JGRG28

The 28th Workshop on General Relativity and Gravitation in Japan – JGRG28
Tachikawa Memorial Hall, Rikkyo University
5-9 November 2018

Volume III

Proceedings of the 28th Workshop on General Relativity and Gravitation in Japan

November 5th–9th 2018
Tachikawa Memorial Hall, Rikkyo University,
3-34-1 Nishi-Ikebukuro, Toshima, Tokyo, Japan

Volume III

Poster Presentations

JGRG : http://www-tap.scphys.kyoto-u.ac.jp/jgrg/index.html

Contents

Poster session

Chiaki Nasu
Rikkyo University

“Stars in K-mouflage gravity”

[JGRG28 (2018) PA1]

PA01

Stars in K-mouflage gravity

M2 Chiaki Nasu(Rikkyo Univ.)
Collaborator Tsutomu Kobayashi(Rikkyo Univ.)

What is K-mouflage gravity[1]?

→ One of scalar-tensor theories(modified gravity)

To explain latetime cosmological expansion

Introducing Λ    Modified gravity

In solar system, theory of gravity should recover GR

screening mechanism

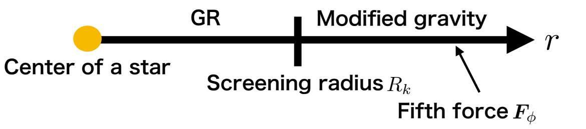

- **We consider** $\tilde{g}_{\mu\nu} = A^2(\phi) g_{\mu\nu}$

  Jordan metric   Einstein metric

geodesic equation in Jordan frame $(\tilde{g}_{\mu\nu})$
$$\frac{\mathrm{d}^2 x^\alpha}{\mathrm{d}\tau^2} + \tilde{\Gamma}^\alpha_{\mu\nu}\frac{\mathrm{d}x^\mu}{\mathrm{d}\tau}\frac{\mathrm{d}x^\nu}{\mathrm{d}\tau} = 0$$

in Einstein frame $(g_{\mu\nu})$ $\left(\frac{\mathrm{d}\ln A}{\mathrm{d}\phi} = \frac{\beta}{\mathrm{M_{Pl}}}\right)$
$$\frac{\mathrm{d}^2 x^\alpha}{\mathrm{d}\tau^2} + \left[\Gamma^\alpha_{\mu\nu} + \underbrace{\frac{\beta}{\mathrm{M_{Pl}}}(\nabla_\nu\phi\delta^\alpha_\mu + \nabla_\mu\phi\delta^\alpha_\nu - \nabla_\lambda\phi g^{\alpha\lambda}g_{\mu\nu})}_{\text{Fifth force}}\right]\frac{\mathrm{d}x^\mu}{\mathrm{d}\tau}\frac{\mathrm{d}x^\nu}{\mathrm{d}\tau} = 0$$

- **K-mouflage gravity**

$$S = \int d^4x\sqrt{-g}\left[\frac{M_{Pl}^2}{2}R + \mathcal{M}^4 K(\chi)\right] + \int d^4x\sqrt{-\tilde{g}}\mathcal{L}_{\mathrm{m}}(\psi^{(i)}_{\mathrm{m}}, \tilde{g}_{\mu\nu})$$

$$\begin{cases} K(\chi) = -1 + \chi + K_0\chi^3 \quad K_0 > 0 \\ \tilde{g}_{\mu\nu} = A^2(\phi)g_{\mu\nu} \quad \chi = -\frac{1}{2\mathcal{M}^4}(\nabla\phi)^2 \end{cases}$$
← **Kinetic function**

Energy momentum tensor

In Einstein frame $T_{\mu\nu} = -2\frac{1}{\sqrt{-g}}\frac{\delta}{\delta g^{\mu\nu}}\sqrt{-\tilde{g}}\mathcal{L}_{\mathrm{m}}(\psi^{(i)}_{\mathrm{m}}, \tilde{g}_{\mu\nu})$

In Jordan frame $\tilde{T}_{\mu\nu} = -2\frac{1}{\sqrt{-\tilde{g}}}\frac{\delta}{\delta \tilde{g}^{\mu\nu}}\sqrt{-\tilde{g}}\mathcal{L}_{\mathrm{m}}(\psi^{(i)}_{\mathrm{m}}, \tilde{g}_{\mu\nu})$

in the theory,

fifth force $F_\phi \propto \frac{1}{K'(\chi)}$

Screening radius $R_k \propto M^{1/2}$ (M is mass of a star)

Feature of this theory

$|\chi| \gg 1$ F_ϕ is suppressed (screening effect)

$|\chi| \ll 1$ F_ϕ is not suppressed

Motivation

Only the case of a point source has been studied[2]

What about the stellar structure?

- To consider a star (not point source)

In the vicinity of the stellar center,
the gradient of the scalar field is small
because of the regularity

Does sufficient screening occur?

Purpose :

Verify a scalar effect on a star in K-mouflage gravity

Numerical solution

- **Setup**

Metric $ds^2 = g_{\mu\nu}dx^\mu dx^\nu = -e^{\nu(r)}dt^2 + e^{\lambda(r)}dr^2 + r^2 d\Omega^2$

Perfect fluid $\{\tilde{T}^\nu_\mu\} = diag\{-\tilde{\rho}, \tilde{P}, \tilde{P}, \tilde{P}\}$

Equation of state
$$\begin{cases} \tilde{P} = K\tilde{\rho}^{\frac{4}{3}}, \quad K = \frac{3^{1/3}\pi^{2/3}}{4}m_p^{-4/3} \quad (\text{white dwarf}) \\ \tilde{\rho} = \left(\frac{\tilde{P}}{K}\right)^{\frac{1}{2}} + \tilde{P}, \quad K = 7.73\times 10^{-3}(8\pi G_N)^3 M_\odot^2 \quad (\text{neutron star}) \end{cases}$$

KG: $K_0 = 1$

Linear: $K_0 = 0$

$\beta = 0.1$ $\left(\tilde{m} = \frac{M_{Pl}^2}{M_\odot}\right)$

Density-Mass relation

White dwarf

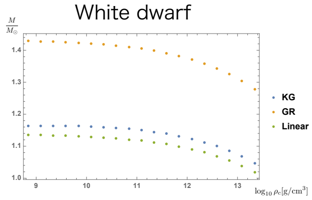

Neutron star

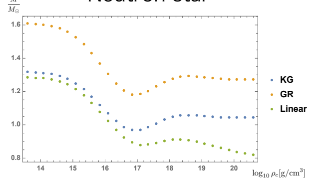

Mass-Radius relation

White dwarf

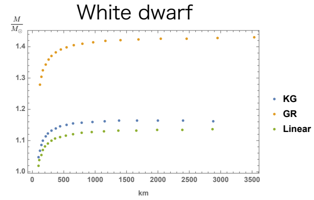

Neutron star

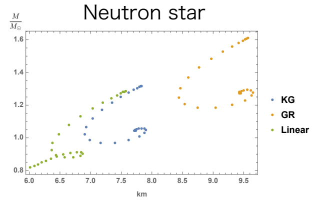

Compactness(M/R)

White dwarf

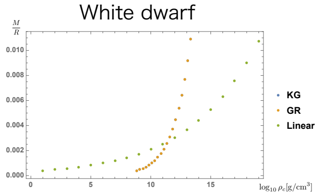

Neutron star

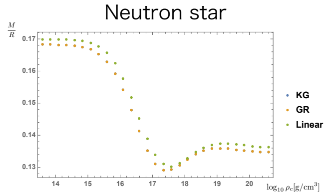

- $\rho_c = 3.89\times 10^{15}\mathrm{g/cm^3}$

Density in a star

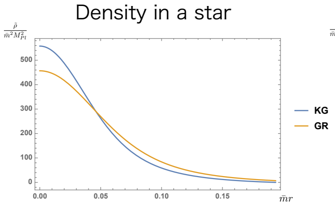

$\rho + \mathcal{M}^4 K(\chi)$ and ρ

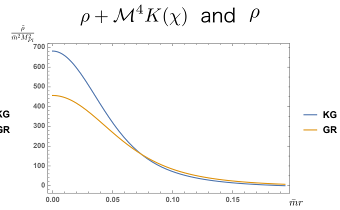

Conclusion and Discussion

- The star solution In K-mouflage gravity is **similar** to that in GR
- There is **difference** between K-mouflage gravity and GR in inner structure

Reference

[1]E. Babichev, C. Deffayet and R. Ziour, Int. J. Mod. Phys. D **18**, 2147 (2009)
[2]A. Barreira, et al., Phys. Rev. D **91**, no. 12, 123522 (2015)
[3]T. Kobayashi and T. Hiramatsu, Phys. Rev. D **97**, no. 10, 104012 (2018)

Hiromu Ogawa
Rikkyo Univ.

“Relativistic stars in a cubic Galileon universe”

[JGRG28 (2018) PA2]

Relativistic stars in a cubic Galileon Universe

Hiromu Ogawa (Rikkyo Univ.)

Collaborators: Tsutomu Kobayashi (Rikkyo Univ.), Kazuya Koyama (Portsmouth Univ., ICG)

1.Introduction

Abstract

Recently it was pointed out that the de Sitter-like black hole solution with nontrivial scalar hair which depends **linearly on time** exists in the cubic Galileon theory. The non-trivial scalar hair **modifies the cosmological constant**, corresponding to three branches (black hole solutions): self-accelerating and self-tuning solutions. We numerically construct relativistic star solutions where the external spacetime is the de Sitter spacetime obtained in the previous work.

Modified gravity theory

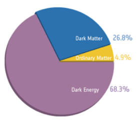

Origin of cosmological expansion is still unknown

fundamental and intriguing problems in cosmology

sign of "new physics"?

beyond standard model, exotic matter, **modification to general relativity**

Modification to GR is tightly constrained in solar system

many modified gravity models are equipped with **a screening mechanism**

can evade the strong constraint from experiments

2.Cubic Galileon

After GW170817/GRB 170817A [1]

Provides tight constraints on modified gravity

$$|c_{\rm GW}/c-1|<10^{-15}$$

The propagation speed of gravitational waves is close to that of light

Surviving theory [2]

General relativity, quintessence, Brans-Dicke, Kinetic Gravity Braiding,…

simplest models survive (also DHOST, vector-tensor so on)

TO DO in surviving theory

find and study star solutions and its structures

Black holes, Neutron stars: natural laboratory for testing theory of gravity

In this poster, we focus on cubic Galileon theory

Cubic Galileon theory[3]

$$S=\int d^4x\sqrt{-g}\,[\zeta R-\eta(\partial\phi)^2+\gamma\Box\phi(\partial\phi)^2] \qquad \zeta,\eta,\gamma \text{ constants}$$

has been studied in the context of cosmology

self accelerating/tuning solution, cosmological perturbation…

not excluded by gravitational waves constraint

equipped with Vainshtein mechanism

3.BHs and NSs

Black holes in Galielon theory

No-hair theorem holds in many cases[4]

Shift-symmetric Galileon theory **with time-dependent scalar**

→ BH solutions are found with non-trivial **scalar hair [5]**

BH solutions in cubic Galileon theory (with cosmological constant) [6]

$$S=\int d^4x\sqrt{-g}[\zeta(R-2\Lambda)-\eta(\partial\phi)^2+\gamma\Box\phi(\partial\phi)^2]\,,\quad \phi(r,t)=\boxed{qt}+\int dr\frac{\chi(r)}{h(r)}$$

$$ds^2=-h(r)dt^2+\frac{dr^2}{f(r)}+r^2d\Omega^2$$

$h(r)=f(r)=1-\frac{\Lambda_{\rm eff}}{3}r^2,\ \chi(r)=\frac{\eta r}{3\gamma}$:asymptotic behaviour at large r

$$\Lambda_{\rm eff}=\begin{cases}\Lambda_< = \frac{1}{2}\left(\Lambda+\sqrt{\Lambda^2+4\Lambda_{\rm KGB}^2}\right) & \text{if } \eta<0 \\ \Lambda_>^+ = \frac{1}{2}\left(\Lambda+\sqrt{\Lambda^2-4\Lambda_{\rm KGB}^2}\right) & \text{if } \eta>0 \text{ and } |\Lambda|>2\Lambda_{\rm KGB} \\ \Lambda_>^- = \frac{1}{2}\left(\Lambda-\sqrt{\Lambda^2-4\Lambda_{\rm KGB}^2}\right) & \text{if } \eta>0 \text{ and } |\Lambda|>2\Lambda_{\rm KGB}\end{cases}$$

:self accelerating sol.

:self tuning sol.

are found numerically within $q\sim\mathcal{O}(q_0)$

$$\Lambda_{\rm KGB}=\left(\frac{|\eta|^3}{6\zeta\gamma^2}\right)^{1/2}$$

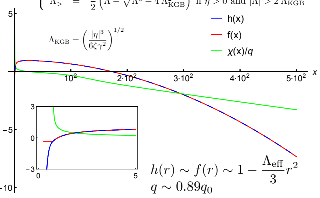

$h(r)\sim f(r)\sim 1-\frac{\Lambda_{\rm eff}}{3}r^2$

$q\sim 0.89q_0$

$h(r)=f(r)=1-\frac{\Lambda_{\rm eff}}{3}r^2,\ \chi(r)=\frac{\eta r}{3\gamma}$

can be mapped to homogeneous solution

$$ds^2=-d\tau^2+e^{2H\tau}(d\rho^2+\rho^2d\Omega^2)$$

$$\phi(\tau)=\boxed{q_0}\tau$$

$$q_0^\pm\equiv\left[\frac{\zeta\Lambda}{\eta}\pm\sqrt{\left(\frac{\zeta\Lambda}{\eta}\right)^2-\frac{2\eta\zeta}{3\gamma^2}}\right]^{1/2}$$

4.Our Setup

Neutron stars in a cubic Galileon universe (minimally coupled matter)

Ansatz

spherical symmetric spacetime

$$ds^2=-h(r)dt^2+\frac{dr^2}{f(r)}+r^2d\Omega^2$$

lineally time-dependent scalar field

$$\phi(r,t)=qt+\int dr\frac{\chi(r)}{h(r)}$$

perfect fluid and EoS

$$T^\nu_\mu={\rm diag}(-\rho,P,P,P)\ ,\rho=\left(\frac{P}{K}\right)^{1/2}+P, K=123M_\odot^2$$

Dimension less quantities

$$\bar m=\frac{M_{\rm Pl}^2}{M_\odot}$$

$$\bar\rho=\frac{\rho}{\bar m^2M_{\rm Pl}^2},\quad \bar P=\frac{P}{\bar m^2M_{\rm Pl}^2},\quad \bar r=\bar m r$$

$$\alpha_1=-\frac{\gamma q\bar m}{\eta},\quad \alpha_2=-\frac{\eta q^2}{\zeta\bar m^2},\quad \alpha_3=\frac{\Lambda}{\bar m^2}$$

$\alpha_1,\ \alpha_2,\ \alpha_3$:parameters

Using shooting method, we solve the field equations numerically

$$\alpha_1\left(\bar r^4h\right)'\frac{f}{h}y^2+2\bar r^4hy-\alpha_1\bar r^4h'=0$$

$$\alpha_2\bar r^2\left[1-\frac{f}{h}y^2\right]+2h\left(-1+f+\alpha_3\bar r^2\right)+2\bar rfh'-2\bar r^2h\bar P=0$$

$$2\bar r^2h^2(-1+\alpha_3\bar r^2+(\bar rf)')-\alpha_2\bar r^4h\left(1+\frac{f}{h}y^2\right)$$

$$+\alpha_1\alpha_2\left[-2\bar r^4hf\left(\frac{y}{h}\right)'+2\bar r^4f^2y^2\left(\frac{y}{h}\right)'-y(\bar r^4f)'+\bar r^4y^3\frac{f'}{h}\right]+2r^4h^2\bar\rho=0$$

$$y=\frac{\chi}{q}$$

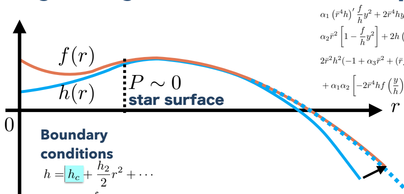

Boundary conditions

$$h=\boxed{h_c}+\frac{h_2}{2}r^2+\cdots$$

$$f=1+\frac{f_2}{2}r^2+\cdots$$

$$\chi=\chi_c r+\cdots$$

$$P=P_c+\frac{P_2}{2}r^2+\cdots$$

→ **given central density** →

Tune

h_c :shooting parameter to match external solutions

$h(r)=f(r)=1-\frac{\Lambda_{\rm eff}}{3}r^2$ at large r

5.Results(preliminary)

Star structure and external geometry $\alpha_1=30,\ \alpha_2=10^{-6},\ \alpha_3=10^{-4},\ q\sim0.51q_0$

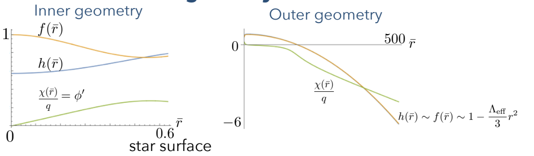

Scalar profile with various q

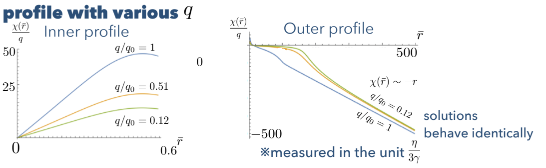

※measured in the unit $\frac{\eta}{3\gamma}$

Comparison to GR $\mathcal{L}=R-2\boxed{\Lambda_{\rm eff}}+\mathcal{L}_{\rm m}$ $(\Lambda_{\rm eff}\neq\Lambda)$ Λ :in Galileon theory

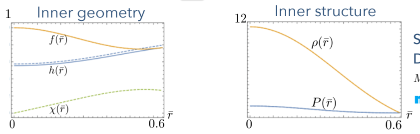

Solid Line:GR,

Dash:cubic Galileon

$M=1.3M_\odot,\ R_{\rm star}\sim 10{\rm km}$

no difference?

6.Summary

Relativistic stars in a cubic Galileon theory

two solutions are found: self accelerating and tuning universe

structure seemed to be same as that in general relativity

Outlook

Why is there no difference between general relativity and Galileon?

We should check the Vainshtein screening around the stars

corresponding Newtonian potential, Galileon force…

We should explore solutions with various parameters $\alpha_1,\ \alpha_2,\ \alpha_3$

We should check our numerical code…

References

[1]e.g., B. P. Abbott et al., Astrophys. J. **848**, no. 2, L13 (2017) [arXiv:1710.05834 [astro-ph.HE]].
[2]e.g., J. M. Ezquiaga and M.~Zumalacárregui, arXiv:1807.09241 [astro-ph.CO].
[3]e.g., A. Nicolis, R. Rattazzi and E. Trincherini, Phys. Rev. D **79**, 064036 (2009) [arXiv:0811.2197 [hep-th]].
[4]E. Babichev, C. Charmousis and A. Lehébel, Class. Quant. Grav. **33**, no. 15, 154002 (2016) [arXiv:1604.06402 [gr-qc]].
[5]e.g., E. Babichev, C. Charmousis, JHEP **1408** (2014), 106, [arXiv:1312.3204 [gr-qc]].
T. Kobayashi and N. Tanahashi, PTEP **2014** (2014) 7, 073E02 [arXiv:1403.4364 [gr-qc]].
[6]E. Babichev, C. Charmousis, A. Lehébel and T. Moskalets, JCAP **1609**, no. 09, 011 (2016) [arXiv:1605.07438 [gr-qc]].

Yuta Hiranuma
Niigata University

“Data Analysis of Gravitational Waves from Core Collapse Supernovae with Hilbert-Huang Transform (I)”

[JGRG28 (2018) PA3]

Data Analysis of Gravitational Waves from Core Collapse Supernovae with Hilbert-Huang Transform (I)

JGRG28

Yuta Hiranuma (¹Niigata University)

collaborated with

Y. Watanabe[1], K. Hayama[2], N. Kanda[3], K. Kotake[2], T. Kuroda[4], K. Oohara[1],
K. Sakai[5], Y. Sakai[1], T. Sawada[3], H. Takahashi[6], T. Takiwaki[7], S. Tsuchida[3], T. Yokozawa[8]
([2]Fukuoka U., [3]Osaka City U., [4]T. U. Darmstadt, [5]Nagaoka CT, [6]Nagaoka U. of Tech., [7]NAOJ, [8]ICRR)

JGRG28
@Rikkyo University (Nov. 5-9, 2018)

1. Introduction

- Hilbert-Huang Transform (HHT) [1] is one of the time-frequency analysis with the high resolution.
- HHT has been adapted to the various fields: e.g.) Nonlinear ocean wave analysis [2]
- HHT was applied to Gravitational Wave (GW) data analysis first by Jordan et al. [3], and Japanese group follows them
  - Binary black hole merger [4]
  - Binary neutron star merger [5]
  - Quasinormal modes in ringdown [6]
- We apply HHT to GW signals from core collapse supernovae. In this poster, we focus on the discussion of (E)EMD parameters.

2. Hilbert-Huang Transform

Hilbert-Huang Transform consists of two parts
✓ **Empirical Mode Decomposition (EMD)**
✓ **Hilbert Spectral Analysis (HSA)**

A target signal $h(t)$
EMD (Like high pass filter)
Intrinsic Mode Functions (IMFs)
HSA
Instantaneous Amplitude (IA)
Instantaneous Frequency (IF)

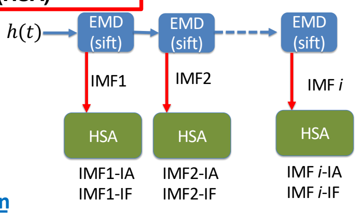

Empirical Mode Decomposition

0. $r_0(t) \leftarrow h(t)$
1. $r(t) \leftarrow r_0(t)$
2. $r(t) \leftarrow r(t) - m(t)$

$(m(t) = (U(t) + L(t))/2)$

if a stoppage criterion is satisfied *then*
get IMF = $r(t)$,
$r_0(t) \leftarrow r_0(t) - r(t)$,
goto 1.
else
goto 2.
end if

"EMD stoppage criterion"

$$\frac{\sum_i |m(t_i)|^2}{\sum_i |r(t_i)|^2} < \boldsymbol{\varepsilon}$$

(In this poster, ε is fixed to be 10^{-1})

($U(t)$: envelope of local maximum of $r(t)$,
$L(t)$: envelope of local minimum of $r(t)$)

Hilbert Spectral Analysis

$x(t)$:IMF

$$y(t) = \frac{1}{\pi} PV \int_{-\infty}^{\infty} \frac{x(t)}{t-\tau} d\tau$$

(PV: Principal value)

$$z(t) = x(t) + iy(t) = a(t)e^{i\theta(t)}$$

$(\theta(t) = \tan^{-1}\left\{\frac{y(t)}{x(t)}\right\}$:Phase)

$a(t) = \sqrt{x^2 + y^2}$: **Instantaneous Amplitude (IA)**
$f(t) = \frac{1}{2\pi}\frac{d\theta}{dt}$: **Instantaneous Frequency (IF)**

3. Ensemble Empirical Mode Decomposition

Ensemble Empirical Mode Decomposition (EEMD):

(i) Add a white Gaussian noise with a standard deviation σ_e to the original data $h(t)$. (σ_h:standard deviation of $h(t)$)
($\sigma_e = \sigma_h \times \sigma_{eemd}$ with a pre-determined $\boldsymbol{\sigma_{eemd}}$)
(ii) Decompose the data with the white noise into IMFs.
(iii) Repeat steps (i) and (ii) many times but with different white Gaussian noise series at each time.
(iv) Obtain the ensemble means for the series of the obtained IMFs. The number of ensemble trials, $\boldsymbol{N_{eemd}}$, has to be large enough. N_{eemd} is fixed to be 1000 in this poster.

(E)EMD parameters
$\boldsymbol{\varepsilon}$: stoppage criterion
$\boldsymbol{N_{eemd}}$: ensemble number,
$\boldsymbol{\sigma_{eemd}}$: injection noise parameter

4. Target Signal

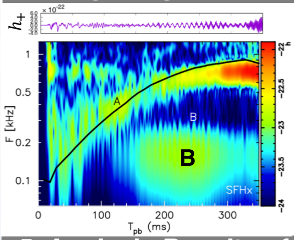

SFHx: (h_+) [7]
- 3-D core collapse supernova simulation of a no-rotating $15M_\odot$ star.
- Standing accretion shock instability (SASI) is active in this case (B part in the left figure)

T. Kuroda, K. Kotake, and T. Takiwaki, ApJ, **827**, L14 (2016)

5. Analysis Results of the Target Signal

5.1 IMFs

EXAMPLE1: (Small noise added)
$\varepsilon = 10^{-1}, N_{eemd} = 1000, \sigma_{eemd} = 10^{-1}$

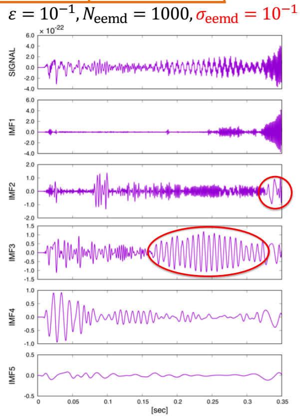

EXAMPLE2: (Large noise added)
$\varepsilon = 10^{-1}, N_{eemd} = 1000, \sigma_{eemd} = 10$

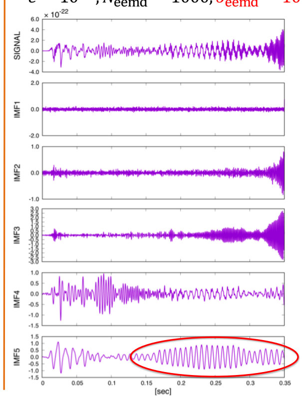

- The SASI signal is split into IMF2 and 3 in EXAMPLE1.

5.2 Time-Frequency Map

EXAMPLE1: (Small noise added)
$\varepsilon = 10^{-1}, N_{eemd} = 1000, \sigma_{eemd} = 10^{-1}$

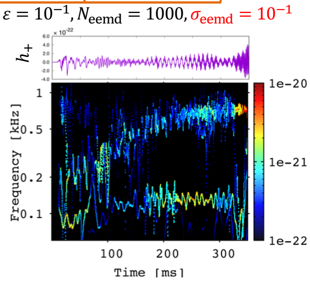

EXAMPLE2: (Large noise added)
$\varepsilon = 10^{-1}, N_{eemd} = 1000, \sigma_{eemd} = 10$

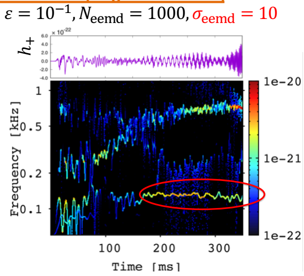

- The SASI signal in EXAMPLE2 is more visible than in EXAMPLE1.

6. Conclusion and Future Works

- We found that the selection of EEMD parameters is IMPORTANT!
- We found that it is likely to be better to **add noises larger than we expected** to the original wave in making an ensemble for the EEMD, which is an essential part of the HHT.
- We need to find the optimal values of EEMD parameters.
- To do this, we should consider how to quantitatively evaluate the time-frequency map of HHT.

Reference

[1] N. E. Huang, and S. S P Shen, *Hilbert-Huang Transform and Its Applications*, World Scientific (2005)
[2] P. A. Hwang, N. E. Huang, D. W. Wang, and J. M. Kaihatu, CHAPTER 10 of [1], pp. 211-225
[3] J. B. Camp, J. K. Cannizzo, and K. Numata, Phys. Rev. D **75**, 061101 (2007)
[4] A. Stroeer, J. K. Cannizzo, and J. B. Camp, Phys. Rev. D **79**, 124022 (2009)
[5] M. Kaneyama, K. Oohara, H. Takahashi, Y. Sekiguchi, H. Tagoshi, and M. Shibata, Phys. Rev. D **93**, 1203010 (2016)
[6] K. Sakai, K. Oohara, H. Nakano, M. Kaneyama, and H. Takahashi, Phys. Rev. D **96**, 044047 (2017)
[7] T. Kuroda, K. Kotake, and T. Takiwaki, ApJ, **827**, L14 (2016)

Kodai Ueda
Department of Physics, Kindai University

"Massive vector field perturbations on extremal static black holes"

[JGRG28 (2018) PA4]

JGRG28

11/5 – 11/9 (2018)

PA4

Massive vector field perturbations on extremal static black holes

Phys. Rev. D**97** 124050 (2018) arXiv:1805.02479

Department of physics, Kindai University, Kodai Ueda and Akihiro Ishibashi

By expanding (near) extremal Reissner-Nordstrom geometry and massive vector field with respect to λ, we show that the Proca equation for the scalar-type components at each order of λ can reduce to a set of two mutually decoupled wave equations of which the source terms consist only of the lower-order variables.

Introduction

In 2015, LIGO directly observed a gravitational wave.

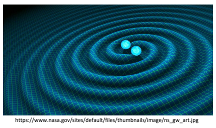

Beginning of the new era of gravitational-wave astronomy

In the future, we may possibly verify…

The existence of ultralight axions
A. Arvanitaki et al. Phys. Rev. D**81**, 123530 (2010)

the candidates of dark matter

Verification measure:

To investigate the interaction between black hole and ultralight boson fields

We can use "Black Hole Bomb"

"Black Hole Bomb" (Superradiant instability):

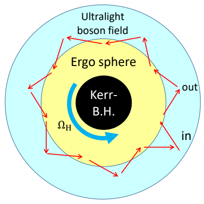

If Compton wavelength $\approx$ black hole radius

Supperradiance will occur repeatedly.

Observation of this phenomenon could lead to the verification of dark matter.

W. H. Press and S. A. Teukolsky, Nature **238**, 211 (1972)

Our objective:

To analyze the dynamics of massive boson field perturbations on Kerr spacetime

Our strategy for massive vector and tensor fields on extremal black holes

Proca equation:

$$\nabla_\mu F^{\mu\nu} = \mu^2 A^\nu$$

degrees of freedom: 3

Massive tensor field equation:

$$\bar{\Box} h_{\mu\nu} + 2R_{\alpha\mu\beta\nu}h^{\alpha\beta} - 2R^{\alpha}_{(\mu}h_{\nu)\alpha} = \mu^2 h_{\mu\nu}$$

degrees of freedom: 5

In the massive case, analytical study is very difficult due to the mass term.

Analysis approach 1:

3 strategies for analysis

1: **the extremal case**

2: **scaling transformation**

3: **perturbation expansion**

Analysis approach 2:

As a practice, we apply 3 strategies to Reissner-Nordstrom case.

Advantage1: extremal case can be used

Advantage2: easy to separate variables

our goal:

field equation

decoupled ODE

It's not achieved even in Schwarzschild spacetime case.

J. G. Rosa and S. R. Dolan, Phys. Rev. D**85**, 044043 (2012)

Massive vector/tensor fields on RN spacetime

(Near) extremal RN metric: (Strategy 1,2)

$$\frac{ds^2}{r_+^2} = -F(x)dv^2 + 2dvdx + R^2(x)d\Omega^2$$

$$\left[F(x) = \frac{x(x+\sigma)}{(1+\lambda x)^2}\ , R(x) = (1+\lambda x)\right]$$

$\lambda \to 0$: a near horizon geometry

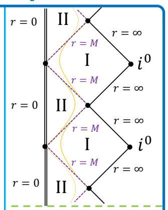

extremal RN spacetime

Near horizon region: $\lambda \to 0$

Decoupled homogeneous master equations can be obtained.

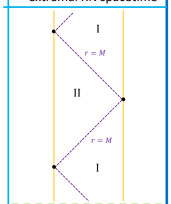

near horizon EX RN

Far region:

Strategy 3 : perturbation expansion

$$A_\mu(\lambda) = A_\mu^{(0)} + \lambda A_\mu^{(1)} + \lambda^2 A_\mu^{(2)} + \cdots$$

$$g_{\mu\nu}(\lambda) = g_{\mu\nu}^{(0)} + \lambda g_{\mu\nu}^{(1)} + \lambda^2 g_{\mu\nu}^{(2)} + \cdots$$

We view λ as a perturbation parameter and expand $A_\mu, g_{\mu\nu}$ around $\lambda = 0$.

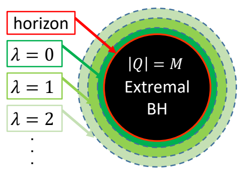

Perturbation expansion method

Results of the perturbation expansion

For simplicity, in what follows we describe our result in the massive vector case.

Proca equation at the nth order of λ : (even parity mode)

$$\begin{pmatrix} L^{(0)}_{\alpha1} & 0 & 0 \\ 0 & L^{(0)}_{\beta2} & 0 \\ 0 & L^{(0)}_{\gamma2} & L^{(0)}_{\gamma3} \end{pmatrix} \begin{pmatrix} \Phi^{(n)}_{S1} \\ \Phi^{(n)}_{S2} \\ \Phi^{(n)}_{S3} \end{pmatrix} = -\sum_{m=1}^{n} \left[\begin{pmatrix} L^{(m)}_{\alpha1} & L^{(m)}_{\alpha2} & L^{(m)}_{\alpha3} \\ 0 & L^{(m)}_{\beta2} & L^{(m)}_{\beta3} \\ 0 & L^{(m)}_{\gamma2} & L^{(m)}_{\gamma3} \end{pmatrix} \begin{pmatrix} \Phi^{(n-m)}_{S1} \\ \Phi^{(n-m)}_{S2} \\ \Phi^{(n-m)}_{S3} \end{pmatrix} \right]$$

$L^{(0)}_{\alpha2} = L^{(0)}_{\alpha3} = L^{(0)}_{\beta3} = 0$

RHS is a source term

2 decoupled inhomogeneous master wave equations

Summary and outlook

- We have developed a new perturbation method to study the massive vector/tensor field in (near) extremal RN spacetimes.
- Proca equation reduces to a set of 3 decoupled inhomogeneous master wave equations.
- Massive vector/tensor case on Kerr black hole case
  $\Rightarrow$ work in progress (w/ Igata, Ishibashi, Cardoso)

Priti Gupta
Waseda University

“Gravitational Waves and Chaos”

[JGRG28 (2018) PA6]

Gravitational Waves And Chaos

Priti Gupta・Kei-ichi Maeda / Waseda University. @ JGRG28, Rikkiyo University

Motivation

- **Gravitational waves from chaotic systems has generated considerable interest.**
- **In particular [Kiuchi at el.(2007)] showed signature of chaos in gravitational waves and energy spectra from a chaotic system : A Point Mass with a Disk**
- **Goal : We aim at studying the energy spectra of gravitational waves from chaotic orbits taking into account radiation reaction mechanism.**
- **We will not consider quadrupole radiation damping as a secular effect, but include radiation reaction terms in the Hamiltonian equations of motion.**

Model : A point mass with a disk

We consider the Newtonian limit of a black hole-disk system.
The dynamics of a test particle (mass μ) in this background is governed by the following Hamiltonian.

$$H = \mu\left[\frac{\dot{\varpi}^2}{2} + \frac{\dot{z}^2}{2} + \frac{L^2}{2\mu^2\varpi^2} - \frac{M}{\sqrt{\varpi^2+z^2}} + \alpha z_0 \ln\cosh\left(\frac{z}{z_0}\right)\right]$$

$\alpha \rightarrow$ *the surface mass density of the disk*
$L \rightarrow$ *angular momentum of the particle*
$Zo \rightarrow$ *thickness of the disk.*

This model mimics a system of blackhole with a massive accretion disk.

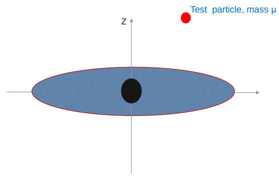

A point mass (M) located at origin while a disk exists on equatorial plane z = 0.

Indication of Chaos in GRWs (No Radiation Reaction)

- **As considering the same model, we first reproduced results of (Kiuchi et al.;2007).**
- **We use Implicit Runge Kutta (Order-6) for numerical analysis. [FORTRAN]**
- **The integrated time is such that particle moves thousand times around central mass.**
- **The numerical accuracy is monitored by conservation of Hamiltonian which is 10^{-8}.**

M=1 to fix unit, and G=c=1

Thickness of the disk is fixed
$Z_0 = 0.5$

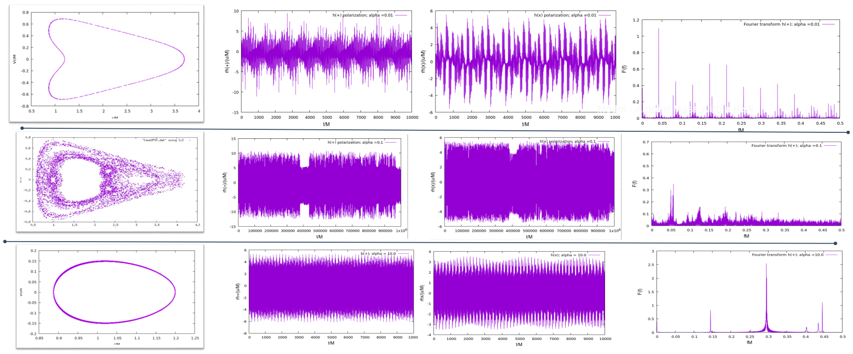

Poincare maps GR waves (+) and (x) modes Fourier transforms

$(surface\ density\ of\ disk\ \alpha)$
$\alpha = 0.01$ **onset of chaos**

$\alpha = 0.1$ **(chaotic orbit)**
comparable mass of disk and point mass leads to chaos [M=1;$\alpha = 0.1$]

$\alpha = 10.0$ **(regular orbit)**

Initial conditions $(r, v_r, z, v_z) = (1.2, 0, 0, 0.76)$
H= - 0.2 ; L=1

Simpler problem: Point mass-test particle (Including Radiation Reaction)

- Including radiation reaction terms in the Hamiltonian.

$$H_{reac}(t) = \frac{G}{5c^5}\dddot{Q}_{ij}(t)\ddot{Q}_{ij}(p,q),$$

$\ddot{Q}_{ij}(p,q)$ denotes that $\ddot{Q}_{ij}$ has to be treated as a function of position and momentum variables.

[G. Schafer, Astron. Nachr. 311, 213 (1990).]

Fig (a) orbit of test particle around a point mass (M=1)
(b) Gravitational Wave (+) polarization mode.
(c) inspiral orbit after including radiation reaction.
(d) Gravitational Wave (+) mode. (CHIRP effect)

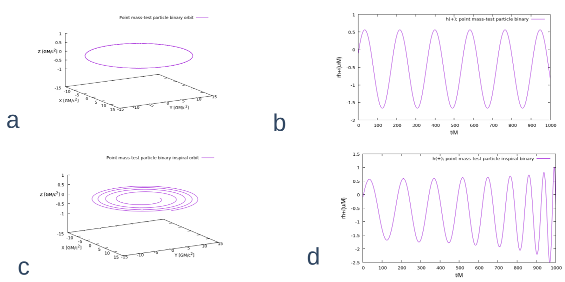

RR terms

NO

YES

Future Works

- As shown above, by **varying surface density** of disks we can have change from regular orbit to a chaotic one.
- Firstly, we want to include radiation reaction effect in our model: Point mass-disk.
- We want to see effect of **radiation reaction in the energy spectra of chaotic orbits.** ($\alpha = 0.1$ *in our case*).

*References

1. Gravitational Wave signals from a chaotic system : A point mass with a disk (Kiuchi et al. 2007)
2. Gravitational waves from a chaotic dynamical system (Kiuchi , K. Maeda 2004)
3. Chaos in Schwarzschild spacetime: The motion of a spinning particle (S.Suzuki , K.Maeda 1997)

STAY TUNED!

Shu Ueda
Tokyo Gakugei University

"Discrete Integrable Systems and Its Application to Discretization of Geodesics"

[JGRG28 (2018) PA7]

$\boxed{\text{PA7}}$ Discrete Integrable Systems and Its Application to Discretization of Geodesics

Shu Ueda and Shinpei Kobayashi
Department of Physics, Tokyo Gakugei University, JGRG28 @Rikkyo University, 5 - 9 November, 2018

Introduction

Quantization of spacetime? cf. { String theory, Noncommutative geometry, Causal Dynamical Triangulation, … }

Universal feature:
minimal length of spacetime
➡ discretized spacetime would appear
Black hole? Early universe?

First step : How to discretize?
What is **"the best"** discretization?

➡ We focus on discrete **integrable systems**

Discretization with preservation of solution structure

e.g., Logistic equation

$$\frac{du}{dt} = au(1-u), a > 0$$

$$a = 2,\ u_0 = 0.1$$

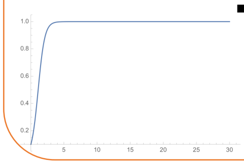

discretize ➡ $t = n\delta$

$$\frac{u_{n+1}-u_n}{\delta} = au_n(1-u_{n+1}) \quad \delta = 1.8$$

$$\frac{u_{n+1}-u_n}{\delta} = au_n(1-u_n) \quad \delta = 1.3$$

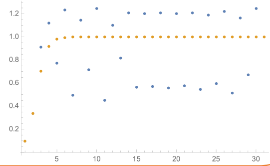

Discretization of geodesics in $(2+1)$-dimensional Massive Gravity

As a first step to discretize geometry, we want to consider the discretization of geodesics (prototype of the discretization of geometry).

Static, circularly symmetric Black hole Oliva et al(2009)

$$ds^2 = -f(r)dt^2 + \frac{1}{f(r)}dr^2 + r^2 d\phi^2$$

b : gravitational hair parameter
μ : mass parameter

$$f(r) = -\Lambda r^2 + br - \mu$$

If $b = 0$, it represents BTZ black hole

Geodesic equation for massive particles

$$\frac{d^2 r}{d\phi^2} = \frac{1}{2L^2}\left[6\Lambda r^5 - 5br^4 + 4\left(E^2 + \mu + \Lambda L^2\right)r^3 - 3bL^2 r^2 + 2\mu L^2 r\right]$$

Hirota's bilinearization method

Bilinear form of the geodesic equation

$$D_\phi^2 g\cdot f + \beta_1\frac{g^4}{f^2} - \gamma_1\frac{g^3}{f} + \epsilon_1 g^2 - \xi_1 gf = 0$$

$$D_\phi^2 f\cdot f - \alpha\frac{g^4}{f^2} - \beta_2\frac{g^3}{f} + \gamma_2 g^2 - \epsilon_2 gf + \xi_2 f^2 = 0$$

where $D_\phi g\cdot f \equiv g_\phi f - g f_\phi$ (D is called Hirota's derivative)

$$\alpha = -\frac{3\Lambda}{L^2}, \beta = \beta_1 + \beta_2 = \frac{5b}{2L^2}, \gamma = \gamma_1 + \gamma_2 = \frac{2(E^2+\mu+\Lambda L^2)}{L^2},$$

$$\epsilon = \epsilon_1 + \epsilon_2 = \frac{3b}{2}, \xi = \xi_1 + \xi_2 = \mu$$

Discretized geodesic equation

$$r_{n+1} = \frac{\left(2+\xi_2\delta^2\right)r_n - r_{n-1}\left[1 - \frac{\xi_1\delta^2}{2} + \frac{\epsilon_2\delta^2}{2}r_n\right]}{\left[1 - \frac{\xi_1\delta^2}{2} + \frac{\epsilon_2\delta^2}{2}r_n\right] - r_{n-1}\delta^2\left[-\alpha r_n^3 - \beta r_n^2 + \gamma r_n - \epsilon_1\right]}$$

➡
- This form is same as that of QRT system, which is an integrable second-order discrete equation.
- We obtained the discrete geodesic equation with keeping integrability by using Hirota's method.

Procedure of discretization with keeping integrability

Nonlinear differential equation

⬇
- Introduction of new functions $r(\phi) = \frac{g(\phi)}{f(\phi)}$
- $r(\phi)$ is invariant under arbitrary gauge transformation $h(\phi)$:**integrability**

Bilinear differential equation $r'(\phi) = \frac{g(\phi)h(\phi)}{f(\phi)h(\phi)} = r(\phi)$

⬇ **Discretization**
- Replace D_ϕ with Δ_ϕ
- $\Delta_\phi g\cdot f \equiv \delta^{-1}[g(\phi+\delta)f(\phi) - g(\phi)f(\phi+\delta)]$
- δ is the interval of difference

Bilinear discrete equation

⬇
- Inverse transformation $g(\phi) = r(\phi)f(\phi)$
- Remove the common term written in $f(\phi)$
- Rewrite to mapping form $\phi = n\delta, r(\phi) = r_n$

Nonlinear discrete equation

Solution of the discretized geodesic equation

	Hirota's method	Other method (numerical)

Bounded orbit

$E = \sqrt{25}, L = 10,$
$r_0 = 10, \phi_0 = \frac{\pi}{2}$
Discrete: $\epsilon_1 = \epsilon_2 = \frac{\epsilon}{2},$
$\xi_1 = \xi_2 = \frac{\xi}{2}, \delta = 0.005$

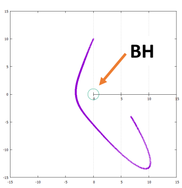

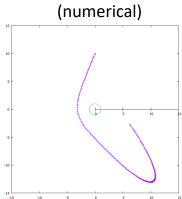

Falling orbit

$E = \sqrt{30}, L = 10,$
$r_0 = 10, \phi_0 = \frac{\pi}{2}$
Discrete: $\epsilon_1 = \epsilon_2 = \frac{\epsilon}{2},$
$\xi_1 = \xi_2 = \frac{\xi}{2}, \delta = 0.005,$

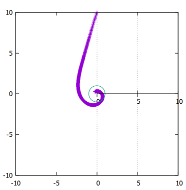

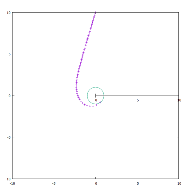

➡ Hirota's bilinearization method gives the same result

Conclusion & Discussions

- We applied the Hirota's method to the geodesic
  -> The discrete geodesics gives the same result
- We will investigate the solution of the discrete geodesic equation for various intervals of difference δ
- Towards discretization of Einstein equation
  -> For stationary axisymmetric spacetime,
  Einstein equation reduces to Masuda et al(1998)

$$\tilde{f}(\tilde{f}_{\rho\rho} + \frac{1}{\rho}\tilde{f}_\rho + \tilde{f}_{zz}) - \tilde{f}_\rho^2 - \tilde{f}_z^2 + \psi_\rho^2 + \psi_z^2 = 0$$

$$\tilde{f}(\psi_{\rho\rho} + \frac{1}{\rho}\psi_\rho + \psi_{zz}) - 2\tilde{f}_\rho\psi_\rho - 2\tilde{f}_z\psi_z = 0$$

Introducing new functions $\tilde{f} \equiv \frac{F}{G}, \psi \equiv \frac{H}{G}$ and $K = \frac{H^2+F^2}{G},$

Bilinear form of Einstein equation

$$\begin{cases}[D_\rho^2 + \frac{1}{\rho}D_\rho + D_z^2]\,G\cdot F = 0\\ [D_\rho^2 + \frac{1}{\rho}D_\rho + D_z^2]\,H\cdot F = 0\\ [D_\rho^2 + \frac{1}{\rho}D_\rho + D_z^2]\,K\cdot F = 0\end{cases}$$

⬇ **discretize**

Discrete Einstein equation

Ryunosuke Kotaki
Hirosaki University

"More accurate equation for the gravitational lens"

[JGRG28 (2018) PA8]

More accurate equation for the gravitational lens

Ryunosuke Kotaki, Masashi Shinoda and Hideaki Suzuki

Hirosaki University, Japan
with T.Ono, A.Ishihara and H.Asada (Hirosaki)

JGRG28 in Tokyo Nov. 5 - 9, 2018

Abstract

We propose a more accurate equation for the gravitational lens, where we assume Schwarzschild spacetime as one example. Our result is compared with previous works.

1 Introduction

The kown lens equations are usually based on the thin lens approximation, in which the effect of gravity is expressed only by the deflection angle and the Euclidean space is assumed except for the lens plane.

2 Previous lens equations

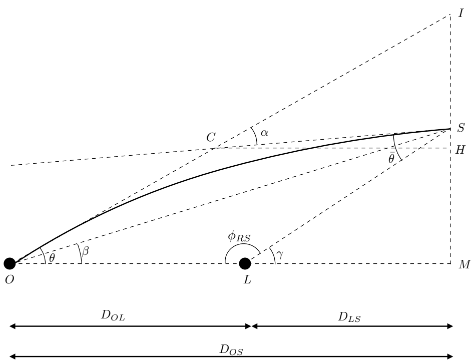

The well-known lens equation is [3]

$$\beta = \theta - \frac{D_{LS}}{D_{OS}}\alpha. \tag{1}$$

Ohanian lens equation is [5]

$$\theta + \bar{\theta} - \alpha = \gamma. \tag{2}$$

Virbhadra and Ellis lens equation is [2]

$$D_{OS}\tan\beta = D_{OS}\tan\theta - D_{LS}[\tan\theta + \tan(\alpha - \theta)]. \tag{3}$$

3 Schwarzschild spacetime

Schwarzschild spacetime as a simple example

$$\mathrm{d}s^2 = -\left(1 - \frac{r_g}{r}\right)\mathrm{d}t^2 + \left(1 - \frac{r_g}{r}\right)^{-1}\mathrm{d}r^2 + r^2\mathrm{d}\Omega^2 \tag{4}$$

Orbit equation for the photon is

$$\left(\frac{\mathrm{d}r}{\mathrm{d}\phi}\right)^2 = \frac{r^4}{b^2} - r^2\left(1 - \frac{r_g}{r}\right). \tag{5}$$

By solving this, we obtain

$$\phi_{RS} = \int_{r_0}^{r_R} \frac{b\mathrm{d}r}{r^2\sqrt{1 - \left(\frac{b}{r}\right)^2\left(1 - \frac{r_g}{r}\right)}} + \int_{r_0}^{r_S} \frac{b\mathrm{d}r}{r^2\sqrt{1 - \left(\frac{b}{r}\right)^2\left(1 - \frac{r_g}{r}\right)}} \tag{6}$$

This is the exact lens equation. Given r_R, r_S, ϕ_{RS}, this determines θ.

- **Weak field approximation**

$\frac{r_g}{b} \ll 1$ equation(6) becomes

$$\begin{aligned}\phi_{RS} =& \pi - \bar{\theta} - \theta + \frac{r_g}{b}(\cos\theta + \cos\bar{\theta}) \\ &+ \left(\frac{r_g}{b}\right)^2 \frac{15}{16}(\pi - \bar{\theta} - \theta + \sin\theta\cos\theta + \sin\bar{\theta}\cos\bar{\theta}) + O\left(\left(\frac{r_g}{b}\right)^3\right)\end{aligned} \tag{7}$$

- **Strong field approximation**

Light ray passing near the photon sphere : $\frac{b}{r_R}, \frac{b}{r_S} \ll 1$

$$\begin{aligned}\phi_{RS} =& 2\int_{r_0}^{\infty} \frac{b\mathrm{d}r}{r^2\sqrt{1 - \left(\frac{b}{r}\right)^2\left(1 - \frac{r_g}{r}\right)}} \\ &- \frac{b}{r_R} - \frac{1}{6}\left(\frac{b}{r_R}\right)^3 + \frac{1}{8}\frac{r_g}{b}\left(\frac{b}{r_R}\right)^4 \\ &- \frac{b}{r_S} - \frac{1}{6}\left(\frac{b}{r_S}\right)^3 + \frac{1}{8}\frac{r_g}{b}\left(\frac{b}{r_S}\right)^4 + O\left(\left(\frac{b}{r_R}\right)^5, \left(\frac{b}{r_S}\right)^5\right)\end{aligned} \tag{8}$$

4 Numerical calculations

We consider Sgr A*, $D_{OL} = 8\text{kpc} \fallingdotseq 2.5 \times 10^{10} r_g$ and $D_{LS} = 1000 r_g$.
We plot the relative error δ in the image positions with respect to the exact lens equation.

$$\delta = \frac{\theta}{\theta_{\mathrm{exact}}} - 1 \tag{9}$$

where

$$\theta_{\mathrm{exact}} = \text{Solution of Eq.(6)}, \tag{10}$$

$$\theta = \text{Solution of Approximation Eqs.(1, 2, 3, 7, 8)}. \tag{11}$$

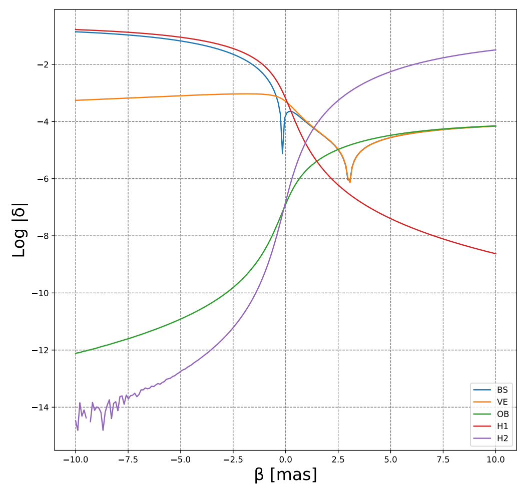

Figure 1: The relative error δ as a function of the source position β for the Basic lens equation(BS),Virbhadra and Ellis lens equation(VE), Ohanian lens equation(OB), Eq.(7) (H1) and Eq.(8) (H2).β is expressed in milli arc-seconds.For $\beta > 0$ the plot represents the primaty image, for $\beta < 0$ it represents the secondary image.

5 Conclusion

1. A more accurate equations for GL is proposed and compared with previous ones.
2. Future work: Astronomical applications.

References

[1] A. Ishihara et al, Phys. Rev. D 94, 084015 (2016)

[2] K.S. Virbhadra and G.F.R. Ellis, Phys. Rev. D 62, 084003 (2000).

[3] P. Schneider, J. Ehlers, and E.E. Falco, Gravitational lenses, Springer-Verlag, Berlin (1992).

[4] V. Bozza, Phys. Rev. D78:103005(2008)

[5] H.C. Ohanian, Am. J. Phys. 55, 428 (1987).

[6] R. Kotaki et al, In preparation.

Shoichiro Miyashita
Waseda University

"Energy spectrum of spacetime: complex saddle points in Euclidean path integral"

[JGRG28 (2018) PA10]

Energy spectrum of spacetime: complex saddle points in Euclidean path integral

Shoichiro Miyashita [Waseda U.]

Abstract : we investigate microcanonical partition function of gravity by mini(micro)superspace model.

Motivation/Previous works

Thermal equilibrium of Gravity may be described by Partition function;

[Gibbons, Hawking, 1977]

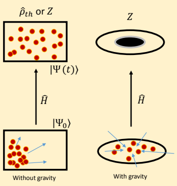

$$Z[\mathfrak{Q},\mathfrak{W}] = \int_{\Gamma} \mathcal{D}g \; e^{-I^{E}_{\{\mathfrak{Q},\mathfrak{W}\}}}$$

① Integration measure

② Action functional

Depending on ensemble, we have to change Action.

③ Integration Contour

For Euclidean path integral of GR,
it is known that integration contour *must be genuinely complex*.

[Gibbons, Hawking, Perry, 1978]

Although complex saddle points have been attracted much attention in a context of Quantum Cosmology, they haven't in a context of gravitational thermodynamics. (However, see[Halliwell, Louko, 1990] and [Whiting, Louko, 1992])

If we only concentrate on only real saddle points, the behavior of free energy or entropy as right figures.

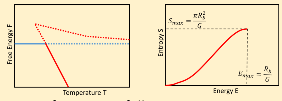

Our aim is to reconsider thermodynamical properties of Gravity in following setups;

- spacetime with rigid spherical boundary (i.e. $\partial\mathcal{M} = \mathbb{R}\times S^2$)
- mini(micro)superspace model
- choosing the contour as (a set of) steepest contour(s)

Especially, we show entropy behavior in microcanonical ensemble in this poster.

(Another motivation is Holography. Assume GKP-Witten like relationships $Z_{gravity} = Z_{field\ theory}$ for the general class of GR.
If we regard the entropy behavior of above panel as (approximately) correct behavior of $Z_{gravity}$, the number of state $N \sim \int dE\, Z_{field\ theory}[E,V]$ becomes finite. This may be peculiar. So the one of the aims is to resolve the boundedness of either (both) of energy or(and) energy in order for N to be infinite which may be required for Z to be the partition function of field theory.)

Minisuperspace model

We approximate Z by minisuperspace functional integral

$$Z[\mathfrak{Q},\mathfrak{W}] = \int dN\, \mathcal{D}f\, \mathcal{D}R\; e^{-I^{E}_{\{\mathfrak{Q},\mathfrak{W}\}}[f,R;N]}$$

$$\simeq \int dN\, e^{-I^{E,on-shell}_{\{\mathfrak{Q},\mathfrak{W}\}}(N)}$$

where corresponding metric is

$$\boldsymbol{g} = f(r)dt^2 + \frac{N^2}{f(r)}dr^2 + R(r)^2 d\Omega^2$$

$$\tau \in (0,\beta_0), \qquad r \in (r_i, r_f)$$

E.O.M.

$$R'' = 0 \qquad \frac{f''R}{N} + \frac{2f'R'}{N} = 0$$

Constraint

$$f(R')^2 + f'RR' = N^2$$

Since

$$\delta I^E\Big|_{r=r_i} \propto \left[-\frac{2RR'}{N}\delta f + R^2\delta\left(\frac{f'}{N}\right) + f(\cdots)\right]$$

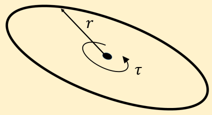

at the "center,"
all off-shell histories must satisfy

$$f\Big|_{r_i} = 0, \qquad \frac{f'}{N}\Big|_{r_i} = \text{const.} \left(= \frac{4\pi}{\beta_0}\right) \qquad \left(or\ R\Big|_{r_i} = 0\right)$$

Microcanonical ensemble $mc \equiv \{E,V\}$

$$I^E_{mc} = \frac{-1}{16\pi G}\int d^4x\sqrt{g}\,R + \frac{-1}{8\pi G}\int d^3y\,\sqrt{\gamma}(\Theta - \Theta_0)$$

$$= \frac{-\beta_0}{2G}\int_{r_i}^{r_f} dr\left[\frac{f(R')^2}{N} + \frac{f'RR'}{N} + N\right] - \frac{\beta_0}{4G}\left(\frac{f'R^2}{N} + \frac{4fRR'}{N}\right)_{r=r_i} + \frac{\beta_0}{G}\frac{RR'f}{N}\Bigg|_{r=r_f}$$

$\Downarrow$ E.O.M. + b.c.

$$\begin{cases} \sqrt{f(r_f)} = \dfrac{(r_f - r_i)N}{(R_b - R_H)}\left(\dfrac{GE}{R_b} - 1\right) \\ R(r_f) = R_b \end{cases}$$

$$I^E_{mc} = -\frac{1}{G}\left[-2\pi R_H(N)\big(R_b - R_H(N)\big) + \frac{1}{2}N\right] - \frac{\pi R_H(N)^2}{G}$$

$$\left[\begin{array}{l} R_H(N) = \dfrac{2}{3}R_b + U(N) + \dfrac{R_b^2}{9}\dfrac{1}{U(N)} \\ U(N) = \sqrt[3]{\dfrac{NL^2R_b}{8\pi} - \dfrac{R_b^3}{27} + \dfrac{NLR_b}{2\pi}\sqrt{\dfrac{1}{16}L^2 - \dfrac{\pi R_b^2}{27N}}}\,, \qquad L = \left(\dfrac{GE}{R_b} - 1\right) \end{array}\right.$$

Since this seems difficult to evaluate, we consider following two alternative "micro"superspace model.

Model I

Instead of integrating over N, integrating over the "distance" between horizon and boundary;

$$z = R_b - R_H(N) \qquad \Rightarrow \qquad N = -\frac{4\pi}{R_bL^2}z^2(z - R_b)$$

Model II

Changing variable N to z by

$$N = \frac{16\pi R_b^2}{27\,L^2}\frac{\left(z^3+1\right)^2}{z^3}$$

Model I $\quad I^E_{mc}(z) = -\dfrac{\pi}{G}\left[R_b^2 - 4LR_bz + \left(3L^2+2\right)z^2 - \dfrac{2L}{R_b}z^3\right]$

$0 < E < R_b$ $\qquad$ $E = R_b$ $\qquad$ $R_b < E$

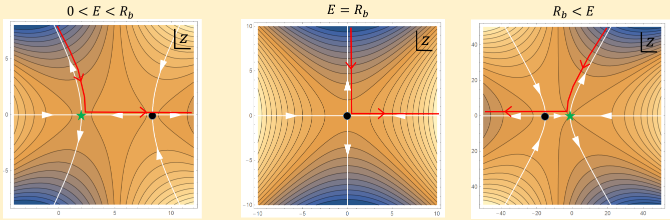

$R_b = 5 \quad E = 3$ $\qquad$ $R_b = 5 \quad E = 5$ $\qquad$ $R_b = 5 \quad E = 20$

: Steepest decent direction

: integration contour

★ : Saddle point and satisfy constraint

● : Saddle point but NOT satisfy constraint

Model II $\quad I^E_{mc}(z) = -\dfrac{\pi R_b^2}{3G}\left[z^2 + 2z + 2 + \dfrac{2}{z} + \dfrac{1}{z^2} + \dfrac{2}{9L^2}\left(z^3 + 2 + \dfrac{1}{z^3}\right)\right]$

$E = 0\,, 2R_b$ $\qquad$ $0 < E < 2R_b$ $\qquad$ $2R_b < E$

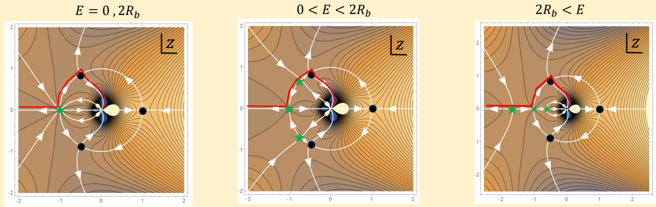

$R_b = 5 \quad E = 0$ $\qquad$ $R_b = 5 \quad E = 0.5$ $\qquad$ $R_b = 5 \quad E = 10.2$

In both cases, if we choose integration contour as above, the energy-entropy relationships are the same.

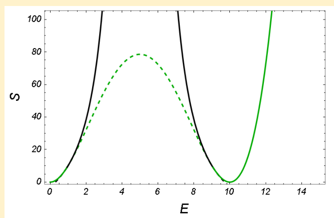

Summary & problems

- We investigated the partition function of gravity by the method of minisuperspace & steepest descent approximation.
- If we choose some contour, both of energy and entropy are shown to be unbounded from above, which is different from the result by evaluating only real saddles.
- # of state may be infinite. This may resolve (one of) the discrepancy(s) between $Z_{gravity}$ and $Z_{field\ theory}$

○ We did NOT evaluate minisuperspace path integral BUT evaluate microsuperspace path integral. It causes the saddle points which are NOT the solution of Euclidean GR.

○ Depending on model and contour, the results are different. But in any cases, there always still remains peculiar behavior, such as the divergence of entropy at finite energy or appearece of negative energy.

Tomohiro Nakamura
Nagoya University

"Instability of stars in screened modified gravity"

[JGRG28 (2018) PA11]

Instability of stars in screened modified gravity

Tomohiro Nakamura

Nagoya University

In collaboration with Chulmoon Yoo(Nagoya U.)

NAGOYA UNIVERSITY

Introduction

- Modified gravitational theories usually have additional degrees of freedom coupled with matter, whose interaction works as "fifth force" on the motion of matter.
- These theories must have a screening mechanism of the fifth force to satisfy experimental constraint within the solar system scale.

Screening mechanism[1]

$$S=\int d^4x\sqrt{-g}\left[-\frac{1}{2}Z^{\mu\nu}(\phi,\partial\phi,\cdots)\partial_\mu\phi\partial_\nu\phi - V(\phi) + g(\phi)T\right]$$

$$Z(\bar\phi)\ddot\varphi - c_s^2(\bar\phi)|\vec\nabla|^2\varphi + m^2(\bar\phi)\varphi = g(\bar\phi)M\delta^3(\vec x)$$

Environment dependence

$$\varphi = \frac{g(\bar\phi)}{Z(\bar\phi)c_s^2(\bar\phi)}\frac{M}{4\pi r}e^{-\frac{m(\bar\phi)}{\sqrt{Z(\bar\phi)}c_s(\bar\phi)}r}$$

example

chameleon, symmetron, environmental dilaton…

For chameleon model,
the fifth force sourced by a constant density star is

$$F_\phi \sim \beta_{eff}^2\frac{GM^2}{r^2} = \frac{1}{m(\bar\phi)R}F_{\mathrm{Newton}}$$

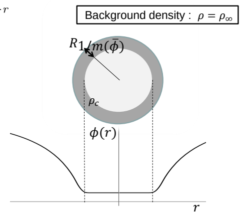

Screening for inhomogeneous objects?

The above calculation is done for a constant density star.
In the case of inhomogeneous density objects, does the screening work properly?

Screening in inhomogeneous density profile

We consider a simple situation where the system composed by spherical shells with same width[2]. We assume static configuration and the inner region is vacuum, then it has extremally inhomogeneous density profile.

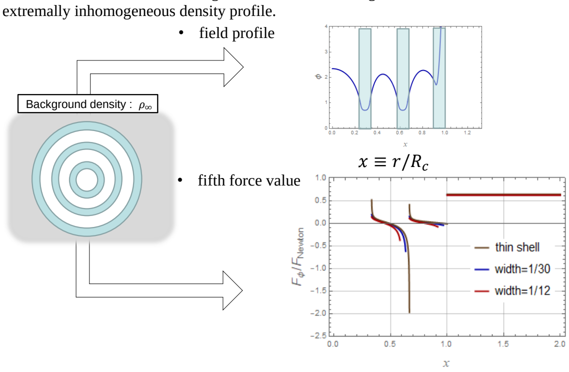

we found the fifth force appears inside the inhomogeneous objects and its value becomes larger as the width of the shells are reduced.

Intuitive explanation

screened $\lambda_\phi < \delta r$ unscreened $\lambda_\phi > \delta r$

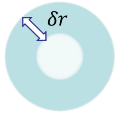

$$\lambda_\phi \equiv \frac{1}{m(\bar\phi)} \propto \rho^{-1/2}$$

mass conservation

$$\delta r \propto \rho^{-1}$$

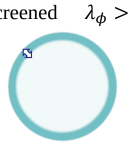

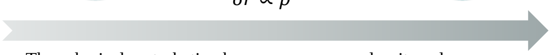

The spherical perturbation becomes unscreened as it evolves.
→Instability in non-linear level?

Instability of simple stellar model

Action

$$S = \int d^4x\sqrt{-g}\left[\frac{M_{\mathrm{pl}}^2}{2}R - \frac{1}{2}\nabla_\mu\phi\nabla^\mu\phi - V(\phi)\right] + S_m\left[\Psi_i; A^2(\phi)g_{\mu\nu}\right].$$

Consider a non-relativistic star consists of perfect fluid.
We concentrated on spherical symmetric system and derive a static solution and equations which a perturbation from the solution follows in linear order.

Equations

$$\nabla^2\Phi_N = 4\pi G\rho$$
$$\frac{\partial\rho}{\partial t} + \vec\nabla\cdot(\rho\vec v) = 0$$
$$\rho\left\{\frac{\partial\vec v}{\partial t} + (\vec v\cdot\vec\nabla)\vec v\right\} = -\vec\nabla p - \rho\vec\nabla\Phi_N - \frac{\beta}{M_{\mathrm{pl}}}\rho\vec\nabla\phi$$
$$-\frac{\partial^2\phi}{\partial t^2} + \frac{1}{r^2}\frac{\partial}{\partial r}\left(r^2\frac{\partial\phi}{\partial r}\right) = V'(\phi) + \frac{\beta}{M_{\mathrm{pl}}}\rho$$

Perturbation

$$p(r,t) = p_0(r) + p_1(r,t)$$
$$\rho(r,t) = \rho_0(r) + \rho_1(r,t)$$
$$\Phi_N(r,t) = \Phi_{N0}(r) + \Phi_{N1}(r,t)$$
$$\phi(r,t) = \phi_0(r) + \phi_1(r,t)$$
$$\zeta \equiv \frac{\delta r}{r}$$

zeroth order

$$\frac{\mathrm{d}}{\mathrm{d}r}\left(r^2\frac{\Gamma_0 p_0}{\rho_0^2}\frac{\mathrm{d}\rho_0}{\mathrm{d}r}\right) = -4\pi G r^2\rho_0 - r^2\frac{\beta}{M_{\mathrm{pl}}}V'(\phi_0) - \frac{\beta^2}{M_{\mathrm{pl}}^2}r^2\rho_0$$
$$\frac{\mathrm{d}}{\mathrm{d}r}\left(r^2\frac{\mathrm{d}\phi_0}{\mathrm{d}r}\right) = r^2V'(\phi_0) + \frac{\beta}{M_{\mathrm{pl}}}r^2\rho_0$$

$$\Gamma_0 = \left.\frac{\mathrm{d}p}{\mathrm{d}\rho}\right|_{\rho=\rho_0, p=p_0}$$

first order

$$\rho_0\frac{\partial^2\zeta}{\partial t^2} = \frac{1}{r^4}\frac{\mathrm{d}}{\mathrm{d}r}\left(r^4\Gamma_0 p_0\frac{\partial\zeta}{\partial r}\right) + \left(\frac{1}{r}\frac{\mathrm{d}}{\mathrm{d}r}[3\Gamma_0 - 4)p_0] - \frac{2}{r}\frac{\beta}{M_{\mathrm{pl}}}\rho_0\frac{\mathrm{d}\phi_0}{\mathrm{d}r} - \frac{\beta}{M_{\mathrm{pl}}}\rho_0\frac{\mathrm{d}^2\phi_0}{\mathrm{d}r^2}\right)\zeta - \frac{\beta}{M_{\mathrm{pl}}}\rho_0\frac{1}{r}\frac{\partial\phi_1}{\partial r}$$

$$\frac{\partial^2\phi_1}{\partial t^2} = \frac{\partial^2\phi_1}{\partial r^2} + \frac{2}{r}\frac{\partial\phi_1}{\partial r} - m_0^2\phi_1 + \frac{\beta}{M_{\mathrm{pl}}}\frac{1}{r^2}\frac{\partial}{\partial r}\left(r^3\rho_0\zeta\right)$$

$$m_0^2 \equiv \left.\frac{\mathrm{d}^2V}{\mathrm{d}\phi^2}\right|_{\phi=\phi_0} + \frac{1}{M_{\mathrm{pl}}}\left.\frac{\mathrm{d}\beta}{\mathrm{d}\phi}\right|_{\phi=\phi_0}\rho_0\frac{\mathrm{d}\phi_0}{\mathrm{d}r}$$

Equation of state

$$p = K\rho^\gamma$$

chameleon model

$$V(\phi) = V_0/\phi^m,\ \beta(\phi) = \mathrm{const}$$

Eigen value problem $\boxed{\text{negative eigen value→instable mode}}$

We solve these equations numerically by shooting method.
We found there is parameter region where imaginary frequency (=negative eigen value) modes are obtained.
For well screened objects, the equations becomes much simpler.
We can assume

$$m_0^2\phi_1 \sim \frac{\beta}{M_{\mathrm{pl}}}\frac{1}{r^2}\frac{\partial}{\partial r}\left(r^3\rho_0\zeta\right)$$

Using dimensionless variables,

$$\omega^2\zeta = -\frac{1}{\theta^n x^4}\frac{\mathrm{d}}{\mathrm{d}\xi}\left\{\left(\gamma\theta^{n+1} - \alpha\theta^{2n}\right)\xi^4\frac{\mathrm{d}\zeta}{\mathrm{d}\xi}\right\} - \left\{(3\gamma-4)(n+1)\frac{1}{\xi}\frac{\mathrm{d}\theta}{\mathrm{d}\xi} - n\alpha\left(3\frac{1}{\xi}\frac{\mathrm{d}\theta}{\mathrm{d}\xi} + \theta^{n-1}\frac{\mathrm{d}^2\theta}{\mathrm{d}\xi^2} + (n-1)\left(\frac{\mathrm{d}\theta}{\mathrm{d}\xi}\right)^2\right)\right\}\zeta$$

$$\left(\xi \equiv r/R,\ \rho_0 = \rho_c\theta^n(\xi),\ p_0 = p_c\theta^{n+1},\ \gamma = 1 + 1/n\right)$$

$$\alpha \equiv \frac{n}{m+1}\frac{\rho_c}{p_c}\frac{\beta\phi_c}{M_{\mathrm{pl}}}$$

If $p_c \sim \dfrac{2GM^2}{\pi R^4}$,

$\Longrightarrow\ \alpha \sim 1/(m_c^2R^2)$: small

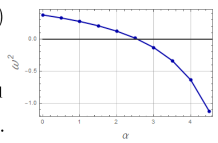

Instability does not occur in linear level.

Conclusions

- We investigate the instability of a star in screened modified gravity.
- We found the coupling between the perturbation of matter and scalar field may leads instability.
- However, the instability happens in only a limited parameter region and it is not the realistic region.
- As we write in the motivation, non-linear effect is significant.

Bibliography

1. **A. Joyce, B. Jain, J. Khoury, and M. Trodden, Phys. Rept. 568, 1 (2015)**
2. **T. Nakamura, T. Ikeda, R. Saito and C. M. Yoo, arXiv:1804.05485**
3. **J. Sakstein, Phys. Rev. D 88, 124013 (2013)**

Hirotaka Yoshino
Osaka City University

"Improved analysis of axion bosenova"

[JGRG28 (2018) PA17]

Improved Analysis
of
Axion Bosenova

Hirotaka Yoshino (Osaka City University)

Hideo Kodama (YITP)

JGRG28 @ Rikkyo University
Nov. 6—7, 2018

AXIVERSE SCENARIO

Arvanitaki, Dimopoulos, Dubvosky, Kaloper, March-Russel, PRD81 (2010), 123530.

- String axions
  - In string theory, many moduli appear when the extra dimensions get compactified.
  - Some of them (10-100) are expected to behave like scalar fields with very tiny mass, which are called string axions.

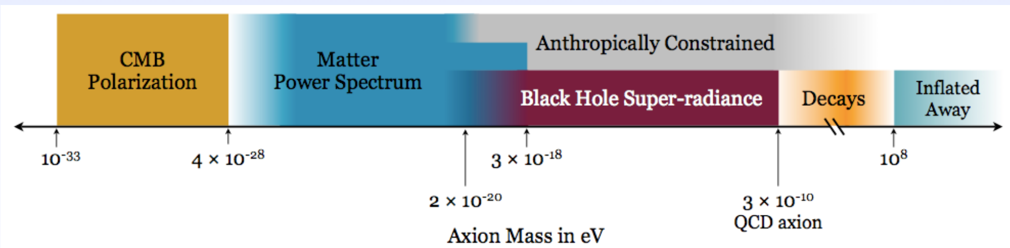

$$\mathcal{L} = -\frac{1}{2}\left(\nabla_a\Phi\nabla^a\Phi + V(\Phi)\right) - \frac{1}{4}g_{a\gamma\gamma}\Phi F_{ab}{}^{*}F^{ab} + \cdots$$

$$V = f_a^2\mu^2[1-\cos(\Phi/f_a)]$$

Energy extraction from a Kerr BH

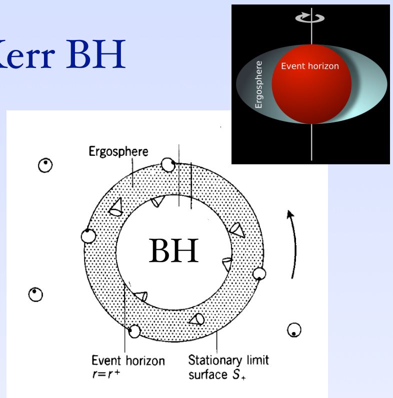

- Metric

$$ds^2 = -\left(\frac{\Delta - a^2\sin^2\theta}{\Sigma}\right)dt^2 - \frac{2a\sin^2\theta(r^2+a^2-\Delta)}{\Sigma}dtd\phi$$
$$+\left[\frac{(r^2+a^2)^2 - \Delta a^2\sin^2\theta}{\Sigma}\right]\sin^2\theta d\phi^2 + \frac{\Sigma}{\Delta}dr^2 + \Sigma d\theta^2$$

- BH's rotational energy

$$M_{\rm rot} = M - M_{\rm irr}$$
$$M_{\rm irr} = \sqrt{\frac{A_H}{16\pi}}$$

- Energy extraction

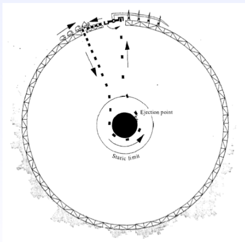

Penrose process

$\Phi = \mathrm{Re}[e^{-i\omega t}R(r)S(\theta)e^{im\phi}]$

Superradiant condition:

$\omega < \Omega_H m$

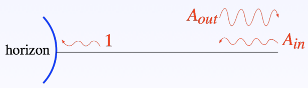

Superradiance

Gravitational Atom

- Massive Klein-Gordon field $\quad \nabla^2\Phi - \mu^2\Phi = 0$

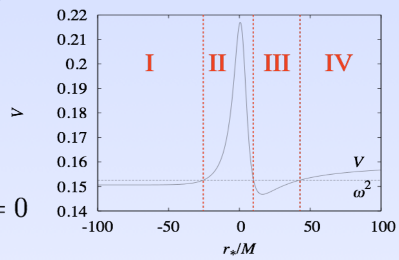

$$\Phi = \mathrm{Re}[e^{-i\omega t}R(r)S(\theta)e^{im\phi}]$$

$$R = \frac{u}{\sqrt{r^2+a^2}} \quad \Rightarrow \quad \frac{d^2u}{dr_*^2} + \left[\omega^2 - V(\omega)\right]u = 0$$

$\omega = \omega_R + i\,\boxed{\omega_I}$ ← Unstable if positive

- Growth rate HY and Kodama, arXiv:1505.00714.

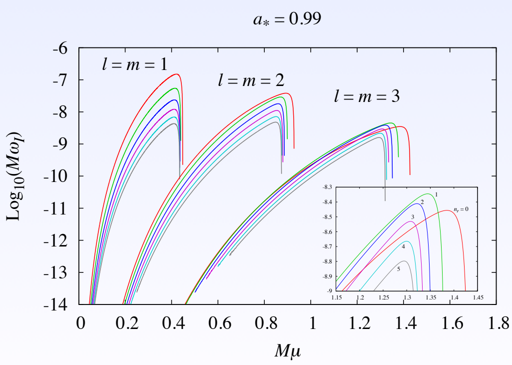

Wavefunctions

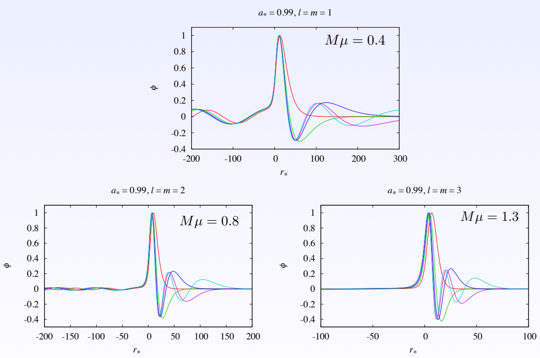

Issues to be explored

- String axion field forms an axion cloud around a rotating astrophysical BH by extracting BH's rotation energy.

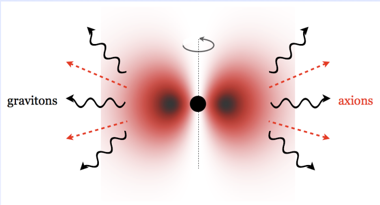

- Superradiant instability
- Nonlinear self-interaction

$$\nabla^2\varphi - \mu^2 \sin\varphi = 0 \qquad \varphi \equiv \frac{\Phi}{f_a}$$

- GW emission
- Long-term evolution of BH parameters

- Simulation:
  - Scalar field

    We have codes that are sufficiently satisfactory.

    But recently, we added improvement on the treatement of the outer boundary..

  - Gravitational waves

    We solve Teukolsky equation in time domain:

$$\left[\frac{(r^2+a^2)^2}{\Delta} - a^2\sin^2\theta\right]\frac{\partial^2\psi}{\partial t^2} + \frac{4Mar}{\Delta}\frac{\partial^2\psi}{\partial t\partial\phi} + \left[\frac{a^2}{\Delta} - \frac{1}{\sin^2\theta}\right]\frac{\partial^2\psi}{\partial\phi^2}$$
$$-\Delta^{-s}\frac{\partial}{\partial r}\left(\Delta^{s+1}\frac{d\psi}{dr}\right) - \frac{1}{\sin\theta}\frac{\partial}{\partial\theta}\left(\sin\theta\frac{\partial\psi}{\partial\theta}\right) - 2s\left[\frac{a(r-M)}{\Delta} + \frac{i\cos\theta}{\sin^2\theta}\right]\frac{\partial\psi}{\partial\phi}$$
$$-2s\left[\frac{M(r^2-a^2)}{\Delta} - r - ia\cos\theta\right]\frac{\partial\psi}{\partial t} + (s^2\cot^2\theta - s)\psi = 4\pi\Sigma T$$

    We have completed the Schwarzschild case.
    A code for a Kerr spacetime is beginning to work.

Improvement of scalar field code

- Outer boundary
  - Previously, we imposed the fixed boundary condition at the boundary.
  - This is because it is difficult to impose outgoing boundary condition in the massive case (there are modes with various velocities!)
  - But there exists reflected waves, and they might have helped the occurrence of the bosenova.
- Improved method

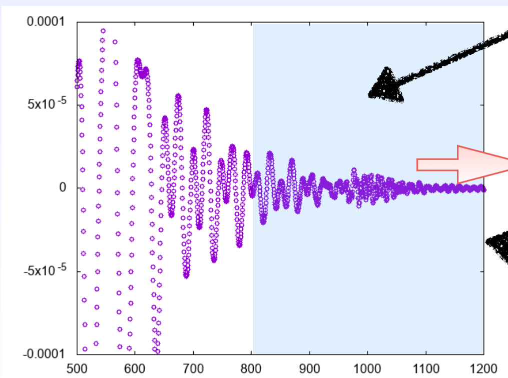

We gradually change the scalar field mass as

$$\mu' = \mu\cos\left[\frac{\pi}{2}\left(\frac{r_* - 800M}{400M}\right)^2\right]$$

works well!

Here, we impose the outgoing BC for massless field.

Current obtained results

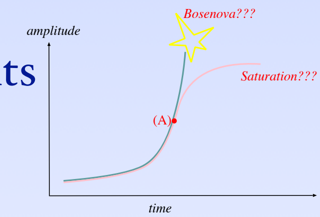

- l = m = 1 mode

$M\mu \lesssim 0.3$ Energy extraction from the BH may stop, and gradually positive energy may fall from scalar cloud.

$M\mu \gtrsim 0.4$ Energy continues to be extracted from the BH.

Require modification from HY and Kodama, CQG32, 214001 (2015)
HY and Kodama, PTP128, 153 (2012)

- l = m = 2 mode

Energy continues to be extracted from the BH.

No modification from HY and Kodama, CQG32, 214001 (2015)

l = m = 2 mode (1)

- Setup

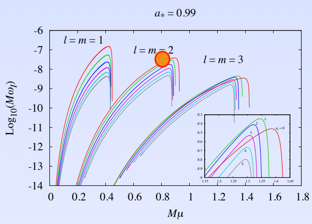

- Kerr black hole $a_* = 0.99$
- $M\mu = 0.8$
- Scalar field
  - The case where (the initial amplitude) $= 1.0$

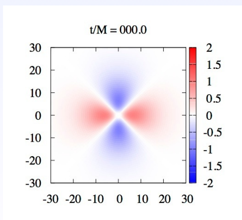

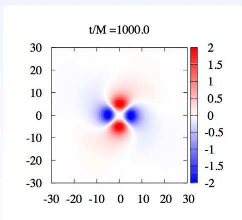

- Energy and angular momentum are continue to be extracted:

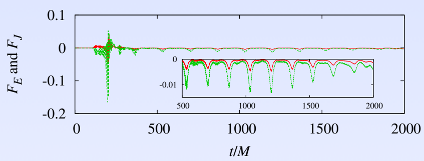

- Energy and angular momentum are continue to be emitted to distant place:

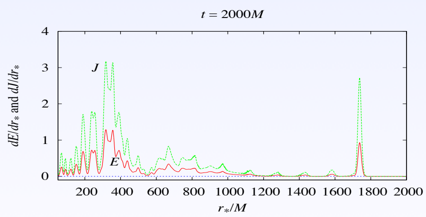

l = m = 2 mode (2)

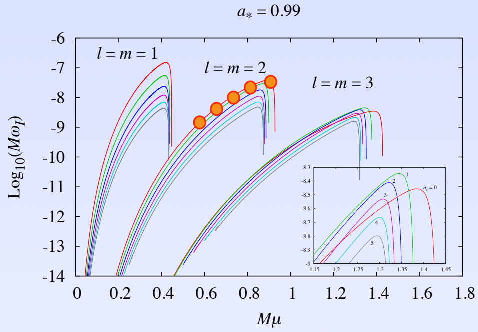

- Growth of the superradiant instability saturates at the energy

$M\mu$	0.5	0.6	0.7	0.8	0.9
$\frac{E}{[(f_a/M_p)^2 M]}$	3245(?)	2150(?)	1863	1550	935

(PRELIMINARY)

l = m = 2 mode (3) (Appendix)

- Emitted Gravitational Waves

Observation point
$r_* = 200M$

(PRELIMINARY)

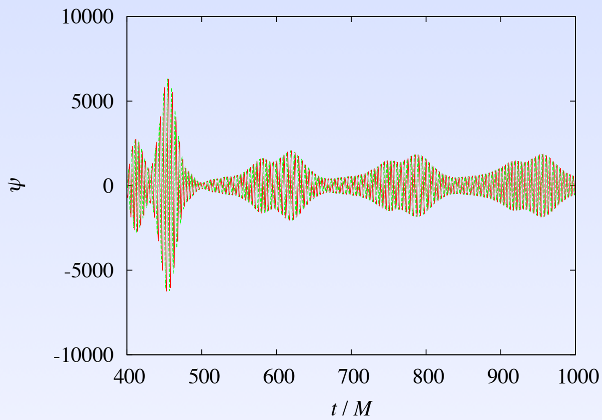

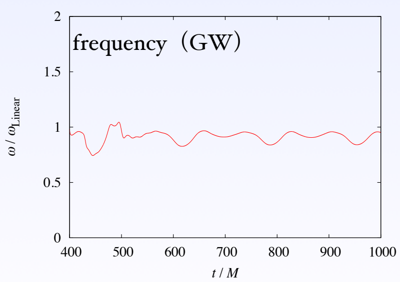

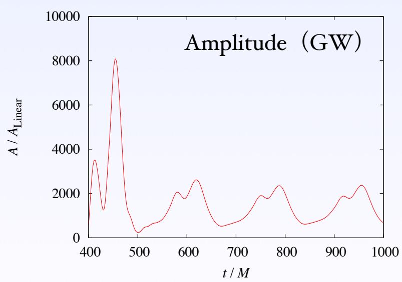

l = m = 1 mode, $M\mu$=0.4 (1)

- Setup
  - Kerr black hole $\quad a_* = 0.99$
  - $M\mu = 0.4$
  - Scalar field
    - Simulation (A): (Initial amplitude) $=$ 0.6
    - Simulation (B):

We adopt the scale transformed data for the results of (A) at t=1000M

$$\varphi^{(B)}(t=0) = C\varphi^{(A)}(t=1000M)$$
$$\dot{\varphi}^{(B)}(t=0) = C\dot{\varphi}^{(A)}(t=1000M)$$

for the results of (A) at t=1000M with C=1.09.

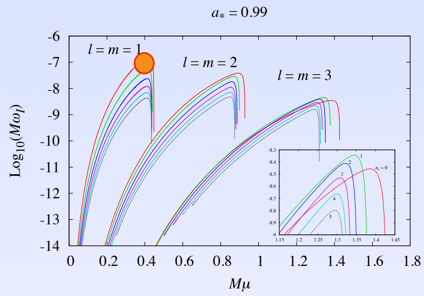

- We calculate gravitational waves of m = 2 mode

l = m = 1 mode, $M\mu$=0.4 (2)

φ

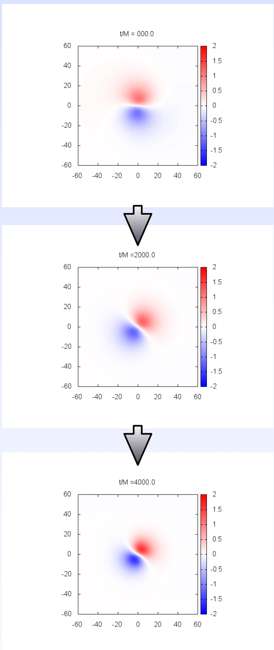

- The superradiant instability continues.

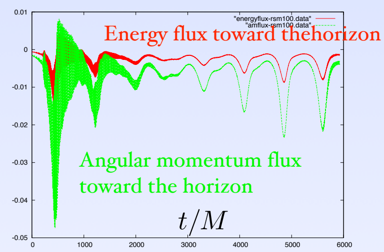

- Total energy in the region $\quad -200M \leq r_* \leq 400M$

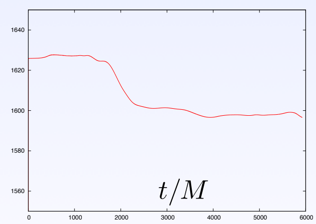

Final state of the axion cloud may extract energy from the BH and emit it to the distant place

(PRELIMINARY)

l = m = 1 mode, $M\mu$=0.3 (1)

- Setup

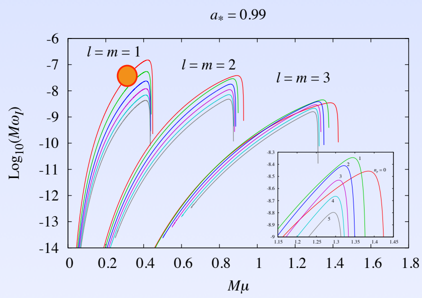

  - Kerr BH $\quad a_* = 0.99$
  - $M\mu = 0.3$

  - As an initial condition
    - Simulation (A): (initial amplitude) = 0.3
    - Simulation (B):

Perform a scale transformation

$$\varphi^{(\mathrm{B})}(t=0) = C\varphi^{(\mathrm{A})}(t=1000M)$$
$$\dot{\varphi}^{(\mathrm{B})}(t=0) = C\dot{\varphi}^{(\mathrm{A})}(t=1000M)$$

to the result of simulation (A) with
C=1.08, 1.07, 1.06, 1.05, 1.04.

l = m = 1 mode, $\quad M\mu$=0.3 (2)

- Energy flux toward the horizon

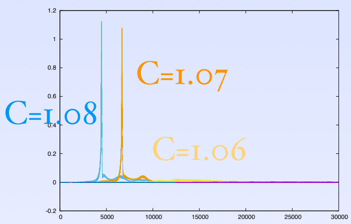

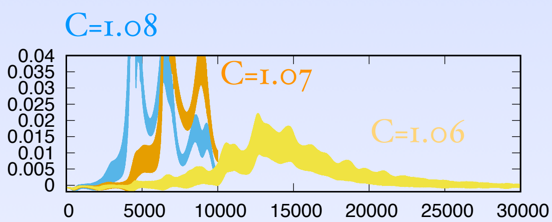

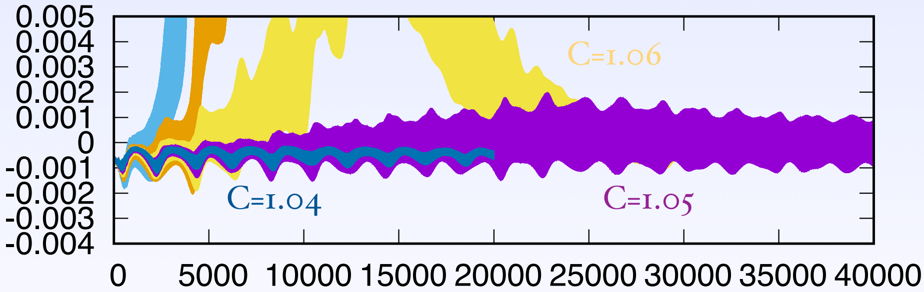

Superradiant instability stops. (PRELIMINARY)

l = m = 1 mode, $M\mu$=0.3 (3)

- Total energy in the C=1.04 and C=1.05 cases

Total energy in the domains $\begin{cases} -100 \leq r_*/M \leq 300 \\ -100 \leq r_*/M \leq 200 \\ -100 \leq r_*/M \leq 100 \end{cases}$

C=1.04 | C=1.05

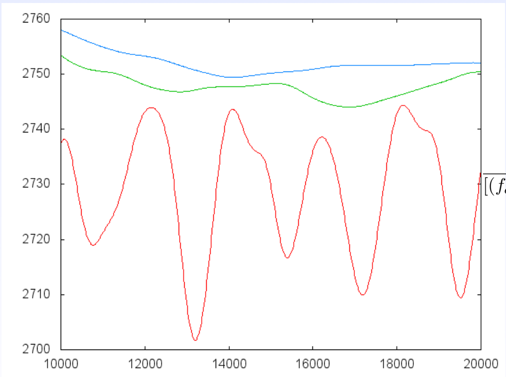

$\frac{E}{[(f_a/M_p)^2 M]}$

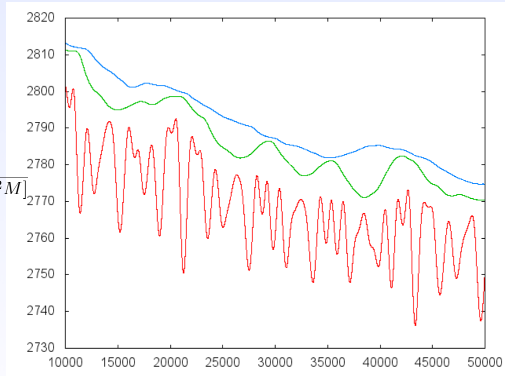

t/M | t/M

Thank you!

Sousuke Noda
Yukawa Institute for Theoretical Physics, Kyoto University

“Optical Berry phase in the gravitational lensing by Kerr black hole”

[JGRG28 (2018) PA18]

Optical Berry phase in gravitational lensing by a Kerr black hole

Sousuke Noda, Marcus Werner (Yukawa Institute for Theoretical Physics, Kyoto University)

Abstract

Chiao and Wu (1986) suggested the optical analogue of the Berry phase for polarization of light, and Tomita and Chiao (1986) observed experimentally the geometrical phase for light rays propagating in an optical fiber for which initial and final directions are identical. The geometrical interpretation of the optical Berry phase was discussed by Segert (1987) and Ryder (1991). According to them, the optical Berry phase can be understood as a classical effect by considering the orbit of light ray in the three dimensional Euclidean space. In this poster, we will try to generalize this for light rays in the Kerr spacetime.

What is the optical Berry phase?

○ **Berry phase in Quantum Mechanics**

The geometrical phase ∝ solid angle

$$|\vec{\sigma}(t_f)\rangle = e^{i\gamma(C)}|\vec{\sigma}(t_i)\rangle, \quad \vec{\sigma}(t_i) = \vec{\sigma}(t_f)$$

geometrical phase

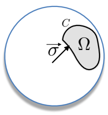

$$\gamma(C) \propto \Omega(C)$$

○ **Optical Berry phase** (Chiao and Wu 1986)

- Linearly polarized light propagating in an optical fiber.
- Directions of both ends of the optical fiber are identical.
- We can understand this at the classical level.

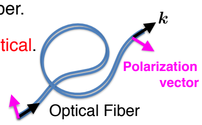

Optical Berry phase

= geometrical phase due to the rotation of polarization vector

Optical Berry phase in the Kerr spacetime

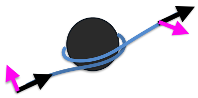

The Polarization vector can rotate due to the black hole's spin

= Gravitational Faraday rotation

(Ishihara and Takahashi 1988)

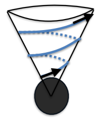

For the initial and final directions of a light ray to be identical, the light ray needs to loop around BH's spin axis.

Optical Berry phase in the Kerr spacetime

~ photon sphere, principal null geodesics

Optical Berry phase in Euclidean space

○ **Setup**

Segert (1987), Ryder (1991)

tangent vector

$$\boldsymbol{k} = \frac{d\boldsymbol{x}}{d\ell}, \quad \boldsymbol{x} \in \text{optical fiber}$$

orthonormal basis

$$(\boldsymbol{k}, \boldsymbol{n}, \boldsymbol{b})$$

geodesic curvature and torsion

$$\frac{d\boldsymbol{k}}{d\ell} = \kappa_g(\ell)\boldsymbol{n}, \quad \frac{d\boldsymbol{b}}{d\ell} = -\tau(\ell)\boldsymbol{n}$$

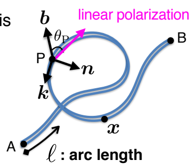

○ **Calculating the rotation of the polarization vector**

We consider the rotation of the polarization plane between two points on the fiber.

$P(\ell_P)$, $Q(\ell_P + d\ell)$

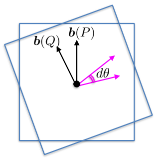

$d\theta$ = angle between $\boldsymbol{b}(P)$ and $\boldsymbol{b}(Q)$ $= -\tau(\ell)d\ell$

From A to B, the change of polarization vector $\Delta\theta$ is

$$\Delta\theta = -\int_A^B \tau(\ell)d\ell = \int_A^B \frac{1}{\kappa_g^2}\boldsymbol{k}\cdot\left(\frac{d\boldsymbol{k}}{d\ell}\times\frac{d^2\boldsymbol{k}}{d\ell^2}\right).$$

○ **Analysis in momentum space**

E_{ij} :Euclidean metric

Since $\boldsymbol{k}$ is normalized as $E_{ij}k^ik^j = 1$, its tip lives on a sphere in the momentum space. This means that we can define the following map at each point on the optical fiber :

$$\boldsymbol{x} \longmapsto \boldsymbol{y} \text{ (tip of } \boldsymbol{k}\text{)},$$

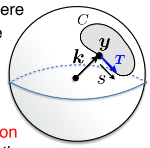

where $\boldsymbol{y}$ is a point on the sphere in the momentum space, and the radius of the sphere does '***not***' depend on the position on the fiber $\boldsymbol{x}$. Moreover, as the initial and final directions of the fiber are identical, $\boldsymbol{y}$ (tip of $\boldsymbol{k}$) traces out a closed curve (C) on the surface.

We define the tangent vector to C as $\boldsymbol{T} = d\boldsymbol{y}/ds$ and represent $\Delta\theta$ in terms of $\boldsymbol{y}$.

$$\Delta\theta = -\oint_C \boldsymbol{y}\cdot\left(\frac{d\boldsymbol{y}}{ds}\times\frac{d^2\boldsymbol{y}}{ds^2}\right)ds$$

$$= -\oint_C \kappa_C\, ds$$

geodesic curvature of C

Gauss-Bonnet theorem

$$\oint_C \kappa_C = 2\pi - \iint \mathcal{K}dA$$

$$\boxed{\Delta\theta = \iint \mathcal{K}dA - 2\pi}$$

→ Solid angle

Optical Berry phase = solid angle on a sphere in momentum space.

Optical Berry phase in the Kerr spacetime

○ **Slowly rotating Kerr BH in the quasi-isotropic coordinates** (t, ρ, θ, ϕ)

$$ds^2 = -\frac{\Delta}{\psi^2\rho^2}dt^2 - \frac{4Ma\sin^2\theta}{\psi\rho}d\phi dt + \psi^2\left[(d\rho^2 + \rho^2 d\theta^2) + \rho^2\sin^2\theta d\phi^2\right]$$

$$\psi = (1 + M/2\rho)^2$$
$$\Delta = (\psi\rho)^2 - 2M\psi\rho$$

From the null condition $ds = 0$, we get

$$dt = \sqrt{\gamma_{ij}dx^idx^j} + \beta_i dx^i, \quad \gamma_{ij} = \frac{\psi^4\rho^2}{\Delta}E_{ij}$$

conformally Euclidean

For fixed A and B, Fermat's principle gives a 3-dimensional curve.

c.f Asada & Kasai (2000)

$$\delta\int_A^B dt = 0 \longrightarrow \nabla^{(3)}_{\boldsymbol{k}}\boldsymbol{k} = \kappa_g\boldsymbol{n},$$

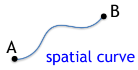

where ℓ is the arc length defined by $d\ell^2 = \gamma_{ij}dx^idx^j$.

Null geodesics in 4d spacetime $(\kappa_g = 0)$ ⟶ Curve in 3d space $(\kappa_g \neq 0)$

○ **Conformal transformation to a model space and optical Berry phase**

$\boldsymbol{k}$ is the tangent vector of which components are defined as $k^i = dx^i/d\ell$, but it is not normalized since γ_{ij} is conformally Euclidean metric: $\gamma_{ij}(\rho)k^ik^j = 1$.

Although we can define the map to the momentum space at each point on the spatial curve (light ray), the radii of the spheres in the momentum space '***do***' depend on the radial coordinate (ρ) due to the conformal factor $\psi^4\rho^2/\Delta$.

Therefore, we obtain a ***open*** curve (C) spanning the multiple different size spheres even for the case that the initial and final directions of the light ray are identical.

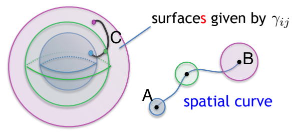

Observable in real space?

Conformal transformation :

$$d\ell^2 \longrightarrow d\ell^2 = E_{ij}dX^idX^j$$

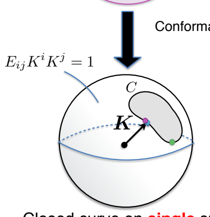

Closed curve on **single** sphere

$$\boldsymbol{K}_A = \boldsymbol{K}_B \longrightarrow$$
$$(\boldsymbol{k}_A = \boldsymbol{k}_B)$$

$$\boxed{\Delta\theta = \iint \mathcal{K}dA - 2\pi}$$

Possible only for looping orbit?

e.g.) photon sphere, principal null geodesics

Summary

1. Optical Berry phase (due to the rotation of the polarization vector) has been observed for light propagating in an optical fiber for which the initial and final directions are identical. $\boldsymbol{k}_A = \boldsymbol{k}_B$
2. This geometrical phase can be understood as a classical effect, and it corresponds to the solid angle on a sphere in the momentum space.
3. Similar situations may be found for light rays in the Kerr spacetime.

   e.g.) photon sphere, principal null geodesics

Questions

1. What is the signature of this phase in an observation?
2. Fixed point of a lensing map ?

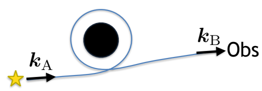

Position of a lensed image

=

Position of a source

3. General spin parameter case

~~conformally Euclidean~~

Tomohiro Harada
Department of Physics, Rikkyo University

"Uniqueness of static, isotropic low-pressure solutions of the Einstein-Vlasov system"

[JGRG28 (2018) PA20]

Uniqueness of static, isotropuc low-pressure solutions of the Einstein-Vlasov system

Tomohiro Harada (Department of Physics, Rikkyo University)

5-9/11/2018 JGRG28@Rikkyo. This presentation is based on Ref. [1].

Introduction

- Beig and Simon (1992) [2] prove that a static solution in the Einstein-Euler (or perfect-fluid) system is spherically symmetric and uniquely determined by the surface potential of the fluid body under certain circumstances.
- The Einstein-Vlasov system consists of infinitely many collisionless particles of infinitesimal mass which follow along geodesics in the background spacetime which is sourced by the stress-energy tensor of the ensemble of the collisionless particles, where we assume all particles have the same mass m.

Beig and Simon's theorem

- Metric
$$g = -V^2\left(x^1, x^2, x^3\right)dt^2 + \gamma_{ab}\left(x^1, x^2, x^3\right)dx^a dx^b, \tag{1}$$
where $V \in C^1$ and γ_{ab} is the Riemannian metric.
- Barotropic EOS: $\varrho = \varrho(p)$ with $d\varrho/dp \geq 0$. We define
$$I = \frac{1}{5}\kappa^2 + 2\kappa + (\varrho + p)\frac{d\kappa}{dp}, \quad \text{where} \quad \kappa = \frac{\varrho + p}{\varrho + 3p}\frac{d\varrho}{dp}. \tag{2}$$
- Theorem (Beig & Simon 1992) [2]
Assume we are given a static perfect fluid model with an EOS satisfying $I \leq 0$, and a spherically symmetric solution. Then the given model and the spherically symmetric solution are isometric.

Vlasov matter

- Mass shell: 7 dimensional submanifold
$$P_m = \{(x, p) \in T\mathscr{M} \,:\, g_{\mu\nu}(x)p^\mu p^\nu = -m^2,\ p \text{ future directed}\}. \tag{3}$$
- Distribution function: $f \in C^1(P_m; \mathbb{R})$
- Vlasov equation (geodesic equation)
$$p^\mu \frac{\partial}{\partial x^\mu} f - \Gamma^i_{\nu\lambda} p^\nu p^\lambda \frac{\partial}{\partial p^i} f = 0. \tag{4}$$
- Stress-energy tensor
$$T^{\mu\nu}(x^\sigma) = \frac{1}{m}\int_{P_{(m,x)}} f(x^\sigma, \mathbf{p}) p^\mu p^\nu \mu_{P_{(m,x)}}, \tag{5}$$
where $P_{(m,x)}$ is the fibre of P_m and $\mu_{P_{(m,x)}}$ is the volume form on it.

Isotropic Einstein-Vlasov system

- Tetrad: $\{e_{(A)}\}$ $(A = 0, 1, 2, 3)$, $p^\mu \partial_{x^\mu} = v^{(A)} e_{(A)}$
- Isotropic distribution function
$f \in C^1(P_m; \mathbb{R})$ is called isotropic if there exist a tetrad basis $\{e_{(A)}\}$ $(A = 0, 1, 2, 3)$ and a function $F : \mathbb{R}^4 \times \mathbb{R}_+ \to \mathbb{R}_+$ such that
$$f(x, \mathbf{p}) = F(x, v), \quad v^2 = \delta_{IJ} v^{(I)} v^{(J)}, \quad (I, J = 1, 2, 3), \tag{6}$$
for all $(x, \mathbf{v}) \in P_m$.
- Equivalence to a perfect fluid
Let F satisfy
$$F(x, v) = \mathcal{O}(v^{-4-\epsilon}), \quad \epsilon > 0. \tag{7}$$
Further let
$$\varrho(x) := 4\pi \int_0^\infty F(x, v) v^2 \sqrt{m^2 + v^2}\, dv, \tag{8}$$
$$p(x) := \frac{4\pi}{3}\int_0^\infty F(x, v) \frac{v^4}{\sqrt{m^2 + v^2}} dv. \tag{9}$$
Then $T^{\mu\nu}$ takes the form
$$T^{\mu\nu} = \varrho u^\mu u^\nu + p\left(u^\mu u^\nu + g^{\mu\nu}\right), \tag{10}$$
where $u(x) := e_{(0)}\big|_x = e^\mu_{(0)}\big|_x \partial_{x^\mu}$ is a timelike unit vector field.
- Energy as a conserved quantity: ϕ
$$F(\mathbf{x}, v) = \Phi(E(\mathbf{x}, v)) =: \phi\left(1 - \frac{E(\mathbf{x}, v)}{E_0}\right). \tag{11}$$

Uniqueness theorem

- Assumption: The energy cutoff be *not too smooth*.
$\phi : (-\infty, 1] \to \mathbb{R}_+$ is an analytic function on $[0, 1]$, $\phi(x) = 0$ if $x < 0$, and that $\exists n \in \mathbb{N}$: $\quad \phi'(+0) = \cdots = \phi^{(n-1)}(+0) = 0, \ \ \phi^{(n)}(+0) > 0$.
- Theorem
Let $E_0 > 0$ and $n \leq 3$. Then, there exists $p_0 > 0$ such that if $\sup_{x \in \Sigma} p(x) \leq p_0$, the model is spherically symmetric and the unique solution determined by ϕ and E_0.
- We omit the proof. If interested, please look at Ref. [1].

Physically interesting limits

- Ultrarelativiastic limit and massless case
The EOS for radiation fluid, $\varrho(p) = 3p$, is recovered. One obtains $I(p) = \frac{24}{5} > 0$ and the Beig-Simon theorem cannot be applied.
- Low-pressure limit
We assume that $\phi(x) = 0$ for $x < 0$ and $\lim_{x \to +0} x^{-n}\phi(x) = C > 0$ for $n \geq 0$, where n is not necessarily integer. If $V < E_0$ and V is sufficiently close to E_0, we obtain the polytropic EOS $p \approx K\rho^\gamma$, where $\gamma = (2n + 5)/(2n + 3)$ and K is a positive constant determined by n and C, and
$$I \approx -\frac{5\gamma - 6}{5\gamma^2} K^{-2\gamma^{-1}} p^{2(1-\gamma)/\gamma}, \tag{12}$$
Therefore, the Beig-Simon theorem applies for $\gamma > 6/5$ or $0 \leq n < 7/2$.

Example: Step-function distribution

- Distribution function: $F(\mathbf{x}, v) = \Phi(E) = \Theta(E_0 - E)$.
We can obtain $\rho(V)$, $p(V)$, $p(\rho)$ and $I(V)$, analytically.

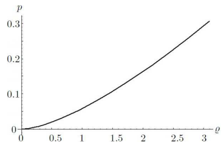

Figure: Plot of $p(\rho)$ for $E_0 = 0.9$.

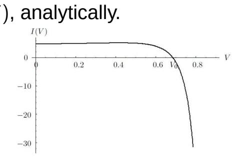

Figure: Plot of $I(V)$ for $E_0 = 0.9$. For each E_0, $I(V)$ has one zero denoted as $V_0(E_0)$.

- Numerical integration of the TOV eq.
There exists a unique spherically symmetric solution for a given E_0 if $V > V_0(E_0)$, while uniqueness may break down in the other regime.

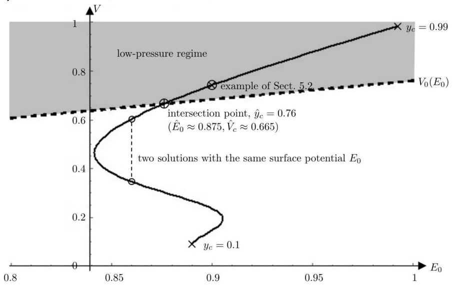

Figure: (E_0, V_0) lie on the dashed line. The solid line represents a succession of (E_0, V_c) obtained by integrating the TOV eq.

Summary

1. **The Vlasov matter reduces to a perfect fluid if the distribution function is isotropic in momentum space.**
2. **A static solution of the Einstein-Vlasov system with isotropic distribution function is necessarily spherically symmetric and unique for a given surface potential provided that the pressure is sufficiently low and the energy cutoff of the distribution function is *not too smooth*.**
3. **For a shallow potential and isotropic distribution function $F(E)$ with $F = 0$ for $E > E_0$ and $F \simeq C(E_0 - E)^n$ near the cutoff E_0, the EOS becomes polytropic. The uniqueness holds for $0 \leq n < 7/2$.**
4. **We analytically and numerically investigated the case of a step-function distribution. There exists a unique spherically symmetric static solution for a shallow potential, while the uniqueness may break down if the regime of a deep potential is included.**

[1] T. Harada and M. Thaller, arXiv:1806.10539 [gr-qc].

[2] R. Beig and W. Simon, Comm. Math. Phys. **144** (1992) 373.

Hideki Ishihara
Osaka City University

“Particle acceleration by ion-acoustic solitons in plasma”

[JGRG28 (2018) PA22]

Particle acceleration by ion-acoustic solitons in plasma

H. Ishihara[1], K. Matsuno[1,2], M. Takahashi[3], S. Teramae[1]

[1]Osaka City University

[2]Osaka Butsuryo University

[3]Aichi University of Education

arXiv: 1807.10460

Introduction

High energy phenomena
in the Universe
⇒ Cosmic rays

Non-thermal energy spectrum
$N(E) \propto E^{-s}$ (s=2〜3)

✓ Fermi acceleration by shock wave is a major candidate.

➢ We propose
a new acceleration mechanism:
Particle acceleration by cylindrical / spherical ion-acoustic soliton in plasma

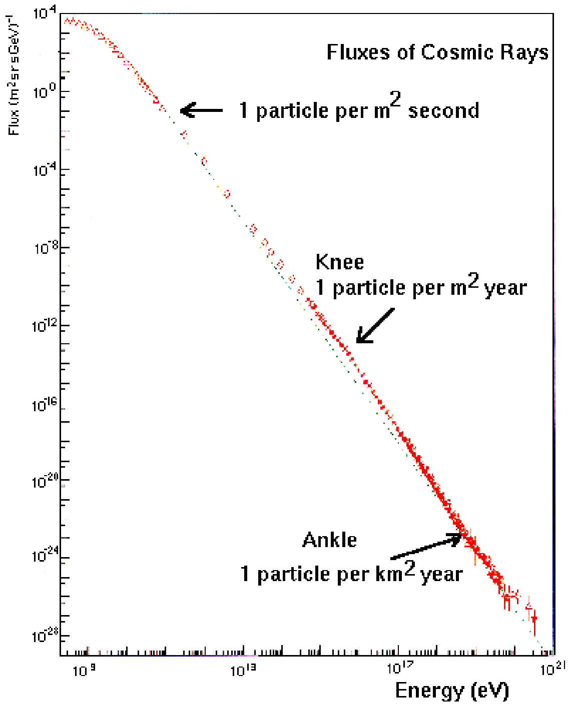

Particle acceleration by ion-acoustic soliton

✓ Acoustic soliton wave, described by cylindrical / spherical Kortweg-de Vries equation, grows in its wave height as wave shrinks to the center.

➢ Charged particles confined by electric potential accompanied with the shrinking wave get energy by reflections.

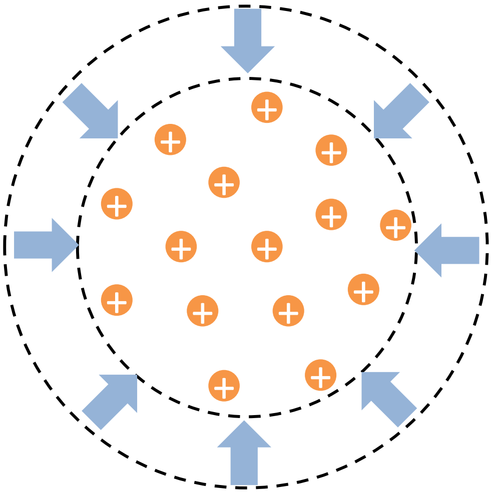

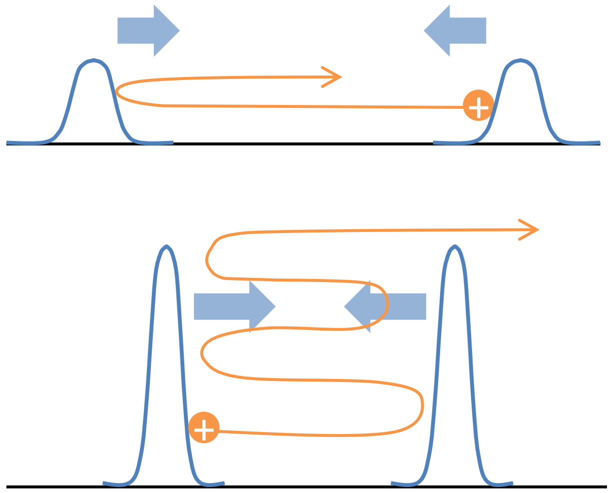

Ion-electron plasma system

$$Mn^{(i)}\left(\frac{\partial \boldsymbol{v}^{(i)}}{\partial t}+\left(\boldsymbol{v}^{(i)}\cdot\nabla\right)\boldsymbol{v}^{(i)}\right)=en^{(i)}\left(\boldsymbol{E}+\boldsymbol{v}^{(i)}\times\boldsymbol{B}\right)-\nabla P^{(i)}$$

$$\frac{\partial n^{(i)}}{\partial t}+\nabla\cdot\left(n^{(i)}\boldsymbol{v}^{(i)}\right)=0,\qquad \Delta\phi=-\frac{e}{\epsilon_0}\left(n^{(i)}-n^{(e)}\right)$$

M: ion mass, $n^{(i)}$, $\boldsymbol{v}^{(i)}$, $P^{(i)}$: number density, velocity, pressure of ion fluid
ϕ : electric potential, $n^{(e)}$: electron number density

✓ Assumption :

No magnetic field, Cold ion and hot electron fluids with cylindrical / spherical symmetry

✓ new variables : $\xi=\frac{\epsilon^{1/2}}{\lambda_D}(r+c_0t)\,,\qquad \tau=\frac{\epsilon^{3/2}}{\lambda_D}c_0t$ Debye length λ_D sound velocity c_0

✓ reductive perturbation :

$$\frac{e\phi}{k_BT^{(e)}}=\epsilon\phi_1+\epsilon^2\phi_2+\cdots\,,\qquad \frac{v^{(i)}}{c_0}=\epsilon v_1+\epsilon^2 v_2+\cdots$$

$$\frac{n^{(i)}}{n_0}=1+\epsilon n_1+\epsilon^2 n_2+\cdots$$

➢ We obtain $\Phi:=\phi_1=-v_1=n_1$

and Korteweg-de Vries (KdV) equation

Korteweg-de Vries equation

$$\frac{\partial\Phi}{\partial\tau} - \Phi\frac{\partial\Phi}{\partial\xi} - \frac{1}{2}\frac{\partial^3\Phi}{\partial\xi^3} + \gamma\frac{\Phi}{\tau} = 0$$

$$\gamma = \begin{cases} 0 & \text{(planar)} \\ 1/2 & \text{(cylindrical)} \\ 1 & \text{(spherical)} \end{cases}$$

$$\tau = \tau_0 \quad \longrightarrow \quad \tau = 0 \ (r = 0)$$

- Early time (large radius and τ): planar soliton like
- Late time (small radius and τ): the last term on l.h.s. becomes important

✓ Cylindrical / spherical soliton wave height grows in time

Evolution of wave form of soliton

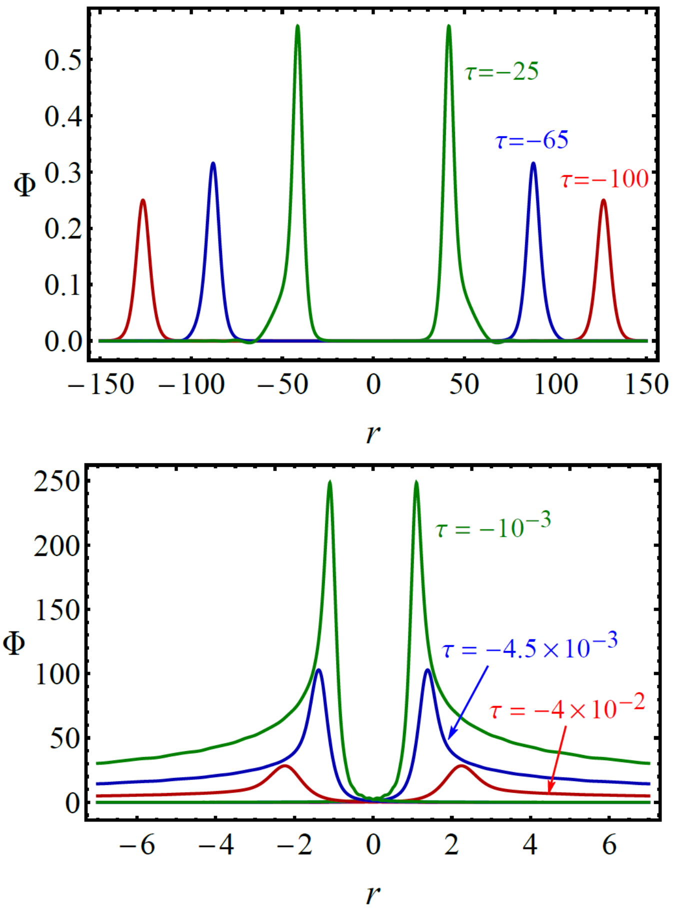

Cylindrical soliton (early stage)

Cylindrical soliton (final stage)

Time evolution of wave height

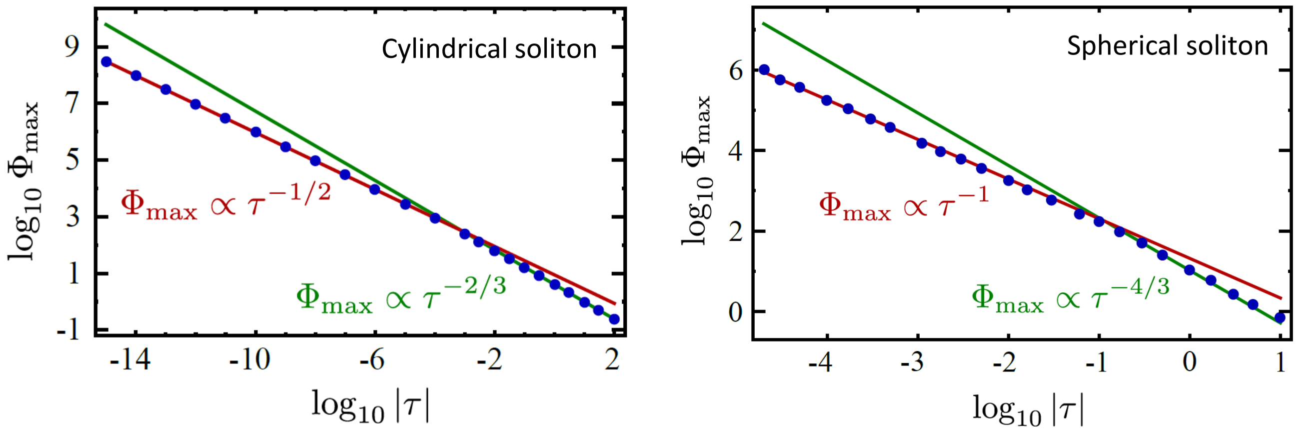

✓ growth rate of wave height is power law in time

- In order to simplify the system, we make a model where the cylindrical/spherical soliton is replaced by a thin shell wall

- We calculate test particle motion enclosed by the shrinking thin shell and obtain energy spectra of accelerated particles

Thin shell wall models

1. Shell wall: Initial radius r_0 of shell at initial time t_0 (<0), moves with sound velocity c_0 $\Rightarrow$ $r(t) = -c_0\, t$
2. Electric potential : $\Phi(t) = \Phi_0\,(t/t_0)^{-\alpha}$

   $\alpha = 1/2$, $2/3$: Cylindrical , $\alpha = 1$, $4/3$: Spherical
3. Final time: (Shell radius) = (Debye length) acceleration stops

A. Test charged particles: Elastic reflection by the moving shell wall

$\Rightarrow$ Particle velocity: $\boldsymbol{v} = (v_\perp,\ v_\parallel) \longrightarrow (-v_\perp - 2c_0,\ v_\parallel)$

B. Escaping particles: (Particle energy) > $\Phi(t)$

$\Rightarrow$ Particles escape to infinity

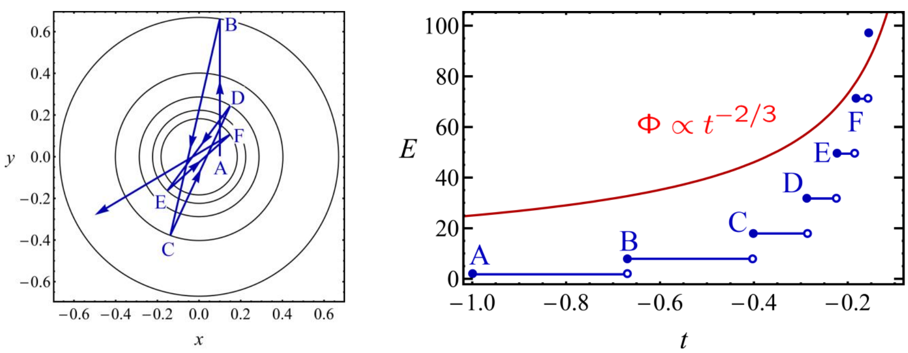

Energy spectra of output particles

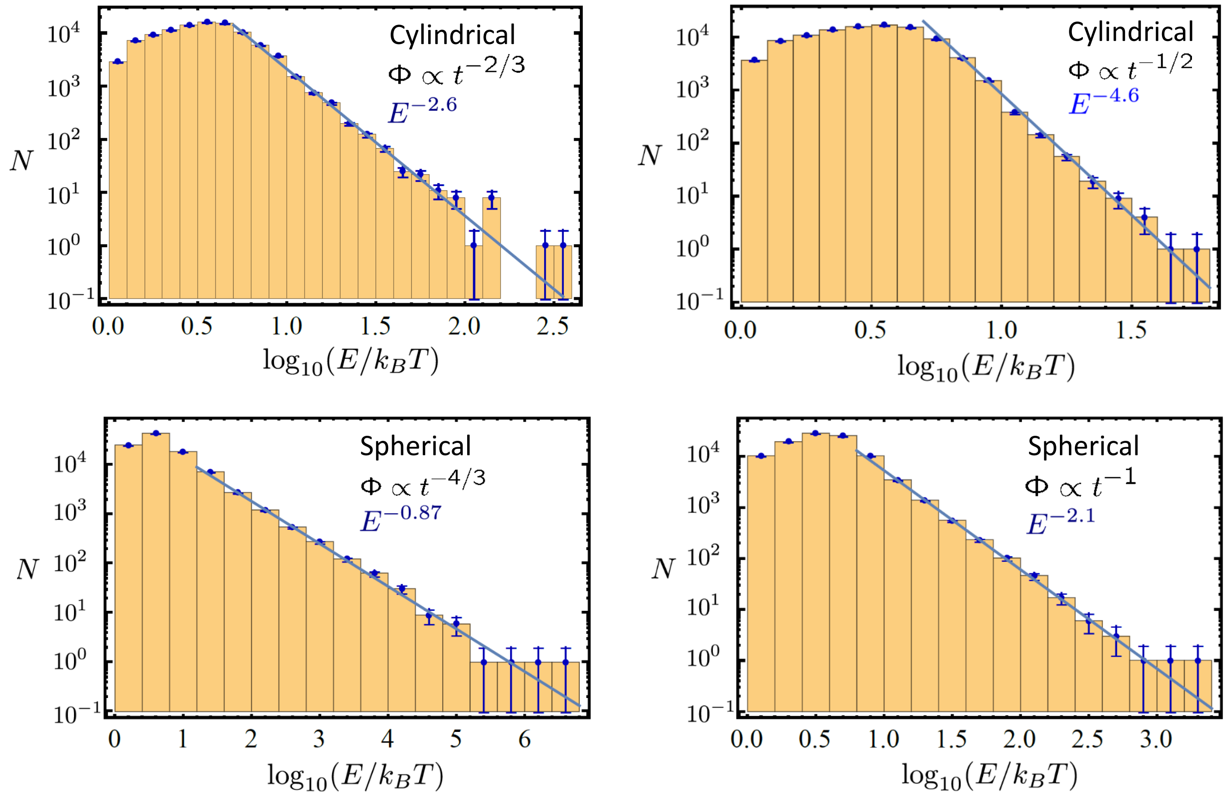

✓ Output energy does not depend on injection energy critically

Energy distribution of output particles

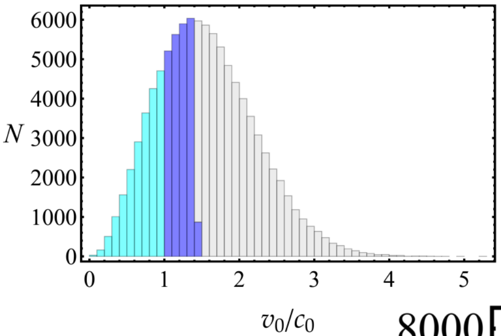

⇦ Initial : Maxwell distribution

✓ Particles with low initial energy are accelerated effectively !

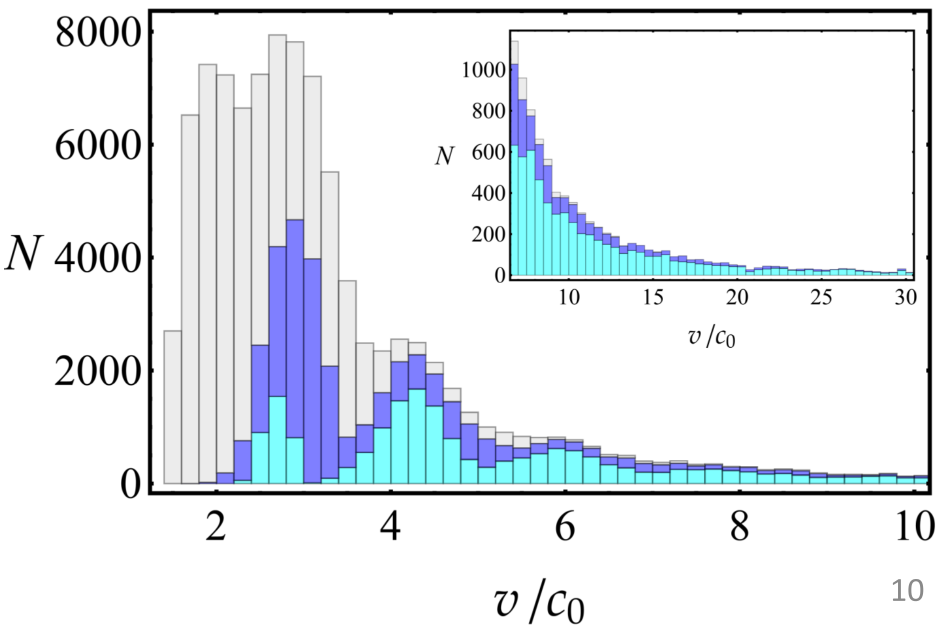

Summary

We propose a new acceleration mechanism for charged particles by using cylindrical / spherical solitons propagating in ion-electron plasma.

Electric potential grows with a power law in time as waves shrink.

⇩

We obtain power law spectra of energy for accelerated particles.

- We expect that the acceleration mechanism by solitons are applicable to cosmic rays associated with Solar flare, etc.

Application to Solar cosmic ray

✓ High energy protons with energy range MeV to GeV are observed when the solar are occurs.

✓ In magnetic reconnection region, a footpoint of the flare, magnetic field becomes negligibly small and solitons would be excited there.

We assume

temperature of solar plasma : 1 ∼ 100 eV
number density of electrons : $10^{15} \sim 10^{16}$ m^{-3}
Debye length λ_D : $10^{-4} \sim 10^{-3}$ m
initial wave radius (size of reconnection region) : $r_0 = 10^4$ m $= 10^7 \sim 10^8 \lambda_D$

If our model is applicable till the cylindrical or spherical shell wall shrinks to size of Debye length, maximum energy is estimated as

$$E_{\max} \approx \Phi_0 \left(\frac{t_f}{t_0}\right)^{-4/3} = k_B T^{(e)} \left(\frac{r_0}{\lambda_D}\right)^{4/3} \approx 2\ \text{GeV} \sim 5\ \text{TeV}$$

Soliton acceleration would be a candidate for origin of the solar cosmic rays energetically.

Yasunari Kurita
Kanagawa Institute of Technology

“Emergence of AdS3 thermodynamic quantities in extremal CFTs”

[JGRG28 (2018) PA25]

Emergence of AdS$_3$ thermodynamic quantities in extremal CFTs

Yasunari Kurita
Kanagawa Institute of Technology

AdS$_3$ pure gravity and Witten's idea

- Basically trivial (no gravitational waves)
- But, existence of BTZ black hole (finite size ⇒ entropy)
- AdS/CFT ⇒ finding CFT!
- 3-dim. Gravity ⇒ Chern-Simons description (gauge invariant)

$$\mathcal{I}_{\rm grav} = \frac{1}{16\pi G}\int d^3x\sqrt{g}\left[\mathcal{R}+\frac{2}{\ell^2}\right]$$

$$\mathcal{I}_{\rm grav} = \frac{k_L}{4\pi}\mathcal{I}_{\rm CS}\left(\mathcal{A}_L\right) - \frac{k_R}{4\pi}\mathcal{I}_{\rm CS}\left(\mathcal{A}_R\right)$$

where

$$\mathcal{I}_{\rm CS}\left(\mathcal{A}\right) = \int {\rm Tr}\left[\mathcal{A}\wedge d\mathcal{A}+\frac{2}{3}\mathcal{A}\wedge\mathcal{A}\wedge\mathcal{A}\right]$$

$$k_L = k_R = \underline{k = \ell/16G}$$

⇒ CS normalization will give the value of c !!

- gauge group : SO(2,1) × SO(2,1) or its covering
- Witten's assumption : holomorphic factorization

⇒ k_L, k_R are integer ⇒ $c_L = 24k_L, \quad c_R = 24k_R$

k=1 case

$c = 24k = 24$

- 71 CFTs are known.
- Pure gravity (no matter field)

⇒ FLM model (uniquely determined!)

Frenkel, Lepowsky, Meurman('88) having monster symmetry

- In FLM model, the Lowest dimension of primary field (other than identity) is 2(=k+1)

- Witten considered k>1 extenstion.

Witten, arXiv:0706.3359

Witten's conjecture

Pure 3-dim. AdS quantum gravity is extremal CFT

k: positive integer

- extremal CFT is CFT whose central charge is c=24k and its lowest dimension of primary operators (other than identity) is precisely k+1

- k=1: **FLM model** is known

- k≥2 : extremal CFTs have not been found

Why k+1 ?

- The ground state energy:

$$L_0 = \bar{L}_0 = -\frac{c}{24} = -k$$

- The mass of BTZ : $Ml = L_0 + \bar{L}_0$
- $M > 0 \Rightarrow L_0 \geq 1$

- The difference between the ground state and minimum (finite size) BTZ is $k+1$
- In Witten's interpretation, primaries (whose lowest conformal dimension is $k+1$) create BTZ black hole states

The Partition function of ECFT

$$Z(\tau) = \mathrm{Tr}\left[q^{L_0 - \frac{c}{24}}\right] = q^{-k}\left[\underbrace{\prod_{n=2}^{\infty}\frac{1}{1-q^n}}_{\text{Ground state and Virasoro descendants}} + \underbrace{\mathcal{O}(q^{k+1})}_{\text{BTZ (primary field) contributions}}\right]$$

Pole structure of the partition function and modular invariance require that $Z(\tau)$ should be polynomial of J-function (mathematically known, see Apostol p.40 for example)

$$\underbrace{J(q)}_{\text{Klein's modular invariant}} = 1728j(q) - 744 = q^{-1} + 196884q + 21493760q^2 + 864299970q^3 + \cdots$$

$$q = e^{2\pi i \tau}$$

moduli parameter of boundary torus

$$\tau = \frac{1}{2\pi T}\left(\Omega_E + \frac{i}{\ell}\right)$$

ECFT $\Rightarrow$ uniquely determined!

Witten, arXiv:0706.3359

The partition function of ECFT on g=1 torus

- The result for the first several k

index is k

$$Z_1(q) = |J(q)|^2 = \left|\frac{41E_4(\tau)^3 + 31E_6(\tau)^2}{72\eta(\tau)^{24}}\right|^2$$

The holomorphic part was found in FLM('84)

$$Z_2(q) = |J(q)^2 - 393767|^2$$
$$Z_3(q) = |J(q)^3 - 590651J(q) - 64481279|^2$$
$$Z_4(q) = |J(q)^4 - 787535J(q)^2 - 85975039J(q) + 74069025266|^2$$

Partition functions are computable for any k, for example

$$\begin{aligned} Z_{10} \quad = \quad & \big|J^{10} - 1968839J^8 - 214937599J^7 + 1348071256190J^6 \\ & +253704014739574J^5 - 361538450036076764J^4 \\ & -824143081027930253 30J^3 + 30123373072315438416085J^2 \\ & +621970556517352063759 2236J - 264390492553551717748100292\big|^2 \end{aligned}$$

Expansion of the partition functions

- Note the coefficients!

FLM interprets the number of primaries with dim.= 2=k+1

$$Z_1(q) = |q^{-1} + \underline{196884q} + \mathcal{O}(q^2)|^2$$

$$Z_2(q) = |q^{-2} + 1 + \underline{42987520q} + \mathcal{O}(q^2)|^2$$

$$Z_4(q) = |q^{-4} + q^{-2} + q^{-1} + 2 + \underline{81026609428q} + \mathcal{O}(q^2)|^2$$

- Take log!

k=1	$\ln 196883 \approx 12.19$	$\Longleftrightarrow$	$4\pi\sqrt{1} \approx 12.57$
k=2	$\ln 42987519 \approx 17.58$		$4\pi\sqrt{2} \approx 17.77$
k=4	$\ln 81026609426 \approx 25.12$		$4\pi\sqrt{4} \approx 25.13$

$\boxed{\text{Good!} \quad \text{close agreement!!}}$

Witten, arXiv:0706.3359

Entropy of BTZ black holes

$$S = \pi\left(\frac{\ell}{2G}\right)^{1/2}\left(\sqrt{M\ell - J} + \sqrt{M\ell + J}\right) = 4\pi\sqrt{k}\left(\sqrt{L_0} + \sqrt{\bar{L}_0}\right)$$

$$\boxed{M\ell = L_0 + \bar{L}_0, \quad J = L_0 - \bar{L}_0, \quad c = \frac{3\ell}{2G} = 24k}$$

- For $L_0 = 1$, Log of coefficients are nearly equals to entropy (for each holomorphic sector and anti-holomorphic sector)
- The coefficients are (almost nearly) the number of primary operators that create BTZ black holes.

Petersson-Rademacher formula

- Asymptotic behavior of the coefficients of the J-function:

$$J(q) = \sum_{m=-1}^{\infty} c_m q^m, \qquad \ln c_m \sim 4\pi\sqrt{m} - \frac{3}{4}\ln m - \frac{1}{2}\ln 2 + \ldots.$$

- Asymptotic behavior of the coefficients of the partition function

$$Z_k(\tau) = \sum_{n=-k}^{\infty} b_{k,n} q^n \qquad \ln b^0_{k,n} \sim 4\pi\sqrt{kn} + \underbrace{\frac{1}{4}\ln k - \frac{3}{4}\ln n - \frac{1}{2}\ln 2}_{} + \ldots.$$

Comparing BTZ entropy and this asymptotic behavior, one can read the correspondence: $\mathrm{n} \sim L_0$

This part vanishes when k=4 and n=1.
The difference (between BH entropy and the coefficients) remain always.
Quantum correction?

Canonical ensemble

Internal Energy obtained from ECFT partition functions

（we set J=0, for simplicity）

- k=1 case

$\langle E\rangle = T^2\partial_T \ln Z_1$

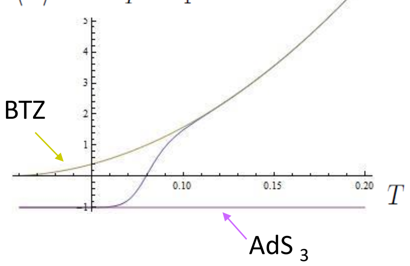

- k=10 case

$\langle E\rangle = T^2\partial_T \ln Z_{10}$

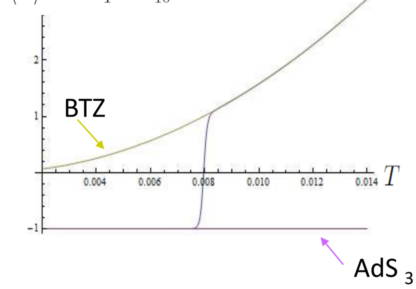

It agrees with mass of AdS_3 at low T and with mass of BTZ at high T. The transition becomes sharper as k increases (thermodynamic limit).

Canonical ensemble

Canonical entropy, canonical angular momentum from ECFT partition function

k=2, Ω_E=0.2 (rotational case)

$$S_C = -\frac{\partial F_k}{\partial T} = \partial_T\,(T\,LogZ_k)$$

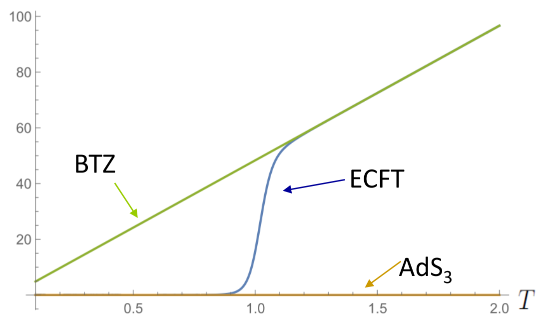

Euclidean

$$J_C = \frac{\partial F_k}{\partial \Omega_E} = -\partial_{\Omega_E}\,(T\,LogZ_k)$$

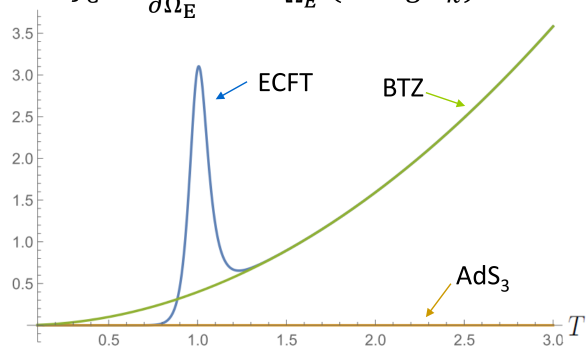

At low temperature, ECFTs give AdS_3 behavior, even when the boundary rotates (non-zero Ω).
Thermodynamic relation gives correct thermodynamic quantities.

Canonical ensemble

Canonical entropy, canonical angular momentum from ECFT partition function

k=4, Ω_E=0.2 (rotational case)

Euclidean

$$S_C = -\frac{\partial F_k}{\partial T} = \partial_T\,(T\,LogZ_k)$$

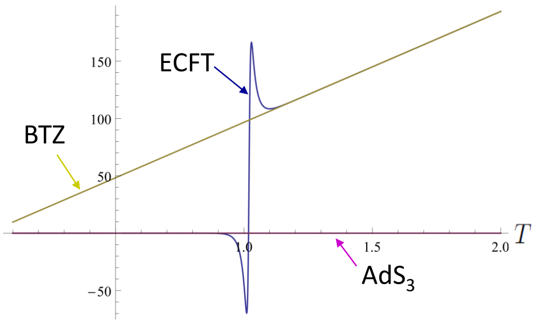

$$J_C = \frac{\partial F_k}{\partial \Omega_{\mathrm{E}}} = -\partial_{\Omega_E}\,(T\,LogZ_k)$$

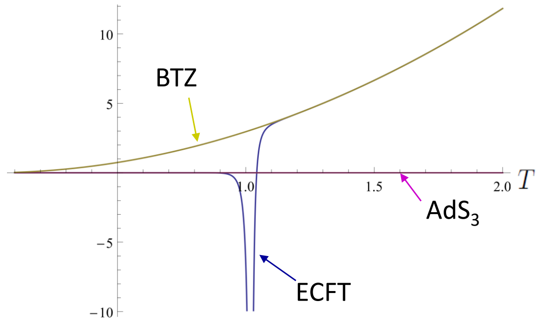

At low temperature, ECFTs give AdS_3 behavior, even when the boundary rotates (non-zero Ω).
Thermodynamic relation gives correct thermodynamic quantities.

Discussion
Tirivial?

The dominant contribution to the partition function : Z_4 case

By use of dimensionless temperature and angular velocity, $\ell = 2k,\ \hat{T} = 2\pi\ell T,\ \hat{\Omega} = \ell\Omega$

the lowest Virasoro op. can be written as $L_0 = k\left(\frac{\hat{T}}{1-\hat{\Omega}}\right)^2 \qquad \bar{L}_0 = k\left(\frac{\hat{T}}{1+\hat{\Omega}}\right)^2$

Canonical ensemble representation

When $\widehat{\Omega} = 0$ and $\hat{T} = \sqrt{2},\ \ L_0 = 8.$
The term q^8 (including the coefficient) gives dominant contribution.

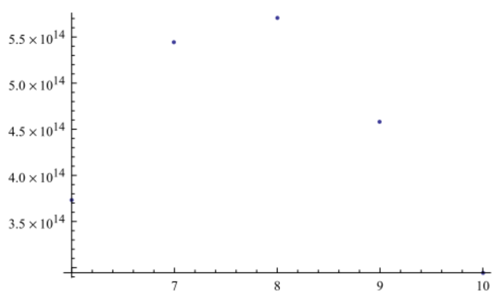

When $\widehat{\Omega} = 0$ and $\hat{T} = 2,\ \ L_0 = 16.$
The term q^{16} (including the coefficient) gives dominant contribution.

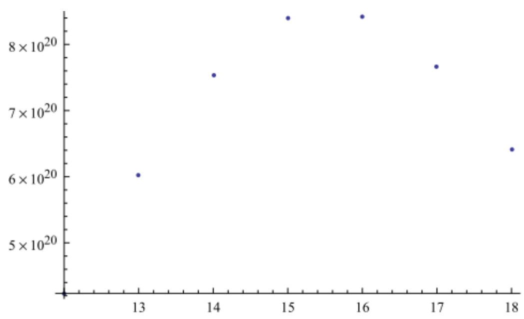

Discussions

- Extremal CFTs are a good candidate for pure AdS_3 quantum gravity. (though it is not found for k > 1)
- The partition functions give expected thermodynamic behavior.
- The critical temperature of Hawking-Page transition is at $|\tau| = 1$ in the moduli space. The transition becomes sharper as $k, c \to \infty$ (semiclassical limit).
- How can we understand microscopic origin of BTZ entropy? There is always a bit difference between Bekenstein-Hawking entropy and microscopic entropy (log of # of BTZ primaries).
- What is quantum gravity? What should we investige further in this model?

Some More Discussions

- What is microscopic understanding of angular momentum, which emerges as thermodynamic quantity at high temperature?
- For $L_0 \geq 2$, ECFT states will include some information of massive BTZ black hole. How should we count the number of states? It will relate with some microscopic understanding of black holes.

Hajime Sotani
National Astronomical Observatory of Japan

“Pulse profiles of highly compact pulsars in general relativity”

[JGRG28 (2018) PA26]

Pulse profiles of highly compact pulsars in general relativity

Hajime SOTANI (NAOJ)

Physical Review D 98, 04417 (2018)

photon trajectory & deflection angle

- metric: $g_{\mu\nu}dx^\mu dx^\nu = -A(r)dt^2 + B(r)dr^2 + C(r)(d\theta^2 + \sin^2\theta d\psi^2)$
- deflection angle and impact parameter:

$$\psi(R) = \int_R^\infty \frac{dr}{C}\left[\frac{1}{AB}\left(\frac{1}{b^2} - \frac{A}{C}\right)\right]^{-1/2} \quad \text{where} \quad b = \sin\alpha\sqrt{\frac{C(R)}{A(R)}}.$$

- maximum value of ψ corresponds to the value when $\gamma = \pi/2$

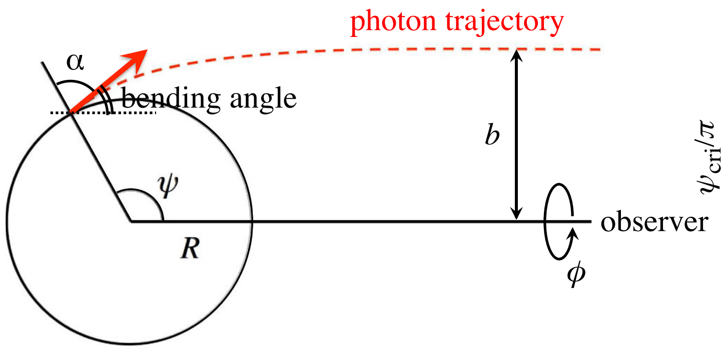

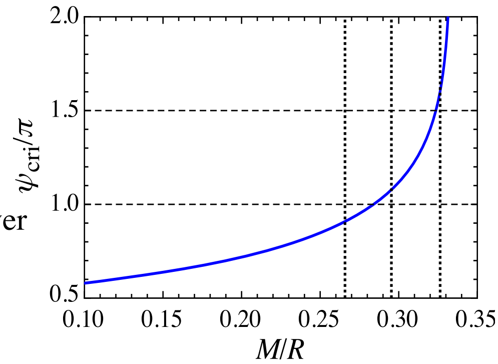

pulse profile from NSs

- adopting a pointlike spot approximation (Beloborocov 02),
- assuming the black body emission from the hot spot with isotropic intensity I_0
- Flux from area of $S_0 := \int dS = 4R^2\delta\psi\delta\phi\sin\psi$: $F_*(\psi) = F_0\sin\alpha\cos\alpha\frac{d\alpha}{d\psi}$, $F_0 := \frac{4I_0A(R)R^2\delta\psi\delta\phi}{D^2}$
- The observed flux: $F(\psi) = F_1\cos\alpha\frac{d(\cos\alpha)}{d\mu}$ where $F_1 := I_0\frac{sA(R)}{D^2}$
- Considering the observation of the pulse profile from rotating NS with angular velocity Ω with angles Θ & i

$$\mu(t) = \sin i \sin\Theta\cos(\omega t) + \cos i\cos\Theta$$

where $\mu = \cos\psi = \boldsymbol{n}_\mathrm{p}\cdot\boldsymbol{d}$

- observed flux from pulsar:

$$F_\mathrm{ob}(t) = F(t) + F_\mathrm{a}(t)$$

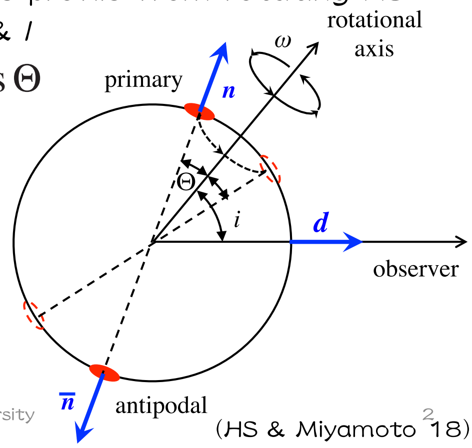

(HS & Miyamoto '18)

NS models

- we consider three NS models with M/M⊙=1.8, 2.0, & 2.21, fixing the radius to be 10 km.
  - $\psi_\mathrm{cri} = 0.908\pi$, $\psi_\mathrm{cri} = 1.078\pi$, $\psi_\mathrm{cri} = 1.604\pi$

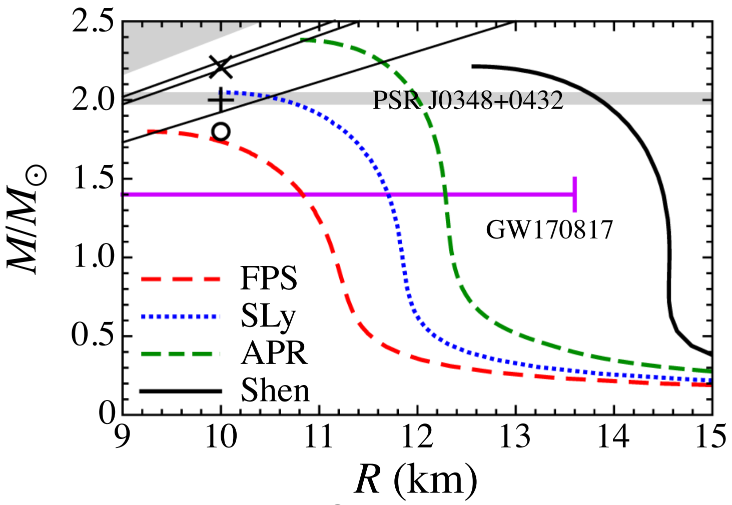

how to observe the hot spots 1

- depending on the angles Θ & I
  - I) only the primary spot can be observed at any time
  - II) the primary spot can be observed at any time and the antipodal spot can also be observed sometime
  - III) only the primary spot can be observed, or both spots can be observed, or only the antipodal spot can be observed
  - IV) the both stops can be observed at any time

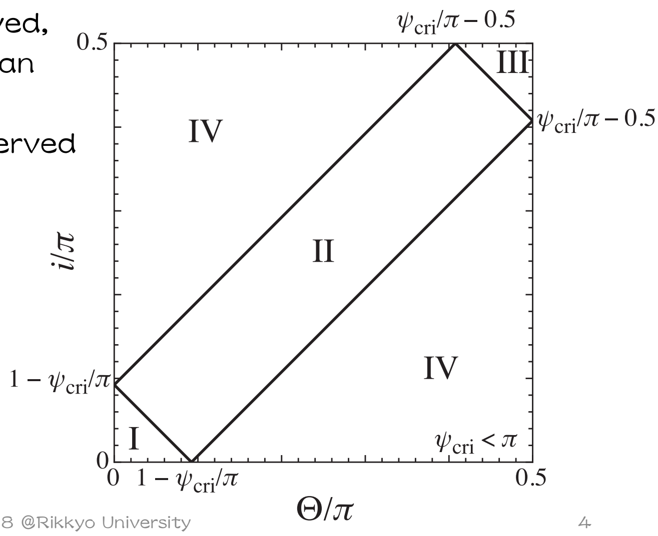

how to observe the hot spots 2

- depending on the angles Θ & I
  - i) the primary has always 1 path, the antipodal has always 2 paths
  - ii) the primary has always 1 path, the antipodal has sometime 2 paths
  - iii) the both have sometime 2 paths
  - iv) the both hot spots have always 1 path

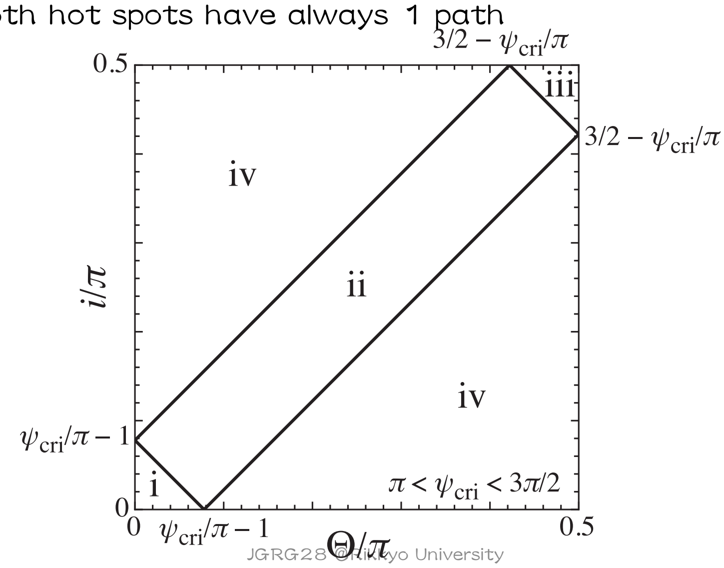

how to observe the hot spots 3

- depending on the angles Θ & *I*
  i) the primary has always 1 path, the antipodal has always 2 paths
  ii) the primary has sometime 2 paths, the antipodal has always 2 path
  iii) the both have sometime 2 paths
  iv) the both hot spots have always 2 paths

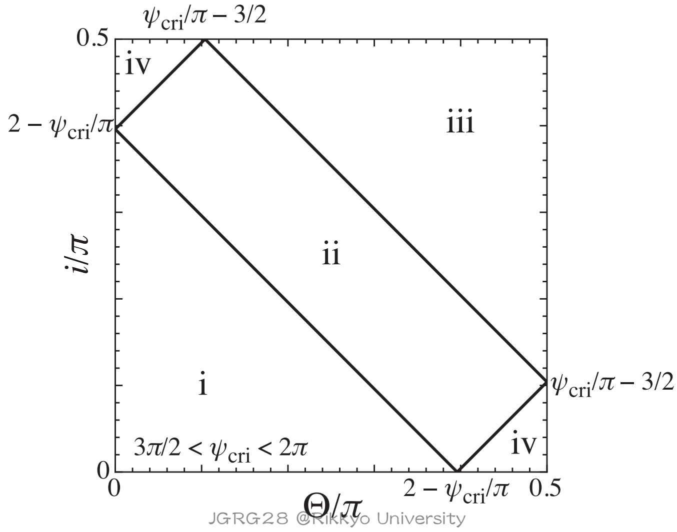

behavior of F/F$_1$, adopted (i, Θ)

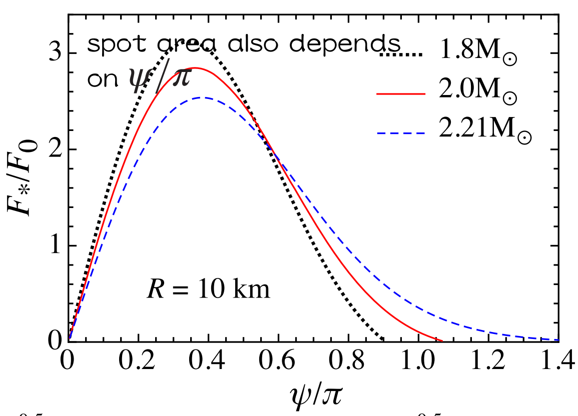

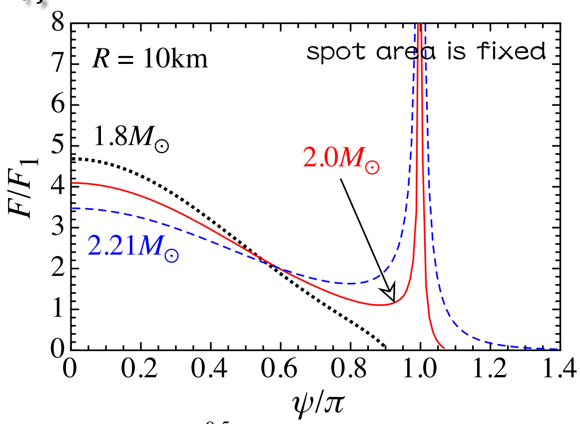

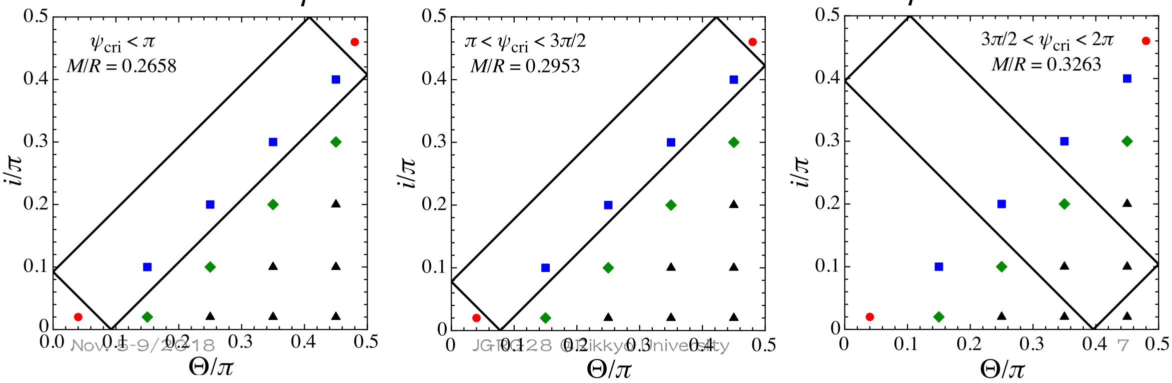

pulse profile from 1.8$M_\odot$ NS

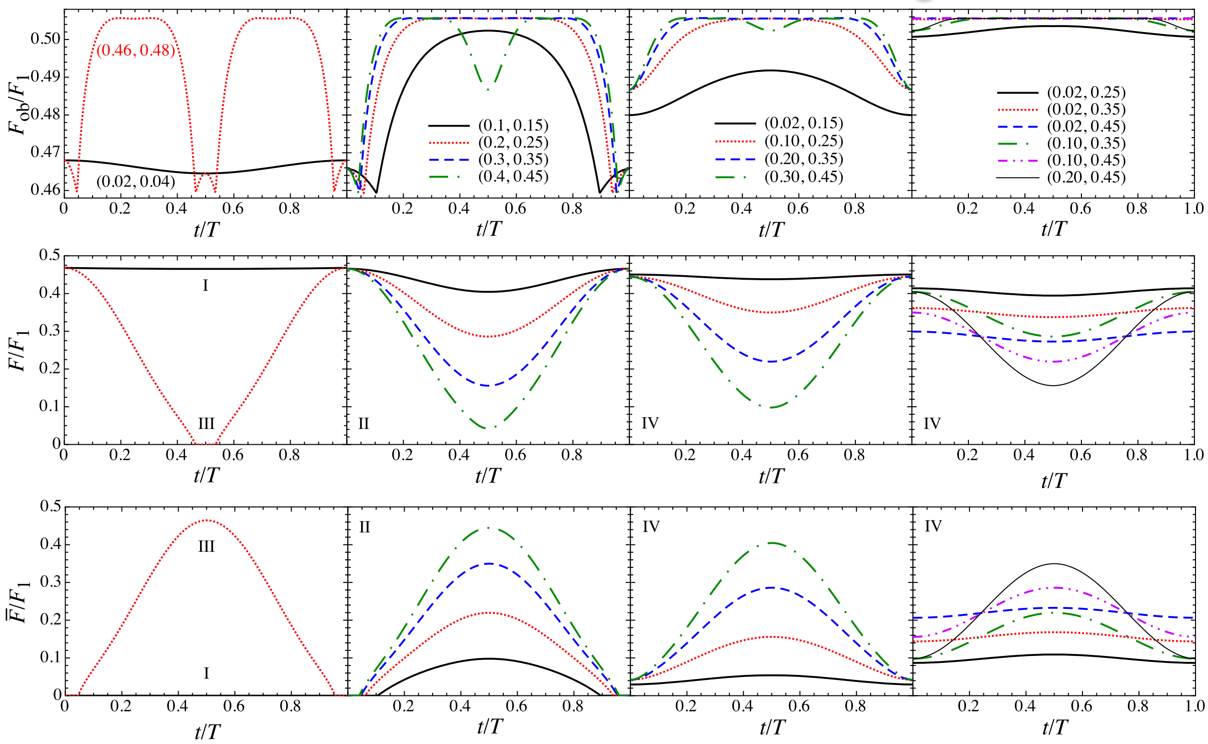

pulse profile from 2.0$M_\odot$ NS

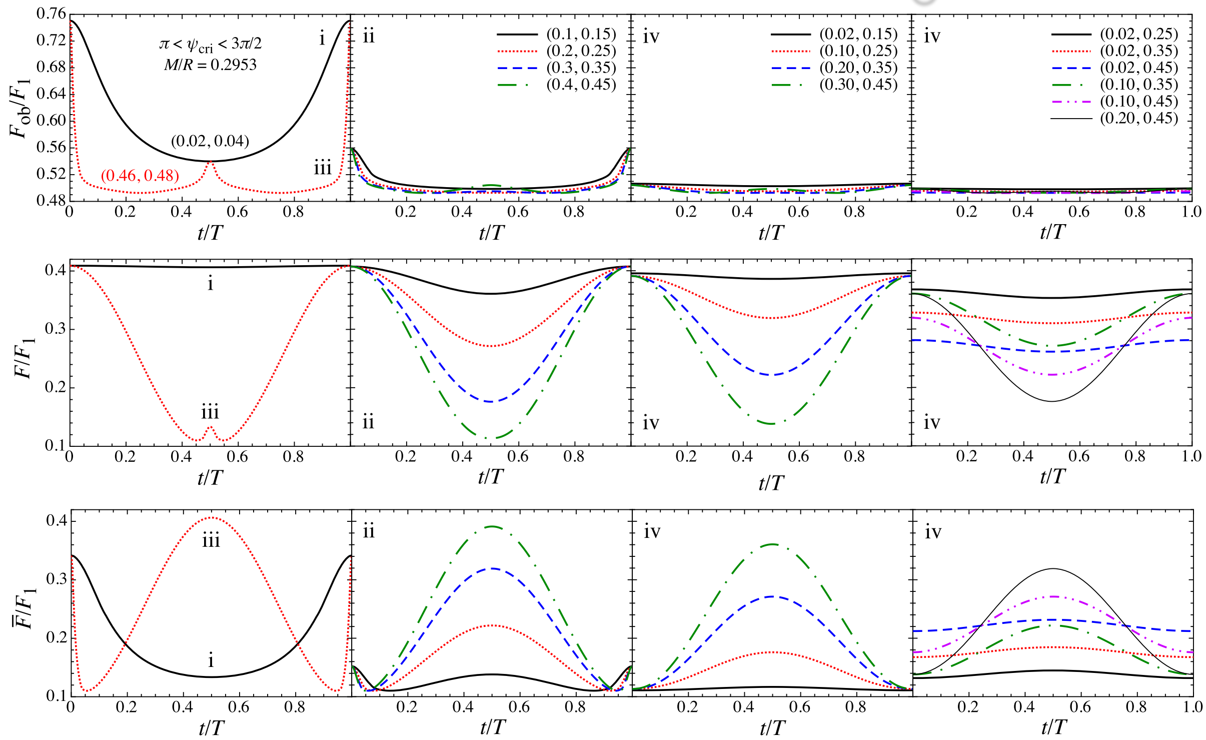

pulse profile from 2.21 $M_\odot$ NS

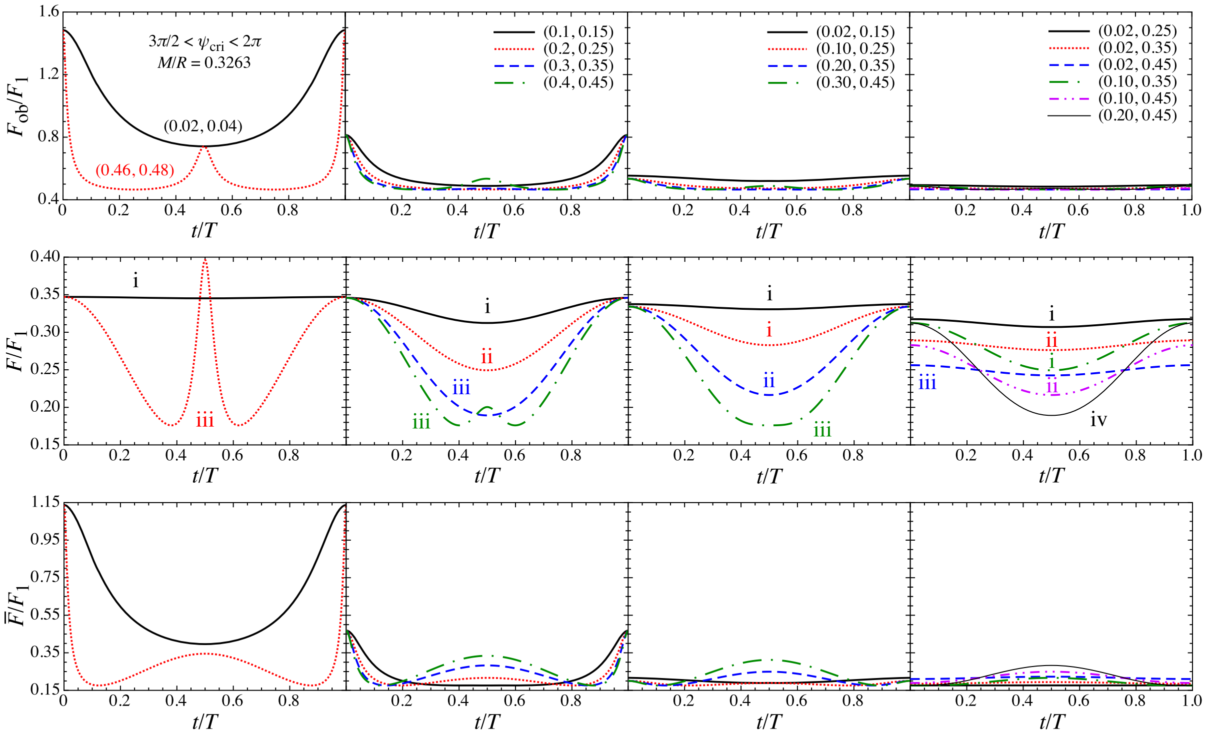

F_{max}/F_{min}

- Fmax/Fmin becomes very large for the NSs with M/R > 0.284 and for smaller (Θ - i)

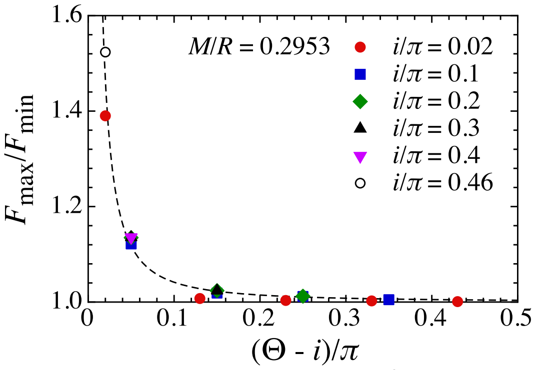

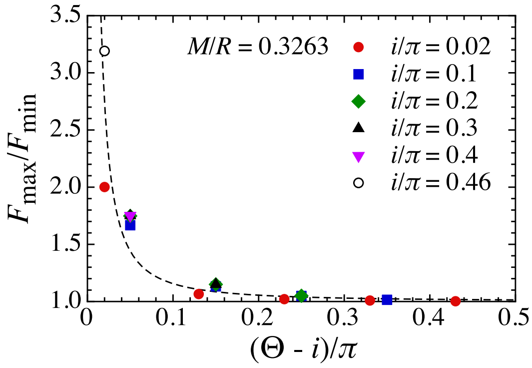

$$F_{max}/F_{min} = \frac{1.311 \times 10^{-3}}{|\Theta - i|^{3/2}} \pi^{3/2} + 1 \qquad F_{max}/F_{min} = \frac{4.935 \times 10^{-3}}{|\Theta - i|^{3/2}} \pi^{3/2} + 1$$

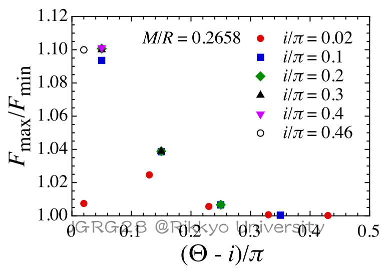

conclusion

- We investigate the pulse profile of highly compact rotating NS for which the bending angle exceeds $\pi/2$ ($M/R > 0.284$).
- We make a classification of the number of path from the primary and antipodal hot spots, dpending on the angles (i, Θ).
- We find that the pulse profiles of highly compact NSs are qualitatively different from those for the standard NSs.
  - In particular, F_{max}/F_{min} is significantly larger for highly compact NSs
- One would be able to constrain the EOS for NSs through the observations of pulse profiles with the help of the observational constraint on (i, Θ).

Norichika Sago
Kyushu University

"Gravitational radiation from a spinning particle orbiting a Kerr black hole"

[JGRG28 (2018) PA28]

Gravitational radiation from a spinning particle orbiting a Kerr black hole

Kyushu University
Norichika Sago
with
Ryuichi Fujita (YITP)

28th workshop on General Relativity and Gravitation
Rikkyo University, 5–9 November 2018

Motivation

To study extreme-mass ratio inspirals (EMRIs) as GW sources by using the black hole perturbation theory.

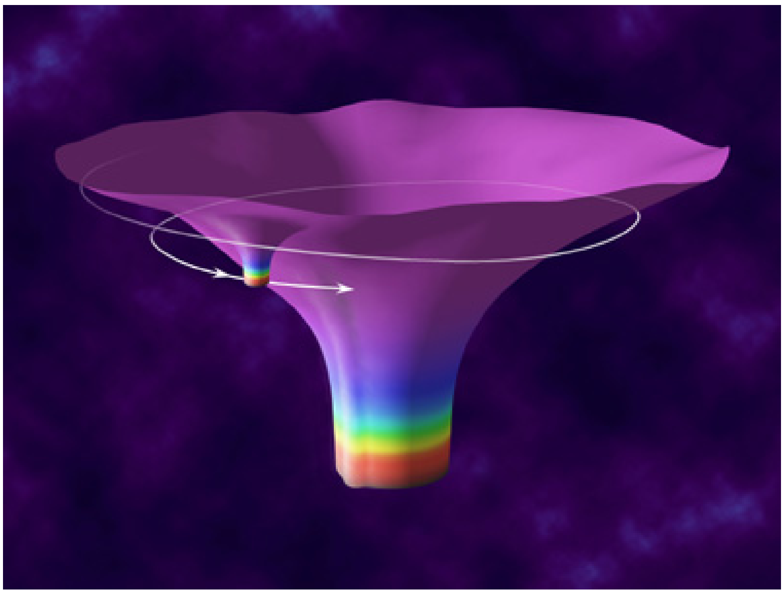

Motion of a spinning particle in Kerr geometry

Test particle case $[\approx O((\mu/M)^0)]$

The particle moves along a geodesic, characterized by E, L, C.

E : energy
L : azimuthal angular momentum
C : Carter constant

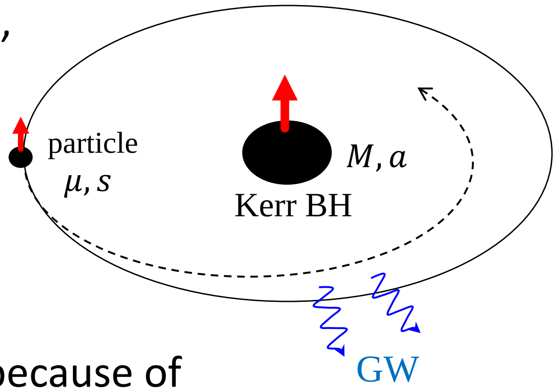

At 1st order $[\approx O((\mu/M)^1)]$

Deviation from the geodesic orbits because of

- radiation reaction effect
- effect of the particle's spin

Question
How does the spin affect the particle's orbit and the GW?

EOM of a spinning particle

Mathisson-Papapetrou-Pirani(MPP) equation

$$\frac{D}{d\tau}p^{\mu}(\tau) = -\frac{1}{2}R^{\mu}{}_{\nu\rho\sigma}v^{\nu}(\tau)S^{\rho\sigma}(\tau)$$

$$\frac{D}{d\tau}S^{\mu\nu}(\tau) = 2p^{[\mu}(\tau)v^{\nu]}(\tau)$$

v^{μ}: 4-velocity
p^{μ}: 4-momentum
$S^{\mu\nu}$: spin tensor

（Neglect higher multipoles than quadropole, accurate up to the linear order of spin）

14 degree of freedom for 10 equations
→ 4 additional conditions are required to close the system.

Spin supplementary condition

$$S^{\mu\nu}(\tau)p_{\nu}(\tau) = 0$$

(correspond to deciding the CoM)

Simplification of MPP equation

Introduce the tetrad frame

$$e_\mu^0 = \left(\frac{\sqrt{\Delta}}{\sqrt{\Sigma}}, 0, 0, -a\sin^2\theta\frac{\sqrt{\Delta}}{\sqrt{\Sigma}}\right) \qquad e_\mu^1 = \left(0, \frac{\sqrt{\Sigma}}{\sqrt{\Delta}}, 0, 0\right)$$

$$e_\mu^2 = \left(0, 0, \sqrt{\Sigma}, 0\right) \qquad e_\mu^3 = \left(-\frac{a}{\sqrt{\Sigma}}\sin\theta, 0, 0, \frac{r^2+a^2}{\sqrt{\Sigma}}\sin\theta\right)$$

Rewrite MPP equation in the tetrad frame up to O(S¹),

$$\boxed{\frac{dv^a}{d\tau} = \omega_{bc}{}^a v^b v^c - SR^a \qquad \frac{d\zeta^a}{d\tau} = \omega_{bc}{}^a v^b \zeta^c - Sv^a\zeta^b R_b}$$

where $v^a = u^a + O(S^2)$ $\quad \zeta^a \equiv \frac{S^a}{S} = -\frac{1}{2\mu S}\epsilon^a{}_{bcd}u^b S^{cd}$

$\omega_{ab}{}^c = e_a^\mu e_b^\nu e_{\nu;\mu}^c$ $\quad R^a \equiv R^{*a}{}_{bcd}v^b u^c \zeta^d = \frac{1}{2\mu S}R^a{}_{bcd}v^b S^{cd}$

Formal expression of energy flux

$$\boxed{\left\langle\frac{dE}{dt}\right\rangle = \sum_n \frac{\mu^2}{4\pi\omega_n^2}\left[|Z_{lmn}^\infty|^2 + \alpha_{lmn}\left|Z_{lmn}^H\right|^2\right]}$$

$$Z_{lmn}^{\infty/H} \approx \int dr\,\underbrace{R_{\ell mn}^{\mathrm{in/up}}(r)}_{\text{homogeneous solution of radial Teukolsky eq.}}\;\underbrace{T_{\ell mn}(r)}_{\text{source term constructed from energy-momentum tensor}}$$: Amplitude of partial wave

homogeneous solution of radial Teukolsky eq.

source term constructed from energy-momentum tensor

Energy-momentum tensor

$$T^{\alpha\beta}(x) = \int d\tau\left\{p^{(\alpha}v^{\beta)}\frac{\delta^{(4)}(x-z(\tau))}{\sqrt{-g}} - \underbrace{\nabla_\gamma\left(S^{\gamma(\alpha}v^{\beta)}\frac{\delta^{(4)}(x-z(\tau))}{\sqrt{-g}}\right)}_{\text{contribution from spin}}\right\}$$

contribution from spin

Calculate the energy flux

- Solve the EOM for a spinning particle
- Construct the energy-momentum tensor to derive the source term
- Solve the Teukolsky equation (by analytic technique [Mano et al.(1995)])
- Calculate the amplitude of each mode
- Sum over all modes

Setup

- circular, slightly inclined orbit
- particle's spin also slightly misaligned to the BH spin

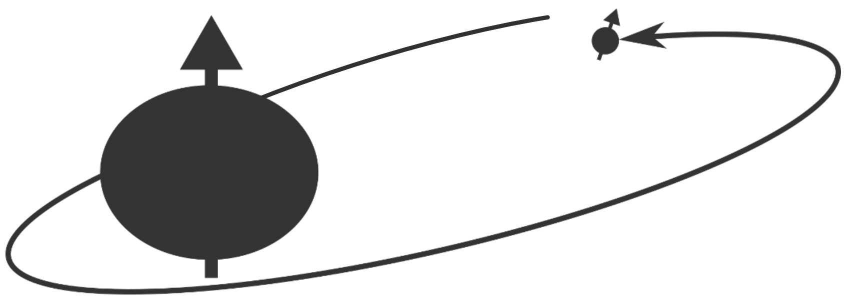

Construct the energy-momentum tensor from the solution of MPP equation, then calculate the energy flux.

circular, slightly inclined orbit, slightly misaligned

Orbital part

$r = \text{const.} \qquad (v^2 = 0) \qquad \Longrightarrow$ circular

$\theta - \frac{\pi}{2} = y \cos \Omega_\theta \tau + O(y^3), \quad (y \ll 1) \quad \Longrightarrow$ slightly inclined

$$t = \Omega_t \tau + y^2 \tilde{t}_2 \cos 2\Omega_\theta \tau + O(y^3)$$

$$\varphi = \Omega_\varphi \tau + y^2 \tilde{\varphi}_2 \cos 2\Omega_\theta \tau + O(y^3)$$

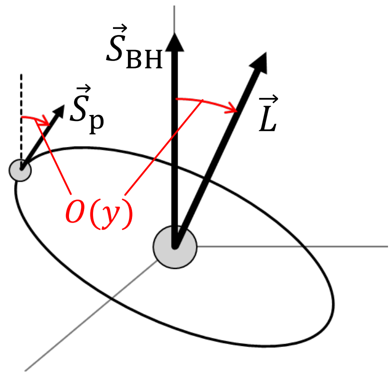

Spin part

$$\zeta^2 = \tilde{\zeta}_0^2 + y^2 \tilde{\zeta}_2^2 \cos 2\Omega_\theta \tau + O(y^3)$$

$$\left.\begin{aligned} \zeta^0 &= y \tilde{\zeta}_1^0 \sin \Omega_\theta \tau + O(y^3) \\ \zeta^1 &= y \tilde{\zeta}_1^1 \sin \Omega_\theta \tau + O(y^3) \\ \zeta^3 &= y \tilde{\zeta}_1^3 \sin \Omega_\theta \tau + O(y^3) \end{aligned}\right\} \text{slightly misaligned}$$

Results

$v^2 = M/r$: PN parameter
$q = a/M$: spin parameter of central BH
$s = S/M$: spin parameter of particle
y : inclination parameter

$$\begin{aligned}
\left\langle \frac{dE}{dt} \right\rangle_\infty &= \frac{32}{5} \left(\frac{\mu^2}{M^2} \right) v^{10} \\
&\times \Bigg\{ 1 - \frac{1247}{336} v^2 + \left[4\pi - \left(\frac{73}{12} - \frac{73}{24} y^2 \right) q - \left(\frac{25}{4} - \frac{2}{3} y^2 \right) s \right] v^3 \\
&\quad + \left[-\frac{44711}{9072} + \left(\frac{33}{16} - \frac{527}{96} y^2 \right) q^2 + \left(\frac{71}{8} - \frac{637}{144} y^2 \right) sq \right] v^4 \\
&\quad + \left[-\frac{8191}{672} \pi + \left(\frac{3749}{336} - \frac{3749}{672} y^2 \right) q + \left(\frac{2403}{112} - \frac{2741}{1792} y^2 \right) s + \frac{463}{72} y^2 q^2 s \right] v^5 \\
&\quad + \Bigg[\frac{6643739519}{69854400} - \frac{1712}{105} \gamma - \frac{3424}{105} \ln(2) + \frac{16}{3} \pi^2 - \frac{1712}{105} \ln v \\
&\qquad - \frac{169}{12} (2 - y^2) \pi q - \left(\frac{187}{6} - \frac{8}{3} y^2 \right) \pi s \\
&\qquad + \left(\frac{3419}{168} - \frac{73}{21} y^2 \right) q^2 + \left(\frac{2411}{168} - \frac{1859}{252} y^2 \right) qs + \frac{737}{144} y^2 q^3 s \Bigg] v^6 \Bigg\}
\end{aligned}$$

Summary and future works

Summary

- Calculate the energy flux of GW from a spinning particle moving along a circular, slightly inclined orbit in Kerr spacetime.
- Consistent with the circular, equatorial case [Tanaka et al.(1996)]
- Consistent with the nonspinning particle case [NS-Fujita(2015)]
- Not trivial to compare our result to the standard PN result because v (or r) and y are gauge dependent.

Future works

- Re-express the flux formula in terms of gauge invariant variables in order to compare with PN result.
- GW waveform including the effect of the particle’s spin
- Beyond the linear order of particle's spin

Yuki Hagihara
Hirosaki University

“GW polarizations with aLIGO, Virgo and KAGRA”

[JGRG28 (2018) PB1]

GW polarizations with aLIGO, Virgo and KAGRA

Yuki Hagihara, Naoya Era, Daisuke Iikawa

Hirosaki University, Japan
with H. Asada (Hirosaki)

JGRG28 in Rikkyo University Nov. 5 - 9, 2018

Abstract: Based on Phys. Rev. D 98, 064035 (2018), We are giving a poster presentation on GW polarizations with Advanced LIGO, Advanced Virgo and KAGRA. Assuming that, for a given source of GWs, we know its sky position, as a case of GW events with an electromagnetic counterpart such as GW170817, we discuss a null stream method to probe GW polarizations including spin-0 (scalar) GW modes and spin-1 (vector) modes.

1 Introduction

There are two polarizations of gravitational wave (GW) in GR or some theories of gravity. But six polarizations are possible in general metric theories of gravity. We can test theories of gravity by probing GW polarization. So, we study null stream method as one polarization test.

The null stream is particular linear combination that cancels out a spin-2 modes signal. Extra GW polarization will make the null stream non-zero.

We investigated the direction in which extra polarization are more likely to be detected when using the null stream method.

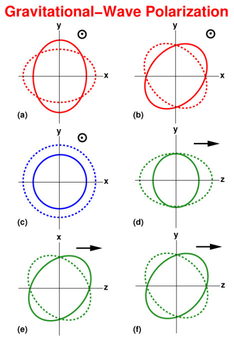

Fig 1: Six GW polarizations in a general metric theory of gravity. [2] (a) and (b) are spin-2 modes, (c) and (d) are spin-0 modes and (e) and (f) are spin-1 modes. In GR, only (a) and (b) are present.

2 Null stream method

The null stream is particular linear combination that cancels out a spin-2 modes signal. A GW signal in a laser interferometer is the phase difference of laser lights. The phase difference$\Delta\Phi$ is expressed as

$$\Delta\Phi = \frac{4\pi\nu L_0}{c} S(t), \tag{1}$$

where ν is frequency of the laser light, L_0 is unperturbed length of each arm. We call $S(t)$ a signal of GW. For a detector labeled by a ($a = 1, 2, 3$, and 4), the signal from a GW source at the location denoted as (θ, ϕ) on the sky is

$$S_a(t) = F_a^+ h^+ + F_a^\times h^\times + F_a^S \left(h^S - h^L\right) + F_a^V h^V + F_a^W h^W, \tag{2}$$

where h^+ and $h^\times$ denote the spin-2 modes called the plus and cross mode, respectively; h^S and h^L denote the spin-0 modes called the breathing and longitudinal mode, respectively; and h^V and h^W denote the spin-1 modes often called the vector-x and vector-y mode, respectively; and F_a^+ , $F_a^\times$, F_a^S , F_a^V , and F_a^W are the antenna patterns for polarizations of GWs. The antenna patterns are functions of a GW source location θ and ϕ.

If GW has only spin-2 modes, by eliminating the two modes in signals at three detectors in the ideal case, we obtain a null stream as, for a= 1, 2, and 3 for instance,

$$\delta_{23} S_1(t) + \delta_{31} S_2(t) + \delta_{12} S_3(t) = 0, \tag{3}$$

where

$$\delta_{ab} = F_a^+ F_b^\times - F_a^\times F_b^+. \tag{4}$$

Next, we consider four detectors and incorporate scalar and vector polarization modes. Let us denote two null streams including spin-0 and spin-1 polarizations as

$$\begin{aligned} P_a S_a =& \delta_{23} S_1(t) + \delta_{31} S_2(t) + \delta_{12} S_3(t) \\ =& P_b F_b^S \left(h^S - h^L\right) + P_c F_c^V h^V + P_d F_d^W h^W, \end{aligned} \tag{5}$$

$$\begin{aligned} Q_a S_a =& \delta_{34} S_2(t) + \delta_{42} S_3(t) + \delta_{23} S_4(t) \\ =& Q_b F_b^S \left(h^S - h^L\right) + Q_c F_c^V h^V + Q_d F_d^W h^W, \end{aligned} \tag{6}$$

where we use Eq. (2) and the summationis taken over $a = 1, 2, 3$ and 4. Note that the tensor null stream is built in and hence h^+ and $h^\times$ do not appear in the above equations. Without loss of generality, we can choose P_a and Q_a as $(P_a) = (\delta_{23}, \delta_{31}, \delta_{12}, 0)$ and $(Q_a) = (0, \delta_{34}, \delta_{42}, \delta_{23})$.

3 Numerical calculations

In numerical calculations for the HLVK network, we choose H=1, L=2, V=3, and K=4 for a=1, 2, 3, and 4 for its simplicity. See Figs. 2 and 3 for the network of HLVK.

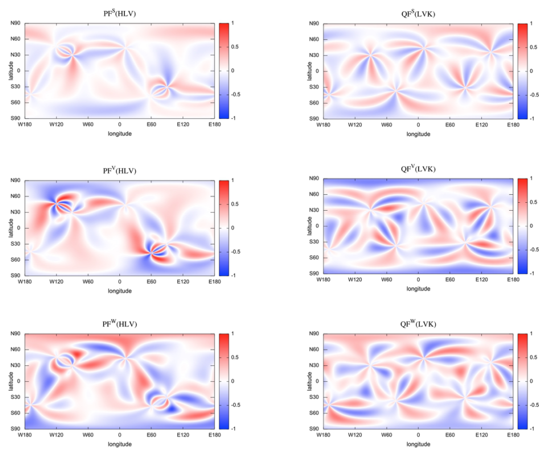

Fig 2: Contour map of the coefficients in the null stream, respectively.

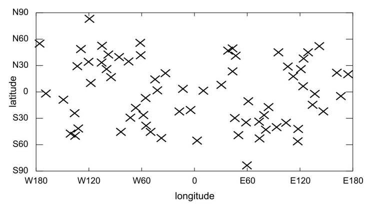

Fig 3: The 70 sky positions that satisfy simultaneously $P_a F_a^S = 0$ and $Q_a F_a^S = 0$. If we are extremely lucky to observe such a GW event with an electromagnetic counterpart at the location at which spin-0 modes fade out from the null streams, Eqs.(5) and (6) will enable us to constrain h^V and h^W, separately.

4 Conclusion

In expectation of the near-future network of Advanced LIGO, Advanced Virgo, and KAGRA, we discussed a null stream method to probe GW polarizations including spin-0 (scalar) GW modes and spin-1 (vector) modes, where we assumed that, for a given source of GWs, we know its sky position, as is the case for GW events with an electromagnetic counterpart such as GW170817. We studied a location on the sky, exactly at which the spin-0 modes of GWs vanish in null streams for the GW detector network, though the strain output at a detector may contain the spin-0 modes. By numerical calculations, we showed that there are 70 sky positions that kill the spin-0 modes in the null streams. If a GW source with an electromagnetic counterpart is found in one of the 70 sky positions, the spin-1 modes will be testable separately from the spin-0 modes by the null stream method.

References

[1] Y. Hagihara, N. Era, D. Iikawa, and H. Asada, Phys. Rev. D 98, 064035 (2018), arXiv:1807.07234

[2] Clifford M. Will, Living Rev. Relativity 17 (2014), 4

Kazuma Tani
Yamaguchi university

"Possibility of forming unstable circular orbit of photon in boson star"

[JGRG28 (2018) PB2]

Possibility of forming unstable circular orbit of photon in boson star

〇Kazuma Tani , Masashi Kuniyasu ,Nobuyuki Sakai(Yamaguchi univ.)

Abstract: Boson star is one of the soliton solutions. Solitons exist on the scale from elementary particles to astronomical objects. It is expected that boson star can be as compact as Black holes(BHs). The existence of unstable circular orbit of photon(UCOP) is one of the phenomena in massive objects. So as We make the index of boson star's compactness. we investigated the possible that boson star can form UCOP. As the result, we show the existence of UCOP in the case no quartic self-interaction. Next stage in the research is expansion that include quartic self-interaction, and check its stability.

1. Introduction

◆Basic knowledge and background

Boson stars are complex scalar fields which have U(1) symmetry.

It's necessary for observing BH shadow to exist circular orbit of photon(UCOP) . If BSs have UCOP, it must be distinguish between BH shadow and BS one.

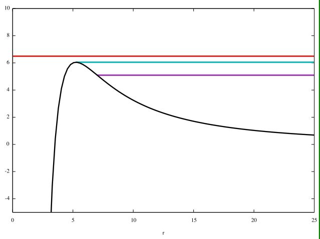

BH's effective potential

◆Purpose

・In my research, we used a model which including nonminimally coupling to scalar curvature.

・In the model, we investigated whether BSs have UCOP or not.

2. Situation and solution of Boson star

◆Setting situation

We assume that spacetime is static and spherical.
So ansatz is given by

$$g_{\mu\nu} = \mathrm{diag}\left(-e^{\nu(r)}, e^{\lambda(r)}, r^2, r^2\sin\theta\right)$$
$$\phi(r,t) = \phi_0(r)e^{-i\omega t}.$$

・the model's action

$$S = \int d^4x\sqrt{-g}\left\{\left(\frac{1}{16\pi G_N} + \xi\varphi^*\varphi\right)R - g^{\mu\nu}\partial_\mu\varphi^*\partial_\nu\varphi - m_\varphi^2\varphi^*\varphi - \frac{\lambda_\phi}{2}(\varphi^*\varphi)^2\right\}$$

(Note) λ_ϕ: quartic self-interaction
ξ: the strength of coupling
m_φ: scalar field's mass

We get the basic equations by varying those of action with respect to $g_{\mu\nu}$ or φ^*. For example, we can get scalar field's equation of motion,

$$\left[\Box - m_\phi^2 - \lambda_\phi\phi^*\phi + \xi R\right]\phi = 0$$

◆Numerical solution example

We show the solution of BSs basic equation below:

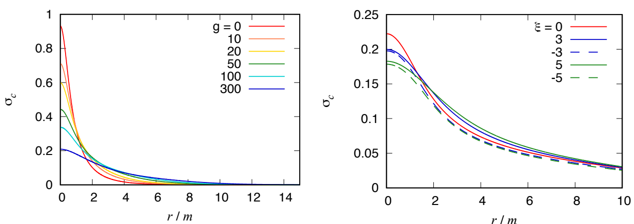

Right panel is the graph which change some values of λ_ϕ .Left panel is the graph which change some values of ξ.

3. Unstable circular orbit of photon

◆Schwarzschild Black hole

By solving geodesics equation with Sch metric. We can get the trajectory of photon around Sch Black hole(like right panel).

The light blue line is unstable circular orbit of photons (UCOP). The phenomenon imply that there is a compact object in center.

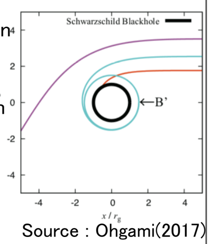

Source : Ohgami(2017)

We can consider the UCOP as index of compactness.

◆Boson star

In similar way, We searched BS's UCOP.

geodesics eq. —Sch. metric→ $\dot{r}^2 + V(r;L) = E$

geodesics eq. —Radial symmetric→ $\dot{r}^2 + V(r;L,E) = 0$

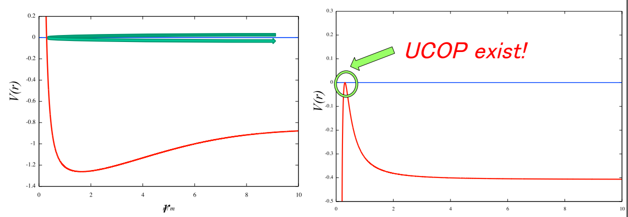

In the constant ξ = 4, we found two case. One has UCOP, another doesn't have. The difference is parameter ω. In above graph, we show the potential in the cases each other. It is not restricted the case ξ = 4. For example, we show the existing UCOP in ξ = 0.1 below. In my research until now, we found UCOP in the case $\xi > 0$ and not found in the case $\xi < 0$

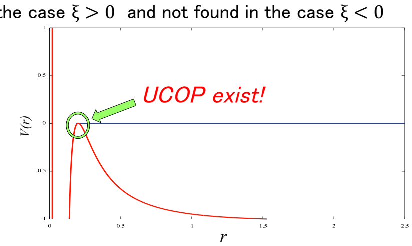

4. Summary and future works

◆Summary

・We focused on the boson stars with nonminimally coupled scalar field to gravity and showed its numerical solution.

・In the case $\lambda_\phi = 0$, We showed that the UCOP in BS exist if $\xi > 0$

◆Future works

We will analyze boson stars for $\lambda_\phi \neq 0$, $\xi \neq 0$ and its their stability. Finally we'll make the parameter map continuously as possible.

Keisuke Nakashi
Rikkyo University

“Negative deflection angle in three-dimensional massive gravity”

[JGRG28 (2018) PB3]

PB3

Negative Deflection Angle in Three-Dimensional Massive Gravity

Keisuke Nakashi (Rikkyo U.), Shinpei Kobayashi (Tokyo Gakugei U.), Shu Ueda (Tokyo Gakugei U.), Hiromi Saida (Daido U.)

JGRG28 @ Rikkyo Univ., 5-8, November, 2018

Abstract

We study the null geodesics in a static circularly symmetric (SCS) black hole spacetime which is a solution in the three-dimensional massive gravity. We obtained the analytic solutions for the geodesic equation for massless particles and the explicit form of the deflection angle. We found that for various values of the impact parameter the deflection angle can be positive, negative, even zero in this black hole spacetime. The negative deflection angle indicates the repulsive behavior of the gravity.

BHT Massive Gravity

Bergshoeff, *et al.* (2009)

- Action

$$S = \frac{1}{16\pi G}\int d^3x\sqrt{-g}\left[R - 2\lambda - \frac{1}{m^2}\left(R_{\mu\nu}R^{\mu\nu} - \frac{3}{8}R^2\right)\right]$$

▶ Two DoFs of the massive graviton (Ghost free).

▶ Some nontrivial solution of BH spacetimes.

- SCS BH Spacetime

$$ds^2 = -(-\Lambda r^2 + br - \mu)dt^2 + \frac{dr^2}{-\Lambda r^2 + br - \mu} + r^2 d\phi^2$$

b : gravitational hair parameter Oliva, *et al.* (2009)

μ : mass parameter

$\boxed{\Lambda = 2\lambda = 2m^2}$ $\boxed{b > 0,\ \mu > 0,\ \Lambda < 0}$

▶ Curvature

$$R = 6\Lambda - \frac{2b}{r}$$

▶ Horizon

$$r_h = \frac{-b + \sqrt{b^2 - 4\Lambda\mu}}{-2\Lambda}$$

➡ $\Lambda = 0$: Asymptotically locally flat

Behavior of Null Geodesics

- Effective Potential V_{eff}

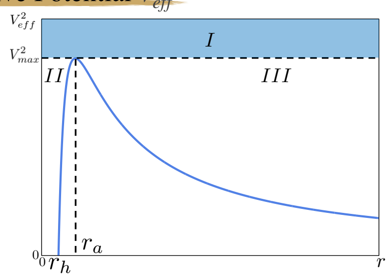

▶ One unstable circular orbit at r_a.

- Behavior of Null Geodesics in Region III

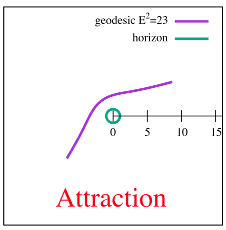

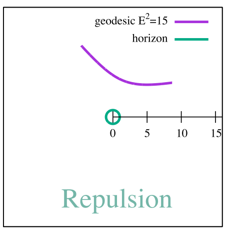

▶ In region III the gravity works repulsively for null geodesics with $E < L\sqrt{\frac{b^2}{4\mu} - \Lambda}$.

Deflection Angle

- Explicit Form

$$\alpha = \frac{1}{\sqrt{\mu}}\log\left|\frac{b\bar{D} + 2\sqrt{\mu}}{b\bar{D} - 2\sqrt{\mu}}\right| - \pi, \quad \bar{D}^2 = \frac{D^2}{1 + D^2\Lambda}$$

D : impact parameter

▶ We can obtain the expression for α exactly.

▶ α can be positive, negative, even zero for various values of $\bar{D}$

- Critical Value $\bar{D}_{\alpha=0}$

$$\bar{D}_{\alpha=0} = \frac{2\sqrt{\mu}}{b\tanh\frac{\pi\sqrt{\mu}}{2}}$$

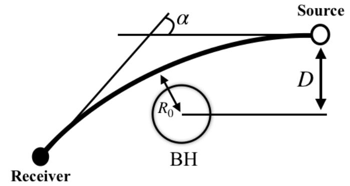

▶ This value is the boarder of the positive and negative deflection angle.

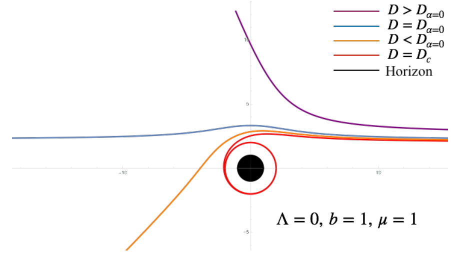

▶ b is essential for the repulsive behavior and the repulsive behavior appears only when b>0.

➡ It does not appear in the BTZ BH background.

Summary and Discussion

- We obtain the analytic solution for the geodesic eq. for massless particles in the SCS BH spacetime of the BHT MG.
- We derive the deflection angle analytically and find that it can be positive, negative, even zero.
- The negative deflection angle denotes the repulsive behavior of the gravity and the linear term br is essential for the repulsive behavior.
- Since BH solution of the Weyl gravity and dRGT MG contains the linear term, the repulsive behavior may also appear in four dimensions.

Yashmitha Kumaran
University of Sussex

“Gravitational waves from plasma turbulence”

[JGRG28 (2018) PB4]

GRAVITATIONAL WAVES FROM PLASMA TURBULENCE

Triggered by First-order Phase Transitions in the Early Universe

Prof Mark Hindmarsh, Yashmitha Kumaran

University of Sussex, United Kingdom

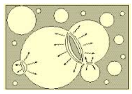

Principle: Gravitational wave emission ensuing from plasma turbulence driven by first-order phase transitions conveniently peaks at the Kolmogorov de-coherence frequency.

Symmetry Breaking: For a scalar field ϕ, vacuum expectation value corrected for temperature T, with coupling (α) and decoupling (λ) constants is given by:

$$V(|\phi|^2, T) = [(-m^2 + \alpha T^2)]\ |\phi|^2 + \lambda^2\ |\phi|^4$$

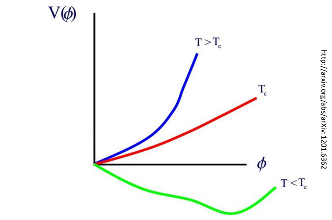

Figure 1: Variation of scalar field with its Potential for different values of temperatures

From Condensed Matter Physics of gauge bosons with mass m, $T_c^2 \equiv -m^2/\alpha$ is the critical temperature.

- $T^2 > T_c^2$ → Symmetric
- $T^2 < T_c^2$ → Symmetry broken!

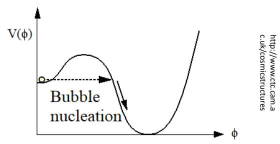

Figure 2: True vacuum bubble breaking the symmetry of the universe, instigating phase transition

Through broken phase bubbles, first-order phase transitions cooled the infant universe below T_c breaking symmetry.

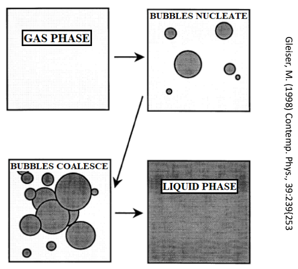

Figure 3: Gas phase undergoes phase transition into hydrodynamic phase resulting in plasma turbulence

While both first-order and second-order phase transitions are believed to have led to inflation, the dramatic effect of first-order phase transition is chosen over the smooth second-order phase transition.

Hydrodynamic turbulence: During the phase transition, plasma enters turbulent phase due to the formation of eddies through TURBULENT CASCADE!

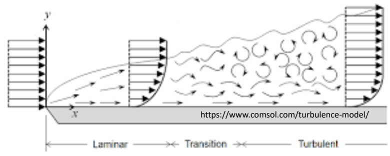

Figure 4: Transition to turbulence through eddies

According to the Kolmogorov model of eddies, **similarity principle** states that:

As Reynolds number of the fluid tends to infinity, the energy spectrum becomes independent of viscosity.

Velocity correlation function is the root mean squared velocity averaged over a physical time. Auto-correlation function of a system consistent with Kolmogorov turbulence is defined as:

$$\eta_k = \frac{1}{\sqrt{2\pi}} \varepsilon^{1/3} k^{2/3}$$

k : wavenumber; ε: energy dissipation rate per unit enthalpy; t: physical time.

Reference Models:

1. Stationary turbulence model: GKK[1]
2. Top-hat decorrelation model: CDS[2]

De-correlation function is obtained from the Kraichnan's *square exponential time dependence* equation by GKK model:

$$f(\eta_k, t) = \exp\left(-\frac{\pi}{4}\eta_k^2 t^2\right)$$

Induced anisotropic stress spectrum is positive when integrated, if the TOP HAT APPROXIMATION is applied, as done by CDS model:

$$\Pi(k, t_1, t_2)$$
$$\propto \Pi(k, t_1, t_1)\ \Theta\,(t_2 - t_1)\ \Theta\left(\frac{x_c}{k} - (t_2 - t_1)\right)$$
$$+\ \Pi(k, t_2, t_2)\ \Theta\,(t_1 - t_2)\ \Theta\left(\frac{x_c}{k} - (t_1 - t_2)\right)$$

This is taken as de-correlation function over the one proposed by GKK for the new model. Here, Θ is the Heaviside function.

Source:

To neglect expansion of universe when turbulence was on, the source is taken to be finite, continuous and short-lasting. Energy spectrum of stationary turbulent source with an anisotropic stress Π, is:

$$\frac{d\Omega_{GW}}{d\log k} \propto \int dt \cos(kt)\ \tilde{\Pi}(k, t_1, t_2)$$

SWEEPING HYPOTHESIS:

It assumes that spacetime correlations are pre-dominantly determined by root mean square velocity of the plasma.

Results of these models were replicated and the procedure was applied to the proposed model (DTM). Final plot of gravitational wave power spectrum with respect to k obtained from the analysis:

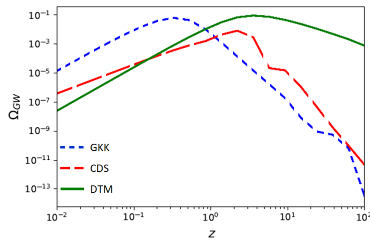

Figure 5: Variation of gravitational wave power spectrum against non-dimensionalised wavenumber

Unlike the reference models, this model is not limited to low Reynold's number, while it still retains the characteristics of the spectrum such as range and slope, as inferred by the reference models.

Amplitude (h_G) varies with frequency (f) in a similar fashion:

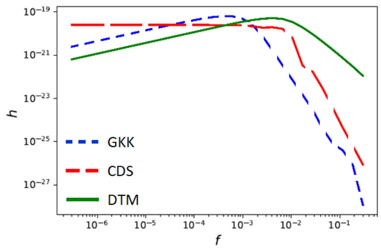

Figure 6: Variation of amplitude with frequency

Although the spectral behaviours have improved over the predicted range, this model possesses an inability to account for freely decaying turbulence.

Conclusion: Added to honing the peaks of the spectra, the source term demands modifications so that turbulence lasts longer than one Hubble time. Finer adjustments can improve experimental sensitivity of the gravitational wave detectors, enhancing the chances of successful detection in the future.

REFERENCES

1. Gogoberidze, G., et al (2007) Phys. Rev., D76:083002
2. Caprini, C., et al (2009) JCAP, 0912:024

ACKNOWLEDGEMENT

I sincerely thank my supervisor Prof Mark Hindmarsh for supporting me throughout this project.

Yukinobu Watanabe
Niigata University

“Data Analysis of Gravitational Waves from Standing Accretion Shock Instability of Core Collapse Supernovae with Hilbert-Huang Transform”

[JGRG28 (2018) PB5]

Data Analysis of Gravitational Waves from Standing Accretion Shock Instability of Core Collapse Supernovae with Hilbert-Huang Transform

Yukinobu Watanabe[1] ([1]Niigata University)

Y. Hiranuma[1], K. Oohara[1], K. Hayama[2], N. Kanda[3], K. Kotake[2], T. Kuroda[4],
K. Sakai[5], Y. Sakai[1],T. Sawada[3], H. Takahashi[6], T. Takiwaki[7], S. Tsuchida[3], T. Yokozawa[8]
([2]Fukuoka U., [3]Osaka City U., [4]T. U. Darmstadt, [5]Nagaoka CT, [6]Nagaoka U. of Tech., [7]NAOJ, [8]ICRR)

1. Introduction

We perform analysis of gravitational waves (GWs) by using Hilbert-Huang transform (HHT).We focus on the signal from standing accretion shock instability (SASI) [1]. In this poster, we report on the current results.

2. HHT of gravitational waves from a core collapse supernova

The GWs are decomposed into some Intrinsic Mode Functions (IMFs) by the Ensemble Empirical Mode Decomposition (EEMD) as Fig.1. The signal from SASI is captured in the 5th IMF (IMF5), the Instantaneous Amplitude (IA) and Instantaneous Frequency (IF) are plotted in Fig.2 as a function of time.

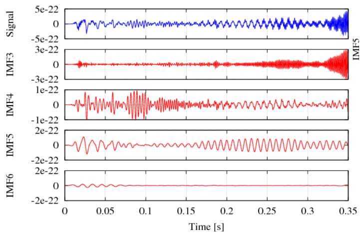

Fig.1

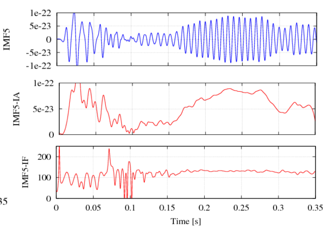

Fig.2

3. Time interval when the SASI mode appears

We will determine the time when the SASI mode appears in the waveform and characteristics of frequency.

- The frequency is apparently constant at $0.1\mathrm{s} \lesssim t \lesssim 0.35$ s.
- To determine the region where the frequency is constant,

- For $T_{\min} \lesssim T \lesssim T_{\max}$, $N_{\min} \lesssim N \lesssim N_{\max}$, where $N = T/\Delta t$ and Δt is the sampling interval of the data:
  - For various n_0, in the interval from $n = n_0$ to $n = n_0 + N$,
    - Calculate the average(*) of the frequency $\langle f \rangle$ and the standard deviation σ.
    - Find the value of n_0 for which σ is minimal.
  - Plot σ as a function N.

(*) The average is weighted by the amplitude (IA), assuming that the accuracy of the frequency (IF) is proportional to IA.

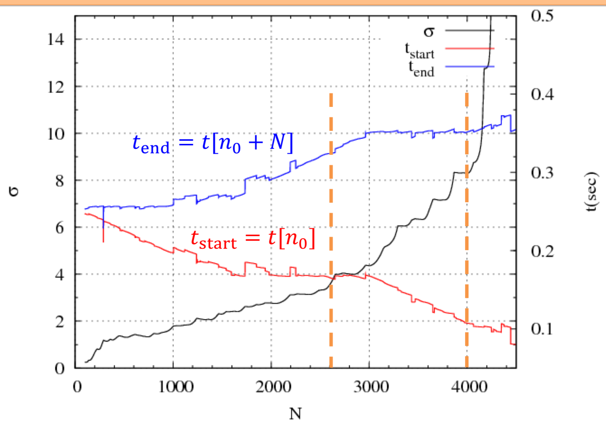

Fig.3

- The optimal interval is
  - $0.16\mathrm{s} \lesssim t \lesssim 0.33$ s (the left vertical line)

  or
  - $0.11\mathrm{s} \lesssim t \lesssim 0.35$ s (the right vertical line)

4. Checking whether the frequency is constant

- The linear and the quadratic regressions

$$f_{\mathrm{lin}}(t) = a_0 + a_1\tau, \qquad f_{\mathrm{quad}}(t) = b_0 + b_1\tau + b_2\tau^2$$

$$\tau = \frac{t - t_c}{t_{\mathrm{end}} - t_{\mathrm{start}}}, \qquad t_c = \frac{1}{2}(t_{\mathrm{start}} + t_{\mathrm{end}})$$

are made with the $(\mathrm{IA})^2$-weighted least-squares fitting to compare them with the constant-frequency.

$$\chi_{\mathrm{A}}^2 = \sum_{i=1}^{N} w(t_i)\left(f(t_i) - f_{\mathrm{A}}(t_i)\right)^2 \qquad [\mathrm{A} = \mathrm{lin}, \mathrm{quad}]$$

$$w(t_i) = \frac{a(t_i)^2}{\sum a(t_i)^2}$$

- Figure 4 shows the result of the interval $0.11\mathrm{s} \lesssim t \lesssim 0.35$ s.

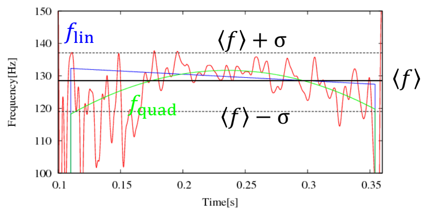

Fig.4

$\langle f \rangle = 128.5 \pm 8.6$

$a_0 = 129.9 \pm 1.0, \quad a_1 = -4.88 \pm 5.02$

$b_0 = 131.7 \pm 1.3, \quad b_1 = 1.51 \pm 5.58, \quad b_2 = -50.9 \pm 19.5$

$\chi_{\mathrm{const}}^2 = \sigma^2 = 74.1, \quad \chi_{\mathrm{lin}}^2 = 21.3, \quad \chi_{\mathrm{quad}}^2 = 14.4$

- For $0.16\mathrm{s} \lesssim t \lesssim 0.33$ s.

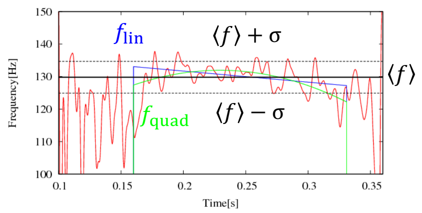

Fig.5

$\langle f \rangle = 129.8 \pm 4.9$

$a_0 = 130.1 \pm 1.0, \quad a_1 = -5.83 \pm 4.22$

$b_0 = 131.7 \pm 1.3, \quad b_1 = -5.20 \pm 4.24, \quad b_2 = -27.6 \pm 15.6$

$\chi_{\mathrm{const}}^2 = \sigma^2 = 23.8, \quad \chi_{\mathrm{lin}}^2 = 12.9, \quad \chi_{\mathrm{quad}}^2 = 9.77$

5. Conclusion and Future Works

- The frequency of the component considered to be SASI can be regarded as constant.
- The quadratic regression may be better, but it is caused by the end of SASI mode, outside of which the frequency of the IMF gets lower.
- We should confirm our proposed analysis method to more realistic case i.e. simulation noise plus signal and real noise plus signal.

6. Reference

[1] T. Kuroda, K. Kotake, and T. Takiwaki, ApJ, 827, L14 (2016)

Tadashi Sasaki
Hokkaido University

“Exact solutions of primordial gravitational waves”

[JGRG28 (2018) PB7]

Exact solutions of primordial gravitational wave

Tadashi Sasaki and Hisao Suzuki, Department of Physics, Hokkaido University, Japan
arXiv:1806.08052[astro-ph.CO]

1. Introduction

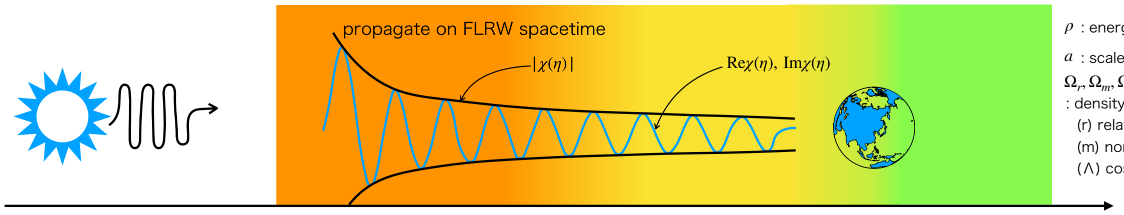

ρ : energy density
a : scale factor
$\Omega_r, \Omega_m, \Omega_\Lambda$
: density parameters of
(r) relativistic matter,
(m) non-relativistic matter,
(Λ) cosmological constant

GWs are produced
(e.g. inflation, phase transition,⋯)

$\rho = \frac{\Omega_r}{a^4}$ radiation dominant

$\rho = \frac{\Omega_m}{a^3}$ matter dominant

$\rho = \Omega_\Lambda$ Λ dominant

GW wave equation
$$\chi''(\eta) + 2\frac{a'(\eta)}{a(\eta)}\chi'(\eta) + k^2\chi(\eta) = 0$$

Friedmann equation
$$\left(\frac{a'}{a^2}\right)^2 = H_0^2\rho$$

- Absolute value of the amplitude $|\chi(\eta)|$ is physically important (strength of signals, energy density of GWs).
- Analytic solutions are known only for single component cases (e.g. radiation dominant, matter dominant,⋯).

We consider the time evolution of $y = |\chi(\eta)|^2$, instead of χ itself, on matter+cosmological constant, $\rho = \Omega_m/a^3 + \Omega_\Lambda$ background.

2. General formalism [1]

Essential idea

Consider 2nd order ODE:
$$\chi''(x) + p(x)\chi'(x) + q(x)\chi(x) = 0. \quad (1)$$
Instead of solving this ODE directly, we treat 3rd order ODE satisfied by the square of the two solutions:
$$y''' + 3py'' + (p' + 4q + 2p^2)y' + (2q' + 4pq)y = 0, \quad (2)$$
$$y \equiv \chi_+\chi_-.$$

How to construct χ from y

If once we obtain the solutions of (2), we can construct a constant associated with χ_+, χ_- :
$$C^2 = -\exp\left(2\int p(x)dx\right)\left[2yy'' + 2pyy' + 4qy^2 - (y')^2\right]. \quad (3)$$
The constant C can be represented by χ_+, χ_- ,
$$C = \exp\left(\int p(x)dx\right)(\chi_+\chi_-' - \chi_-\chi_+'). \quad (4)$$
By differentiating the definition of y,
$$y' = \chi_+\chi_-' + \chi_-\chi_+'. \quad (5)$$
Combining eqs. (3), (4), and (5), solutions for (1) can be derived from solutions of (2),
$$\chi_\pm = \exp\left[\pm\frac{C}{2}\int\frac{1}{y}\exp\left(-\int p(x)dx\right)dx\right]. \quad (6)$$

4. Matching condition

Solution with an initial condition
$$\chi(0) = c, \ \frac{d\chi}{d\eta}(0) = 0$$
is given by the following superposition:
$$\chi_C \equiv (\chi_+ - \chi_-)/2i,$$
$$\frac{\chi_C(a)}{\chi_C(0)} = \frac{3}{2\sqrt{2}\tilde{C}}\sqrt{\frac{1}{a^3} + \frac{8\tilde{k}^2}{a^2} + 4} \times \sin\left[\int_0^a \frac{\sqrt{2}\tilde{C}ada}{\sqrt{a + a^4}(1 + 8\tilde{k}^2 a + 4a^3)}\right]$$

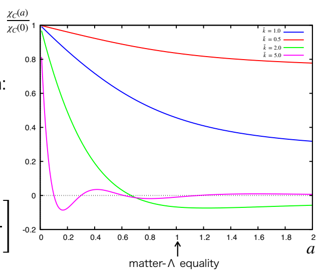

3. Application to GWs

3rd order ODE for the squared amplitude $y = |\chi(\eta)|^2$:
$$\left[\left\{\Omega_m a\left(\theta + \frac{3}{2}\right) + \Omega_\Lambda a^4(\theta + 6)\right\}(\theta + 3) + 4\tilde{k}^2 a^2(\theta + 2)\right] y = 0, \quad (8)$$
$\theta \equiv a\frac{d}{da}$, $\tilde{k} = \frac{k}{H_0}$, H_0 : Hubble constant at a=1

Surprisingly, it has a polynomial solution,
$$y = \frac{\Omega_m}{a^3} + \frac{4\tilde{k}^2}{a^2} + 4\Omega_\Lambda, \quad (9)$$

From the general formula (6), amplitude itself is derived:
$$\chi_\pm(\eta) = \frac{1}{\sqrt{2}}\prod_{j=1}^{3}\sqrt{\wp(\tilde{\eta}) - \wp(c_j)}\left[\frac{\sigma(c_j - \tilde{\eta})}{\sigma(c_j + \tilde{\eta})}e^{2\tilde{\eta}\zeta(c_j)}\right]^{\pm 2\sqrt{2}i\tilde{C}\Theta_j} \quad (10)$$
$\tilde{\eta} \sim H_0\eta$, $c_j, \Theta_j, \tilde{C}$: constants determined by k.
$\wp(z)$: Weierstrass elliptic function,
ζ and σ obey the following relations: $\wp(z) = -\zeta'(z)$, $\zeta(z) = \frac{\sigma'(z)}{\sigma(z)}$

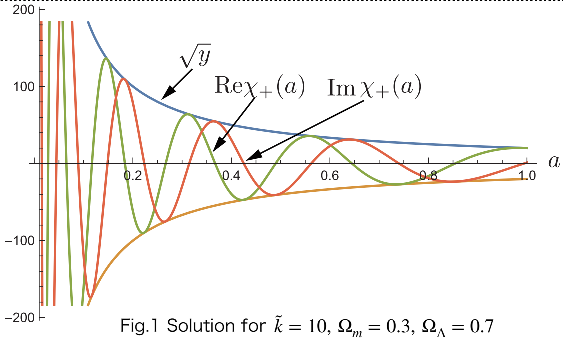

Fig.1 Solution for $\tilde{k} = 10$, $\Omega_m = 0.3$, $\Omega_\Lambda = 0.7$

5. Remarks

・Basic properties (wave number dependence and asymptotic behavior) are investigated in our paper[3].

・When the effect of radiation is included, i.e. $\Omega_r \neq 0$, 3rd order ODE (8) doesn't permit any polynomial solution, therefore we could not obtain closed form solutions.

References

[1] R. Burger, G. Labahn, M. van Hoeij, Proceeding of ISSAC '04 Proceedings of the 2004 international symposium on Symbolic and algebraic computation, (2004) 58-64
[2] For the definition and properties, see, Bateman, Harry, *Higher Transcendental Functions, vol.2,* McGraw-Hill (1953)
[3] T. Sasaki and H. Suzuki, arXiv:1806.08052[astro-ph.CO]

Kanna Takagi
Tokyo Gakugei University

“Realization of the Change of Effective Dimension in Gravity via Multifractional Theories”

[JGRG28 (2018) PB8]

PB8

Realization of the Change of Effective Dimension in Gravity via Multifractional Theories

Kanna Takagi, Shinpei Kobayashi and Arisa Sano
Department of Physics, Tokyo Gakugei University, JGRG28 @ Rikkyo University, 5-9 November, 2018

I. Introduction

candidates of quantum gravity (at small scale (high energy))

causal dynamical triangulation | string theory | noncommutative geometry …

Carlip(2017) Calcagni(2017)

Spacetime becomes effectively lower-dimensional
<- due to existence of minimal length

Example) Hausdorff dimension gets lower for spacetime with fractal structure

$$d_H(l) := \frac{d\ln V(l)}{d\ln l} \Longrightarrow V \propto l^{d_H}$$

(i)Square

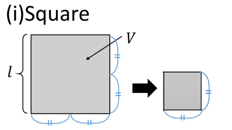

$$\frac{1}{4} = \left(\frac{1}{2}\right)^{d_H} \qquad d_H = 2$$

(ii) Sierpinski gasket (fractal)

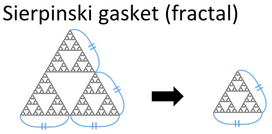

$$\frac{1}{3} = \left(\frac{1}{2}\right)^{d_H} \qquad d_H = \frac{\ln 3}{\ln 2} \sim 1.6$$

less than 2

Is it possible to change effective dimension at different scales?
multifractional theory

Does interesting physics appear?

e.g.) Log oscillation in discrete self-similar geometry

Random walk in Sierpinski gasket

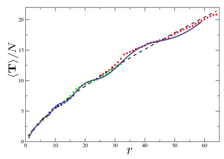

r : the source-target distance
the dotted points : numerical data
(gaskets of generation 3,4,5,6 respectively in yellow, blue, green, red)

Akkermans et al(2009)

II. Multifractional theory

x : coordinate of continuous spacetime
$\downarrow$
$q(x)$: coordinate of discretized spacetime with fractal structure

dimensional flow can be realized by q-coordinate

Definition

$$\frac{\partial}{\partial q^\mu(x)} = \frac{1}{v^\mu(x)}\frac{\partial}{\partial x^\mu} \Longleftrightarrow v^\mu(x) = \frac{\partial}{\partial x^\mu}q^\mu(x)$$

μ is not summed

$$q^\mu(x^\mu) = \begin{cases} x^i + \frac{l_*}{\alpha}\left|\frac{x^i}{l_*}\right|^{\alpha}\left[1 + A\cos\left(\omega\ln\left|\frac{x^\mu}{l_\infty}\right|\right) + B\sin\left(\omega\ln\left|\frac{x^\mu}{l_\infty}\right|\right)\right] \\ t + \frac{t_*}{\alpha_0}\left|\frac{t}{t_*}\right|^{\alpha_0}\left[1 + \underbrace{A\cos\left(\omega\ln\left|\frac{t}{t_\infty}\right|\right) + B\sin\left(\omega\ln\left|\frac{t}{t_\infty}\right|\right)}_{\text{log oscillation}}\right] \end{cases}$$

l_*, t_* : fundamental length scale
l_∞, t_∞ : Planck scale, Planck time
α, α_0 : fractional exponent (lacunarity(空隙性))
($0 < \alpha, \alpha_0 < 1$)

$$dV = dxdydz \to dq^1dq^2dq^3 \ , \quad q \sim x + Cx^\alpha$$

large scale $V \sim l^3 \to d_H = 3$
small scale $V \sim l^{3\alpha} \to d_H = 3\alpha < 3$ (dimensional flow)

III. Effect of dimensional flow

What should we see using multifractional theory? — e.g., Inflation Calcagni et al(2016)

reduction of dimension
$\downarrow$

- Reduction of DoF -> GW (and other waves) can exist?
- Propagation of GW in discretized spacetime would change?
- Log oscillation?

GW with maltifractional theory

$$\boxed{\begin{aligned} g_{\mu\nu}(q(x)) &= \eta_{\mu\nu} + h_{\mu\nu}(q(x)) \qquad |h_{\mu\nu}(q(x))| \ll 1 \\ \phi_{\mu\nu}(q(x)) &= h_{\mu\nu}(q(x)) - \frac{1}{2}hg_{\mu\nu}(q(x)) \end{aligned}}$$

$${}^q\Gamma^\rho_{\mu\nu} := \frac{1}{2}g^{\rho\sigma}(g_{\sigma\mu|\nu} + g_{\sigma\nu|\mu} - g_{\mu\nu|\sigma}) \qquad (\because \ | = \partial_q)$$

$${}^qR^\rho_{\mu\sigma\nu} := {}^q\Gamma^\rho_{\mu\nu|\sigma} - {}^q\Gamma^\rho_{\mu\sigma|\nu} + {}^q\Gamma^\gamma_{\mu\nu}{}^q\Gamma^\rho_{\gamma\sigma} - {}^q\Gamma^\gamma_{\mu\sigma}\Gamma^\rho_{\gamma\nu}$$

$${}^qR_{\alpha\mu\sigma\nu} = \frac{1}{2}(h_{\alpha\nu|\mu\sigma} - h_{\mu\nu|\alpha\sigma}) - \frac{1}{2}(h_{\alpha\sigma|\mu\nu} - h_{\mu\sigma|\alpha\nu})$$

Linearized Einstein equation

$$\phi^\sigma{}_{\mu|\nu\sigma} + \phi^\sigma{}_{\nu|\mu\sigma} - {}^q\Box\phi_{\mu\nu} - \eta_{\mu\nu}\phi^{\alpha\beta}{}_{|\beta\alpha} = 0$$

$\Downarrow$ TT gauge ($\phi^\sigma_{\mu|\sigma} = 0$, $\phi = 0$)

$$\frac{v^\nu{}_{,\sigma}}{v^\sigma(v^\nu)^2}\phi^\sigma{}_{\mu,\nu} + \frac{v^\mu{}_{,\sigma}}{v^\sigma(v^\mu)^2}\phi^\sigma{}_{\nu,\mu} + {}^q\Box\phi_{\mu\nu} = 0$$

$\Downarrow$ approximation

$$\left(\begin{aligned} &q^\mu \sim x^\mu + \epsilon\beta(x^\mu) \ , v^\mu \sim 1 + \epsilon F(x^\mu) \\ &\phi_{\mu\nu} = \phi^{(0)}_{\mu\nu} + \epsilon\phi^{(1)}_{\mu\nu} \ , \quad |\epsilon| \ll 1 \\ &\phi^{(0)}_{\mu\nu} = a_{\mu\nu}e^{-i(kt-kz)} + a_{\mu\nu}e^{-i(kt+kz)} \end{aligned}\right)$$

$$\Box\phi^{(1)}_{\mu\nu} = -\eta^{\alpha\sigma}[F(x^\nu)_{,\sigma}\phi^{(0)}_{\alpha\mu,\nu} - F(x^\mu)_{,\sigma}\phi^{(0)}_{\alpha\nu,\mu} - F(x^\sigma)_{,\alpha}\phi^{(0)}_{\mu\nu,\sigma}]$$

Preliminary result
: discretization in spatial direction $\left(F(t)_{,t} = 0, \ F(z)_{,z} = \left(\frac{z}{l_*}\right)^{\alpha-1}_{,z}\right)$

if $\alpha = \frac{1}{2}$ $\Longrightarrow$

$$\phi^{(1)}_{\mu\nu} = b_{\mu\nu}De^{-i(kt-kz)} + b_{\mu\nu}\beta'(i+1)\sqrt{k}\sqrt{\pi}\mathrm{Erf}[(1+i)\sqrt{k}\sqrt{z}]e^{-i(kt-kz)}$$

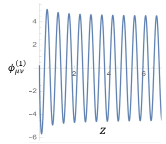

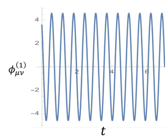

$$\beta' = \frac{a_{11}}{b_{11}}\frac{\alpha-1}{l_*^{\alpha-1}}$$

$b_{\mu\nu}$: amplitude tensor of $\phi^{(1)}_{\mu\nu}$

Amplitude changes at small scale.

IV. Summary & future works

- Using multifractional theory, we found GW can exist, even if there is dimensional flow.
- Propagation of GW in discretized spacetime changes at small scale.
- Effect of log oscillation? -> $F(z) = 1 + A\cos\left(\omega\ln\left|\frac{z}{l_\infty}\right|\right) + B\sin\left(\omega\ln\left|\frac{z}{l_\infty}\right|\right)$
- What $\phi_{|\mu\nu}$ means?
- Possibility of observation? -> evaluate of $<\phi^2>$

Satoru Sugimoto
Fukushima University Faculty of Symbiotic Systems Science

“The Research of Inflation Fields in Anisotropic Inflationary Cosmology”

[JGRG28 (2018) PB9]

The Research of Inflation Fields in Anisotropic Inflationary Cosmology

Satoru Sugimoto, Kazuharu Bamba
Fukushima University Faculty of Symbiotic Systems Science

Abstract

I research the cosmological magnetic fields and primordial gravitational waves in anisotropic inflationary cosmology. To clarify the origin of initial density fluctuations for the source of cosmological structure, I study the behavior of inflation fields by numerically.

1. Introduction

In the early universe, cosmic accelerated expansion occurred, called inflation. The fields caused inflation, inflaton, expand the space, after the fields decay the other particles and bring the generation of radiation.

In addition, the quantum fluctuations of fields are extended by the inflation, then those are the macroscopic fluctuations, which have been the seeds of structure formation of stars and galaxies in the universe.

Anisotropic inflation model considering the gauge fields has been proposed. The inflaton coupled to the gauge fields are caused anisotropic inflation.

2. Method

I researched the behavior of inflaton ϕ numericaly. The following simultaneous differential equation of three variables calculated.

$$\dot{\alpha}^2 = \dot{\sigma}^2 + \frac{1}{6}\kappa^2\dot{\phi}^2 + \frac{1}{6}\kappa^2 m_{pl}^2\phi^2 + \frac{1}{6}\kappa^2 p_A^2 e^{-c\kappa^2\phi^2-4\alpha-4\sigma} \quad (1)$$

$$\ddot{\alpha} = -3\dot{\alpha}^2 + \frac{1}{2}\kappa^2 m_{pl}^2\phi^2 + \frac{1}{6}\kappa^2 p_A^2 e^{-c\kappa^2\phi^2-4\alpha-4\sigma} \quad (2)$$

$$\ddot{\sigma} = -3\dot{\alpha}\dot{\sigma} + \frac{1}{3}\kappa^2 p_A^2 e^{-c\kappa^2\phi^2-4\alpha-4\sigma} \quad (3)$$

$$\ddot{\phi} = -3\dot{\alpha}\dot{\phi} - m_{pl}^2\phi + c\kappa^2 p_A^2 \phi e^{-c\kappa^2\phi^2-4\alpha-4\sigma} \quad (4)$$

e^{α} is a isotropic scale factor, σ is the variance from the isotropy. ($\dot{}\ = \frac{d}{dt}$ is derivative with time t, κ^2 is reduced gravitational constant, m_{pl} is plank mass, p_A is integral constant, c is a coupling constant.)

I studied the time evolution of these variables α, σ, ϕ.

3. Results

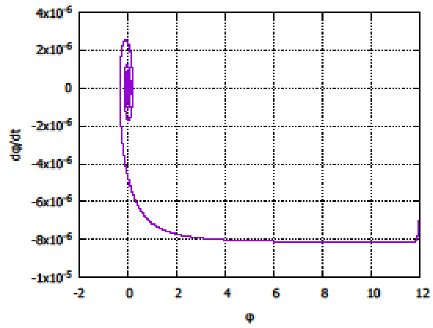

Fig.1 Phase space diagram of inflaton ϕ in isotropic inflation

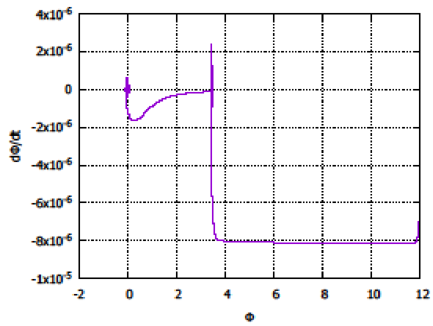

Fig.2 Phase space diagram of inflaton ϕ in anisotropic inflation

According to the method, I carried out numerical calculation. As the parameter, coupling constant is $c = 2$, $\kappa = 1.0$, $m_{pl} = 1.0 \times 10^{-5}$.

Calculation results show in the above figures. The case of the anisotropic inflation (Fig.2), the behavior of inflaton ϕ are different from the case of the isotropic one (Fig.1).

Conclusion

I researched the behavior of inflaton ϕ in anisotropic inflationary cosmology. The model is that inflaton interacted the gauge fields cause anisotropic inflation. I studied it by numerical calculation, and indicated the difference with isotropic inflation.

Keitaro Tomikawa
Rikkyo University

"Gauge dependence of gravitational waves induced by curvature perturbations"

[JGRG28 (2018) PB11]

Gauge dependence of gravitational waves induced by curvature perturbations

立教大学 RIKKYO UNIVERSITY

Keitaro Tomikawa Collaborator: Tsutomu Kobayashi

Background

Cosmological perturbation theory

$$\boxed{M_{\rm Pl}^2 G_{\mu\nu} = T_{\mu\nu}}$$

$$\downarrow \quad g+\delta g \quad T+\delta T \quad \textbf{+SVT decomposition}$$

Perturbed EoM for Scalar / Vector / Tensor mode

EoM of tensor mode

Linear $\quad h_{ij}^{(1)\prime\prime} + 2\mathcal{H}h_{ij}^{(1)\prime} - \Delta h_{ij}^{(1)} = 0$

2nd-order $\quad h_{ij}^{(2)\prime\prime} + 2\mathcal{H}h_{ij}^{(2)\prime} - \Delta h_{ij}^{(2)} = \partial_i\zeta^{(1)}\partial_j\zeta^{(1)} + \cdots$

2nd-order GWs are induced by scalar perturbations[1]

Power spectrum of 2nd-order GWs

$$P_h(k,\eta) = \frac{1}{a^2(\eta)}\int_0^\eta \mathrm{d}\eta_1 \int_0^\eta \mathrm{d}\eta_2 \int \mathrm{d}\tilde{\boldsymbol{k}}\ \underbrace{F(\boldsymbol{k},\tilde{\boldsymbol{k}},\eta_1,\eta_2)}_{\text{Time evolution of source terms}} \underbrace{P_\zeta(\tilde{k})P_\zeta(|\boldsymbol{k}-\tilde{\boldsymbol{k}}|)}_{\text{Primordial curvature spectrum}}$$

2nd-order GWs depend on

- **Barotropic parameter** w
- **Primordial curvature perturbation** $P_\zeta(k)$

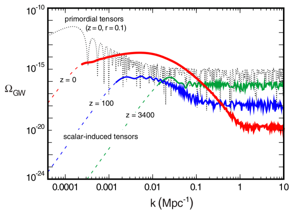

2nd-order GWs can be detected by future CMB observations[2]

$$P_\zeta(k) = A_\zeta = const$$

Problem

2nd-order tensor mode is Gauge dependent!!

Linear $\quad x^\mu \to x^\mu - \xi^{(1)\mu} \qquad \xi^\mu = (s, v^i)$

$$h_{ij}^{(1)} \to h_{ij}^{(1)}$$

2nd-order $\quad x^\mu \to x^\mu - \xi^{(1)\mu} + \frac{1}{2}\left(\xi^{(1)\mu}_{,\nu}\xi^{(1)\nu} - \xi^{(2)\mu}\right)$

$$h_{ij}^{(2)} \to h_{ij}^{(2)} + \partial_i s^{(1)}\partial_j s^{(1)} + \cdots$$

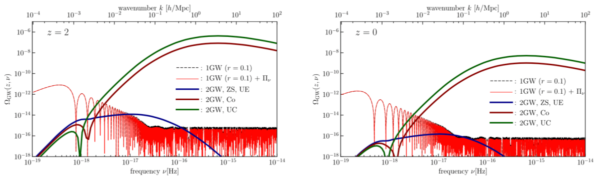

Gauge dependence of 2nd-order GWs at a large scale(MD)[3]

EoM of 2nd-order GWs

$$h_{ij}'' + 2\mathcal{H}h_{ij}' - \partial^2 h_{ij} = \underbrace{\Lambda_{ij}{}^{,kl}}_{\text{TT-projection tensor}} S_{kl}$$

Newtonian gauge

$$\mathrm{d}s^2 = -a^2(1+2\Phi)\mathrm{d}\eta^2 + a^2\left((1-2\Psi)\delta_{ij} + \frac{1}{2}h_{ij}\right)\mathrm{d}x^i\mathrm{d}x^j$$

Neglect the
- vector perturbation
- 1st-order GWs
- anisotropic stress

$$S_{ij} = 4\left[4\Phi\partial_i\partial_j\Phi + 2\partial_i\Phi\partial_j\Phi - \frac{4}{3(1+3w)}\partial_i\left(\mathcal{H}^{-1}\Phi' + \Phi\right)\partial_j\left(\mathcal{H}^{-1}\Phi' + \Phi\right)\right]$$

Comoving gauge

$$\mathrm{d}s^2 = -a^2(1+\delta N)\mathrm{d}\eta^2 + 2a\partial_i\chi\mathrm{d}\eta\mathrm{d}x^i + a^2\left((1+2\zeta)\delta_{ij} + \frac{1}{2}h_{ij}\right)\mathrm{d}x^i\mathrm{d}x^j$$

$$S_{ij} = 2\zeta_{,i}\zeta_{,j} - 4\delta N_{(,i}\zeta_{,j)} - 2\delta N_{,i}\delta N_{,j} - \frac{2}{a}\delta N'\chi_{,ij} + \frac{6}{a}\zeta'\chi_{,ij} + \frac{1}{a^2}\partial^2\left(\chi_{,i}\chi_{,j}\right)$$

The difference between the two gauges appears in the source term

- **The 2nd-order GWs were mainly calculated only in the Newtonian gauge**
- **Ref[3] shows the gauge dependence of the 2nd-order GWs at a large scale (in Matter Dominant era)**
- **Is there gauge dependence even in a small scale?**

Formalism and Results

$$S = \int \mathrm{d}^4x\sqrt{-g}\left[\frac{M_{\rm Pl}^2}{2}R + P(\phi, X)\right] \qquad X := -\frac{1}{2}g^{\mu\nu}\partial_\mu\phi\partial_\nu\phi$$

$$\mathrm{d}s^2 = -(1+2\delta N)\mathrm{d}t^2 + 2\partial_i\chi\mathrm{d}t\mathrm{d}x^i + a^2e^{2\zeta}\left(e^h\right)_{ij}\mathrm{d}x^i\mathrm{d}x^j$$

$\delta N, \chi, \zeta, h_{ij}$ **: Perturbations** $\quad s = (\delta N, \chi, \zeta)$

$P(\phi, X) = X^{\frac{1+w}{2w}} \Leftrightarrow$ **Perfect fluid satisfying** $p = w\rho$ **[4]**

$$S = S_{hh} + S_{hss} + S_{ss}$$

Integrate out

$\xrightarrow{\frac{\delta}{\delta(\delta N)}\ \frac{\delta}{\delta\chi}}$ **Hamiltonian / Momentum constraint** $\delta N(\zeta), \chi(\zeta)$

$\xrightarrow{\frac{\delta}{\delta\zeta}}$ **EoM of** $\zeta \longrightarrow \underline{\zeta = \zeta(\eta)}$

$\downarrow \frac{\delta}{\delta h^{ij}}$ **EoM of GWs**

$$h_{ij}'' + 2\mathcal{H}h_{ij}' - \Delta h_{ij} = \partial_i\zeta\partial_j\zeta + \cdots =: S$$

Fourier tr.
Using Green's function

$$h_{\boldsymbol{k}}^{\pm}(\eta) = \frac{1}{a(\eta)}\int^\eta \mathrm{d}\overline{\eta}\ G_k(\eta, \overline{\eta})a(\overline{\eta})S_{\boldsymbol{k}}^{\pm}(\overline{\eta})$$

$$\zeta_{\boldsymbol{k}}(\eta) = \underbrace{\zeta(k\eta)}_{\text{Transfer function}}\underbrace{Z_{\boldsymbol{k}}}_{\text{Primordial perturbation}}$$

$$\left\langle h_{\boldsymbol{k}}^{\pm}(\eta)h_{\boldsymbol{k}'}^{\pm}(\eta)\right\rangle = \frac{1}{a^2(\eta)}\int^\eta \mathrm{d}\eta_1\int^\eta \mathrm{d}\eta_2 G_k(\eta,\eta_1)a(\eta_1)G_{k'}(\eta,\eta_2)a(\eta_2)\underline{\left\langle S_{\boldsymbol{k}}^{\pm}(\eta_1)S_{\boldsymbol{k}'}^{\pm}(\eta_2)\right\rangle}$$

Using Wick's theorem

$$\langle Z_{\boldsymbol{k}}Z_{\boldsymbol{k}'}\rangle = \frac{2\pi^2}{k^3}P_\zeta(k)\delta(\boldsymbol{k}+\boldsymbol{k}')$$

Power spectrum of curvature perturbation

$$\left\langle h_{\boldsymbol{k}}^{\pm}(\eta)h_{\boldsymbol{k}'}^{\pm}(\eta)\right\rangle = \frac{2\pi^2}{k^3}P_h^{\pm}(k,\eta)\delta\left(\boldsymbol{k}+\boldsymbol{k}'\right)$$

The fraction of the GW energy density

$$\Omega_{GW}(k,\eta) = \frac{1}{24}\left(\frac{k}{a(\eta)H(\eta)}\right)P_h(k,\eta)$$

$$P_h(k,\eta) = \frac{1}{a^2(\eta)}\int_0^\eta \mathrm{d}\eta_1 \int_0^\eta \mathrm{d}\eta_2 \int \mathrm{d}\tilde{\boldsymbol{k}}\ \underbrace{F(\boldsymbol{k},\tilde{\boldsymbol{k}},\eta_1,\eta_2)}_{\text{contains transfer function depends on } w}P_\zeta(\tilde{k})P_\zeta(|\boldsymbol{k}-\tilde{\boldsymbol{k}}|)$$

- **In the RD universe** $\quad w = 1/3$
- **For the monochromatic curvature perturbation** $\quad P_\zeta(k) = A_\zeta\delta\left(\log\left(\frac{k}{k_*}\right)\right)$

e.g) $k_* = 3.5\times10^5\mathrm{Mpc}^{-1}$ **for PBH**

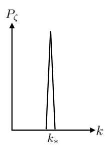

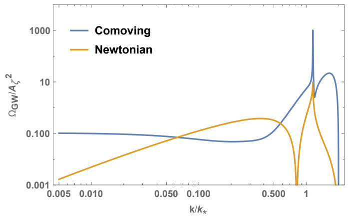

The gauge dependence of 2nd-order GWs is significant even in a small scale

References

[1] K.N.Ananda, et al. Phys.Rev.D75.1235188 (2007) [2] D.Baumann, et al. Phys.Rev.D76, 084019 (2007)
[3] J.Hwang, et al. Astrophys. J. 842, no. 1, 46 (2017) [4] L.Boubekeur, et al. JCAP 0808, 028 (2008)

Daiske Yoshida
Kobe University

"Separability of Equations of Form field in Schwartzschild spacetime"

[JGRG28 (2018) PB12]

JGRG2018 @ Rikkyo Univ.

Separability of Equations of Form field in Schwarzschild spacetime

Daiske Yoshida, Jiro Soda (Kobe University)

Motivation

- In higher dimensions, the form field generally. For examples, in 6 dimensions, there are the metric, the scalars, the vectors and the 2-form fields.
- But, there isn't the formalism of the master equations of the form field in arbitrary dimensions even on spherical BH solutions.
- So, we study the master equation of the form field in arbitrary dimensions.
- In this poster, we give the master equations of the 2-form field in arbitrary dimensions on spherical BH solution.

Spherical BH solution

- We are interested in spherical static solution for simplicity.
- One example is Schwarzschild-Tangherlini solution. The metric is given by $n \equiv D-2$

$$ds^2 = -f(r)\,dt^2 + \frac{1}{f(r)}dr^2 + r^2 q_{AB}dx^A dx^B. \quad f = 1 - \frac{\mu}{r^{n-1}}$$

- In 4-dimension, this solution becomes the Schwarzschild solution.

GWs on Schwarzschild solution

- Schwarzschild Spacetime(1916)

$$ds^2 = -f(r)\,dt^2 + \frac{1}{f(r)}dr^2 + r^2 q_{AB}dx^A dx^B, \quad f(r) \equiv 1 - \frac{2GM}{r}$$

- Perturbation on Schwarzschild BH(Regge-Wheeler(1957), Zerilli(1970)) $ds^2 = g^{\rm SBH}_{\mu\nu}dx^\mu dx^\nu + h_{\mu\nu}dx^\mu dx^\nu$

$$h^{\rm RW}_{\mu\nu} = \begin{pmatrix} 0 & 0 & v\mathscr{V}_A \\ 0 & 0 & w\mathscr{V}_A \\ v\mathscr{V}_A & w\mathscr{V}_A & {\rm O} \end{pmatrix} \quad h^{\rm Z}_{\mu\nu} = \begin{pmatrix} f\bar{H}Y & H_1 Y & 0 \\ H_1 Y & f^{-1}HY & 0 \\ 0 & 0 & r^2 KY q_{AB} \end{pmatrix}$$

$$\Delta_q \mathscr{V}^A_{lm} = (1-\gamma)\mathscr{V}^A_{lm} \qquad D_A \mathscr{V}^A_{lm} = 0 \qquad \Delta_q Y = -\gamma Y$$

- Master variable Ψ

Regge-Wheeler : $\dot{v} = f\,(fw)' \qquad w = \frac{r}{f}\Psi_{\rm RW}$

Zerilli : $\bar{H} = H = rK' - \frac{1}{2f}(\gamma+1-3f)K - \frac{\gamma}{2f}\Phi, \quad H_1 = \frac{r}{f}\left(\dot{\Phi} + \dot{K}\right)$

$$\Phi = \frac{\gamma+1-3f}{r}\Psi_{\rm Z}$$

Master equation of GWs

- The equations of motion of the GWs on Schwarzschild spacetime is

$$-\partial_x^2\Psi_A + V_A\Psi_A = \omega^2\Psi_A \qquad A = {\rm RW\ or\ Z}$$

$$V_{\rm RW} \equiv \frac{f}{r^2}\left(l\,(l+1) - 3\cdot\frac{2M}{r}\right)$$

$$V_{\rm Z} \equiv -\frac{f}{r^2}\frac{\gamma^3 - (3f+1)\,\gamma^2 + \left(9f^2 - 6f + 1\right)\gamma - \left(9f^3 - 9f^2 + 3f - 3\right)}{(3f-\gamma-1)^2}$$

- There is the method to the extension to higher dimensional theory. 例)Schwarzschild-Tangherlini: Kodama & Ishibashi (2003) Spherical and static Lovelock BH: Takahashi & Soda (2009)
- From these formulations, we can get the information of the higher dimensions. For examples, we study the stability of the BH solutions, QNMs, etc.

Form fields

- The form field is defined by $\boldsymbol{A} \equiv \frac{1}{p!}A_{a_1\cdots a_p}dx^{a_1}\wedge dx^{a_2}\wedge\cdots\wedge dx^{a_p}.$
- The equations of motion of the form field is given by

$$d\boldsymbol{F} = 0 \quad \text{and} \quad *d*\boldsymbol{F} = 0. \quad (\boldsymbol{F} \equiv d\boldsymbol{A})$$

- The existence of the form field in each dimensions are
in 4-dim : 0-form, 1-form, (2-form),
in 5-dim : 0-form, 1-form, (2-form, 3-form).
or in 6-dim : 0-form, 1-form, 2-form, (3-form, 4-form).
- The 2-form field in arbitrary dimensions is decomposed as follows,

$$A_{ab} = \begin{pmatrix} 0 & A_{tr} & A_{tA} \\ -A_{tr} & 0 & A_{rA} \\ -A_{tA} & -A_{rA} & A_{AB} \end{pmatrix} = \begin{pmatrix} 0 & \mathcal{A} & v_{:A} + V_A \\ -\mathcal{A} & 0 & w_{:A} + W_A \\ -(v_{:A} + V_A) & -(w_{:A} + W_A) & 2Z_{[A:B]} + A_{AB} \end{pmatrix}.$$

Here, we chose ${V_A}^{:A} = 0, \quad {W_A}^{:A} = 0 \quad \text{and} \quad {Z_A}^{:A} = 0$ for vector part and ${A_{AB}}^{:B} = 0$ for tensor part.

Gauge fixing method

- The p-form field have the gauge invariance as follows,

$$\boldsymbol{A} \to \tilde{\boldsymbol{A}} = \boldsymbol{A} + d\boldsymbol{\xi}. \qquad \boldsymbol{\xi} \to \tilde{\boldsymbol{\xi}} = \boldsymbol{\xi} + d\boldsymbol{\Lambda} \qquad d^2 = 0$$

For 2-form field, it is transformed by

$$A_{ab} \to \tilde{A}_{ab} = A_{ab} + \partial_a\xi_b - \partial_b\xi_a\,. \qquad \xi_a = \begin{pmatrix} T \\ R \\ s_{:A} + S_A \end{pmatrix} \qquad {S_A}^{:A} = 0$$

- But the scalar component s of ξ is automatically removed by the gauge transformation.
- The gauge transformation of the components of the 2-form field is given by

scalar $\tilde{\mathcal{A}} = \mathcal{A} + \dot{R} - T'\,, \quad \tilde{v} = v - T\,, \quad \tilde{w} = w - R\,,$

vector $\tilde{V}_A = V_A + \dot{S}_A\,, \quad \tilde{W}_A = W_A + S'_A\,, \quad \tilde{Z}_A = Z_A - S_A\,,$

and tensor $\tilde{A}_{AB} = A_{AB}\,.$

- We can choose the gauge condition as follows,

$$v \to \tilde{v} = v - T = 0, \quad w \to \tilde{w} = w - R = 0$$

$$\text{and} \quad Z_A \to \tilde{Z}_A = Z_A - S_A = 0\,.$$

This gauge is completely fixed.

- Finally, the 2-form field becomes $A_{ab} = \begin{pmatrix} 0 & \mathcal{A} & V_A \\ -\mathcal{A} & 0 & W_A \\ -V_A & -W_A & A_{AB} \end{pmatrix}.$
- This is similar to the Regge-Wheeler gauge or Zerilli gauge (1957).
- We use the scalar, vector, tensor harmonics.

Master equation of 2-form field

- From those ansatz, we can derive the master equations.

Scalar part is $\mathcal{A} = 0$.

Vector part is $V^{(n)}_{\mathscr{V}} \equiv \frac{f}{r^2}\left(\gamma^{(n)}_{\mathscr{V}} + (n-1)\,K + \frac{4-n}{2}\left(rf' - \left(\frac{n-2}{2}\right)f\right)\right).$

Tensor part is $V^{(n)}_{\mathscr{T}} = \frac{1}{r^2}f\left(\gamma^{(n)}_{\mathscr{T}} + 2K\,(n-2) + \frac{4-n}{2}\left(\left(\frac{6-n}{2}\right)f - rf'\right)\right) \quad (n \geq 3)\,.$

- The plots of the effective potential are given below.

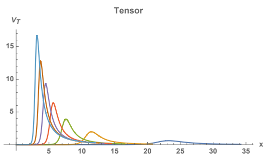

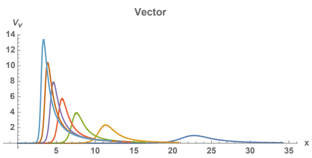

Quasinormal modes of 2-form field

- We can calculate the quasinormal mode if the potentials are positive definite.
- We use the 9-th order WKB method for the quasinormal mode which is invented by Schutz & Will (1985) and Iyer & WIll (1987).
- The results are

Tensor	QNM(preliminary)
D=6	1.2618 - 0.4615 i
7	1.7509 - 0.5920 i
8	2.2231 - 0.7192 i
9	2.6681 - 0.8555 i
10	3.0791 - 1.0080 i

and

Vector	QNM(preliminary)
D=6	1.2618 - 0.4615 i
7	1.5387 - 0.5652 i
8	1.8352 - 0.7345 i
9	2.2630 - 0.8521 i
10	2.6910 - 0.9444 i

Conclusion

- We studied the master equations of the 2-form field in arbitrary dimensions.
- We checked the relations between the master equations of the scalar field or the vector field and the master equations of the 2-form field.
- We found the positivity of the potential of the 2-form field in 6 - 10 dimensions under some parameter sets.
- We gave the QNM of the 2-form field in 6 - 10 dimensions.
- We must study the S-deformed potentials of the 2-form field.
- This analysis gives the hints of the extension for the master equation of the p-form field.

Masashi Kuniyasu
Yamaguchi-University

"Integrable higher-dimensional cosmology with separable variables in an Einstein-dilaton-antisymmetric field theory"

[JGRG28 (2018) PB13]

Integrable higher-dimensional cosmology with separable variables in an Einstein-dilaton-antisymmetric field theory

Masashi Kuniyasu, Kiyoshi Shiraishi, Kohjiroh Takimoto (Yamaguchi University)
Nahomi Kan (Gifu College)

based on Phys. Rev D **98**, 044054 (2018). (arXiv:1806.10263) [1]

We consider a D-dimensional cosmological model with a dilaton field and two $(D-d-1)$-form field strengths which have nonvanishing fluxes in extra dimensions. Exact solutions for the model with a certain set of couplings are obtained by separation of three variables. Some of the solutions describe accelerating expansion of the d-dimensional space. Quantum cosmological aspects of the model are also briefly mentioned.

1.Introduction

・Scalar fields may play important role of inflationary scenario or dark energy problem. Several models (for example, scalar field with exponential potential) have exact cosmological solutions.

・Dilaton gravity arises form low-energy effective theory of string theory.
→Scalar fields naturally appears with exponential potential. (Such theories often contains totally anti-symmetric tensor fields.)

・ In this work, we consider analytical solvable models of D-dimensional cosmology with a scalar dilaton and anti-symmetric tensor fields. Our model in which equation of motion can be expressed by three separate equations of Liouville-type.

Why exact solutions?

Exact solutions play the most important role in understanding and growing the crude concepts in many areas of physics!

2.Analytically Solvable Model

・D-dimensional model (there are **two** p-form field strengths)

$$S=\int d^Dx\sqrt{-g}\left[R-\sigma\frac{1}{2}(\nabla\Phi)^2-\frac{l}{2p!}e^{2\kappa\alpha\Phi}F^{(l)2}_{[p]}-\frac{r}{2p!}e^{-2\kappa\frac{\sigma}{\alpha}\Phi}F^{(r)2}_{[p]}\right] \quad ①$$

R ; Ricci scalar derived from the metric g_{MN} $(M,N=0,1,\dots,D-1)$

Φ ; s rela scalar field which has dilaton-like coupling to the p-form field strength $F^{(l)}_{[p]}$ and $F^{(r)}_{[p]}$

κ, α, l, r; constants, $\sigma=\pm1$ (+ ; canonical, − ; phantom)

・Ansatze (FLRW universe with $D-d-1$ extra dimensions)

$$ds^2=g_{MN}dx^Mdx^N=-e^{2n(t)}dt^2+e^{2a(t)}d\mathbf{x}^2+e^{2b(t)}d\Omega^2_{D-d-1}$$

Ricci tensor of the extra space is written by $\tilde{R}_{mn}=k_b(D-d-2)\tilde{g}_{mn}$

$\tilde{g}_{mn}$; metric of the extra space

k_b ; normalized to be −1, 0, 0

We futher consistently assume that the p-form field strength

$$p=D-d-1\,,\ F^{(l)}_{[D-d-1]\,d+1,d+2,\cdots,D-1}=F^{(r)}_{[D-d-1]\,d+1,d+2,\cdots,D-1}=f>0$$

p –form field strengths take ''constant'' (flux) value in the extra space

・Separation of variables

gauge choice $n(t)=da(t)+(D-d-1)b(t)$

Substituting the ansatze to our model ①, we get

$$S\propto\int dt\Big\{-d(d-1)\dot{a}^2-2d(D-d-1)\dot{a}\dot{b}-(D-d-1)(D-d-2)\dot{b}^2+\sigma\frac{1}{2}\dot{\Phi}^2$$
$$+(D-d-1)(D-d-2)k_be^{2[da+(D-d-2)b]}-\frac{1}{2}f^2\left[le^{2[da+\kappa\alpha\Phi]}+re^{2[da-\kappa\sigma\Phi/\alpha]}\right]\Big\}$$

If we set the constant $\kappa\equiv\sqrt{\frac{d(D-d-2)}{2(D-2)}}$, action as $S=\int L\,dt$ with

$$L=-\frac{1}{2}\frac{2(D-d-1)}{D-d-2}\left[d\dot{a}+(D-d-2)\dot{b}\right]^2+\frac{1}{2}\frac{\sigma}{\alpha^2+\sigma}\frac{2(D-2)}{d(D-d-2)}\left[d\dot{a}+\kappa\alpha\dot{\Phi}\right]^2$$
$$+\frac{1}{2}\frac{\alpha^2}{\alpha^2+\sigma}\frac{2(D-2)}{d(D-d-2)}\left[d\dot{a}-\kappa\frac{\sigma}{\alpha}\dot{\Phi}\right]^2$$
$$-\frac{V_1}{2}e^{2[da+(D-d-2)b]}-\frac{1}{2}f^2\left[le^{2[da+\kappa\alpha\Phi]}+re^{2[da-\kappa\sigma\Phi/\alpha]}\right],$$

where $V_1\equiv(D-d-1)(D-d-2)(-2k_b)$

The action can be written in three independent variables !

$$x(t)\equiv\sqrt{\frac{2(D-d-1)}{D-d-2}}[da+(D-d-2)b]\quad \lambda_2y\equiv da+\kappa\alpha\Phi\quad \lambda_3z\equiv da-\frac{\kappa}{\alpha}\Phi$$

Hereafter, we restrict σ=1 (canonical case)

with $\lambda_2\equiv\sqrt{\alpha^2+1}\,\kappa$, $\lambda_3\equiv\sqrt{\alpha^{-2}+1}\,\kappa$

Finally, we get the reduced cosmological Lagrangian

$$L=-\frac{1}{2}\dot{x}^2+\frac{1}{2}\dot{y}^2+\frac{1}{2}\dot{z}^2-\frac{V_1}{2}e^{2\lambda_1x}-\frac{lf^2}{2}e^{2\lambda_2y}-\frac{rf^2}{2}e^{2\lambda_3z}$$

This is just a Liouville type Lagrangian !
Then, we can derive exact solutions of the model.

However, there are so many solutions in our model. Detail discussion of them were done in our paper [1].

3.Accelerating Universe

・`` Physical '' ($d+1$)-dimensional metric and cosmic time

$$ds^2=e^{-\frac{2(D-d-1)b}{d-1}}g_{\mu\nu}dx^\mu dx^\nu+e^{2b}\tilde{g}_{mn}dx^mdx^n$$

is considered to define the Einstein frame of the (d+1)-dimensional space-time

thus,

$$ds^2=-e^{2[da(t)+(D-d-1)b(t)]}dt^2+e^{2a(t)}d\mathbf{x}^2+e^{2b(t)}d\Omega^2_{D-d-1}$$
$$=e^{-\frac{2(D-d-1)b}{d-1}}(-d\eta^2+S^2(\eta)d\mathbf{x}^2)+e^{2b}d\Omega^2_{D-d-1}\,,$$

where $S(\eta)=e^{a(t)+\frac{D-d-1}{d-1}b(t)}$, $d\eta=\pm e^{d[a(t)+\frac{D-d-1}{d-1}b(t)]}dt=\pm S^ddt$

・Judgments of the accelerating physical universe

$$\frac{dS}{d\eta}=S^{-d}\frac{dS}{dt}=-\frac{1}{d-1}\frac{dS^{1-d}}{dt},\quad \frac{d^2S}{d\eta^2}=-\frac{1}{d-1}S^{-d}\frac{d^2S^{1-d}}{dt^2}$$

$A(t)\equiv-S(t)^{d-1}\frac{d^2S^{1-d}(t)}{dt^2}>0$ Accelerating !

S is the `` physical '' scale factor of d -dimensional space in flat space in ($d+1$) dimensional view and η is the cosmic time for the ($d+1$)-dimensional space-time

・One of the example ($D=6$, $d=3$, $l=r=1$, $\alpha=1$, $q=1$ and $t_1=0$)

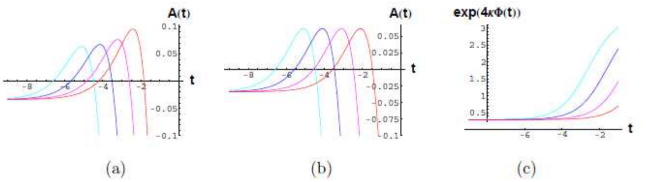

FIG. 1. $A(t)$ for $k_b=-1$ as a function of t in the canonical case. The curves correspond to the cases with $t_2=-3,-2,-1,0$ and $t_2-t_3=1$, according to location of the peak from left to right. (b) $A(t)$ for $k_b=0$ as a function of t. The choice of parameters are the same as (a). (c) exp $(4\kappa\Phi(t))$ as a function of t. The color of the curve corresponds to (a).

4.Quantum Cosmology

(We choose the natural unit $\hbar=1$)

・We can get Wheeler - De Witt equation $H\Psi=0$ by replacing $\dot{x}_a\to-i\frac{\partial}{\partial x_a}$

wave function of the universe

where $$H=\frac{1}{2}\frac{\partial^2}{\partial x^2}+\frac{V_1}{2}e^{2\lambda_1x}-\frac{1}{2}\frac{\partial^2}{\partial y^2}+\frac{lf^2}{2}e^{2\lambda_2y}-\frac{1}{2}\frac{\partial^2}{\partial z^2}+\frac{rf^2}{2}e^{2\lambda_3z}$$

・Normalizable wave function ($\sigma=1$, $l>0$ and $r>0$)

$$\Psi(x,y,z)=\int_{-\infty}^{\infty}dq\int_0^{2\pi}d\theta\,\mathcal{A}(q,\theta)\left[c_1F_{i\frac{q}{\lambda_1}}(\sqrt{V_1}e^{\lambda_1x}/\lambda_1)+c_2G_{i\frac{q}{\lambda_1}}(\sqrt{V_1}e^{\lambda_1x}/\lambda_1)\right]$$
$$\times\frac{2(\sqrt{l}f/(2\lambda_2))^{-iq\cos\theta/\lambda_2}}{\Gamma(-iq\cos\theta/\lambda_2)}K_{i\frac{q\cos\theta}{\lambda_2}}(\sqrt{l}fe^{\lambda_2y}/\lambda_2)$$
$$\times\frac{2(\sqrt{r}f/(2\lambda_3))^{-iq\sin\theta/\lambda_3}}{\Gamma(-iq\sin\theta/\lambda_3)}K_{i\frac{q\sin\theta}{\lambda_3}}(\sqrt{r}fe^{\lambda_3z}/\lambda_3)\,,$$

where $F_\nu(z)=\frac{1}{2\cos(\nu\pi/2)}[J_\nu(z)+J_{-\nu}(z)]$, $G_\nu(z)=\frac{1}{2\sin(\nu\pi/2)}[J_\nu(z)-J_{-\nu}(z)]$

c_1 and c_2 are constants

・Normarization of wave function

We refer C. de Lacroix, H. Erbin and E. E. Svanes, Phys. Lett. **B758** (2016) 186

coefficient of incomming planer waves are unity at $-\infty$

・Wave function $|\psi_q(\xi_1,\xi_2)|^2$

To simplify, we assume amplitude A is independent of θ. We define

$$\psi_q(\xi_1,\xi_2)\equiv\int_0^{2\pi}d\theta\,\frac{2(2)^{iq\cos\theta}}{\Gamma(-iq\cos\theta)}K_{iq\cos\theta}(e^{\xi_1})\frac{2(2)^{iq\sin\theta}}{\Gamma(-iq\sin\theta)}K_{iq\sin\theta}(e^{\xi_2})$$

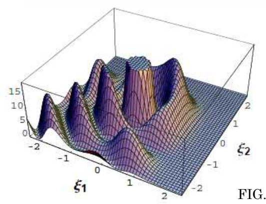

Many peaks of the function are located in the region $(\xi_1<0,\xi_2<0)$ and considerably high peaks are found $\xi_1\sim\xi_2$.

Probably density $|\Psi|^2$ appear at discrete positions where $\lambda_2y\sim\lambda_3z$, i.e., $\Phi\sim0$ for $\alpha\sim1$.
→ Stationary value of dilaton field.

FIG. 2. $|\psi_q(\xi_1,\xi_2)|^2$ with $q=4$

Yamato Matsuo
Hiroshima University

"Chameleonic Dark Matter in Logarithmic F(R) gravity"

[JGRG28 (2018) PB14]

Chameleonic Dark Matter in Logarithmic F(R) gravity

Hiroshima University Yamato Matsuo in collaboration with T. Inagaki, S. D. Odintsov, H. Sakamoto

Motivation

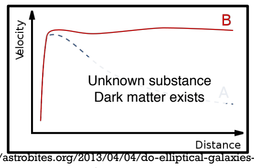

https://astrobites.org/2013/04/04/do-elliptical-galaxies-have-dark-matter-halos/

The universe expands

The unknown energy source Dark matter exists

Bring new particles or Expand general relativity

Introduce new particle →**Explain dark matter**

Modified gravity theory →**Explain dark energy**

We explain the dark matter by F(R) gravity of modified gravity theory

What is Dark Matter ?

F(R) gravity is ...

Einstein–Hilbert action

$$S=\frac{1}{2\kappa^2}\int d^4x\sqrt{-g}R$$

F(R)gravity

$$S=\frac{1}{2\kappa^2}\int d^4x\sqrt{-g}F(R)$$

For a review, S. Nojiri and S. D. Odintsov, Phys, Rept, 505 (2011) 59-144

$$g_{\mu\nu}\to\tilde g_{\mu\nu}=e^{2\kappa\varphi(x)/\sqrt6}g_{\mu\nu} \qquad F'(R)=e^{2\kappa\varphi/\sqrt6}$$

$$S=\frac{1}{2\kappa^2}\int d^4x\sqrt{-\tilde g}\tilde R+\int d^4x\sqrt{-\tilde g}\left[-\frac12\tilde g^{\mu\nu}(\partial_\mu\varphi)(\partial_\nu\varphi)-V(\varphi)\right]+\tilde S_{Matter}$$

We call the scalar particle "scalaron".

Interaction term

vector	Fermion	Boson
$\frac{\kappa m_V^2}{\sqrt6}\varphi\tilde g^{\mu\nu}A_\mu A_\nu$	$\frac{\kappa m_F}{\sqrt6}\varphi\bar\xi\xi$	$\frac{2\kappa m_S^2}{\sqrt6}\varphi\Theta^*\Theta$

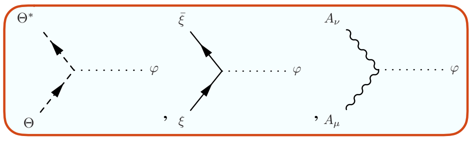

Contradiction from observation ??

This problem is solved by the mechanism of scalaron mass

The definition of scalaron mass

If the effective potential has a minimum, there is a stable ground state for the scalaron field

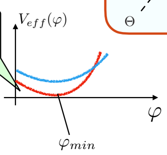

The effective potential of scalaron

$$V_{eff}(\varphi)\equiv\frac{1}{2\kappa^2}\frac{F'(R(\varphi))R(\varphi)-F(R(\varphi))}{F^2(R(\varphi))}-\frac14 e^{-4\kappa\varphi/\sqrt6}T^\mu_\mu$$

The EoM of scalaron

$$\left(\tilde\Box-V''_{eff}\big|_{\varphi=\varphi_{min}}\right)\varphi=0$$

regard as mass m_φ^2

The effective potential depends on the trace of Energy-Momentum Tensor

The scalaron mass also depends on the trace of EMT → $m_\varphi(T^\mu_\mu)$

The scalaron mass varies with background

In a vacuum Light = $V_{eff}(\varphi)$ is constant → cause the effect of DE

On the matter field Heavy → the interaction is screened out

Because the wave length becomes short

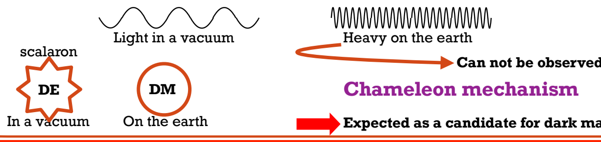

Can not be observed

Chameleon mechanism

Expected as a candidate for dark matter

Logarithmic F(R)

$$F(R)=R-\Lambda_{DE}\left[1-\alpha\frac{R}{R_C}\ln\left(\frac{R}{R_C}\right)\right]+\kappa^2\gamma_0\left[1+\gamma_1\ln\left(\frac{R}{R_0}\right)\right]R^2$$

S. D. Odintsov, V. K. Oikonomou and L. Sebastiani, Nucl. Phys. B923, 608 (2017) doi: 10.1016/j.nuclphy.

α,γ_0,γ_1 : free constant parameters
R_0 : inflation scale parameter
R_C : DE scale parameter

Our F(R) model is motivated by one-loop corrections to coupling constants.

The Starobinsky inflation model

$$F(R)=R+f_{DE}(R)+\kappa^2\gamma(R)R^2$$

Cause DE effect **Cause inflation effect**

We assume following replacement and DE term also transform as logarithmic.

$$\gamma(R)\to\gamma_0\left[1+\gamma_1\ln\left(\frac{R}{R_0}\right)\right]$$

We impose constraints for parameters by following condition,

(1)explain inflation era and DE era →**Either the Λ_{DE} term or the R^2 term becomes effective**
(2)Inflation dominant era →**Parameters are constrained by the observed value of CMB**
(3)DE dominant era (explain DM) →**The scalaron explains the current DM in DE dominant era**

Constraint (1)

For a small curvature the DE term should be neglected,

$$R_0,\kappa^2\gamma_0\left[1+\gamma_1\ln(O(1))\right]R_0^2\gg\Lambda_{DE}\left[1-\alpha\frac{R_0}{R_C}\ln\left(\frac{R_0}{R_C}\right)\right].$$

For a large curvature the R² term should be neglected,

$$R_C,\Lambda_{DE}[1-\alpha\ln(O(1))]\gg\kappa^2\gamma_0\left[1+\gamma_1\ln\left(\frac{R_C}{R_0}\right)\right]R_C^2.$$

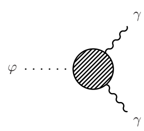

For example,
Massive boson loop
Massive fermion loop

Scalaron lifetime should be longer than the age of the universe

$$\Gamma^{-1}_{\varphi\to\gamma\gamma}>10^{17}s$$

Upper bound for the scalaron mass is obtained

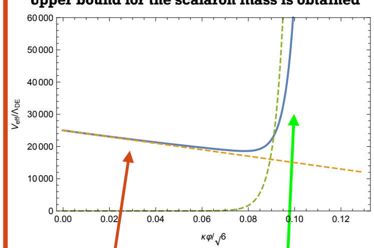

For a small φ, $V_{eff}(\varphi)$ becomes linear function.
For a large φ, $V_{eff}(\varphi)$ becomes increasing function.
For a large ρ, $V_{eff}(\varphi)$ has a stable point.

$$\rho>\left(\frac{R_C}{e\kappa^2}-\frac{2\alpha\Lambda_{DE}}{e\kappa^2}-\frac{2\Lambda_{DE}}{\kappa^2}\right)$$

Constraint (2)

To satisfy the current CMB fluctuations, the model parameters are constrained as follow,

$N\sim 50-60$
$n_s=0.9652\pm0.0042$
$\ln(10^{10}A_s)=3.043\pm0.014$
$r<0.106$

$\gamma_0=(0.88\sim1.2)\times10^9$
$\gamma_1=(1.0\sim1.4)\times10^{-6}$
$R_0/\Lambda_{DE}=1.8$

N. Aghanim *et al.* [Planck Collaboration], arXiv:1807.06209 [astro-ph.CO].

The upper bound for the scalaron mass

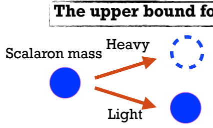

Most of scalarons have already decayed, and washed out.

Scalarons rarely decay and remain in the current universe

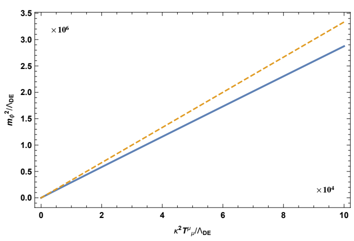

The solid line corresponds to the numerical result.
The dashed line corresponds to the approximated values.

$$m_\varphi^2\simeq\frac{\kappa^2R_C\rho}{3\alpha\Lambda_{DE}} \quad\Rightarrow\quad \frac{R_C}{\Lambda_{DE}}\le O(10^{55})\alpha$$

We obtain the constraint from the upper bound of mass.

Constraint (3)

The scalaron which is the candidate for DM must have a stable vacuum solution, and the life time of scalaron is long enough.

The scalaron decay to $\gamma\gamma$ via the SM particle from $\tilde S_{Matter}$

→**γ γ decay occurs**

In the solar system scale, the upper bound is

$$\rho_\odot\sim10^{-17}\text{GeV}^4 \qquad m_\varphi\le O(1)\text{GeV}.$$

*The effect of pressure is ignored

T. Katsuragawa, S.Matsuzaki. Phys.Rev. D95 (2017)

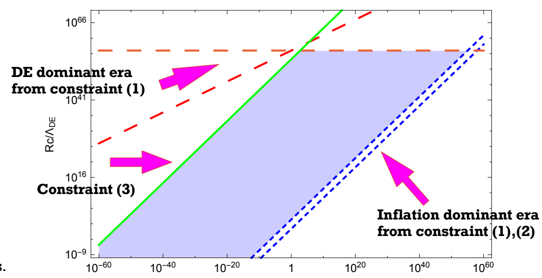

Constraints for α and R_C/Λ_{DE} : Colored area is allowed region.
In the area, our model can explain the inflation era and the DE era with DM, $V_{eff}(\varphi)$ has a stable point and the life time of scalaron is large enough.

Conclusion

We have checked if the logarithmic F(R) gravity can explain both the inflation dominant and the DE dominant era. Furthermore, we obtain constraints of the model parameters to explain DM, the scalaron gives a stable vacuum and the life time is longer than the age of the universe. To obtain a concrete constraint for the life time we have to evaluate the relic abundance of the DM. It can be obtained from the relation between the decay rate of scalaron and the energy density.

Kouji Nakamura
National Astronomical Observatory of Japan

"Extension of the input-output relation for a Michelson interferometer to arbitrary coherent-state light sources: Gravitational-wave detector and weak-value amplification"

[JGRG28 (2018) PB15]

Poster No. PB15

Extension of the input-output relation for a Michelson interferometer to arbitrary coherent state light sources:

--- Gravitational-wave detector and weak-value amplification ---

JGRG28@Rikkyo Univ. (Nov. 5th – 9th, 2018)

Kouji Nakamura (NAOJ)

Contents :

References:

K.N. and M.-K. Fujimoto, Ann. Phys. **392** (2018), 71.
A. Nishizawa, PRA **92** (2015), 032123.
A. Nishizawa, K.N., and M.-K. Fujimoto, PRA **85** (2012), 062108.
H. Miao, PhD Thesis, The Univ. of Western Australia (2010).

I. Introduction

1-1. Weak measurement in terms of density matrix:

Density matrix for the total system : $\rho = \rho_s \otimes \rho_d$

System : $\rho_s = |\psi_i\rangle\langle\psi_i|$ Measuring device : $\rho_d = |\phi\rangle\langle\phi|$

Pre-selection

Weak interaction : $\mathcal{H} = g\delta(t-t_0)\mathbf{A}\otimes P \qquad (g\Delta P \ll 1)$

$\mathbf{A}$: an operator associated with the System ρ_s

P : the momentum conjugate to the pointer variable Q associated with the Measuring device : ρ_d

Post-selection of the system : $\rho' \to \rho'\Pi_f \qquad \Pi_f = |\psi_f\rangle\langle\psi_f|$

The density matrix of the detector after the post-selection : $\rho'_d = \dfrac{\mathrm{tr}_s\rho'\Pi_f}{\mathrm{tr}\rho'\Pi_f}$

When $\langle P|\phi\rangle$ is even, $\langle P^n\rangle = 0, \quad (n\text{: odd}) \qquad \delta Q := \mathrm{tr}_d\left(Q\rho'_d\right) - \mathrm{tr}_d\left(Q\rho_d\right)$

$$\delta Q = g\mathrm{Re}\mathbf{A}_w + g\mathrm{Im}\mathbf{A}_w\langle\{Q,P\}\rangle + O(g^2),$$
$$\delta P = 2g\mathrm{Im}\mathbf{A}_w\langle P^2\rangle + O(g^2).$$
Jozsa (2007)

Weak value : $\mathbf{A}_w := \dfrac{\langle\psi_f|\mathbf{A}|\psi_i\rangle}{\langle\psi_f|\psi_i\rangle},$ --> **Weak-Value Amplification (WVA)**

I-2. Nishizawa model (1)

The Nishizawa model is a simple application of WM to GW detectors. (Michelson interferometer, A. Nishizawa, PRA **92** (2015), 032123.)

(Cf. N. Brunner and C. Simon, PRL **105** (2010), 010405.)

- The operator of the system to be measured is which path information in Michelson int..

  $\mathbf{A} = |y\rangle\langle y| - |x\rangle\langle x|$ $\boxed{\mathbf{A}^2 = 1}$

- Pre-selection : $|\psi_i\rangle = \frac{1}{\sqrt{2}}\left(ie^{i\phi/2}|y\rangle + e^{-i\phi/2}|x\rangle\right).$

- The observable of the measuring device is photon's momentum "p" (frequency) (which measures the phase shift induced by the mirror displacements).

- Weak interaction :

  $\mathcal{H} = gp \otimes \mathbf{A}\delta(t - t_0), \quad g = -2l.$

- Post-selection :

  $|\psi_f\rangle = \frac{1}{\sqrt{2}}(|y\rangle - |x\rangle).$

- Weak value : $\boxed{\frac{\langle\psi_f|\mathbf{A}|\psi_i\rangle}{\langle\psi_f|\psi_i\rangle} = -i\cot\frac{\phi}{2}.}$

  (imaginary)

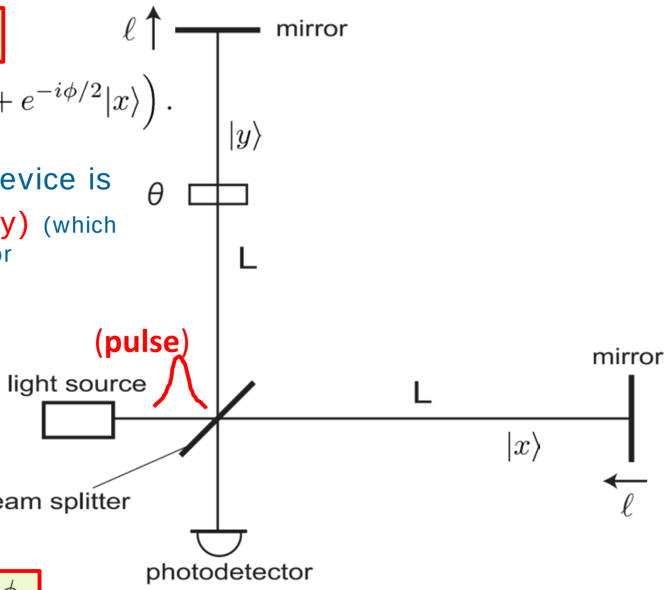

I-2. Nishizawa model (2) : Shot-noise in phase measurements

The density matrix of MD after the post-selection : $\rho'_d = \frac{|\Phi'\rangle\langle\Phi'|}{\langle\Phi'|\Phi'\rangle}, \quad |\Phi'\rangle = \int dp\Phi(p)|p\rangle\langle\psi_f|e^{-ig\mathbf{A}p}|\psi_i\rangle.$

For a single photon, the "signal" (the frequency shift) is given by

$$\langle\omega\rangle' = \int d\omega\omega\langle\omega|\rho'_d|\omega\rangle, \qquad \int d\omega\langle\omega|\rho'_d|\omega\rangle = 1,$$ ($\langle\omega\rangle'$ includes weak value.)

Assume that the output in each frequency mode is a coherent state.

---> The photon number $n(\omega)$ fluctuates (Poisson distribution).

$n(\omega) = \overline{n(\omega)} + \Delta n(\omega),$ averaged photon number : $\overline{n(\omega)} = N_{out}\langle\omega|\rho'_d|\omega\rangle,$

The observed frequency shift : $\tilde{\omega} = \frac{1}{N_{out}}\int d\omega\omega n(\omega) = \langle\omega\rangle' + \Delta\omega$

Shot noise : $\Delta\omega := \frac{1}{N_{out}}\int d\omega\omega\Delta n(\omega),$ $\boxed{\mathrm{Var}[\Delta\omega] = \langle(\Delta\omega)^2\rangle_P = \frac{1}{N_{out}}\langle\omega^2\rangle'}$

Here, we used mode independency: $\boxed{\langle\Delta n(\omega)\Delta n(\omega)\rangle_P = \overline{n(\omega)}\delta(\omega - \omega').}$

Detection limit of the mirror displacement: we set "signal"/"shot noise" =1 and solve for l.

$$\boxed{l_{min} = \underbrace{\frac{\lambda_0}{4\pi\sqrt{2N_{in}}\cos(\theta/2)}}_{\text{Detection limit for the conventional continuous monochromatic laser.}}\left(\frac{\sigma_\omega}{\omega_0}\right)^{-1}.}$$

Nishizawa model is weaker against shot noise.

I-2. Nishizawa model (3) : Radiation-pressure noise

In the research on quantum noise in GW detectors, not only the shot noise in the laser but also the radiation-pressure noise is important.

- **Radiation-pressure noise:**

  random shot noise in laser ---> random motion of mirrors (EOM of mirrors)
  ---> random noise in the reflected laser
  ---> radiation-pressure noise in data

To treat this radiation-pressure noise, (as far as I know,) QED treatments of the interferometer (a standard treatment of quantum noise in GW detectors) is necessary.

If we want to discuss the problem whether the ideas of weak-measurements are applicable to gravitational-wave detectors, or not, QED treatments, which are same level of the standard treatment of quantum noise in GW detector, is necessary.

I-4. A. Nishizawa, PRA 92 (2015), 032123.

- Shot noise and radiation-pressure noise in this model are evaluated through the QED analyses. However, **it is assumed that the mirror displacements are almost constant in the analyses.**
- The weak-value amplification in this model is realized only by classical carrier field.
- This model is weaker than the conventional gravitational-wave detector against shot noise (as previous analyses).
- The weak-value amplification cannot reduce radiation-pressure noise, neither.
  - The radiation-pressure noise is arose from the random motion of the mirrors and weak-value amplification also amplifies this random motion. Then, there is no improvement in the signal-to-noise ratio.
- There is a “standard quantum limit” as in the usual gravitational-wave detectors.

I-5. K.N. and M.-K. Fujimoto, Ann. Phys. 392 (2018), 71.

- We consider the “extension of the input-output relation for the Michelson interferometer to arbitrary coherent light-sources.”
- This extension enable us to discuss the conventional Michelson gravitational-wave detector and weak-value amplification from the same input-output relation.
- The key difference from [A. Nishizawa, PRA 92 (2015), 032123.]:
  - We consider the continuous measurement of the time-dependent end-mirrors’ displacement through the pulse train. (No correlated each mode coherent state.)
    - Nishizawa discussed the shot noise and the radiation-pressure noises in each pulse.
    - We want to measure gravitational-wave signals in the frequency range 10 Hz – 10 kHz.
  - If we inject the femtosecond pulses, a sufficiently large number of pulses are used to measure the signal with 10 kHz and the output signal is averaged these many pulses.
    - **We regard that the output signals in the frequency domain are given as the result of this average of many pulses.**

- The meaning of the “constant displacement in time”?

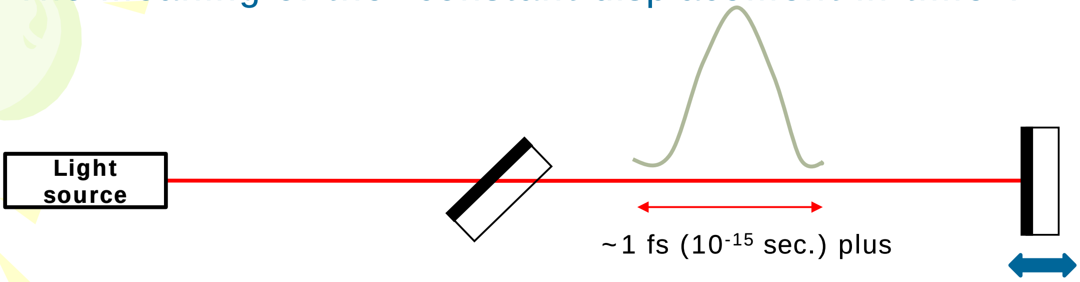

If we concentrate on 1 plus, the time-variation due to GW is extremely small.

<u>However, we cannot regard GW-signal as a signal within this treatment.</u>

- Then, ・・・・・

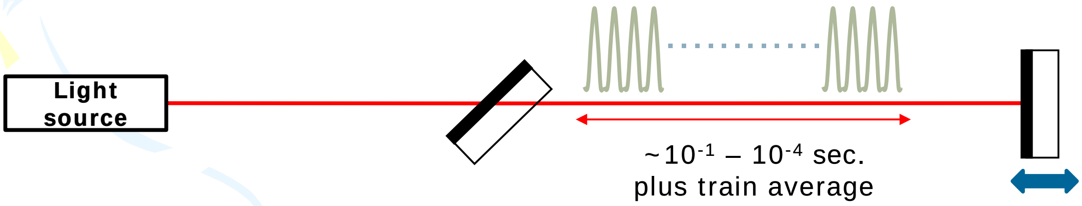

$$E(\omega) := \int_{-\infty}^{+\infty} dt E(t) e^{+i\omega t}$$

: We regard the time-integration in Fourier transformations as “the average of many pulses.

Further, we regard the system is almost stationary as the result of the average of many pulses.

II. Michelson weak measurement setup

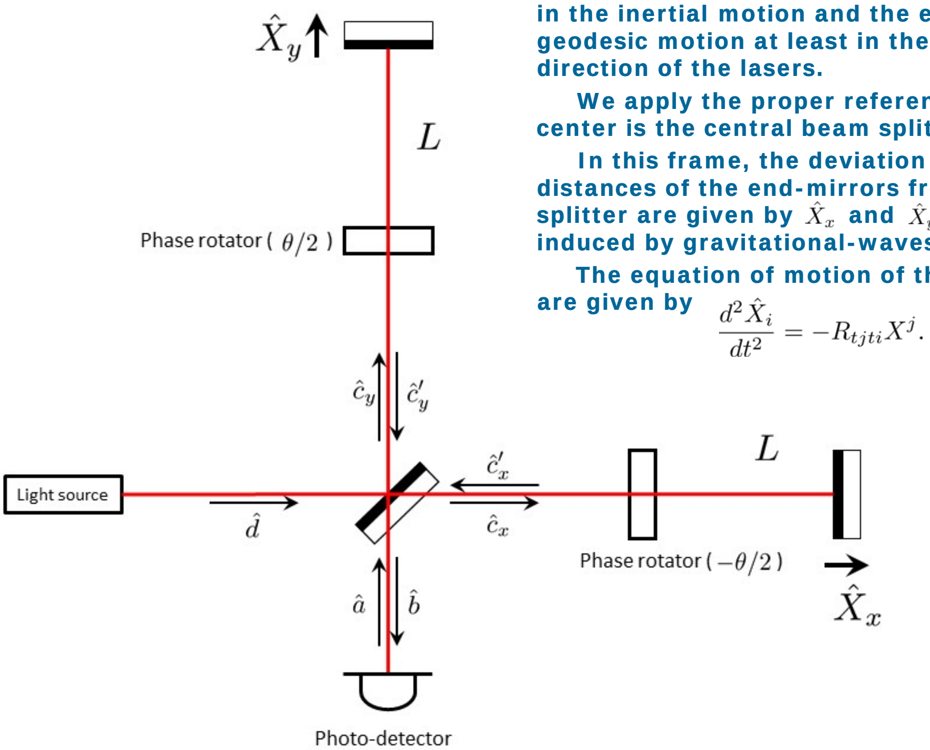

We assume that the central beam splitter is in the inertial motion and the end-mirrors in the geodesic motion at least in the longitudinal direction of the lasers.

We apply the proper reference frame whose center is the central beam splitter.

In this frame, the deviation of the geodesic distances of the end-mirrors from the beam splitter are given by $\hat{X}_x$ and $\hat{X}_y$, which are induced by gravitational-waves.

The equation of motion of the end-mirrors are given by $\frac{d^2 \hat{X}_i}{dt^2} = -R_{tjti} X^j.$

III. Extension of input-output relation to arbitrary coherent state

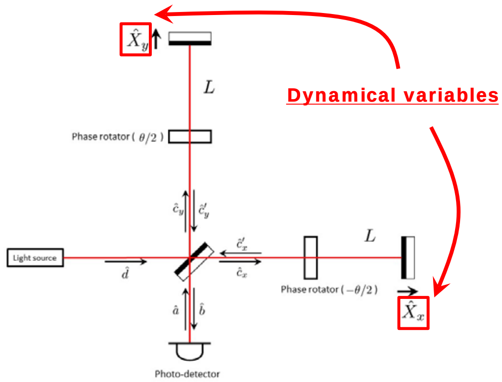

Here, we regard the mirrors are under the free motion (geodesic motion) except for the radiation pressure due to the light source.

In this case, we have to treat the Bogolyubov transformation and it is convenient to introduce the notation for the electric field as

$$\hat{E}_a(t-z) = \int_{-\infty}^{+\infty} \frac{d\omega}{2\pi} \sqrt{\frac{2\pi\hbar|\omega|}{\mathcal{A}c}} \hat{A}(\omega) e^{-i\omega(t-z)},$$

where the operator $\hat{A}(\omega)$ is defined by

$$\hat{A}(\omega) := \hat{a}(\omega)\Theta(\omega) + \hat{a}^\dagger(-\omega)\Theta(-\omega) = \begin{cases} \hat{a}(\omega) & (\omega \geq 0), \\ \hat{a}^\dagger(-\omega) & (\omega < 0), \end{cases}$$

and $\Theta(\omega)$ is the Heaviside step function and $\hat{a}(\omega)$ is the annihilation operator satisfies the commutation relations

$$\left[\hat{a}(\omega), \hat{a}^\dagger(\omega')\right] = 2\pi\delta(\omega-\omega'), \quad \left[\hat{a}(\omega), \hat{a}(\omega')\right] = \left[\hat{a}^\dagger(\omega), \hat{a}^\dagger(\omega')\right] = 0.$$

We can derive the inverse relation from the definition of the δ-function :

$$\hat{A}(\omega) = \sqrt{\frac{\mathcal{A}c}{2\pi\hbar|\omega|}} \int_{-\infty}^{+\infty} dt e^{+i\omega t} \hat{E}_a(t), \qquad \int_{-\infty}^{+\infty} dt e^{+i(\omega-\omega')t} = 2\pi\delta(\omega-\omega').$$

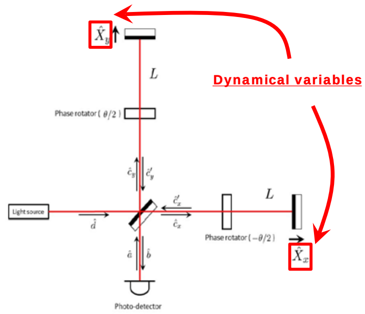

- Beam splitter junctions :

$$\hat{E}_b(t) = \frac{\hat{E}_{c'_y}(t) - \hat{E}_{c'_x}(t)}{\sqrt{2}}, \quad \hat{E}_{c_x}(t) = \frac{\hat{E}_d(t) - \hat{E}_a(t)}{\sqrt{2}}, \quad \hat{E}_{c_y}(t) = \frac{\hat{E}_d(t) + \hat{E}_a(t)}{\sqrt{2}}.$$

---> $$\boxed{\hat{B}(\omega) = \frac{\hat{C}'_y(\omega) - \hat{C}'_x(\omega)}{\sqrt{2}}, \quad \hat{C}_x(\omega) = \frac{\hat{D}(\omega) - \hat{A}(\omega)}{\sqrt{2}}, \quad \hat{C}_y(\omega) = \frac{\hat{D}(\omega) + \hat{A}(\omega)}{\sqrt{2}}.}$$

- Arm propagation conditions:

$$\hat{E}_{c'_x}[t] = \hat{E}_{c_x}\left[t - 2(\tau + \hat{X}_x/c) + \Delta t_\theta\right], \quad \hat{E}_{c'_y}[t] = \hat{E}_{c_y}\left[t - 2(\tau + \hat{X}_y/c) - \Delta t_\theta\right],$$

$$\omega\Delta t_\theta := \frac{\theta}{2}, \quad \tau = L/c.$$

- Fourier transformation of displacements:

$$\hat{X}_x(t) =: \int_{-\infty}^{+\infty} \frac{d\Omega}{2\pi} \hat{Z}_x(\Omega) e^{-i\Omega t}, \quad \hat{X}_y(t) =: \int_{-\infty}^{+\infty} \frac{d\Omega}{2\pi} \hat{Z}_y(\Omega) e^{-i\Omega t},$$

$$\hat{Z}_x(\Omega) = \int_{-\infty}^{+\infty} dt e^{+i\Omega t} \hat{X}_x(t), \quad \hat{Z}_y(\Omega) = \int_{-\infty}^{+\infty} dt e^{+i\Omega t} \hat{X}_y(t).$$

----> Arm propagation conditions:

$$\boxed{\begin{aligned} \hat{C}'_x(\omega) &= e^{-i\theta/2} e^{+2i\omega\tau} \hat{C}_x + e^{-i\theta/2} e^{+2i\omega\tau} \frac{2i}{c\sqrt{|\omega|}} \int_{-\infty}^{+\infty} \frac{d\Omega}{2\pi} e^{-i\Omega\tau} \sqrt{|\omega-\Omega|}(\omega-\Omega)\hat{C}_x(\omega-\Omega)\hat{Z}_x(\Omega), \\ \hat{C}'_y(\omega) &= e^{+i\theta/2} e^{+2i\omega\tau} \hat{C}_y + e^{+i\theta/2} e^{+2i\omega\tau} \frac{2i}{c\sqrt{|\omega|}} \int_{-\infty}^{+\infty} \frac{d\Omega}{2\pi} e^{-i\Omega\tau} \sqrt{|\omega-\Omega|}(\omega-\Omega)\hat{C}_y(\omega-\Omega)\hat{Z}_y(\Omega). \end{aligned}}$$

- State of the incident photon : $|\psi\rangle = \hat{D}_d|0\rangle_d \otimes |0\rangle_a, \quad \hat{D}_d := \exp\left[\int \frac{d\omega}{2\pi}\left\{\alpha(\omega)\hat{d}^\dagger(\omega) - \alpha(\omega)^*\hat{d}(\omega)\right\}\right].$
- We may treat the electric field as $\hat{D}_d^\dagger \hat{E}_d D_d$ with the state $|0\rangle_d|0\rangle_a$.
  - The operators $\hat{d}(\omega)$ and $\hat{d}^\dagger(\omega)$ are regarded as $D_d^\dagger \hat{d}(\omega) D_d$ and $D_d^\dagger \hat{d}^\dagger(\omega) D_d$, respectively. Then,

$$D_d^\dagger \hat{D}(\omega) D_d = \hat{D}_c(\omega) + \hat{D}_v(\omega),$$

$$\hat{D}_c(\omega) := \alpha(\omega)\Theta(\omega) + \alpha^*(-\omega)\Theta(-\omega), \quad \hat{D}_v(\omega) := \hat{d}(\omega)\Theta(\omega) + \hat{d}^\dagger(-\omega)\Theta(-\omega).$$

  - Neglecting the terms $\hat{A}\hat{Z}$ and $\hat{D}_v\hat{Z}$, we obtain the **input-output relation** :

$$\begin{aligned} e^{-2i\omega\tau}\hat{D}_d^\dagger \hat{B}(\omega)\hat{D}_d \;=\;& i\sin(\theta/2)\hat{D}_c(\omega) \quad \text{(Classical carrier)} \\ & + i\sin(\theta/2)\hat{D}_v(\omega) + \cos(\theta/2)\hat{A}(\omega) \quad \text{(Shot noise)} \\ & + \frac{2i}{c\sqrt{|\omega|}}\int_{-\infty}^{+\infty}\frac{d\Omega}{2\pi}e^{-i\Omega\tau}\sqrt{|\omega-\Omega|}(\omega-\Omega)\hat{D}_c(\omega-\Omega) \\ & \times\left[i\sin(\theta/2)\hat{D}_d^\dagger\hat{Z}_{com}(\Omega)\hat{D}_d - \cos(\theta/2)\hat{D}_d^\dagger\hat{Z}_{dif}(\Omega)\hat{D}_d\right]. \end{aligned}$$

(Radiation pressure + GW signal)

$$\hat{Z}_{com}(\Omega) := \frac{1}{2}\left(\hat{Z}_x(\Omega) + \hat{Z}_y(\Omega)\right), \quad \hat{Z}_{dif}(\Omega) := \frac{1}{2}\left(\hat{Z}_x(\Omega) - \hat{Z}_y(\Omega)\right), \quad \hat{Z}_x = \hat{Z}_{com} + \hat{Z}_{dif}, \quad \hat{Z}_y = \hat{Z}_{com} - \hat{Z}_{dif}.$$

- Eq. of motion for mirror displacements :

$$\frac{m}{2}\frac{\partial^2}{\partial t^2}\hat{X}_x(t) = \hat{F}_{rp(x)}(t) + \frac{1}{2}\frac{m}{2}L\frac{\partial^2}{\partial t^2}h(t), \quad \frac{m}{2}\frac{\partial^2}{\partial t^2}\hat{X}_y(t) = \hat{F}_{rp(y)}(t) - \frac{1}{2}\frac{m}{2}L\frac{\partial^2}{\partial t^2}h(t).$$

- Radiation pressure force :
  - We evaluate the radiation pressure to the mirrors from

$$\hat{F}_{rp(x)}(t) = 2\frac{\mathcal{A}}{4\pi}\left(\hat{E}_{c_x}\left[t - (\tau + \hat{X}_x/c) + \Delta t_\theta/2\right]\right)^2, \quad \hat{F}_{rp(y)}(t) = 2\frac{\mathcal{A}}{4\pi}\left(\hat{E}_{c_y}\left[t - (\tau + \hat{X}_y/c) - \Delta t_\theta/2\right]\right)^2,$$

- **Summary of the input-output relation**
  - Input-output relation :

$$\begin{aligned} e^{-2i\omega\tau}\hat{D}_d^\dagger \hat{B}(\omega)\hat{D}_d \;=\;& i\sin(\theta/2)\hat{D}_c(\omega) \quad \text{(Classical carrier)} \\ & + i\sin(\theta/2)\hat{D}_v(\omega) + \cos(\theta/2)\hat{A}(\omega) \quad \text{(Shot noise)} \\ & + \frac{2i}{c\sqrt{|\omega|}}\int_{-\infty}^{+\infty}\frac{d\Omega}{2\pi}e^{-i\Omega\tau}\sqrt{|\omega-\Omega|}(\omega-\Omega)\hat{D}_c(\omega-\Omega) \\ & \times\left[i\sin(\theta/2)\hat{D}_d^\dagger\hat{Z}_{com}(\Omega)\hat{D}_d - \cos(\theta/2)\hat{D}_d^\dagger\hat{Z}_{dif}(\Omega)\hat{D}_d\right]. \end{aligned}$$

(Radiation pressure + GW signal)

  - Eqs. of the mirror motion :

$$\begin{aligned} m\Omega^2 D_d^\dagger\hat{Z}_{com}(\Omega)D_d \;=\;& -\frac{\hbar}{2c}e^{+i\Omega\tau}\cos(\theta/2)\int\frac{d\omega}{2\pi}\sqrt{|\omega(\Omega-\omega)|}\hat{D}_c(\omega)\hat{D}_c(\Omega-\omega) \\ & -\frac{\hbar}{c}e^{+i\Omega\tau}\int\frac{d\omega}{2\pi}\sqrt{|\omega(\Omega-\omega)|}\hat{D}_c(\omega)\left(\cos(\theta/2)\hat{D}_v(\Omega-\omega) - i\sin(\theta/2)\hat{A}(\Omega-\omega)\right) \\ & -i\cos(\theta/2)\frac{\hbar}{2c^2}\iint\frac{d\omega}{2\pi}\frac{d\omega'}{2\pi}\sqrt{|\omega\omega'|}(\omega+\omega')\hat{D}_c(\omega)\hat{D}_c(\omega')D_d^\dagger\hat{Z}_{com}(\Omega-\omega-\omega')D_d e^{+i(\omega+\omega')\tau} \\ & -\sin(\theta/2)\frac{\hbar}{2c^2}\iint\frac{d\omega}{2\pi}\frac{d\omega'}{2\pi}\sqrt{|\omega\omega'|}(\omega+\omega')\hat{D}_c(\omega)\hat{D}_c(\omega')D_d^\dagger\hat{Z}_{dif}(\Omega-\omega-\omega')D_d e^{+i(\omega+\omega')\tau}, \end{aligned}$$

$$\begin{aligned} m\Omega^2 D_d^\dagger\hat{Z}_{dif}(\Omega)D_d \;=\;& i\frac{\hbar}{2c}e^{+i\Omega\tau}\sin(\theta/2)\int\frac{d\omega}{2\pi}\sqrt{|\omega(\Omega-\omega)|}\hat{D}_c(\omega)\hat{D}_c(\Omega-\omega) \\ & +\frac{\hbar}{c}e^{+i\Omega\tau}\int\frac{d\omega}{2\pi}\sqrt{|\omega(\Omega-\omega)|}\hat{D}_c(\omega)\left[i\sin(\theta/2)\hat{D}_v(\Omega-\omega) - \cos(\theta/2)\hat{A}(\Omega-\omega)\right] \\ & -\sin(\theta/2)\frac{\hbar}{2c^2}\iint\frac{d\omega}{2\pi}\frac{d\omega'}{2\pi}\sqrt{|\omega\omega'|}(\omega+\omega')\hat{D}_c(\omega)\hat{D}_c(\omega')D_d^\dagger\hat{Z}_{com}(\Omega-\omega-\omega')D_d e^{+i(\omega+\omega')\tau} \\ & -i\cos(\theta/2)\frac{\hbar}{2c^2}\iint\frac{d\omega}{2\pi}\frac{d\omega'}{2\pi}\sqrt{|\omega\omega'|}(\omega+\omega')\hat{D}_c(\omega)\hat{D}_c(\omega')D_d^\dagger\hat{Z}_{dif}(\Omega-\omega-\omega')D_d e^{+i(\omega+\omega')\tau} \\ & +\frac{1}{2}mL\Omega^2 h(\Omega). \quad \text{(Gravitational-wave signal)} \end{aligned}$$

IV. Rederivation of the conventional input-output relation

Here, we consider the monochromatic light source case, where

$$\alpha(\omega) = 2\pi N \delta(\omega - \omega_0), \quad N := \sqrt{\frac{I_0}{\hbar\omega_0}}, \quad \hat{D}_c(\omega) = 2\pi N \left(\delta(\omega - \omega_0)\Theta(\omega) + \delta(\omega + \omega_0)\Theta(-\omega)\right).$$

In conventional gravitational-wave detectors, we concentrate on the sideband frequencies $\omega_0 \pm \Omega$ with carrier frequency ω_0, and consider the situation where $\omega_0 \gg \Omega$. In this case the above $\hat{D}_c(\omega)$ is given by

$$\hat{D}_c(\omega_0 \pm \Omega) = 2\pi N \left(\delta(\pm\Omega) + \underbrace{\delta(2\omega_0 \pm \Omega)}_{\text{rapidly oscillating term : we neglect this term.}}\right) \sim 2\pi N \delta(\pm\Omega).$$

Through the same approximation, we obtain

Input-output relation :

$$\begin{aligned} e^{-2i(\omega_0 \pm \Omega)\tau} D_d^\dagger \hat{B}(\omega_0 \pm \Omega) D_d &= i \sin\left(\frac{\theta}{2}\right) \hat{D}_c(\omega_0 \pm \Omega) + i \sin\left(\frac{\theta}{2}\right) \hat{D}_v(\omega_0 \pm \Omega) + \cos\left(\frac{\theta}{2}\right) \hat{A}(\omega_0 \pm \Omega) \\ &\quad + \frac{2iN\omega_0^{3/2} e^{\mp i\Omega\tau}}{c\sqrt{|\omega_0 \pm \Omega|}} \left[i \sin\left(\frac{\theta}{2}\right) D_d^\dagger \hat{Z}_{com}(\pm\Omega) D_d - \cos\left(\frac{\theta}{2}\right) D_d^\dagger \hat{Z}_{diff}(\pm\Omega) D_d \right], \end{aligned}$$

Eqs. of motion :

$$\begin{aligned} m\Omega^2 D_d^\dagger \hat{Z}_{com}(\Omega) D_d &= -\frac{\hbar N e^{+i\Omega\tau}\sqrt{\omega_0}}{c} \cos\left(\frac{\theta}{2}\right) \left(\sqrt{|\Omega - \omega_0|} \hat{D}_c(\Omega - \omega_0) + \sqrt{|\Omega + \omega_0|} \hat{D}_c(\Omega + \omega_0) \right) \\ &\quad - \frac{2\hbar N e^{+i\Omega\tau}\sqrt{\omega_0}}{c} \left\{ \sqrt{|\Omega - \omega_0|} \left(\cos\left(\frac{\theta}{2}\right) \hat{D}_v(\Omega - \omega_0) - i \sin\left(\frac{\theta}{2}\right) \hat{A}(\Omega - \omega_0) \right) \right. \\ &\qquad \left. + \sqrt{|\Omega + \omega_0|} \left(\cos\left(\frac{\theta}{2}\right) \hat{D}_v(\Omega + \omega_0) - i \sin\left(\frac{\theta}{2}\right) \hat{A}(\Omega + \omega_0) \right) \right\}, \\ m\Omega^2 D_d^\dagger \hat{Z}_{diff}(\Omega) D_d &= +\frac{i\hbar N e^{+i\Omega\tau}\sqrt{\omega_0}}{c} \sin\left(\frac{\theta}{2}\right) \left\{ \sqrt{|\Omega - \omega_0|} \hat{D}_c(\Omega - \omega_0) + \sqrt{|\Omega + \omega_0|} \hat{D}_c(\Omega + \omega_0) \right\} \\ &\quad + \frac{2\hbar N e^{+i\Omega\tau}\sqrt{\omega_0}}{c} \left\{ \sqrt{|\Omega - \omega_0|} \left[i \sin\left(\frac{\theta}{2}\right) \hat{D}_v(\Omega - \omega_0) - \cos\left(\frac{\theta}{2}\right) \hat{A}(\Omega - \omega_0) \right] \right. \\ &\qquad \left. + \sqrt{|\Omega + \omega_0|} \left[i \sin\left(\frac{\theta}{2}\right) \hat{D}_v(\Omega + \omega_0) - \cos\left(\frac{\theta}{2}\right) \hat{A}(\Omega + \omega_0) \right] \right\} \\ &\quad + \frac{1}{2} m L \Omega^2 h(\Omega). \end{aligned}$$

We also apply <u>the approximation in which $\omega_0 \pm \Omega$, in the coefficients of the input-output relation are regarded as $\omega_0 \pm \Omega \sim \omega_0$</u>, since $\omega_0 \gg \Omega$. $(\omega_0 \pm \Omega > 0, \quad \Omega - \omega_0 < 0)$.

Furthermore, we choose arm length L so that $\omega_0 \tau = \omega_0 \frac{L}{c} = 2n\pi, \quad n \in \mathbb{N}$, and we introduce variables $\kappa := \frac{8\omega_0 I_0}{mc^2\Omega^2}, \quad h_{SQL} := \sqrt{\frac{8\hbar}{m\Omega^2 L^2}}$. Then, the input-output relation is given by

$$\boxed{\begin{aligned} D_d^\dagger \hat{b}_\pm D_d &= \underbrace{\sin\left(\frac{\theta}{2}\right)\left(i + \kappa\cos\left(\frac{\theta}{2}\right)\right)\sqrt{\frac{I_0}{\hbar\omega_0}} 2\pi\delta(\Omega)}_{\text{carrier leakage}} \\ &\quad \underbrace{+ e^{\pm 2i\Omega\tau}\left[i\sin\left(\frac{\theta}{2}\right)\hat{d}_\pm + \cos\left(\frac{\theta}{2}\right)\hat{a}_\pm \right]}_{\text{shot noise}} + \underbrace{\frac{\kappa e^{\pm 2i\Omega\tau}}{2}\left[\sin\theta\left(\hat{d}_\mp^\dagger + \hat{d}_\pm\right) + i\cos\theta\left(\hat{a}_\mp^\dagger + \hat{a}_\pm\right)\right]}_{\text{radiation-pressure noise}} \\ &\quad \underbrace{- i\sqrt{\kappa}e^{\pm i\Omega\tau}\cos\left(\frac{\theta}{2}\right)\frac{h(\pm\Omega)}{h_{SQL}}}_{\text{gravitational-wave signal}}, \end{aligned}}$$

where $\hat{a}_\pm(\Omega) := \hat{a}(\omega_0 \pm \Omega), \quad \hat{b}_\pm(\Omega) := \hat{b}(\omega_0 \pm \Omega), \quad \hat{d}_\pm(\Omega) := \hat{d}(\omega_0 \pm \Omega)$.

Introducing amplitude and phase quadratures as

$$\hat{a}_1 = \frac{1}{\sqrt{2}}(\hat{a}_+ + \hat{a}_-^\dagger), \quad \hat{a}_2 = \frac{1}{\sqrt{2}i}(\hat{a}_+ - \hat{a}_-^\dagger), \quad \hat{b}_1 = \frac{1}{\sqrt{2}}(\hat{b}_+ + \hat{b}_-^\dagger), \quad \hat{b}_2 = \frac{1}{\sqrt{2}i}(\hat{b}_+ - \hat{b}_-^\dagger), \quad \hat{d}_1 = \frac{1}{\sqrt{2}}(\hat{d}_+ + \hat{d}_-^\dagger), \quad \hat{d}_2 = \frac{1}{\sqrt{2}i}(\hat{d}_+ - \hat{d}_-^\dagger),$$

The above input-output relation is given by

$$\boxed{\begin{aligned} D_d^\dagger \hat{b}_1 D_d &= \frac{1}{\sqrt{2}} \sin\theta\,\kappa \sqrt{\frac{I_0}{\hbar\omega_0}} 2\pi\delta(\Omega) + e^{+2i\Omega\tau}\left\{ -\sin\left(\frac{\theta}{2}\right)\hat{d}_2 + \cos\left(\frac{\theta}{2}\right)\hat{a}_1 \right\} + e^{+2i\Omega\tau}\kappa\sin\theta\hat{d}_1, \\ D_d^\dagger \hat{b}_2 D_d &= \sqrt{2}\sin\left(\frac{\theta}{2}\right)\sqrt{\frac{I_0}{\hbar\omega_0}} 2\pi\delta(\Omega) + e^{+2i\Omega\tau}\left\{ \sin\left(\frac{\theta}{2}\right)\hat{d}_1 + \cos\left(\frac{\theta}{2}\right)\hat{a}_2 \right\} + \cos\theta e^{+2i\Omega\tau}\kappa\hat{a}_1 - e^{+i\Omega\tau}\cos\left(\frac{\theta}{2}\right)\sqrt{2\kappa}\frac{h(\Omega)}{h_{SQL}}. \end{aligned}}$$

When $\theta = 0$, these input-output relation yields a well-known form:

$$\boxed{D_d^\dagger \hat{b}_1 D_d = e^{+2i\Omega\tau}\hat{a}_1, \quad D_d^\dagger \hat{b}_2 D_d = e^{+2i\Omega\tau}\left(\hat{a}_2 + \kappa\hat{a}_1\right) - e^{+i\Omega\tau}\sqrt{2\kappa}\frac{h(\Omega)}{h_{SQL}}.}$$

Therefore, our extended input-output relation is a natural extension of the conventional input-output relation for the Michelson gravitational-wave detector.

V. Weak-value amplification from the extended input-output relation

Here, we show the weak-value amplification from our extended input-output relation. To do this, we consider the case $\omega > 0$. In this case, our input-output relation is given by

$$
\begin{aligned}
e^{-2i\omega\tau} D_d^\dagger \hat{b}(\omega) D_d \;=\;& \underbrace{i\sin\left(\frac{\theta}{2}\right)\alpha(\omega)}_{\text{carrier leakage}} + \underbrace{i\sin\left(\frac{\theta}{2}\right)\hat{d}(\omega) + \cos\left(\frac{\theta}{2}\right)\hat{a}(\omega)}_{\text{shot noise}} \\
& \underbrace{+\frac{2i}{c}\int_{-\infty}^{+\infty}\frac{d\Omega}{2\pi}e^{-i\Omega\tau}\sqrt{\left|\frac{\omega-\Omega}{\omega}\right|}(\omega-\Omega)\left[i\sin\left(\frac{\theta}{2}\right)\hat{D}_c(\omega-\Omega)D_d^\dagger\hat{Z}_{com}(\Omega)D_d - \cos\left(\frac{\theta}{2}\right)\hat{D}_c(\omega-\Omega)D_d^\dagger\hat{Z}_{diff}(\Omega)D_d\right]}_{\text{Radiation-pressure + GW signal}}.
\end{aligned}
$$

To discuss the weak measurement from this input-output relation, we concentrate on the output-photon number operator $\hat{n}(\omega) := \hat{b}^\dagger(\omega)\hat{b}(\omega)$ to the photo-detector and its expectation value $\overline{\hat{n}(\omega)}$ under the state $|\psi\rangle = \hat{D}_d|0\rangle_d \otimes |0\rangle_a$, $\hat{D}_d := \exp\left[\int \frac{d\omega}{2\pi}\left\{\alpha(\omega)\hat{d}^\dagger(\omega) - \alpha(\omega)^*\hat{d}(\omega)\right\}\right]$.

For simplicity, we consider the situation where $\hat{Z}_{com}$ and $\hat{Z}_{diff}$ are classical and their frequency-dependence are negligible in this case we obtain

$$
\overline{n(\omega)} = \underbrace{\sin^2\left(\frac{\theta}{2}\right)\alpha^2(\omega)}_{\overline{\hat{n}_0(\omega)}} \underbrace{- \sin^2\left(\frac{\theta}{2}\right)\frac{8}{2\pi c\omega^{1/2}}\mathcal{I}_{s+3/2}(\tau,\alpha)\alpha(\omega)\left(\cos(\omega\tau)\hat{Z}_{com} + \underbrace{\cot\left(\frac{\theta}{2}\right)}_{\text{Imaginary part of the weak vlaue}}\sin(\omega\tau)\hat{Z}_{diff}\right)}_{\delta n(\omega)},
$$

where $\mathcal{I}_{s+3/2}(\tau,\alpha) := \int_0^{+\infty} dx x^{3/2}\sin(x\tau)\alpha(x)$.

To consider the weak-value amplification, we introduce the conditional distribution function $f(\omega)$ defined by

$$
f(\omega) := \frac{\overline{n(\omega)}}{\int_0^{+\infty} d\omega \overline{n(\omega)}} = \frac{N_{out}\langle\omega|\rho_d'|\omega\rangle}{N_{out}} = \langle\omega|\rho_d'|\omega\rangle.
$$

Under the conditional distribution function $f(\omega)$ defined by

$$
f(\omega) := \frac{\overline{n(\omega)}}{\int_0^{+\infty} d\omega \overline{n(\omega)}},
$$

we evaluate the expectation value of the frequency ω by

$$
\langle\omega\rangle := \int_0^{+\infty} d\omega\omega f(\omega) \sim \omega_0 + \frac{\int_0^{+\infty} d\omega(\omega-\omega_0)\delta n(\omega)}{\int_0^{+\infty} d\omega\overline{n_0(\omega)}}, \quad \overline{n(\omega)} =: \overline{n_0(\omega)} + \delta n(\omega), \quad \omega_0 := \frac{\int_0^{+\infty} d\omega\omega\overline{n_0(\omega)}}{\int_0^{+\infty} d\omega\overline{n_0(\omega)}}.
$$

Then, we obtain

$$
\begin{aligned}
\langle\omega\rangle - \omega_0 \;\sim\;& \hat{Z}_{com}\frac{8}{2\pi c\mathcal{J}(\alpha)}\mathcal{I}_{s+3/2}(\tau,\alpha)\left(\omega_0\mathcal{I}_{c-1/2}(\tau,\alpha) - \mathcal{I}_{c+1/2}(\tau,\alpha)\right) \\
& + \cot\left(\frac{\theta}{2}\right)\hat{Z}_{diff}\frac{8}{2\pi c\mathcal{J}(\alpha)}\mathcal{I}_{s+3/2}(\tau,\alpha)\left(\omega_0\mathcal{I}_{s-1/2}(\tau,\alpha) - \mathcal{I}_{s+1/2}(\tau,\alpha)\right) \\
\sim\;& \underbrace{+\frac{2}{\theta}}_{\text{Weak-value amplification!!}}\hat{Z}_{diff}\frac{8}{2\pi c\mathcal{J}(\alpha)}\mathcal{I}_{s+3/2}(\tau,\alpha)\left(\omega_0\mathcal{I}_{s-1/2}(\tau,\alpha) - \mathcal{I}_{s+1/2}(\tau,\alpha)\right) \quad \text{when} \quad \theta \ll 1,
\end{aligned}
$$

where $\mathcal{J}(\alpha) := \int_0^{+\infty}\alpha^2(\omega)$, $\mathcal{I}_{c-1/2}(\tau,\alpha) := \int_0^{+\infty} dx x^{-1/2}\cos(x\tau)\alpha(x)$, and $\mathcal{I}_{s-1/2}(\tau,\alpha) := \int_0^{+\infty} dx x^{-1/2}\sin(x\tau)\alpha(x)$.

VI. Summary and Discussions

Here, we considered the extension of the input-output relation for a conventional Michelson gravitational-wave detector to include the situation of the weak-value amplification. Specifically, we extended the photon state injected from the light source into their interferometer to a coherent state with an arbitrary complex amplitude $\alpha(\omega)$.

Due to this extension, we can discuss a conventional input-output relation for a Michelson gravitational-wave detector and the situation of the weak-value amplification from the same input-output relation. (Main result of this work.)

1. Weak-value amplification effect is determined by $\alpha(\omega)$.
2. Weak-value amplification also amplifies the shot noise and the radiation pressure noise which are important for the sensitivity of gravitational-wave detectors.
3. The effect of the weak-value amplification corresponds to the **common mode rejection** in conventional gravitational-wave detectors, which is achieved by the complete dark port in conventional gravitational-wave detectors. *In this sense, a weak-value amplification is already and implicitly included in a conventional gravitational-wave detector.*

In ***the weak measurement***, we evaluated the photon number expectation value

$$\overline{n(\omega)} := \langle \hat{n}(\omega) \rangle = \langle 0 | D_d^\dagger \hat{b}^\dagger(\omega) \hat{b}(\omega) D_d | 0 \rangle = \langle 0 | D_d^\dagger \hat{b}^\dagger(\omega) D_d D_d^\dagger \hat{b}(\omega) D_d | 0 \rangle$$

from the input-output relation

These terms do not contribute to $\langle \hat{n}(\omega) \rangle$ but contribute to noise.

$$e^{-2i\omega\tau} D_d^\dagger \hat{b}(\omega) D_d = \underbrace{i \boxed{\sin\left(\frac{\theta}{2}\right)} \alpha(\omega)}_{\text{“zeroth-order”}} + \boxed{i \sin\left(\frac{\theta}{2}\right) \hat{d}(\omega) + \cos\left(\frac{\theta}{2}\right) \hat{a}(\omega)}$$

$$\underbrace{+ \frac{2i}{c} \int_{-\infty}^{+\infty} \frac{d\Omega}{2\pi} e^{-i\Omega\tau} \sqrt{\left|\frac{\omega-\Omega}{\omega}\right|} (\omega - \Omega) \left[i \boxed{\sin\left(\frac{\theta}{2}\right)} \hat{D}_c(\omega-\Omega) D_d^\dagger \hat{Z}_{com}(\Omega) D_d - \boxed{\cos\left(\frac{\theta}{2}\right)} \hat{D}_c(\omega-\Omega) D_d^\dagger \hat{Z}_{diff}(\Omega) D_d \right]}_{\text{“first-order”}}.$$

Conditional photon frequency distribution: $f(\omega) := \frac{\overline{n(\omega)}}{N_{out}}, \quad N_{out} := \int_0^\infty \overline{n(\omega)}.$

$$\langle \omega \rangle - \omega_0 \sim \frac{\int_0^{+\infty} d\omega (\omega - \omega_0) \delta n(\omega)}{\int_0^{+\infty} d\omega \overline{n_0(\omega)}} \sim \frac{\text{“first-order”}}{\text{“zeroth-order”}} \sim \frac{\bigcirc \sin(\theta/2) + \square \cos(\theta/2)}{\triangle \sin(\theta/2)} = \frac{\bigcirc}{\triangle} + \frac{\square}{\triangle} \underbrace{\cot\left(\frac{\theta}{2}\right)}_{\text{“weak value”}}.$$

Since “zeroth-order” term is proportional to $\sin(\theta/2)$, the term in the “first-order” which proportional to $\cos(\theta/2)$ in the input-output relation is amplified by the weak-value amplification.

The input-output relation for ***the conventional Michelson GW detector***:

$$\begin{aligned} D_d^\dagger \hat{b}_\pm D_d = & \boxed{\sin\left(\frac{\theta}{2}\right)} \left(i + \kappa \cos\left(\frac{\theta}{2}\right) \right) \sqrt{\frac{I_0}{\hbar\omega_0}} 2\pi\delta(\Omega) \\ & + e^{\pm 2i\Omega\tau} \left[i \boxed{\sin\left(\frac{\theta}{2}\right)} \hat{d}_\pm + \boxed{\cos\left(\frac{\theta}{2}\right)} \hat{a}_\pm \right] + \frac{\kappa e^{\pm 2i\Omega\tau}}{2} \left[\boxed{\sin\theta} \left(\hat{d}_\mp^\dagger + \hat{d}_\pm \right) + i \boxed{\cos\theta} \left(\hat{a}_\mp^\dagger + \hat{a}_\pm \right) \right] \\ & - i\sqrt{\kappa} e^{\pm i\Omega\tau} \boxed{\cos\left(\frac{\theta}{2}\right)} \frac{h(\pm\Omega)}{h_{SQL}}, \end{aligned}$$

If we regard that the effect of the weak-value amplification is reduction of the terms proportional to $\sin(\theta/2)$ but the terms proportional to $\cos(\theta/2)$ is finite, **we should say that we can reduce both the shot noise and the radiation-pressure noise from the light source but we cannot reduce neither the shot noise nor radiation-pressure noise from the dark port.**

Within this work, we did not evaluate the quantum noises (shot noise and radiation-pressure noise) in the situation where the weak-value amplification occurs. This evaluation will be possible in our framework.

In this evaluation, we have to take care of the differences in the weak measurement from conventional gravitational-wave detectors. In the theory of conventional gravitational-wave detectors, we used three assumptions to derive the input-output relation:

1. Concentrate quadratures of the mode $\omega_0 \pm \Omega$;
2. Ignore the term of the rapid oscillation $2\omega_0 \pm \Omega$;
3. Apply $\omega_0 \gg \Omega$ in the coefficients of input-output relation.

We have to discuss whether these assumptions are valid even for the situation of the weak measurement, or not.

Furthermore, we have to investigate the following problem:

- What is the signal indicator in this setup???? (Noise spectral density?, photon number expectation value?)
- How to treat the divergence Ω^{-2} in the response function ??? (Technical?)

These should be clarified to discuss the relation between the current understanding of gravitational wave detectors and weak measurement.

Takahisa Igata
Rikkyo University

“Bright edge of a near extremal Kerr black hole shadow”

[JGRG28 (2018) PB16]

Bright edge of a near-extremal Kerr black hole shadow

Takahisa IGATA

Rikkyo University

collaborators: H. Ishihara and Y. Yasunishi (Osaka City University)

in preparation

Introduction & Motivations

- Black hole shadow edge is related to spherical photon orbits
- Rapidly rotating black hole has the throat geometry near the horizon.

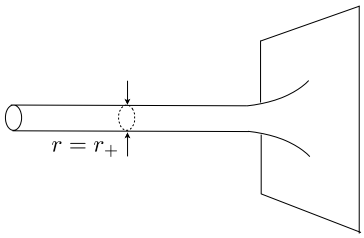

Question

Observational signature of the near-horizon extremal Kerr throat on the black hole shadow?

The spherical photon orbits on the throat turn around and around at almost the horizon radius and are related to a part of the shadow edge at a distant observer. The photons feel the geometry near the horizon radius. We consider the null congruence, which is closely related to the intensity of the shadow edge.

Kerr geometry

- Metric (M: mass, a: specific angular momentum, $|a| \leq M$):

$$g_{\mu\nu}\mathrm{d}x^\mu \mathrm{d}x^\nu = -\frac{\Delta\Sigma}{A}\mathrm{d}t^2 + \frac{\Sigma}{\Delta}\mathrm{d}r^2 + \Sigma \mathrm{d}\theta^2 + \frac{A}{\Sigma}\sin^2\theta\left[\mathrm{d}\varphi - \frac{2Mar}{A}\mathrm{d}t\right]^2, \tag{1}$$

$$\Sigma = r^2 + a^2\cos^2\theta, \quad \Delta = r^2 + a^2 - 2Mr, \quad A = \left(r^2+a^2\right)^2 - a^2\Delta\sin^2\theta. \tag{2}$$

- Killing vectors: $\xi^a = (\partial/\partial t)^a$ and $\psi^a = (\partial/\partial\varphi)^a$
- Horizon radius, angular velocity, and generator: (use units in which $M = 1$)

$$r_+ := 1 + \sqrt{1-a^2}, \quad \Omega_{\mathrm{h}} = a/(r_+^2 + a^2), \quad \chi = (\partial/\partial t)^a + \Omega_{\mathrm{h}}(\partial/\partial\varphi)^a, \tag{3}$$

- Conformal Killing–Yano 2-form

$$h = r\left[\mathrm{d}t - a\sin^2\theta\mathrm{d}\varphi\right]\wedge\mathrm{d}r + a\cos\theta\sin\theta\left[a\mathrm{d}t - \left(r^2+a^2\right)\mathrm{d}\varphi\right]\wedge\mathrm{d}\theta. \tag{4}$$

- Killing–Yano 2-form $f = {}^*h$, Killing tensor: $K_{ab} = f_{ac}f_b{}^c$, conformal Killing tensor: $C_{ab} = h_{ac}h_b{}^c$

Null geodesics

- Null geodesic tangent: k^a (λ: affine parameter)
- Conserved quantities

$$E = -k_a(\partial/\partial t)^a(\neq 0), \quad b = k_a(\partial/\partial\varphi)^a/E, \quad q = E^{-2}K_{ab}k^ak^b - (b-a)^2, \tag{5}$$

- Equations of motion (σ_r, $\sigma_\theta = \pm 1$)

$$\dot{t} = \frac{1}{\Sigma}\left[a\left(b - a\sin^2\theta\right) + \frac{r^2+a^2}{\Delta}P\right], \dot{r} = \frac{\sigma_r}{\Sigma}\sqrt{-V}, \dot{\theta} = \frac{\sigma_\theta}{\Sigma}\sqrt{-U}, \dot{\varphi} = \frac{1}{\Sigma}\left[\frac{b}{\sin^2\theta} - a + \frac{a}{\Delta}P\right],$$

$$V = \Delta\left[q + (b-a)^2\right] - P^2, \; U = \cos^2\theta\left[\frac{b^2}{\sin^2\theta} - a^2\right] - q, \; P = r^2 + a(a-b).$$

- $V = 0$ & $V' = 0$:

$$b = \left[\frac{1}{a} - a\right]\frac{2}{r-1} - \frac{(r-1)^2}{a} + \frac{3}{a} - a, \quad q = \frac{r^3(4a^2 - 9r + 6r^2 - r^3)}{a^2(r-1)^2}. \tag{6}$$

Spherical photon orbits (SPOs)

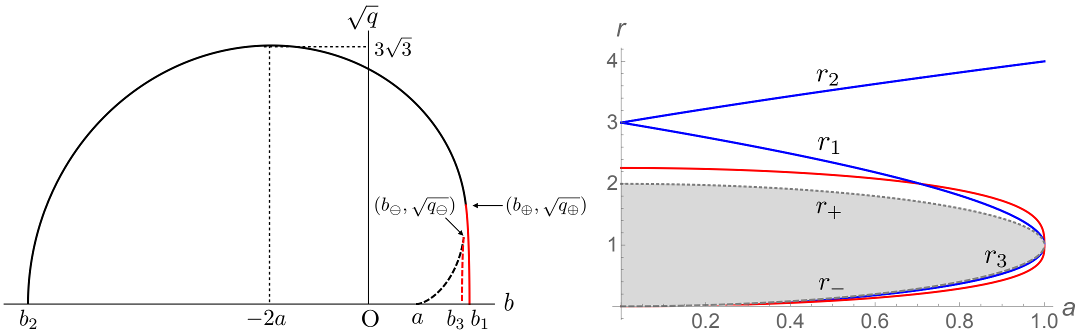

Shape of the shadow for $a \simeq 1$. Photons with parameters on the red comes from the Kerr throat.

- SPOs exist in the range

$$r_1 \le r \le r_2, 0 < r \le r_3, \tag{7}$$

Convergence of SPOs to the horizon in $a \to 1$

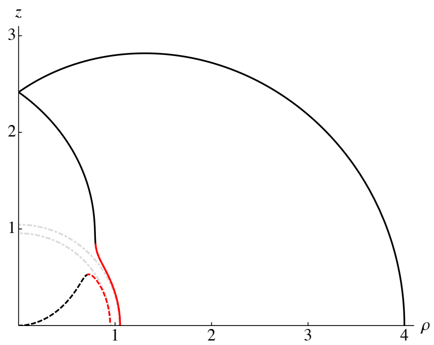

Allowed range of θ ($U < 0$) for spherical photon orbits in the limit $a \to 1$.

- Near extremal & near horizon

$$a = 1 - \epsilon, \quad r = 1 + \delta \quad (\epsilon \ll \delta \ll 1) \tag{8}$$

- limiting values

$$b \to 2, \; q \to q_0 \in [0, 3] \text{ (finite range)} \quad \left(\epsilon \ll \sqrt{\frac{8}{3}}\epsilon^{1/2} \le |\delta| \ll 1\right) \tag{9}$$

- The SPO radii degenerate into r_+ while the variable θ takes a value in a finite range

$$|\cos\theta| \le \frac{1}{\sqrt{2}}\left[\sqrt{(q+1)(q+9)} - q - 3\right]^{1/2} \le \sqrt{2\sqrt{3} - 3}, \tag{10}$$

Weyl curvature on SPOs

- parallelly propagated tetrad

$$m^a = \frac{h_k{}^a - \lambda \xi_k k^a}{\sqrt{C_{kk}}},\ n^a = \frac{f_k{}^a}{\sqrt{K_{kk}}},\ l^a = \frac{h_m{}^a}{\sqrt{C_{kk}}} + \frac{C_k{}^d C_{dk} + \lambda^2 \xi_k^2 C_{kk}}{2C_{kk}^2} k^a, \tag{11}$$

- $\{\tilde{k}^a, \tilde{l}^a, \tilde{m}^a, \tilde{n}\}$: regularized tetrad in the limit $\epsilon \to 0$ and $\delta \to 0$
- Weyl curvature components $C_{\tilde{k}AB\tilde{k}} := C_{abcd}\tilde{k}^a (e_A)^b (e_B)^c \tilde{k}^d$ on SPOs

$$C_{\tilde{k}\tilde{m}\tilde{m}\tilde{k}} = -C_{\tilde{k}\tilde{n}\tilde{n}\tilde{k}} \simeq \frac{12(1 - 10\cos^2\theta + 5\cos^4\theta)}{(1+\cos^2\theta)^5}(\delta^2 - 4\epsilon) \to 0, \tag{12}$$

$$C_{\tilde{k}\tilde{m}\tilde{n}\tilde{k}} = C_{\tilde{k}\tilde{n}\tilde{m}\tilde{k}} \simeq \frac{12\cos\theta(5 - 10\cos^2\theta + \cos^4\theta)}{(1+\cos^2\theta)^5}(\delta^2 - 4\epsilon) \to 0, \tag{13}$$

- The Weyl curvature does NOT generate the shear of SPOs in the limit $\epsilon \to 0$ and $\delta \to 0$:

$$\overset{\circ}{\Theta} = -\frac{\Theta^2}{2} - \sigma^{AB}\sigma_{AB}, \quad \overset{\circ}{\sigma}_{AB} = -\Theta\sigma_{AB} + \cancel{C_{\tilde{k}AB\tilde{k}}}, \tag{14}$$

Conclusions & Discussions

- When photons on the spherical photon orbits have impact parameters within a certain range, the radii collect on the event horizon in $a \to 1$ while each photon moves in a different range of θ.
- Weyl curvature components do not generate the shear for the congruence of the special SPOs.
- This result implies that the intensity of the black hole shadow edge becomes large when the black hole rotates rapidly.
- The tangent of the special class of SPOs must be proportional to the null generator on the event horizon, which is identified with the outgoing principal null vector. Hence, the Weyl curvature components correspond to the complex Weyl scalar ψ_0 associated with the principal null. Since $\psi_0 = 0$ in the Kerr geometry (Petrov type D), the Weyl curvature components also vanish for the special class of SPOs.

Naoki Tsukamoto
Tohoku University

“Linear stability analysis of a rotating thin-shell wormhole”

[JGRG28 (2018) PB18]

Linear stability analysis of a rotating thin-shell wormhole

Naoki Tsukamoto (Tohoku University)

(From this December, a limited-term assistant professor at National Institute of Technology, Hachinohe College)

Phys. Rev. D 98, 044026 (2018) with Takafumi Kokubu (KEK and Rikkyo University)

Abstract: Rotation is expected to make wormholes stable. We construct a rotating BTZ thin-shell wormhole by using a cut-and-paste method in a corotating frame on a throat. We investigate the linear stability of the thin shell of the rotating wormhole against the radial perturbations of the throat at $x = x_0$. The larger its dimensionless angular momentum $|j|$ is, the more the wormhole becomes stable $|j|$ until it reaches 1. The behavior of a condition for its stability significantly changes when $|j| > 1$. The rapidly rotating wormhole with the throat at $x_0 = |j|/\sqrt{2}$ is stable regardless of the equation of state for the barotropic fluid. Stable regions on a plane $x_0\beta_0^2$, where $\beta_0^2 \equiv (\partial p/\partial\sigma)_{x=x_0}$ and p and σ are the surface pressure and energy density of the shell, respectively, are shown in the following figures. Shaded regions indicate the stable regions. For $|j| = 0$ and 0.99, solid lines denote the radius of the event horizon.

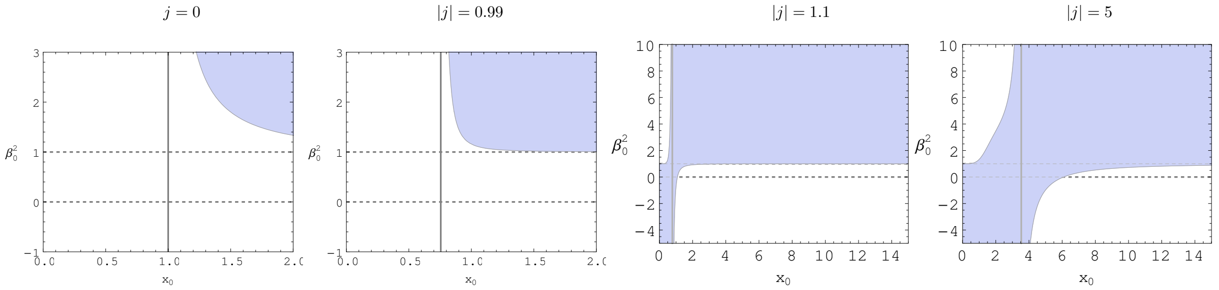

Introduction

A wormhole is a spacetime structure which connects two regions in our universe or multiverse. Existence of wormholes in nature will require their stability. Dzhunushaliev *et al.* [V. Dzhunushaliev, V. Folomeev, B. Kleihaus, J. Kunz, and E. Radu, Phys. Rev. D **88**, 124028 (2013)] investigated a five-dimensional rotating wormhole with equal angular momenta filled with a ghost scalar field and discussed its stability. They found that the unstable mode of the five-dimensional wormhole disappears when the wormhole rotates fast. Their result might show that rotation makes wormholes stable.

Construction of rotating BTZ wormhole

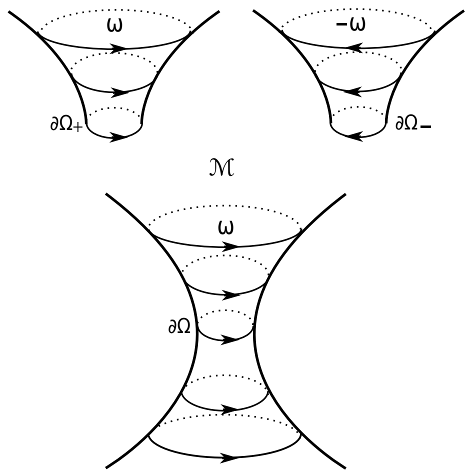

We cut and paste two BTZ spacetimes with a line element, in a corotating frame on a throat, given by

$$ds_\pm^2 = -f_\pm(r_\pm)dt_\pm^2 + \frac{dr_\pm^2}{f_\pm(r_\pm)} + r_\pm^2\left[d\phi_\pm + \frac{J_\pm}{2}\left(\frac{1}{a^2(t_\pm)} - \frac{1}{r_\pm^2}\right)dt_\pm\right]^2,$$

where

$$f_\pm(r_\pm) \equiv -M_\pm + \frac{r_\pm^2}{l_\pm^2} + \frac{J_\pm^2}{4r_\pm^2}$$

and where $M_\pm$, $J_\pm$, and $l_\pm \equiv \sqrt{-1/\Lambda_\pm}$ are a mass parameter, an angular momentum, and the scale of a curvature related to a negative cosmological constant $\Lambda_\pm < 0$, respectively. Here we have permitted that the radius of the throat a is a function of time, $a = a(t)$. As shown in a left figure, we identify the boundaries of the manifolds $\partial\Omega_\pm$ which are the timelike hypersurfaces $\partial\Omega \equiv \partial\Omega_+ = \partial\Omega_-$ and we obtain a manifold $\mathcal{M}$ describing a rotating thin-shell wormhole.

Stability of the rotating wormhole

We assume that the thin shell is filled with a barotropic fluid with the surface pressure $p = p(\sigma)$, where σ is the surface density. From the the Darmois-Israel junction conditions, the motion of the shell is described by

$$\left(\frac{da}{dt}\right)^2 + V(a) = 0,$$

where

$$V(a) \equiv f(a) - \frac{\pi^2 a^2\sigma^2(a)}{4}.$$

We investigate the stability of the rotating wormhole with the throat which stays in the radial direction at $r = a_0$, where a_0 is a constant. By introducing $x \equiv a/(l\sqrt{M})$ and $x_0 \equiv a_0/(l\sqrt{M})$, the effective potential $V(x)$ can be expanded in the power of $x - x_0$ as

$$V(x) = \frac{1}{2}\left.\frac{d^2V}{dx^2}\right|_{x=x_0}(x-x_0)^2 + O\left((x-x_0)^3\right).$$

The thin shell is stable (unstable) for

$$\left.\frac{d^2V}{dx^2}\right|_{x=x_0} = \frac{1}{Mx_0^4}\left[\frac{-8x_0^6 + 12j^2x_0^4 - 6j^2x_0^2 + j^4}{4x_0^4 - 4x_0^2 + j^2} + (2x_0^2 - j^2)\beta_0^2\right] > 0\ (< 0),$$

where $j \equiv J/(lM)$ and

$$\beta_0^2 \equiv \left(\frac{\partial p}{\partial\sigma}\right)_{x=x_0},$$

against linearized fluctuations in the radial direction. We can rewrite the stable condition as

$$\frac{-8x_0^6 + 12j^2x_0^4 - 6j^2x_0^2 + j^4}{4x_0^4 - 4x_0^2 + j^2} + \left(2x_0^2 - j^2\right)\beta_0^2 > 0.$$

The behavior of the stable condition with $|j| > 1$ is different from the behavior with $|j| \le 1$ as shown in the figures of the abstract.

Takashi Hiramatsu
Rikkyo University

"CMB bispectra induced by lensing"

[JGRG28 (2018) PB19]

CMB Bispectra induced by lensing

Takashi Hiramatsu
Rikkyo University

Collaboration with Daisuke Yamauchi (Kanagawa)

Introduction : Cosmic Microwave Background

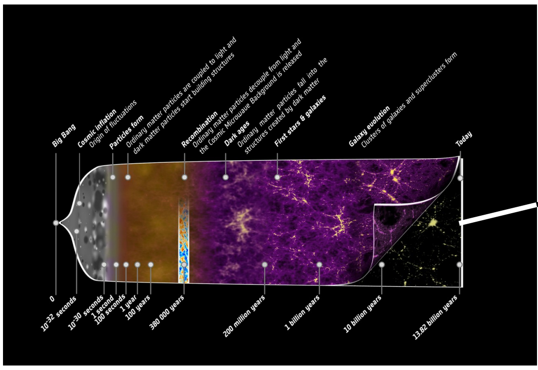

Microwave radiation from last-scattering surface at $z = 1089$

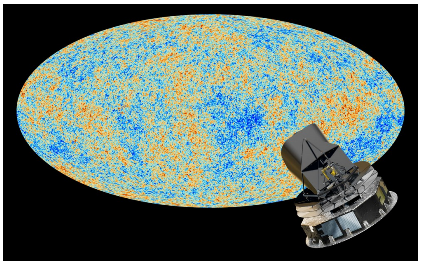

- The remnant of Big-Bang
- Almost isotropic
- Almost complete blackbody radiation with $2.726\mathrm{K}$

$$\rho_\gamma = \frac{\pi^2}{15}T^4$$

(cf. COBE)

- Tiny anisotropic fluctuations with $\mathcal{O}(10)\mu\mathrm{K}$ are induced

Introduction : CMB observation

Takashi Hiramatsu

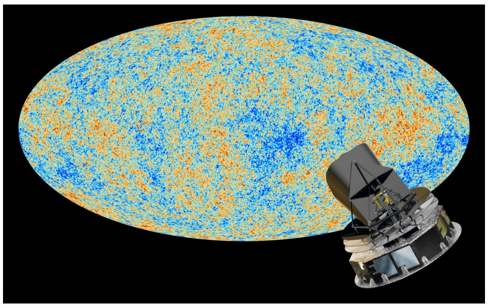

Many kinds of information on the history of the Universe come out.

http://www.sciops.esa.int

From the angular power spectrum,

$$C_\ell^{TT} = \frac{1}{2\ell+1}\sum_m \langle |a_{\ell m}^T|^2\rangle$$

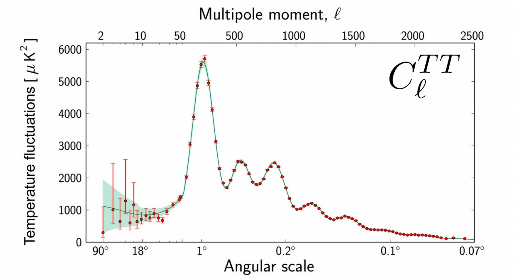

we can estimate the primordial curvature pertubation

$$\langle \zeta(\mathbf{k}_1)\zeta(\mathbf{k}_2)\rangle = (2\pi)^3 P_\zeta(k_1)\delta^{(3)}(\mathbf{k}_1+\mathbf{k}_2)$$

$$P_\zeta(k) = A\left(\frac{k}{k_*}\right)^{n_s-1} \qquad A = 2.196^{+0.080}_{-0.078}\times 10^{-9}, \quad n_s = 0.968\pm 0.006$$

Planck Collaboration, arXiv://1502.01589

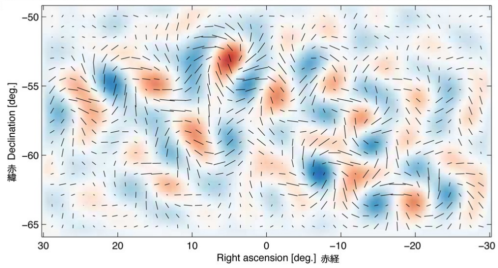

Observations of E/B-mode polarisation give more information on, for instance, primordial gravitational waves.

Introduction : Non-Gaussianity

Takashi Hiramatsu

We focus on the 3-point function (Bispectrum)

$$\langle \zeta(\mathbf{k}_1)\zeta(\mathbf{k}_2)\zeta(\mathbf{k}_3)\rangle = (2\pi)^3 B_\zeta(k_1,k_2,k_3)\delta^{(3)}(\mathbf{k}_1+\mathbf{k}_2+\mathbf{k}_3)$$

Primordial curvature fluctuations

Bispectrum gives the statistical properties beyond the power specttrum,

Gaussian : $\langle \zeta(\mathbf{k}_1)\zeta(\mathbf{k}_2)\zeta(\mathbf{k}_3)\rangle = 0$

Non-Gaussian : $\langle \zeta(\mathbf{k}_1)\zeta(\mathbf{k}_2)\zeta(\mathbf{k}_3)\rangle \neq 0$

Non-Gaussianity is quantified by

$$f_{\rm NL}^{(i)} = \frac{(B_\zeta\cdot B^{\mathrm{temp}(i)})}{(B^{\mathrm{temp}(i)}\cdot B^{\mathrm{temp}(i)})}$$

e.g., Komatsu, Spergel, PRD 63 (2001) 063002

Some inflation models predict large $f_{\rm NL}$ and such models have been roled out by recent Planck observations, $f_{\rm NL} = 0.8\pm 5.0$ Planck Collaboration, A&A 594A (2016) 17

In the next decade, the focus would move to the non-Gaussianity of primordial tensor perturbations that generate the B-mode signals such as $\langle BBB\rangle \propto \langle hhh\rangle$

Introduction : Non-Gaussianity by CMB lensing

We cannot see ζ or h_{ij} directly, but observe $\Theta \equiv \delta T/T$ and E/B-modes.

If the corresponding bispectra are linearly related, $\Theta(\boldsymbol{k}) = \mathrm{factor} \times \zeta(\boldsymbol{k})$, it's easy to get the primordial contribution, $\langle \zeta(\boldsymbol{k}_1)\zeta(\boldsymbol{k}_2)\zeta(\boldsymbol{k}_3)\rangle = \mathrm{factor}^{-3}\,\langle \Theta(\boldsymbol{k}_1)\Theta(\boldsymbol{k}_2)\Theta(\boldsymbol{k}_3)\rangle$

But, unfortunately, it is not the case….

New inflation
Chaotic inflation
Power-law inflation
DBI inflation
K-inflation
Hybrid inflation
MSSM inflation
Brane inflation
⋮

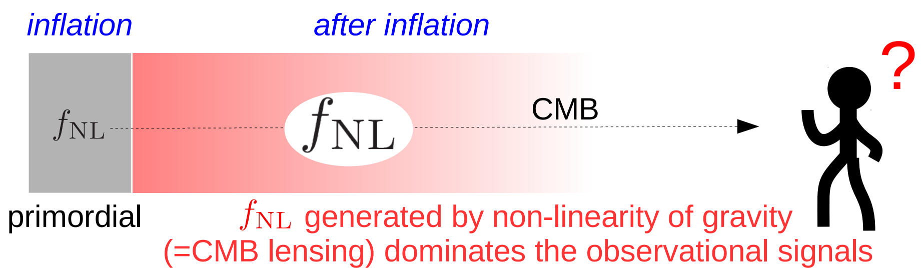

It is crutial to correctly remove the non-linear contributions to estimate the primordial one. If done, we can kill a large number of inflation models. Here we revisit the influence of CMB lensing, and estimate the significance of all kinds of lensing contributions to the CMB bispectra.

Formulation of CMB lensing

Multipole expansion

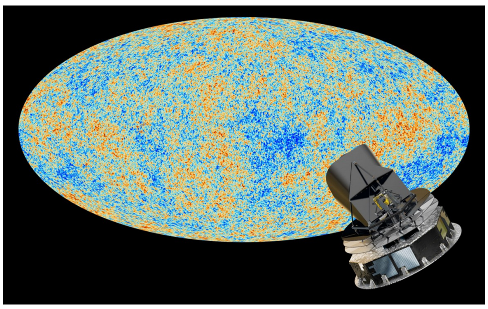

Given the temperature or polarisation map, $X(\hat{\boldsymbol{n}})$,
as a function of the directional vector $\hat{\boldsymbol{n}}$,
the next step is to quantify the pattern on the celestial sphere.

CMB signal $X = \Theta/E/B$ is expanded by the spherical harmonics,

$$X_{LM} = \int d\hat{\boldsymbol{n}}\, X(\hat{\boldsymbol{n}}) Y^*_{LM}(\hat{\boldsymbol{n}})$$

The harmonics coeffient is related with the primordial fluctuations,

$$X^{(Z)}_{LM} = 4\pi(-i)^\ell \int \frac{d^3k}{(2\pi)^3} \sum_s \lambda_{sx} \xi^s(\boldsymbol{k}) \mathcal{T}^{(Z)X}_\ell(k) Y^{-s*}_{\ell m}(\hat{k}) \qquad \lambda_{sx} := (\mathrm{sgn}\ s)^{s+x}$$

$$Z = S(\mathrm{calar}), V(\mathrm{ector}), T(\mathrm{ensor}) \quad [s = 0, \pm 1, \pm 2]$$

CMB Lensing

CMB lensing is characterised in terms of the defelection vector $\boldsymbol{d} = \boldsymbol{\nabla}\phi + (\star\boldsymbol{\nabla})\varpi$,

Gradient-mode

Curl-mode

Yamauchi, Namikawa, Taruya, JCAP 1308 (2013) 051

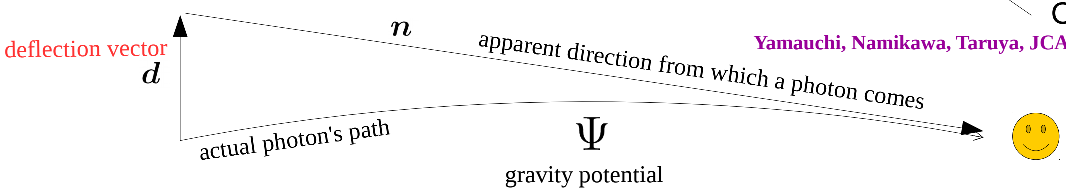

The lensed CMB signal can be written as

$$\widetilde{X}(\hat{\boldsymbol{n}}) = X(\hat{\boldsymbol{n}} + \boldsymbol{d})$$

Expanding it in the assumption that $|\boldsymbol{d}|$ is small, we have

$$\widetilde{X}_{LM} = X_{LM} + \sum_{x\overline{X}\ell\ell' mm'} \mathcal{M}^{L\ell\ell';x;X\overline{X}}_{Mmm'} x_{\ell m}\overline{X}_{\ell' m'} + \frac{1}{2}\sum_{xy\overline{X}\ell\ell'\ell'' mm'm''} \mathcal{M}^{L\ell\ell'\ell'';xy;X\overline{X}}_{Mmm'm''} x_{\ell m} y_{\ell' m'} \overline{X}_{\ell'' m''}$$

$$\mathcal{M}^{L\ell\ell';x;X\overline{X}}_{Mmm'} = (-1)^M \underbrace{\begin{pmatrix} L & \ell & \ell' \\ -M & m & m' \end{pmatrix}}_{\text{Wigner's 3j-symbol}} M^{X\overline{X},x}_{L\ell\ell'}$$

The coefficient matrix M will be defined next.

Coefficient matrix

The integration of triple products of spherical harmonics and their derivative with respect to the solid angle yields the coeffient matrix,

$$M^{X\overline{X},x}_{L\ell\ell'} := \begin{array}{c} \begin{array}{ccc} \Theta & E & B \end{array} \\ \begin{pmatrix} S^{(0)x}_{L\ell\ell'} & 0 & 0 \\ 0 & S^{(+)x}_{L\ell\ell'} & -S^{(-)x}_{L\ell\ell'} \\ 0 & S^{(-)x}_{L\ell\ell'} & S^{(+)x}_{L\ell\ell'} \end{pmatrix} \end{array} \begin{array}{c} \Theta \\ E \\ B \end{array}$$

$$\begin{aligned} S^{(0)\phi}_{\ell_1\ell_2\ell_3} &:= c_{\ell_1\ell_2\ell_3} e\mathcal{S}^{(0)\phi}_{\ell_1\ell_2\ell_3}, & S^{(0)\varpi}_{\ell_1\ell_2\ell_3} &:= c_{\ell_1\ell_2\ell_3} \overline{e}\mathcal{S}^{(0)\varpi}_{\ell_1\ell_2\ell_3}, \\ S^{(+)\phi}_{\ell_1\ell_2\ell_3} &:= c_{\ell_1\ell_2\ell_3} e\mathcal{S}^{\phi}_{\ell_1\ell_2\ell_3}, & S^{(+)\varpi}_{\ell_1\ell_2\ell_3} &:= c_{\ell_1\ell_2\ell_3} \overline{e}\mathcal{S}^{\varpi}_{\ell_1\ell_2\ell_3} \\ S^{(-)\phi}_{\ell_1\ell_2\ell_3} &:= c_{\ell_1\ell_2\ell_3} \overline{e}\mathcal{S}^{\phi}_{\ell_1\ell_2\ell_3}, & S^{(-)\varpi}_{\ell_1\ell_2\ell_3} &:= c_{\ell_1\ell_2\ell_3} e\mathcal{S}^{\varpi}_{\ell_1\ell_2\ell_3} \end{aligned}$$

where

$$c_{\ell_1\ell_2\ell_3} := \sqrt{\frac{(2\ell_1+1)(2\ell_2+1)(2\ell_3+1)}{16\pi}}$$

$$e\mathcal{S}^{(0)\phi}_{\ell_1\ell_2\ell_3} := [-\ell_1(\ell_1+1) + \ell_2(\ell_2+1) + \ell_3(\ell_3+1)] \begin{pmatrix} \ell_1 & \ell_2 & \ell_3 \\ 0 & 0 & 0 \end{pmatrix}$$

$$\overline{e}\mathcal{S}^{(0)\varpi}_{\ell_1\ell_2\ell_3} := 2\sqrt{\ell_2(\ell_2+1)\ell_3(\ell_3+1)} \begin{pmatrix} \ell_1 & \ell_2 & \ell_3 \\ 0 & -1 & 1 \end{pmatrix}$$

$$\mathcal{S}^{\phi}_{\ell_1\ell_2\ell_3} := [-\ell_1(\ell_1+1) + \ell_2(\ell_2+1) + \ell_3(\ell_3+1)] \begin{pmatrix} \ell_1 & \ell_2 & \ell_3 \\ 2 & 0 & -2 \end{pmatrix}$$

$$\mathcal{S}^{\varpi}_{\ell_1\ell_2\ell_3} := \mathcal{S}^{\phi}_{\ell_1\ell_2\ell_3} + 2\sqrt{\ell_2(\ell_2+1)}\sqrt{(\ell_3-1)(\ell_3+2)} \begin{pmatrix} \ell_1 & \ell_2 & \ell_3 \\ 2 & -1 & -1 \end{pmatrix}$$

Formulation of CMB lensing

CMB Bispectrum

Bispectrum is defined as a three-point function of $\Theta/E/B$-signal,

$$\langle X_{L_1M_1}Y_{L_2M_2}Z_{L_3M_3}\rangle = B^{XYZ}_{L_1L_2L_3;M_1M_2M_3}$$

Angular-averaged bispectrum is then defined as

$$B^{XYZ}_{L_1L_2L_3} := \sum_{M_1M_2M_3}\begin{pmatrix} L_1 & L_2 & L_3 \\ M_1 & M_2 & M_3\end{pmatrix} B^{XYZ}_{L_1L_2L_3;M_1M_2M_3}$$

Lensed bispectrum up to 2nd-order

After a little bit long but systematic calculations, we finally find

$$\widehat{B}^{XYZ,ss s'}_{L_1L_2L_3} = \sum_{\overline{X}x}\left(M^{X\overline{X},x}_{L_1L_3L_2}C^{\overline{X}Y(s)}_{L_2}C^{xZ(s')}_{L_3} + \widetilde{M}^{Y\overline{X},x}_{L_2L_3L_1}C^{\overline{X}X(s)}_{L_1}C^{xZ(s')}_{L_3}\right) \qquad (s\neq s')$$

$$\begin{aligned}\widehat{B}^{XYZ,sss}_{L_1L_2L_3} = &\sum_{\overline{X}x}\left(M^{X\overline{X},x}_{L_1L_3L_2}C^{\overline{X}Y(s)}_{L_2}C^{xZ(s)}_{L_3} + M^{Y\overline{X},x}_{L_2L_1L_3}C^{\overline{X}Z(s)}_{L_3}C^{xX(s)}_{L_1} + M^{Z\overline{X},x}_{L_3L_2L_1}C^{\overline{X}X(s)}_{L_1}C^{xY(s)}_{L_2}\right)\\ &+\sum_{\overline{X}x}\left(\widetilde{M}^{X\overline{X},x}_{L_1L_2L_3}C^{\overline{X}Z(s)}_{L_3}C^{xY(s)}_{L_2} + \widetilde{M}^{Y\overline{X},x}_{L_2L_3L_1}C^{\overline{X}X(s)}_{L_1}C^{xZ(s)}_{L_3} + \widetilde{M}^{Z\overline{X},x}_{L_3L_1L_2}C^{\overline{X}Y(s)}_{L_2}C^{xX(s)}_{L_1}\right)\end{aligned}$$

$$X = T,E,B \quad x=\phi,\varpi \quad s = \mathrm{Scalar/Vector/Tensor} \quad \widetilde{M}^{X\overline{X},x}_{\ell_1\ell_2\ell_3} = (-1)^{\ell_1+\ell_2+\ell_3}M^{X\overline{X},x}_{\ell_1\ell_2\ell_3}$$

Boltzmann solver "CMB2nd"

CMB2nd

* Angular power spectra, $C^{\Theta\Theta}_\ell, C^{\Theta E}_\ell, C^{EE}_\ell, C^{BB}_\ell$, from Scalar/Vector/Tensor Perturbations, which are consistent to CAMB results with O(0.1)% error.

* Lensed bispectra $\widehat{B}^{XYZ,s_1s_2s_3}_{L_1L_2L_3}$ as well as the lensed power spectra $\widehat{C}^{XY,s}_L$ (not mentioned in this poster) can be computed.

* To quantify the significance of the bispectra, we compute the signal-to-noise ratio, $\frac{S}{N} = \frac{1}{\sqrt{(F_{ii})^{-1}}}$, where F_{ij} is the Fisher matrix,

$$F_{ij} = \sum_{L_1L_2L_3}\frac{\widehat{B}^i_{L_1L_2L_3}\widehat{B}^j_{L_1L_2L_3}}{\Delta_{L_1L_2L_3}C^{XX}_{L_1}C^{YY}_{L_2}C^{ZZ}_{L_3}} \quad (i,j = XYZ)$$

$$\Delta_{L_1L_2L_3} = 6\ (L_1=L_2=L_3), 2\ (L_1=L_2\neq L_3\ \text{etc.}), 1\ (\text{otherwise})$$

* To quantify the shape of bispectra, CMB2nd can compute $f_{\rm NL}$ parameters for the frequently-used template functions, local/equilateral/orthogonal/folded.

* [Future] To see the modified gravity effects, the effective theory of degenerate higher-order scalar-tensor theory (EFT DHOST) is ready for implementation.

Assumptions

* Cosmological parameters

Basically, we use Planck 2015 results, and assume the Lambda-CDM model with

Planck Collaboration, A&A 594A (2016) 13

$$
\begin{aligned}
h &= 0.6774 & Y_{\rm He} &= 0.24667 \\
h^2\Omega_{\rm CDM} &= 0.1188 & \tau &= 0.066 \\
h^2\Omega_{\rm B} &= 0.02230 & T_0 &= 2.7255\ {\rm K} \\
N_{\rm eff} &= 3.046
\end{aligned}
$$

* Initial power spectrum

$$\text{Scalar}: \quad \mathcal{P}^{(S)}(k) = \mathcal{A}^{(S)}\left(\frac{k}{k_0}\right)^{n_s-1} \qquad \mathcal{A}^{(S)} = 2.384\times 10^{-9},\ n_s = 0.9667,\ k_0 = 0.002\ {\rm Mpc}^{-1}$$

$$\text{Vector}: \quad \mathcal{P}^{(V)}(k) = r_V\mathcal{A}^{(S)}\left(\frac{k}{k_0}\right)^{n_v} \qquad r_v = 0.01,\ n_v = 0$$

(Large and flat vector spectrum is not realistic, but we use it to demonstrate the influence of vector modes on the lensing bispectra.)

$$\text{Tensor}: \quad \mathcal{P}^{(T)}(k) = r_T\mathcal{A}^{(S)}\left(\frac{k}{k_0}\right)^{n_t} \qquad r_t = 0.01,\ n_t = 0$$

Results : signal-to-noise ratio (vector)

$(r_V, r_T) = (0.01, 0)$ Cosmic variance limited ——   LiteBIRD ··········

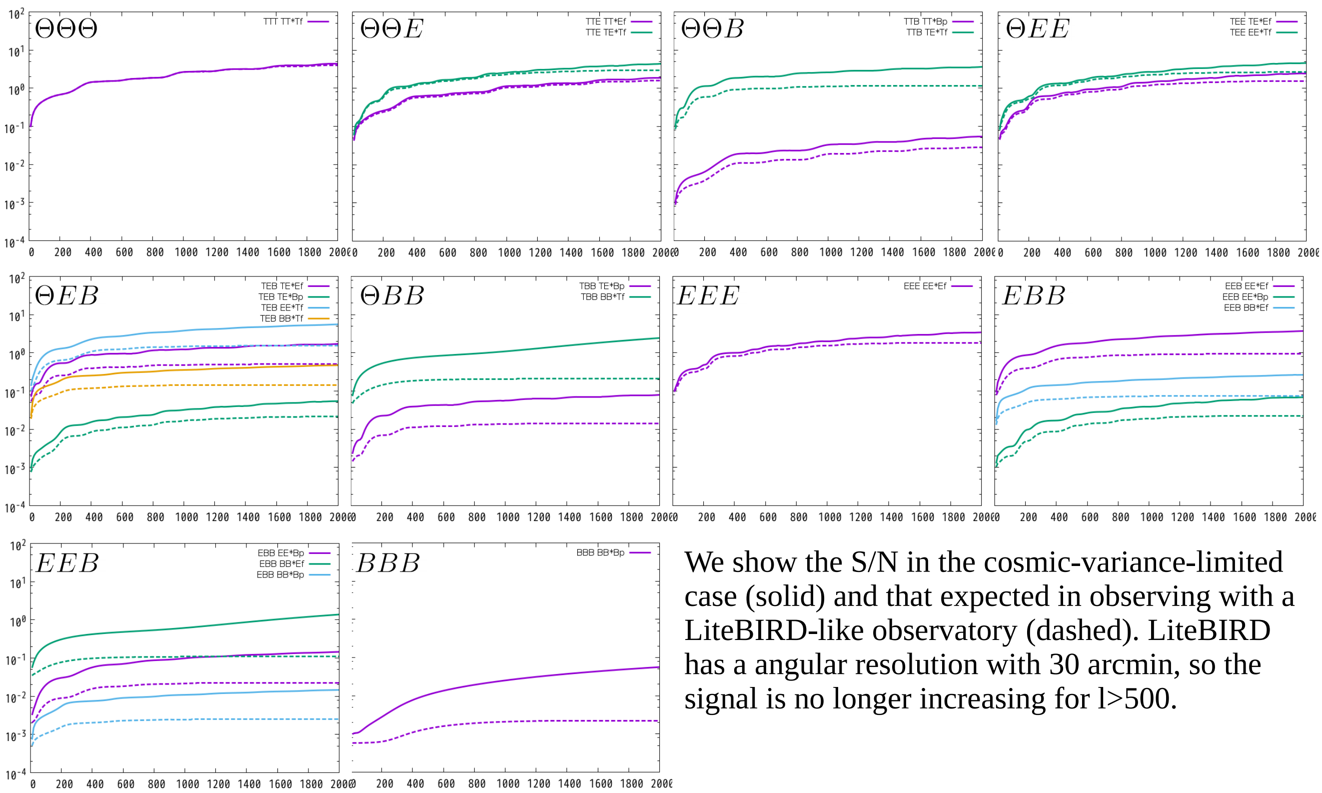

We show the S/N in the cosmic-variance-limited case (solid) and that expected in observing with a LiteBIRD-like observatory (dashed). LiteBIRD has a angular resolution with 30 arcmin, so the signal is no longer increasing for l>500.

Results : signal-to-noise ratio (tensor)

Takashi Hiramatsu

$(r_V, r_T) = (0, 0.01)$ Cosmic variance limited ——— LiteBIRD ....

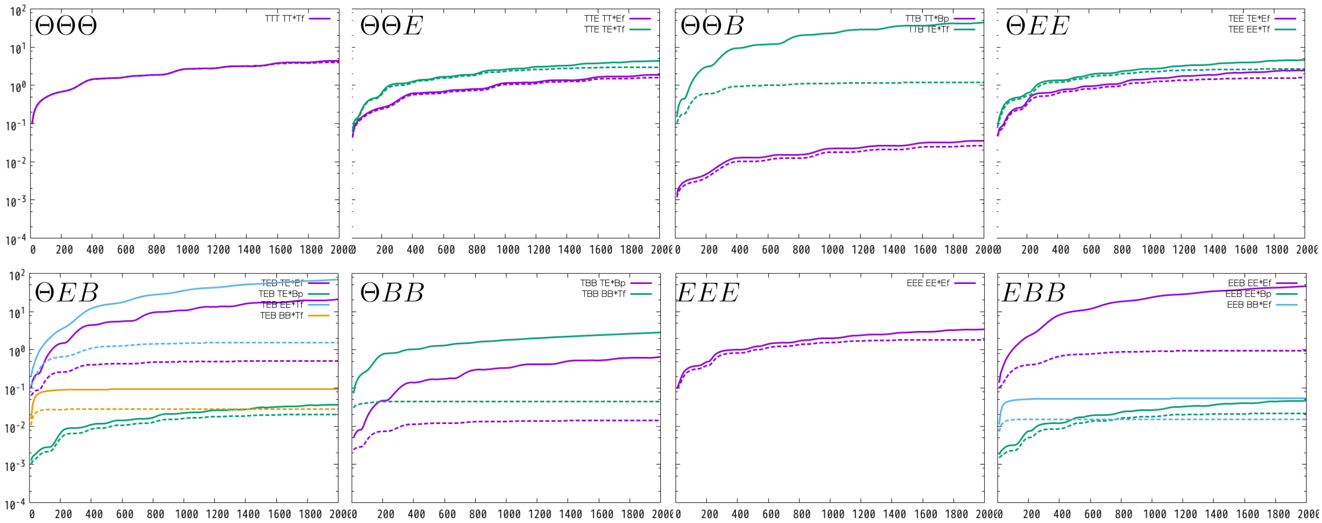

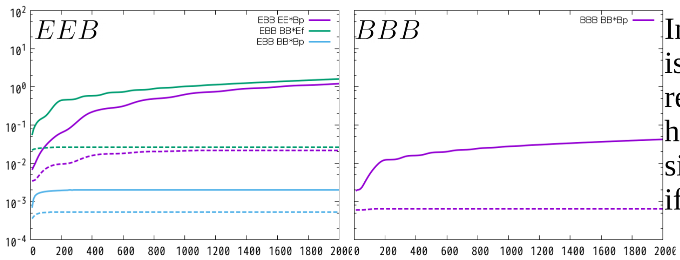

In the absence of vector modes, the cosmic variance is reduced, resulting in the increase of S/N. Our results imply that $\Theta\Theta\Theta/\Theta\Theta E/\Theta EE/\Theta EB/EEE$ have a potential to be observed, and EBB is the only signal sourced by the curl-mode and to be observed if the cosmic-variance-limited observation is possible.

Results : bispectrum shape

Takashi Hiramatsu

Next we focus on the shape of bispectra. In particular, here we compare the squeezed slice $(\ell_1, \ell_2, \ell_3) = (4, \ell, \ell+4)$ with the equilateral slice $(\ell_1, \ell_2, \ell_3) = (\ell-2, \ell, \ell+2)$.
To save the number of slices, we show the case with $(r_V, r_T) = (0, 0.01)$ only.

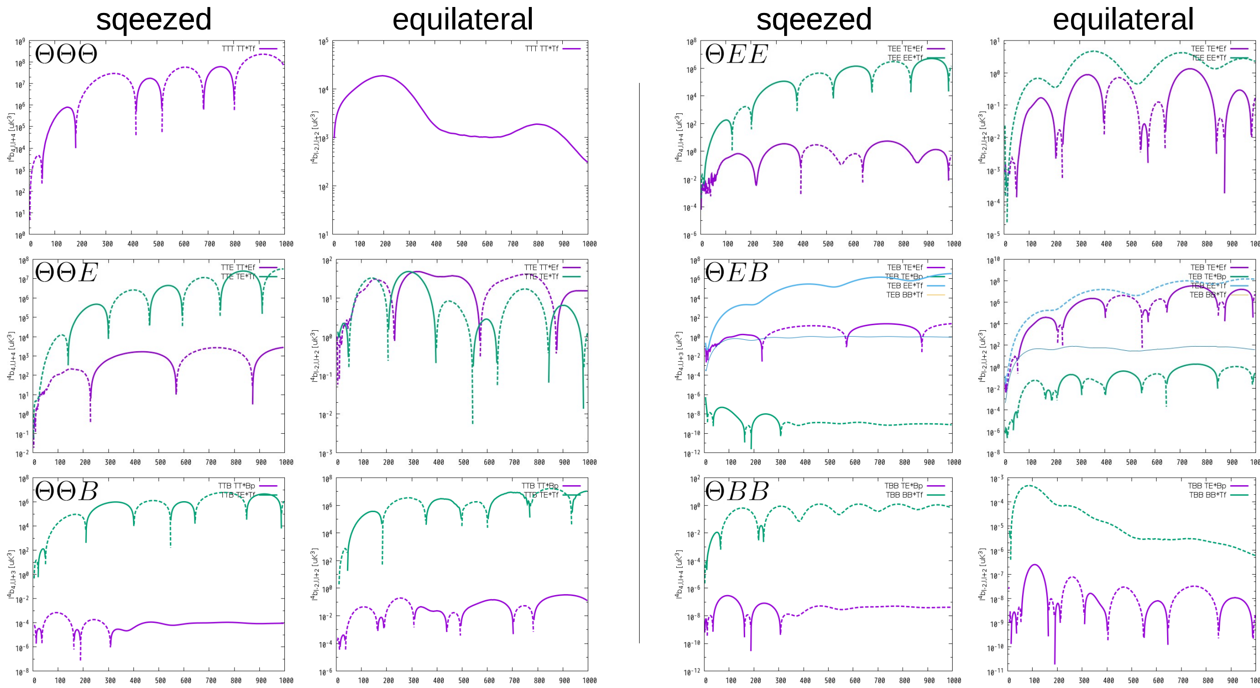

Results : bispectrum shape

Takashi Hiramatsu

sqeezed | equilateral | sqeezed | equilateral

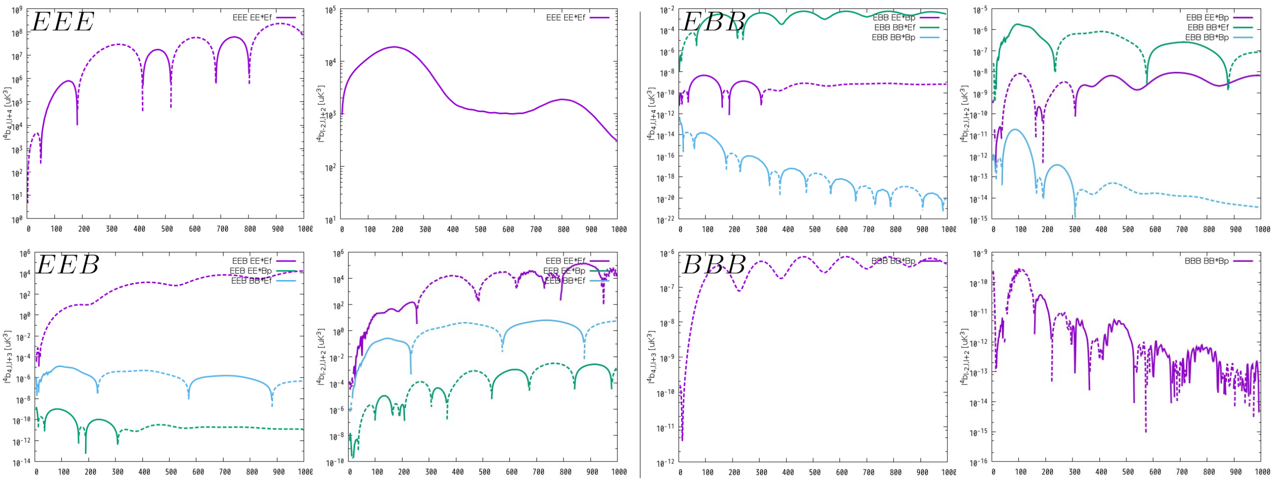

Some signals indicate the equilateral shape rather than local (squeezed) shape.

Results : Estimating “$f_{\rm NL}$”

Takashi Hiramatsu

Fisher analysis

To quantify the shape of bispectra, we introduce the paramter $f_{\rm NL}$, which is defined as a quantity minimising the following chi-square,

$$\chi^2 = \sum_{\ell_1\leq\ell_2\leq\ell_3}\left(B^{XYZ}_{\ell_1\ell_2\ell_3} - f^{XYZ,A}_{\rm NL}B^{({\rm temp}),A}_{\ell_1\ell_2\ell_3}\right)^2$$

where $X,Y,Z=\Theta/E/B$ and $A={\rm local/equilateral/orthogonal/folded}$.

In the usual analysis, a template function is given as a reduced bispectrum $b^A_{\ell_1\ell_2\ell_3}$ and the relation with the angular-averaged bispectrum is

$$B^{({\rm temp}),A}_{\ell_1\ell_2\ell_3} = I^{000}_{\ell_1\ell_2\ell_3}b^A_{\ell_1\ell_2\ell_3} \qquad I^{s_1s_2s_3}_{\ell_1\ell_2\ell_3} := \sqrt{\frac{(2\ell_1+1)(2\ell_2+1)(2\ell_3+1)}{4\pi}}\begin{pmatrix}\ell_1 & \ell_2 & \ell_3\\ s_1 & s_2 & s_3\end{pmatrix}$$

However, $B^{({\rm temp}),A}_{\ell_1\ell_2\ell_3}$ is non-zero only if $\ell_1+\ell_2+\ell_3={\rm even}$. Hence it is impossible to quantify the shapes of odd-parity bispectra (non-zero only if $\ell_1+\ell_2+\ell_3={\rm odd}$) like $\Theta\Theta B/\Theta EB/EEB$ and BBB. Instead we use

$$B^{({\rm temp}),A}_{\ell_1\ell_2\ell_3} = I^{2,-1,-1}_{\ell_1\ell_2\ell_3}b^A_{\ell_1\ell_2\ell_3}$$

Shiraishi, Liguori, Fergusson, JCAP 1405 (2014) 008

This template function has no longer the original meaning, but we use it to quantify the shapes of both even- and odd-parity bispectra.

Results : Estimating “f$_{\rm NL}$” for CVL case

立教大学 RIKKYO UNIVERSITY
Takashi Hiramatsu

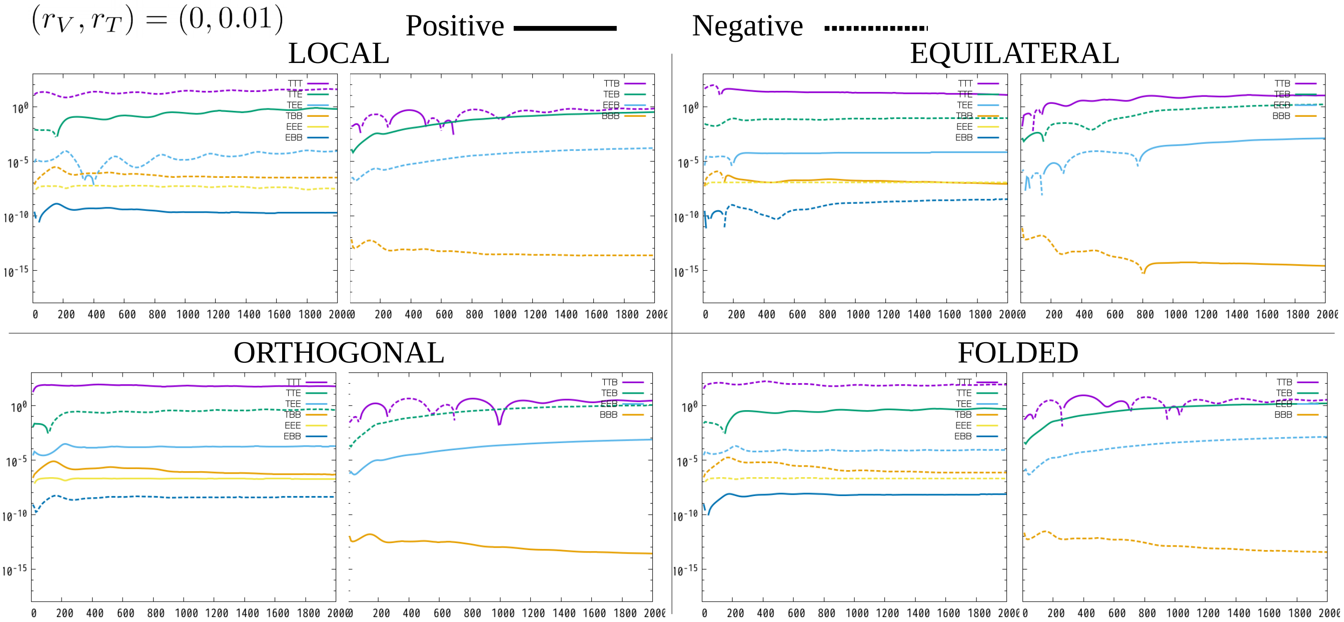

We estimate the $f_{\rm NL}$ paramter with four kinds of frequently-used template functions to quantify the shape of bispectrum in the cosmic-variance-limited case. Here we used $I^{-2,1,1}_{\ell_1\ell_2\ell_3}$ factor to define the templates, so notice that the original role of $f_{\rm NL}$ parameter is lost.

In particular, $\Theta\Theta B/\Theta EB/EEE$ have a equilateral feature in comparison with $\Theta\Theta\Theta$. Besides, BBB seems to be featureless in the sense that the $f_{\rm NL}$ paramter is not highly sensitive to the shape.

Results : Estimating “f$_{\rm NL}$”

立教大学 RIKKYO UNIVERSITY
Takashi Hiramatsu

First we define the ratio of $f_{\rm NL}$'s for equilateral/orthogonal/folded to local-type.

$$R^{A(X)} := \frac{f_{\rm NL}^{A(X)}}{f_{\rm NL}^{{\rm local}(X)}} \qquad \begin{array}{l} A = \text{equilateral, orthogonal, folded} \\ X = \Theta\Theta\Theta, \Theta\Theta E, \Theta\Theta B, \Theta EE, \Theta EB, \Theta BB \\ \quad , EEE, EEB, EBB.BBB \end{array}$$

The statistic R roughly gives the trend of each shape comparing with local-type shape. Next we define the ratio of R for each bispectrum and R for TTT:

$$S^{A(X)} := \frac{R^{A(X)}}{R^{A(\Theta\Theta\Theta)}}$$

The statistic S gives the trend comparing with $\Theta\Theta\Theta$ bispectrum.

	equilateral	orthogonal	folded
TTT	1	1	1
TTE	0.48	0.46	0.38
TTB	50.09	2.85	2.37
TEE	2.49	1.46	0.47
TEB	16.63	2.26	2.32
TBB	0.81	0.96	1.01
EEE	13.39	4.46	3.46
EEB	25.68	3.21	4.00
EBB	54.85	15.60	18.74
BBB	0.37	0.81	0.78

$(r_V, r_T) = (0, 0.01)$

We estimate S for all bispectra (CVL) at $\ell_{\rm max} = 2000$.

S-statistic implies that $\Theta\Theta B/\Theta EB/EEE/EEB$ look “more equilateral” comparing with $\Theta\Theta\Theta$.

All S-statistics for EBB are large, implying that EBB is not local.

Three-lines summary

- In near future, we will succeed to observe the B-mode signal and it will be possible to estimate the CMB bispectra of primordial origin.

- To extract the primordial signals from the real observations, we need to estimate the lensing contributions with a good accuracy.

- We found that $\Theta\Theta\Theta/\Theta\Theta E/\Theta EE/\Theta EB/EEE$ could be observable with a LiteBIRD-like observatory, and the bispectra induced by the curl-mode are highly difficult to be observed.

Kiyoshi Shiraishi
Yamaguchi University

“An ostentatious model of cosmological scalar-tensor theory”

[JGRG28 (2018) PB20]

PB20: An ostentatious model of cosmological scalar-tensor theory

N. Kan (NIT, Gifu College) and K. Shiraishi (Yamaguchi U.)

based on:

An ostentatious model of cosmological scalar-tensor theory

arXiv:1807.10411 [gr-qc]

Nahomi Kan and Kiyoshi Shiraishi

We consider a novel model of gravity with a scalar field described by the Lagrangian with higher order derivative terms in a cosmological context. The model has the same solution for the homogeneous and isotropic universe as in the model with General Relativity (GR), notwithstanding the additional higher order terms. A possible modification scenario is briefly discussed lastly.

§ 1. Introduction

Neutron star merger:
GW170817 / GRB 170817A

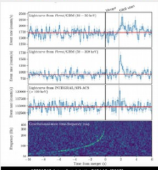

170817A", Astrophys. J. Lett. 848:L13 (2017)

the speed of GW ∼ the light speed *in high accuracy*

e.g. Phys. Rev. Lett. 119 (2017) 251301--251304

↓

Severe constraints on parameters in Modified Gravities (MG) in general!

・Recently, Motohashi and Minamitsuji (Phys. Lett. B781 (2018) 728) proposed a possible form of the Lagrangian for Modified Gravity, which leads to General Relativity solutions.

What is the simplest model of MG which admits GR solutions?

Suppose the gravitating scalar system in GR:

$$I_0=\int d^4x\sqrt{-g}L_0=\int d^4x\sqrt{-g}\left[R-\sigma\frac{1}{2}(\nabla\phi)^2-V(\phi)\right].$$

This leads to GR solution:

$$T_{\mu\nu}\equiv\frac{1}{\sqrt{-g}}\frac{\delta I_0}{\delta g^{\mu\nu}}=R_{\mu\nu}-\frac{1}{2}Rg_{\mu\nu}-\sigma\frac{1}{2}\nabla_\mu\phi\nabla_\nu\phi+\sigma\frac{1}{4}(\nabla\phi)^2g_{\mu\nu}+\frac{1}{2}V(\phi)g_{\mu\nu}$$
$$\equiv\tau_{\mu\nu}-\frac{1}{2}\tau g_{\mu\nu}+\frac{1}{2}V(\phi)g_{\mu\nu}=0.$$

If one considers

$L=L_0+F(T_{\mu\nu})$ (F is 2nd or higher order in $T_{\mu\nu}$),

he can obtain the GR solution $T_{\mu\nu}=0$ (as one of solutions)

A MG model which admits GR solutions!

… Such a model describes Higher-Order Gravity!

higher-derivative→Ghost

$$\text{propagator}\sim\frac{1}{k^2(k^2+m^2)}=\frac{1}{m^2}\left[\frac{1}{k^2}-\frac{1}{k^2+m^2}\right]$$

Is it pathological in quantum field theory?
*many cure methods have been proposed
e.g. Anselmi and Piva, arXiv:1806.03605, etc.,etc..
We won't touch them in this talk.

(semi-) classically, ghost modes cause finite-range force, which may modify the gravitation law at the galactic scale.

Meissner--Olechowski Gravity

(PRL86(2001)3708, PRD65(2002)064017)

which includes ghost tensor modes and no scalar mode, found through the study of "Critical Gravity"(PRL106(2011)181302)
(in a narrow definition, critical means prop.∼$1/k^4$)
[⇔ F(R) theory includes a scalar degree of freedom, no tensor ghost]
is governed by the Lagrangian expressed by LC of:

$$L^{(n)}_{MO}=-\delta^{\mu_1\cdots\mu_n}_{\nu_1\cdots\nu_n}S_R{}^{\nu_1}_{\mu_1}\cdots S_R{}^{\nu_n}_{\mu_n}\equiv-[S_R\cdots S_R]$$

$$S_R^{\mu\nu}=R^{\mu\nu}-\tfrac{1}{6}Rg^{\mu\nu},\qquad \delta^{\mu_1\mu_2\cdots\mu_p}_{\nu_1\nu_2\cdots\nu_p}\equiv\begin{vmatrix}\delta^{\mu_1}_{\nu_1}&\delta^{\mu_1}_{\nu_2}&\cdots&\delta^{\mu_1}_{\nu_p}\\\delta^{\mu_2}_{\nu_1}&\delta^{\mu_2}_{\nu_2}&\cdots&\delta^{\mu_2}_{\nu_p}\\\vdots&\vdots&\ddots&\vdots\\\delta^{\mu_p}_{\nu_1}&\delta^{\mu_p}_{\nu_2}&\cdots&\delta^{\mu_p}_{\nu_p}\end{vmatrix}$$

[Well, we don't want any more scalar modes than ϕ ...]

§ 2. our model

We can use [SS], [SSS] and [SSSS] in the Lagrangian for our model,

where $S_{\mu\nu}\equiv T_{\mu\nu}-\dfrac{1}{3}Tg_{\mu\nu}$

(in the absence of the scalar kinetic and potential term, $S=S_R$)

For example: $L=\alpha L_0+\beta[SS]$

$$L=\alpha\left[R-\sigma\frac{1}{2}(\nabla\phi)^2-V(\phi)\right]-\beta\left[\left(R^\nu_\mu-\sigma\frac{1}{2}\nabla_\mu\phi\nabla^\nu\phi\right)^2-\frac{1}{3}\left(R-\sigma\frac{1}{2}(\nabla\phi)^2\right)^2+\frac{1}{3}V(\phi)\left(R-\sigma\frac{1}{2}(\nabla\phi)^2\right)-\frac{1}{3}V^2(\phi)\right].$$

[SSS] and [SSSS] contribute $O(h_{\mu\nu}{}^3)$ and $O(h_{\mu\nu}{}^4)$ in terms of $h_{\mu\nu}=g_{\mu\nu}-\bar{g}_{\mu\nu}$, deviation from the B.G. $T_{\mu\nu}=0$.

We then consider

$$L=\alpha L_0+\beta[SS]+\gamma[S_\tau SS]+\delta[S_\tau S_\tau SS]$$

where $S_{\tau\mu\nu}\equiv\tau_{\mu\nu}-\frac{1}{6}\tau g_{\mu\nu}$.

Then, we obtain

$$\sqrt{-g}L=\sqrt{-\bar{g}}\left[\alpha\frac{1}{4}h^{\mu\nu}\bar{\nabla}^2h_{\mu\nu}-\left\{\beta+\gamma\frac{V(\bar{\phi})}{3}+\delta\frac{V^2(\bar{\phi})}{18}\right\}\frac{1}{4}h^{\mu\nu}\bar{\nabla}^2\bar{\nabla}^2h_{\mu\nu}+\cdots\right]$$

There is a Ghost tensor mode with mass

$$m^2(\bar{\phi})=\alpha(\beta+\gamma V(\bar{\phi})/3+\delta V^2(\bar{\phi})/18)^{-1},$$

which affects galaxy rotation curve(?)
(possibly time-dependent)

§ 3. not-so-ostentatious model

We consider $L'=L+\beta\left(R^\mu_\nu R^\nu_\mu-\frac{1}{3}R^2\right)$, $L=\alpha L_0+\beta[SS]$.

L' and L lead to the same FLRW GR solution,

because $R^\mu_\nu R^\nu_\mu-\frac{1}{3}R^2\equiv0$ for conformally flat spacetime.

The model includes no ghost tensor mode but higher order of the scalar field ϕ:

$$L'=\alpha\left[R-\sigma\frac{1}{2}(\nabla\phi)^2-V(\phi)\right]+\beta'\left[-\sigma\frac{1}{6}V(\phi)(\nabla\phi)^2+\sigma^2\frac{1}{6}[(\nabla\phi)^2]^2-\frac{1}{3}V^2(\phi)+\frac{1}{3}\left(V(\phi)+\sigma(\nabla\phi)^2\right)R-\sigma R^{\mu\nu}\nabla_\mu\phi\nabla_\nu\phi\right],$$

where $\beta'\equiv-\beta$.

The speed of GW

Kobayashi,Yamaguchi,Yokoyama,PTP126(2011)511,
DeFelice,Tsujikawa,PRD84(2011)083504;JCAP1303(2013)030

$$ds^2=-dt^2+a^2(t)(1+2\Phi)d\mathbf{x}^2$$

$$\int d^4x\sqrt{-g}L'=\int d^4x a^3\left[\frac{w_4}{a^2}(\partial_i\Phi)^2-3w_1\dot{\Phi}^2+\cdots\right]$$

where $w_4=2\left(\alpha+\frac{\beta'}{3}V(\bar{\phi})\right)-\frac{2}{3}\sigma\beta'\dot{\bar{\phi}}^2,\quad w_1=2\left(\alpha+\frac{\beta'}{3}V(\bar{\phi})\right)+\frac{4}{3}\sigma\beta'\dot{\bar{\phi}}^2$

$$c^2_{GW}=\frac{w_4}{w_1}=1-\frac{2\sigma\beta'}{w_1}\dot{\bar{\phi}}^2$$

needs fine tuning

§ 4. Modification?

The 1st model up to 2nd order:

$$L=\alpha L_0-\beta\left(T^{\mu\nu}T_{\mu\nu}-\frac{1}{3}T^2\right)$$

is equivalent to the Lagrangian including an auxiliary symmetric tensor field

$$\tilde{L}=\alpha L_0-\beta(2T_{\mu\nu}\tilde{S}^{\mu\nu}-\tilde{S}_{\mu\nu}\tilde{S}^{\mu\nu}+\tilde{S}^2),$$

$$\text{where }\tilde{S}\equiv\tilde{S}^\mu_\mu$$

The condensation $\langle\tilde{S}^\nu_\mu\rangle=\Lambda\delta^\nu_\mu$ brings about

$$\tilde{L}=(\alpha+2\beta\Lambda)\left(R-\frac{1}{2}\sigma(\nabla\phi)^2\right)-(\alpha+4\beta\Lambda)V(\phi)-\beta\Lambda^2$$

(the condensasion mechanism needs quantum effects of additional fields ...)

§ 5. Summary

We consider a novel model of gravity with a scalar field described by the Lagrangian with higher order derivative terms in a cosmological context. The model has the same solution for the homogeneous and isotropic universe as in the model with General Relativity (GR), notwithstanding the additional higher order terms. A possible modification scenario is briefly discussed.

Ghost condensasion?

future study : relating with
induced gravity / quantum cosmology / higher dimensions / supersymmetry / torsion / helthy quantization?

Hisaaki Shinkai
Osaka Institute of Technology

"INO: Interplanetary Network of Optical Lattice Clocks"

[JGRG28 (2018) PB21]

INO: Interplanetary Network of Optical Lattice Clocks

Hisa-aki Shinkai, with T. Ebisuzaki, H. Katori, J. Makino, A. Noda, and T. Tamagawa
(Osaka Inst. Technology / RIKEN/ U Tokyo / JAXA)

真貝寿明（大阪工業大），戎崎俊一，香取秀俊，牧野淳一郎，玉川徹（理化学研究所），野田篤司（JAXA）

Outline & Summary

The new technique of measuring frequency by optical lattice clocks now approaches to the relative precision of ($\Delta f/f$)=O(10^{-18}).
We propose to place such precise clocks in space and to use Doppler tracking method for detecting low-frequency gravitational wave below 1 Hz.
Our idea is to locate three satellites at one A.U. distance (say at L1, L4 & L5 of the Sun-Earth orbit), and apply the Doppler tracking method by communicating "the time" each other. Applying the current available technologies, we obtain the sensitivity for gravitational wave with three or four-order improvement ($h_n \sim 10^{-17}$ or 10^{-18} level in 10^{-5} Hz -- 1 Hz) than that of Cassini satellite in 2001.
This sensitivity enables us to observe black-hole mergers of their mass greater than 10^5 Msun in the cosmological scale.
Based on the hierarchical growth model of black-holes in galaxies, we estimate the event rate of detection will be 20-50 a year.
We nickname "INO" , named after Tadataka Ino (1745--1818), a Japanese astronomer, cartographer, and geodesist. [arXiv:1809.10317]

伊能忠敬　没後 200 年

Improvement of Doppler-tracking sensitivity

1. Introduction : Optical Lattice Clock

"Optical Lattice Clock"
H. Katori (JPS Journal, 2002, p754)
trap atoms at standing laser wave
read frequency of transient phase

Cs atomic clock $\Delta t/t = 5\times10^{-16}$
Optical Lattice Clock (2015) 10^{-18}
magic freq. compensates multi-polarization
OLC targets $\Delta t/t = 10^{-19}$

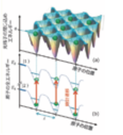

JPS J. 2017, p84

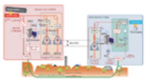

grav. potential of 15m difference
relativistically measured ± 5cm (1 cm on the Earth $\Delta t/t$= 1.1 x10^{-18})

GW detector using Optical Lattice Clocks in Space

3. Principle of GW detection

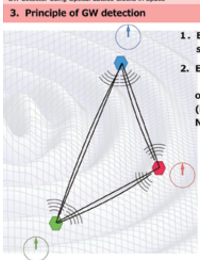

1. Each satellite has Opt Lattice Clock, send out each time to others.
2. Each satellite recognizes direction · distance · velocity of others, and we know all of them (including the potential of the Sun.) Note: effects of planets are O(month).
3. When GW passes, we know its differences. If the events are ~10s (/yr), then we can calibrate them well.

2. Doppler tracking of Cassini Saturn Explorer

Cassini 2001-2002 (Armstrong, LRR 2006)

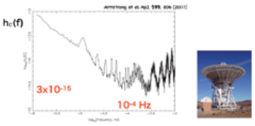

G. Cassini (1625-1712)

Cassini (1997-2017)

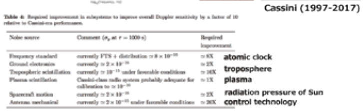

2. Improvement of Doppler sensitivity (1)

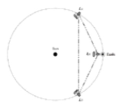

1 AU baseline ▶ 10^{-5}Hz

▶ monitor the time by Opt Lattice Clocks in 3 satellites (need to make it portable)
If radio transmission, use two frequency ranges (double tracking) to check phase differences due to interplanetary plasma
▶ If light transmission, no effects from plasma. (need R&D)

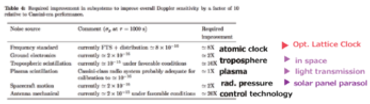

2. Improvement of Doppler sensitivity (2)

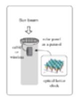

rad. press. F=P/c
P=1.3 kW/m²
1000 kg, 10 m²
acceleration
a=5x10^{-8} m/s²
$\Delta P/P \fallingdotseq 1/1000$
$\Delta a/a \fallingdotseq 10^{-11}$
▶ solar panel parasol
1 AU baseline ▶ 10^{-5}Hz　$\Delta g/g \fallingdotseq 10^{-12}$

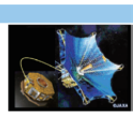

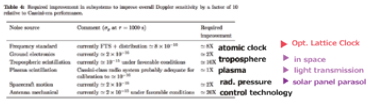

2. Improvement of Doppler sensitivity (3)

With current technologies, we can obtain 3-order less than Cassini !

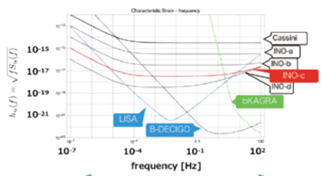

sensitivity f^{-1}
satellite control perturbation

sensitivity $f^{2/3}$+10^{-18}
Opt. Lattice Clock limitation

Detectable Distance

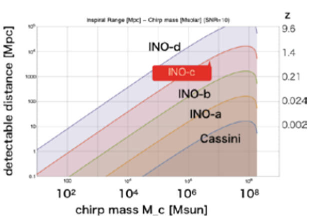

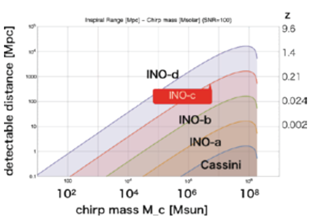

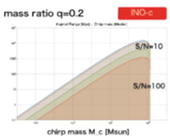

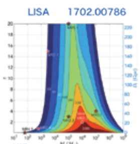

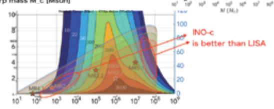

How many BH mergers in 1-year observation ?

Hierarchical growth model of SMBH

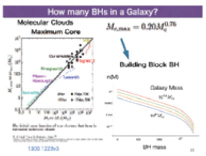

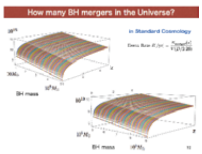

ApJ. 835 (2017) 276

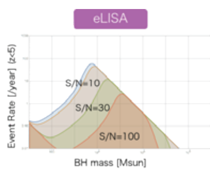

S/N=10　520/year
(range: 550M-3.8x10^5M)
S/N=30　6/year
(range: 5.5x10^3M-3.3x10^4M)

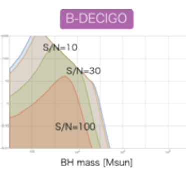

S/N=10　18000/year
(range: 10M-7.9x10^4M)
S/N=30　4300/year
(range: 10M-3.3x10^4M)

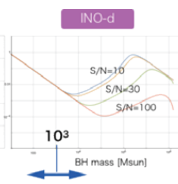

19.2/yr　29.8/yr
S/N=10

Atsushi Miyauchi
Research Organization for Information Science and Technology

"Reformulating Yang-Mills Theory as a Non-Abelian Electromagnetism"

[JGRG28 (2018) PB22]

Reformulating Yang-Mills Theory as a Non-Abelian Electromagnetism

Atsushi Miyauchi

Research Organization for Information Science and Technology (RIST), Kobe, Japan

Motivation

Einstein's equations accompany constraints which reflect gauge invariance. In numerical relativity, constraints are able to be managed rather well recently. However, its instruments are still empirical or intuitive. To understand such constrained system mathematically better, I investigated Yang-Mills theory as a preliminary step to general relativity. Notice that both theories are non-Abelian. Differential forms are consistently employed for manipulation. Discussion proceeds as parallel to Abelian theory(i.e. Maxwell's equations) as possible.

Prerequisite formula

4D exterior derivative of a 3D form can be decomposed into a sum of 3D exterior derivative and temporal form. As an example, 1-form is shown below. With direct manipulation, we can confirm any form can be written in a same formula. Underline in the bottom line designates 3D exterior derivative.

$$\begin{aligned} d\mathbf{A} &= d\left(A_x dx + A_y dy + A_z dz\right) \\ &= dA_x \wedge dx + dA_y \wedge dy + dA_z \wedge dz \\ &= \left(\partial_x A_x dx + \partial_y A_x dy + \partial_z A_x dz + \partial_t A_x cdt\right) \wedge dx \\ &\quad + \left(\partial_x A_y dx + \partial_y A_y dy + \partial_z A_y dz + \partial_t A_y cdt\right) \wedge dy \\ &\quad + \left(\partial_x A_z dx + \partial_y A_z dy + \partial_z A_z dz + \partial_t A_z cdt\right) \wedge dz \\ &= cdt \wedge \dot{\mathbf{A}} + \underline{d}\mathbf{A} \end{aligned}$$

Maxwell's theory

Assume there exists connection A for gauge group $U(1)$, then

Field strength (geometry) $F \equiv dA$

Action (dynamics) $S[A, j] = \int \left(\frac{1}{2} F \wedge {}^*F + j \wedge A\right)$

Equations to be solved $\boxed{\begin{aligned} dF &= 0, \\ d^*F &= j, \end{aligned}}$ Bianchi identity (geometry); Euler-Lagrange equation (dynamics)

3+1 D decomposition $F = -cdt \wedge \mathbf{E} + \mathbf{B}, \quad {}^*F = G = cdt \wedge \mathbf{H} + \mathbf{D}, \quad A = \phi cdt + \mathbf{A}\,,$

Electric and magnetic fields in terms of connection

Applying 3+1D decomposition,

$$dA = d\phi \wedge cdt + d\mathbf{A} = \left(cdt\dot{\phi} + \underline{d}\phi\right) \wedge cdt + cdt \wedge \dot{\mathbf{A}} + \underline{d}\mathbf{A} = cdt \wedge \left(\dot{\mathbf{A}} - \underline{d}\phi\right) + \underline{d}\mathbf{A},$$

$$\therefore \;\; F = dA = cdt \wedge \left(\dot{\mathbf{A}} - \underline{d}\phi\right) + \underline{d}\mathbf{A},$$

Therefore,

$$\mathbf{E} = \underline{d}\phi - \dot{\mathbf{A}}, \qquad \mathbf{B} = \underline{d}\mathbf{A},$$

Bianchi identity

Applying 3+1D decomposition,

$$0 = dF = cdt \wedge d\mathbf{E} + d\mathbf{B} = cdt \wedge \left(cdt \wedge \dot{\mathbf{E}} + \underline{d}\mathbf{E}\right) + +cdt \wedge \dot{\mathbf{B}} + \underline{d}\mathbf{B} = cdt \wedge \left(\underline{d}\mathbf{E} + \dot{\mathbf{B}}\right) + \underline{d}\mathbf{B}$$

Consequently, we have $\boxed{\text{Faraday's law: } \partial_t \mathbf{B} = -\underline{d}\mathbf{E}, \quad \text{Gauss's law: } \underline{d}\mathbf{B} = 0.}$

Euler-Lagrange equation

$$\begin{aligned} j = D^*F &= dG \\ &= -cdt \wedge d\mathbf{H} + d\mathbf{D} \\ &= -cdt \wedge \left(cdt \wedge \dot{\mathbf{H}} + \underline{d}\mathbf{H}\right) + cdt \wedge \dot{\mathbf{D}} + \underline{d}\mathbf{D} \\ &= -cdt \wedge \left(\underline{d}\mathbf{H} - \dot{\mathbf{D}}\right) + \underline{d}\mathbf{D} \end{aligned}$$

Notice that $j \equiv -cdt \wedge \mathbf{i} + \rho$Consequently, we have

$$\boxed{\text{Ampere's law: } \partial_t \mathbf{D} = \underline{d}\mathbf{H} - \mathbf{i}, \quad \text{Gauss's law: } \underline{d}\mathbf{D} = \rho.}$$

Differential forms | **Differential equations**

$$\boxed{\begin{gathered} \partial_t \mathbf{B} = -\underline{d}\mathbf{E}, \\ \partial_t \mathbf{D} = \underline{d}\mathbf{H} - \mathbf{i}, \\ \underline{d}\mathbf{D} = \rho, \\ \underline{d}\mathbf{B} = 0, \end{gathered}} \Longleftrightarrow \boxed{\begin{gathered} \nabla \times \boldsymbol{E} = -\dot{\boldsymbol{B}}\,, \\ \nabla \times \boldsymbol{H} = \boldsymbol{i} + \dot{\boldsymbol{D}}\,, \\ \nabla \cdot \boldsymbol{D} = \rho\,, \\ \nabla \cdot \boldsymbol{B} = 0\,, \end{gathered}}$$

Faraday's law
Ampere's law
Gauss's law

If Gauss's law(i.e. constraint) is fulfilled initially, it remains ever after under charge conservation.

$$\partial_t\left(\underline{d}\mathbf{B}\right) = \underline{d}(\partial_t \mathbf{B}) = -\underline{d}\left(\underline{d}\mathbf{E}\right) = 0,$$

$$\partial_t\left(\underline{d}\mathbf{D} - \rho\right) = \underline{d}(\partial_t \mathbf{D}) - \partial_t \rho = \underline{d}\left(\underline{d}\mathbf{H} - \mathbf{i}\right) - \partial_t \rho = -\left(\partial_t \rho + \underline{d}\mathbf{i}\right) = 0,$$

Yang-Mills theory

Assume there exists connection A for gauge group $SU(N)$, then

Field strength (geometry) $F \equiv DA = dA + A \wedge A$ (D: covariant exterior derivative)

Action (dynamics) $S[A, j] = \int \left(\frac{1}{2} F \wedge {}^*F + j \wedge A\right)$

Equations to be solved $\boxed{\begin{aligned} DF &= 0, \\ D^*F &= j, \end{aligned}}$
} Bianchi identity (geometry)
} Euler-Lagrange equation (dynamics)

3+1 D decomposition $F = -cdt \wedge \mathbf{E} + \mathbf{B}, \quad {}^*F = G = cdt \wedge \mathbf{H} + \mathbf{D}, \quad A = \phi cdt + \mathbf{A}$,

Electric and magnetic fields in terms of connection

(We assume there exists a function ϕ instead of matrix A_0, since at least one component of Hermitian matrices A can be diagonalized through some coordinate transformation. I suppose it corresponds to a local-frame selection such as maximal slicing.)

Applying 3+1D decomposition of A for field strength,

$$
\begin{aligned}
dA &= d\phi \wedge cdt + d\mathbf{A} \\
&= \left(cdt\dot{\phi} + \underline{d}\phi\right) \wedge cdt + cdt \wedge \dot{\mathbf{A}} + \underline{d}\mathbf{A} \\
&= cdt \wedge \left(\dot{\mathbf{A}} - \underline{d}\phi\right) + \underline{d}\mathbf{A}, \\
A \wedge A &= (\phi cdt + \mathbf{A}) \wedge (\phi cdt + \mathbf{A}) \\
&= \phi^2 cdt \wedge cdt + \phi cdt \wedge \mathbf{A} + \mathbf{A} \wedge \phi cdt + \mathbf{A} \wedge \mathbf{A} \\
&= \mathbf{A} \wedge \mathbf{A}. \\
\therefore \quad F &= dA + A \wedge A = cdt \wedge \left(\dot{\mathbf{A}} - \underline{d}\phi\right) + \underline{d}\mathbf{A} + \mathbf{A} \wedge \mathbf{A},
\end{aligned}
$$

Comparing it with 3+1 decomposition of F, we have,

$$
\mathbf{E} = \underline{d}\phi - \dot{\mathbf{A}}, \qquad \mathbf{B} = \underline{d}\mathbf{A} + \mathbf{A} \wedge \mathbf{A}, \qquad (*)
$$

Bianchi identity

$$
\begin{aligned}
0 = DF &= dF + A \wedge F - F \wedge A \\
&= cdt \wedge d\mathbf{E} + d\mathbf{B} + A \wedge (-cdt \wedge \mathbf{E} + \mathbf{B}) - (-cdt \wedge \mathbf{E} + \mathbf{B}) \wedge A \\
&= cdt \wedge (d\mathbf{E} + A \wedge \mathbf{E} + \mathbf{E} \wedge A) + d\mathbf{B} + A \wedge \mathbf{B} - \mathbf{B} \wedge A \\
&= cdt \wedge \left(cdt \wedge \dot{\mathbf{E}} + \underline{d}\mathbf{E} + A \wedge \mathbf{E} + \mathbf{E} \wedge A\right) + cdt \wedge \dot{\mathbf{B}} + \underline{d}\mathbf{B} + A \wedge \mathbf{B} - \mathbf{B} \wedge A \\
&= cdt \wedge \left(\underline{d}\mathbf{E} + \dot{\mathbf{B}} + A \wedge \mathbf{E} + \mathbf{E} \wedge A\right) + \underline{d}\mathbf{B} + A \wedge \mathbf{B} - \mathbf{B} \wedge A \\
&= cdt \wedge \left(\underline{d}\mathbf{E} + \dot{\mathbf{B}} + (\phi cdt + \mathbf{A}) \wedge \mathbf{E} + \mathbf{E} \wedge (\phi cdt + \mathbf{A})\right) + \underline{d}\mathbf{B} + (\phi cdt + \mathbf{A}) \wedge \mathbf{B} - \mathbf{B} \wedge (\phi cdt + \mathbf{A}) \\
&= cdt \wedge \left(\underline{d}\mathbf{E} + \dot{\mathbf{B}} + \mathbf{A} \wedge \mathbf{E} + \mathbf{E} \wedge \mathbf{A}\right) + \underline{d}\mathbf{B} + \mathbf{A} \wedge \mathbf{B} - \mathbf{B} \wedge \mathbf{A}
\end{aligned}
$$

(Notice that $\mathbf{E}$ is 1-form, $\mathbf{B}$ 2-form, respectively)

Substituting $(*)$,

$$
\begin{aligned}
\mathbf{A} \wedge \mathbf{E} + \mathbf{E} \wedge \mathbf{A} &= \mathbf{A} \wedge \left(\underline{d}\phi - \dot{\mathbf{A}}\right) + \left(\underline{d}\phi - \dot{\mathbf{A}}\right) \wedge \mathbf{A} \\
&= \mathbf{A} \wedge \underline{d}\phi - \mathbf{A} \wedge \dot{\mathbf{A}} + \underline{d}\phi \wedge \mathbf{A} - \dot{\mathbf{A}} \wedge \mathbf{A} \\
&= -\mathbf{A} \wedge \dot{\mathbf{A}} - \dot{\mathbf{A}} \wedge \mathbf{A} \\
&= -(\mathbf{A} \dot{\wedge} \mathbf{A}), \\
\mathbf{B} \wedge \mathbf{A} - \mathbf{A} \wedge \mathbf{B} &= \left(\underline{d}\mathbf{A} + \mathbf{A} \wedge \mathbf{A}\right) \wedge \mathbf{A} - \mathbf{A} \wedge \left(\underline{d}\mathbf{A} + \mathbf{A} \wedge \mathbf{A}\right) \\
&= \underline{d}\mathbf{A} \wedge \mathbf{A} - \mathbf{A} \wedge \underline{d}\mathbf{A} \\
&= \underline{d}(\mathbf{A} \wedge \mathbf{A}).
\end{aligned}
$$

Consequently, we have

$$
\boxed{\text{Faraday's law: } \partial_t(\mathbf{B} - \mathbf{A} \wedge \mathbf{A}) = -\underline{d}\mathbf{E}, \qquad \text{Gauss's law: } \underline{d}(\mathbf{B} - \mathbf{A} \wedge \mathbf{A}) = 0.}
$$

Euler-Lagrange equation

$$\begin{aligned}
j = D^*F &= dG + A\wedge G - G\wedge A \\
&= -cdt\wedge d\mathbf{H} + d\mathbf{D} + A\wedge(cdt\wedge\mathbf{H}+\mathbf{D}) - (cdt\wedge\mathbf{H}+\mathbf{D})\wedge A \\
&= -cdt\wedge(d\mathbf{H} + A\wedge\mathbf{H} + \mathbf{H}\wedge A) + d\mathbf{D} + A\wedge\mathbf{D} - \mathbf{D}\wedge A \\
&= -cdt\wedge\left(cdt\wedge\dot{\mathbf{H}} + \underline{d}\mathbf{H} + A\wedge\mathbf{H} + \mathbf{H}\wedge A\right) + cdt\wedge\dot{\mathbf{D}} + \underline{d}\mathbf{D} + A\wedge\mathbf{D} - \mathbf{D}\wedge A \\
&= -cdt\wedge\left(\underline{d}\mathbf{H} - \dot{\mathbf{D}} + A\wedge\mathbf{H} + \mathbf{H}\wedge A\right) + \underline{d}\mathbf{D} + A\wedge\mathbf{D} - \mathbf{D}\wedge A \\
&= -cdt\wedge\left(\underline{d}\mathbf{H} - \dot{\mathbf{D}} + (\phi cdt+\mathbf{A})\wedge\mathbf{H} + \mathbf{H}\wedge(\phi cdt+\mathbf{A})\right) + \underline{d}\mathbf{D} + (\phi cdt+\mathbf{A})\wedge\mathbf{D} - \mathbf{D}\wedge(\phi cdt+\mathbf{A}) \\
&= -cdt\wedge\left(\underline{d}\mathbf{H} - \dot{\mathbf{D}} + \mathbf{A}\wedge\mathbf{H} + \mathbf{H}\wedge\mathbf{A}\right) + \underline{d}\mathbf{D} + \mathbf{A}\wedge\mathbf{D} - \mathbf{D}\wedge\mathbf{A}
\end{aligned}$$

(Notice that $\mathbf{H}$ is 1-form, $\mathbf{D}$ 2-form, respectively)

After some manipulation, we have

$$\tilde{\rho} \equiv \mathbf{A}\wedge\mathbf{D} - \mathbf{D}\wedge\mathbf{A} = -\left([A_x,\dot{A}_x] + [A_y,\dot{A}_y] + [A_z,\dot{A}_z]\right)dx\wedge dy\wedge dz, \quad c.f.\ \mathbf{A} = A_x dx + A_y dy + A_z dz,$$

$$\tilde{\boldsymbol{\imath}} \equiv \mathbf{A}\wedge\mathbf{H} + \mathbf{H}\wedge\mathbf{A} = i_x dy\wedge dz + i_y dz\wedge dx + i_z dx\wedge dy,$$

where, $i_x \equiv [\boldsymbol{\mathcal{A}},\partial_x\boldsymbol{\mathcal{A}}] + [\nabla A_x,\boldsymbol{\mathcal{A}}] + 2\boldsymbol{\mathcal{A}}(A_x\boldsymbol{\mathcal{A}}) - \{\boldsymbol{\mathcal{A}}\boldsymbol{\mathcal{A}},A_x\}$, **Inner product pair**

$$i_y \equiv [\boldsymbol{\mathcal{A}},\partial_y\boldsymbol{\mathcal{A}}] + [\nabla A_y,\boldsymbol{\mathcal{A}}] + 2\boldsymbol{\mathcal{A}}\cdot(A_y\boldsymbol{\mathcal{A}}) - \{\boldsymbol{\mathcal{A}}\cdot\boldsymbol{\mathcal{A}},A_y\},$$

$$i_z \equiv [\boldsymbol{\mathcal{A}},\partial_z\boldsymbol{\mathcal{A}}] + [\nabla A_z,\boldsymbol{\mathcal{A}}] + 2\boldsymbol{\mathcal{A}}\cdot(A_z\boldsymbol{\mathcal{A}}) - \{\boldsymbol{\mathcal{A}}\cdot\boldsymbol{\mathcal{A}},A_z\}, \qquad c.f.\ \boldsymbol{\mathcal{A}} = (A_x,A_y,A_z),$$

Recall that $j = -cdt\wedge\mathbf{i} + \rho$, consequently,

$$\boxed{\text{Ampere's law: } \dot{\mathbf{D}} = \underline{d}\mathbf{H} - \mathbf{i} + \tilde{\boldsymbol{\imath}}, \qquad \text{Gauss's law: } \underline{d}\mathbf{D} = \rho - \tilde{\rho}.}$$

Differentiation of Gauss's law in time gives

$$\partial_t\left(\underline{d}\mathbf{D} - \rho + \tilde{\rho}\right) = \underline{d}\left(\underline{d}\mathbf{H} - \mathbf{i} + \tilde{\boldsymbol{\imath}}\right) - \dot{\rho} + \dot{\tilde{\rho}},$$

Therefore, combining charge conservation and following condition,

$$\underline{d}\tilde{\boldsymbol{\imath}} + \dot{\tilde{\rho}} = 0.$$

Gauss's law is nothing but an initial condition as Maxwell equations are.

Skipping detail calculation, equations above can be rewritten as followings.

$$\dot{\tilde{\rho}} = -\left([A_x,\ddot{A}_x] + [A_y,\ddot{A}_y] + [A_z,\ddot{A}_z]\right)dx\wedge dy\wedge dz,$$

$$\underline{d}\tilde{\boldsymbol{\imath}} = \left([A_x,K_x] + [A_y,K_y] + [A_z,K_z]\right)dx\wedge dy\wedge dz,$$

where, $K_x \equiv \triangle A_x - \partial_x(\nabla\boldsymbol{\mathcal{A}}) + [\nabla\boldsymbol{\mathcal{A}},A_x] + [\partial_x\boldsymbol{\mathcal{A}},\boldsymbol{\mathcal{A}}] + 2[\nabla A_x,\boldsymbol{\mathcal{A}}]$,

$$K_y \equiv \triangle A_y - \partial_y(\nabla\boldsymbol{\mathcal{A}}) + [\nabla\boldsymbol{\mathcal{A}},A_y] + [\partial_y\boldsymbol{\mathcal{A}},\boldsymbol{\mathcal{A}}] + 2[\nabla A_y,\boldsymbol{\mathcal{A}}],$$

$$K_z \equiv \triangle A_z - \partial_z(\nabla\boldsymbol{\mathcal{A}}) + [\nabla\boldsymbol{\mathcal{A}},A_z] + [\partial_z\boldsymbol{\mathcal{A}},\boldsymbol{\mathcal{A}}] + 2[\nabla A_z,\boldsymbol{\mathcal{A}}],$$

Finally, we obtain specific gauge condition as follows.

$$\boxed{\text{Constraints preserving gauge: } \ddot{\boldsymbol{\mathcal{A}}} - \triangle\boldsymbol{\mathcal{A}} + \nabla(\nabla\boldsymbol{\mathcal{A}}) - [\nabla\boldsymbol{\mathcal{A}},\boldsymbol{\mathcal{A}}] - [\nabla\boldsymbol{\mathcal{A}},\boldsymbol{\mathcal{A}}] - 2[\nabla\boldsymbol{\mathcal{A}},\boldsymbol{\mathcal{A}}] = \mathbf{0}}$$

Conclusion

Yang-Mills theory defined in four dimension has been decomposed into 3+1 dimension. Resultant equations turn out to be natural extension of Maxwell's equations. Constraints can be treated similarly under constraints preserving gauge proposed in this presentation. Meanwhile, in the field of computational electromagnetics, it is well known that finite integration technique (FIT) employing Whitney form enables three dimensional differential forms to realize nilpotent relation ($d^2 = 0$) exactly. Therefore, truly-free evolution of Yang-Mills theory is possible using FIT in which constraints can be managed without any loss of accuracy. Application to general relativity is in progress.

Koichi Hirano
Tsuru University

"Inflation inspired by the string theory with Planck and future CMB data"

[JGRG28 (2018) PB23]

Inflation inspired by the string theory with Planck and future CMB data

Koichi Hirano

Department of Teacher Education, Tsuru University, 3-8-1, Tahara, Tsuru, Yamanashi, 402-8555, Japan
E-mail: k_hirano@tsuru.ac.jp

Abstract

We study D-brane inflation model and Kähler-moduli inflation model. These inflation models predict the very small value of the tensor-to-scalar ratio r. The primordial density perturbations are parametrized by the spectral index n_s and the tensor-to-scalar ratio r, and they are constrained by the Planck data combined with other CMB and cosmological observations. We compare the Planck 2018 data with the models. Furthermore, we discuss comparison of future tensor-to-scalar ratio data with the predictions by the inflation models inspired by the string theory, focusing on part of the quantum fluctuation origin.

1 Model

The action we consider is of the form

$$S = \int d^4x\sqrt{-g}\left[\frac{M_{\rm pl}^2}{2}R + X - V(\phi)\right]. \quad (1)$$

$$(X \equiv -\partial^\mu\phi\partial_\mu\phi/2)$$

Under the slow-roll approximations $\dot{\phi}^2/2 \ll V$ and $|\ddot{\phi}| \ll |3H\dot{\phi}|$, the Friedmann equation and the scalar-field equation of motion, respectively, reduce to

$$3M_{\rm pl}^2H^2 \simeq V, \quad 3H\dot{\phi} \simeq -V_{,\phi}. \quad (2)$$

The number of e-foldings can be expressed as

$$N \simeq \frac{1}{M_{\rm pl}^2}\int_{\phi_f}^{\phi}\frac{V}{V_{,\tilde{\phi}}}d\tilde{\phi}. \quad (3)$$

The slow-roll parameter ϵ and parameter η is defined as follows

$$\epsilon \equiv \frac{M_{\rm pl}^2}{2}\left(\frac{V_{,\phi}}{V}\right)^2, \qquad \eta \equiv \frac{M_{\rm pl}^2V_{,\phi\phi}}{V}. \quad (4)$$

The observables reduce to

$$n_s = 1 - 6\epsilon + 2\eta, \quad r = -8n_t, \quad n_t = -2\epsilon. \quad (5)$$

Small-field inflation can be realized by the potential

$$V(\phi) = \Lambda^4[1 - \mu(\phi)]. \quad (6)$$

In D-brane inflation [1] we have

$$\mu(\phi) = \mathrm{e}^{-\phi/M}, \quad (7)$$

in which case n_s and r are

$$n_s \simeq 1 - \frac{2}{N}, \quad r \simeq \frac{8}{N^2}\left(\frac{M}{M_{\rm pl}}\right)^2. \quad (8)$$

For $M < M_{\rm pl}$ and $N = 50 - 60$, it follows that

$$0.960 < n_s < 0.967 \quad \text{and} \quad r < 2.2 \times 10^{-3}. \quad (9)$$

In Kähler-moduli inflation [2] we have

$$\mu(\phi) = c_1\phi^{4/3}\mathrm{e}^{-c_2\phi^{4/3}} \quad (c_1 > 0, c_2 > 0). \quad (10)$$

The inflationary observables are in the ranges, for $N = 50 - 60$

$$0.960 < n_s < 0.967 \quad \text{and} \quad r < 10^{-10}. \quad (11)$$

Table 1: Value of the spectral index n_s and the tensor-to-scalar ratio r

Model	spectral index n_s	tensor-to-scalar ratio r
D-brane	$0.960 < n_s < 0.967$	$r < 2.2 \times 10^{-3}$
Kähler-moduli	$0.960 < n_s < 0.967$	$r < 10^{-10}$

2 Comparison with Planck 2018

We compare the Planck 2018 data with the models.

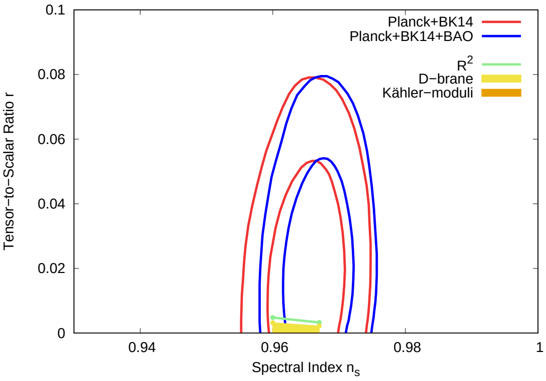

Figure 1: Comparison of the Planck 2018 data with the inflation models. The vertical axis is liner.

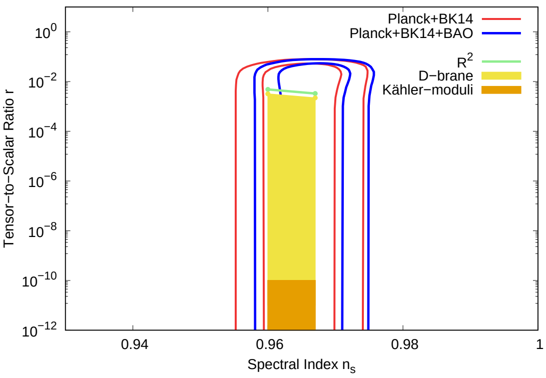

Figure 2: Comparison of the Planck 2018 data with the inflation models. The vertical axis is logarithmic.

3 Summary

The models are inside the 95% CL boundary constrained by the Planck + BK14 + BAO data, are consistent with the observational data as well. In future work, we discuss comparison of future tensor-to-scalar ratio data with the predictions by the inflation models inspired by the string theory, focusing on part of the quantum fluctuation origin.

References

[1] G. R. Dvali and S. H. H. Tye, Phys. Lett. B **450**, 72 (1999).

[2] J. P. Conlon and F. Quevedo, J. High Energy Phys. **0601**, 146 (2006).

Akihiro Yatabe
Waseda University

"Collisional Electric Penrose Process in Flat Spacetime"

[JGRG28 (2018) PB24]

Collisional Electric Penrose Process in Flat Spacetime

Akihiro Yatabe
Advanced Research Institute for Science and Engineering, Waseda University
Mail: yatabe@heap.phys.waseda.ac.jp

Abstract

The Penrose process is an impressive physical process in the framework of general relativity. This process is that an object splits into two objects in the so-called ergoregion of a rotating black hole and that one of them gains energy. Recently, the process of gaining energy is shown to be possible even in the limit of the flat spacetime and energy is extracted from the electric potential energy in this case. In this study, we assume whether the energy gain of two photons is possible when we consider the two-photon pair annihilation, which makes an electron-positron pair. We also consider the case for the Born-Infeld theory, which is a nonlinear theory of electrodynamics, as well as the Maxwell theory.

1. Introduction and Settings

■ Penrose Process

At Kerr Blackhole

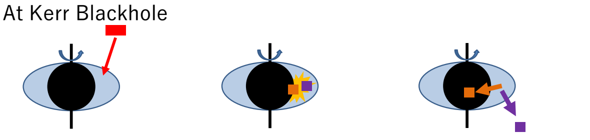

Matter 0 falls into the ergoregion.

Matter 0 splits into matters 1 and 2.

Matter 1 has the negative energy and matter 2 gains energy.

■ Motivation

Recent paper [1] discusses the energy gain around the electric charge. This corresponds to the zero limit of gravitational constant of the Penrose process around Reissner-Nordström black hole.

At Charge

[1]Zaslavskii, arXiv: 1807.05763

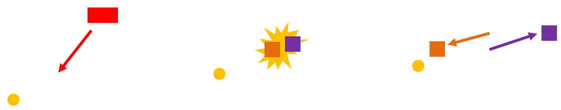

Matter 0 approaches the charge.

Matter 0 splits into matters 1 and 2.

Matters 1 and 2 gain or lose the electrostatic energy.

If matters 1 and 2 are infinitely charged, the electrostatic energy is not bounded. There is no limitation of the energy gain. This is so-called super-Penrose process.

Realistic process? How much is the energy gain?

■ More realistic process: Two-photon pair annihilation

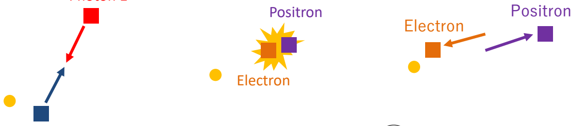

■ Setting of Two-Photon Annihilation

For simplicity, radial motion is only considered.

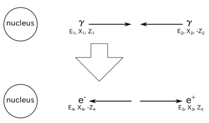

E_i : Total Energy
X_i : Kinetic Energy
Z_i : Momentum

■ Equations

・Total Energy Conservation

$$E_1 + E_2 = E_3 + E_4, \qquad E_i = X_i + q_i\varphi.$$

q_i : Charge
φ : Electrostatic Potential

・Kinetic Energy and Momentum

$$Z_i = \frac{X_i}{c}, \quad \text{for photons}$$

c : Light Speed
m : Electron Mass

$$Z_i = \sqrt{\left(\frac{X_i}{c}\right)^2 - (mc)^2}, \quad \text{for electrons and positrons}$$

・Momentum Conservation

$$X_1 + X_2 = X_3 + X_4.$$

$$\Leftrightarrow \frac{X_1}{c} - \frac{X_2}{c} = \sqrt{\left(\frac{X_3}{c}\right)^2 - (mc)^2} - \sqrt{\left(\frac{X_1}{c} + \frac{X_2}{c} - \frac{X_3}{c}\right)^2 - (mc)^2}.$$

2. Results

■ Solutions of Kinetic Energy (E_1 = 1MeV)

Equation $\frac{X_1}{c} - \frac{X_2}{c} = \sqrt{\left(\frac{X_3}{c}\right)^2 - (mc)^2} - \sqrt{\left(\frac{X_1}{c} + \frac{X_2}{c} - \frac{X_3}{c}\right)^2 - (mc)^2}.$

Solutions of Kinetic Energy of Positron X_3 and Electron X_4

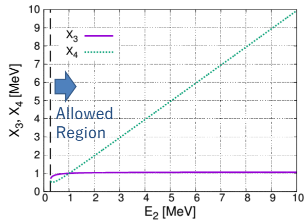

There exist solutions for kinetic energy.
Conservation laws allow the existence of this process.

■ Total Energy vs Place of Annihilation

E_1=1MeV, E_2=2MeV Coulomb Potential $\varphi = \frac{q}{r}$

Au nucleus (q=79e) are considered.

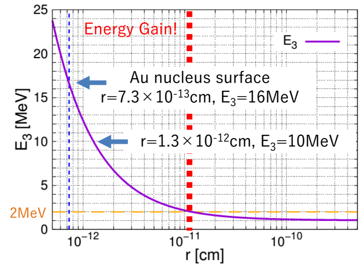

Energy gain is possible when the annihilation occurred enough near to the nucleus.

■ Comparison with Another Theory

We finally compare the case for another theory of electromagnetism, the Born-Infeld theory [2], with the case for now. We will show whether there exist differences between the Maxwell theory and the Born-Infeld theory.

Difference between the two theory

	Maxwell Theory	Born-Infeld Theory
Permeability, Dielectricity	$\mu = \epsilon^{-1} = 1$	$\mu = \frac{1}{\epsilon} = \sqrt{1 + \frac{1}{b^2}(\mathbf{B}^2 - \mathbf{E}^2)},$
Electric Field by a Charge	$E_r = \frac{q}{r^2}$	$E_r = \frac{q}{\sqrt{r^4 + \frac{q^2}{b^2}}},$
Potential by a Charge	$\varphi = \frac{q}{r}$	$\varphi(r) = \int_r^\infty \frac{q}{\sqrt{x^4 + \frac{q^2}{b^2}}}dx,$

b: Maximum Field   Maximum field is determined by experiments.

Comparison of Electrostatic Energy

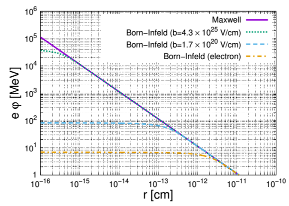

Ellis, Mavromatos, You (2017) [3]
b~100GeV

Soff, Rafelski, Greiner (1973) [4]
b~200MeV

Original assumption by Born (1930's)
b~20MeV

No difference even at the surface of the nucleus with the latest limit. But the energy-gain process can occur in both theory.

Summary

We consider whether the gaining energy by the two-photon annihilation is possible. We solve equations of the conservation of energy and momentum and it is shown that there exist the solution. It is also shown that the initial particle gains energy when the annihilation process occurs near the charge, which is the source of the Coulomb potential. These results are based on the Maxwell theory. We finally, compare the results in the Maxwell theory with those for the Born-Infeld theory. It is found that there is no difference in the case of the process concerned in this poster but the energy gain is possible.

Reference

[1] O. B. Zaslavskii, arXiv: 1807.05763, *Pure electric Penrose and super-Penrose processes in the flat space-time*, [2] M. Born and L. Infeld, Proceedings of the Royal Society of London Series A, 144, 425 (1934), [3] J. Ellis, N. E. Mavromatos, T. You, Phys. Rev. Lett. 118, 261802 (2017), [4] G. Soff, J. Rafelski, W. Greiner, Phys. Rev. A 7, 903 (1973)

Shin'ichirou Yoshida
Department of Earth Science & Astronomy, The University of Tokyo

"Rotating merger remnant models of white dwarf binaries"

[JGRG28 (2018) PB25]

Rotating merger remnant models of white dwarf binaries

Shin Yoshida

Department of Earth Science & Astronomy
The University of Tokyo

Abstract

I present new numerical models of rapidly rotating white dwarfs with large degree of differential rotation and thermal stratification. The model has a core composed of ions and completely degenerate electrons and has an isentropic envelope composed of ions, photons, partially degenerate electrons and positrons. The models are intended to mimic very early phases of remnants of white dwarf binary mergers, some of which may lead to type Ia supernovae.

I. Introduction

<u>mergers of binaries of white dwarfs (BWD)</u>

- progenitors of Type Ia supernovae (SNIa)
  double-degenerate models
- bimodal distribution of mass
- origin of high B (10^6-9G) WD
- gravitational wave emission
  → *foreground noise* for spaceborne detector

bimodal distribution
of white dwarf mass
↓
merger remnants

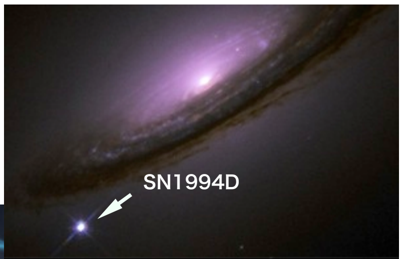

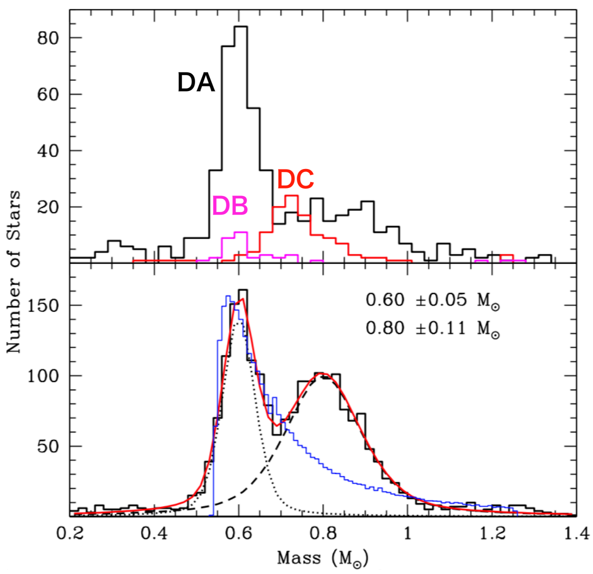

Kilic et al.(2018)

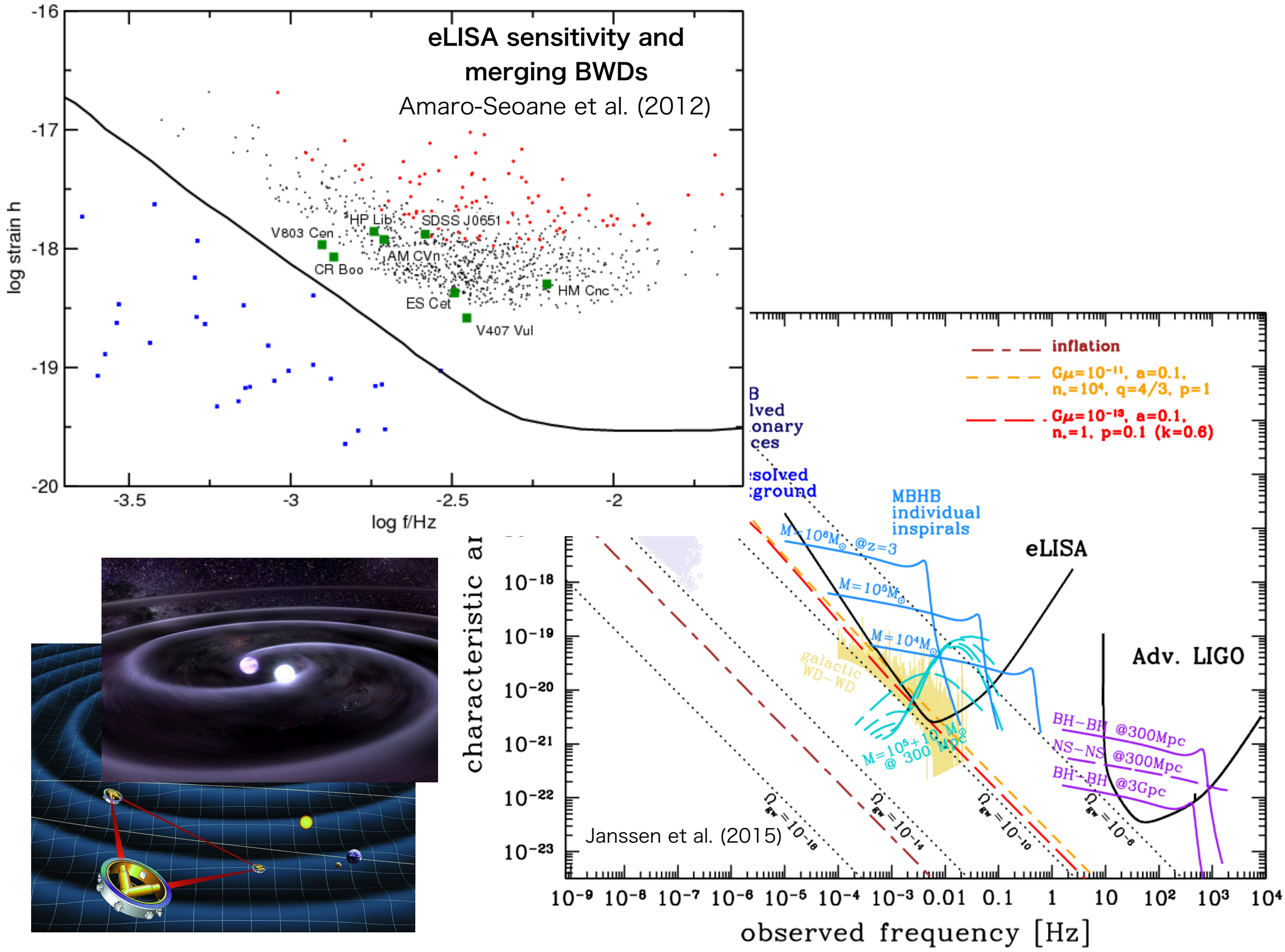

Our interest here is NOT in the merging phase…

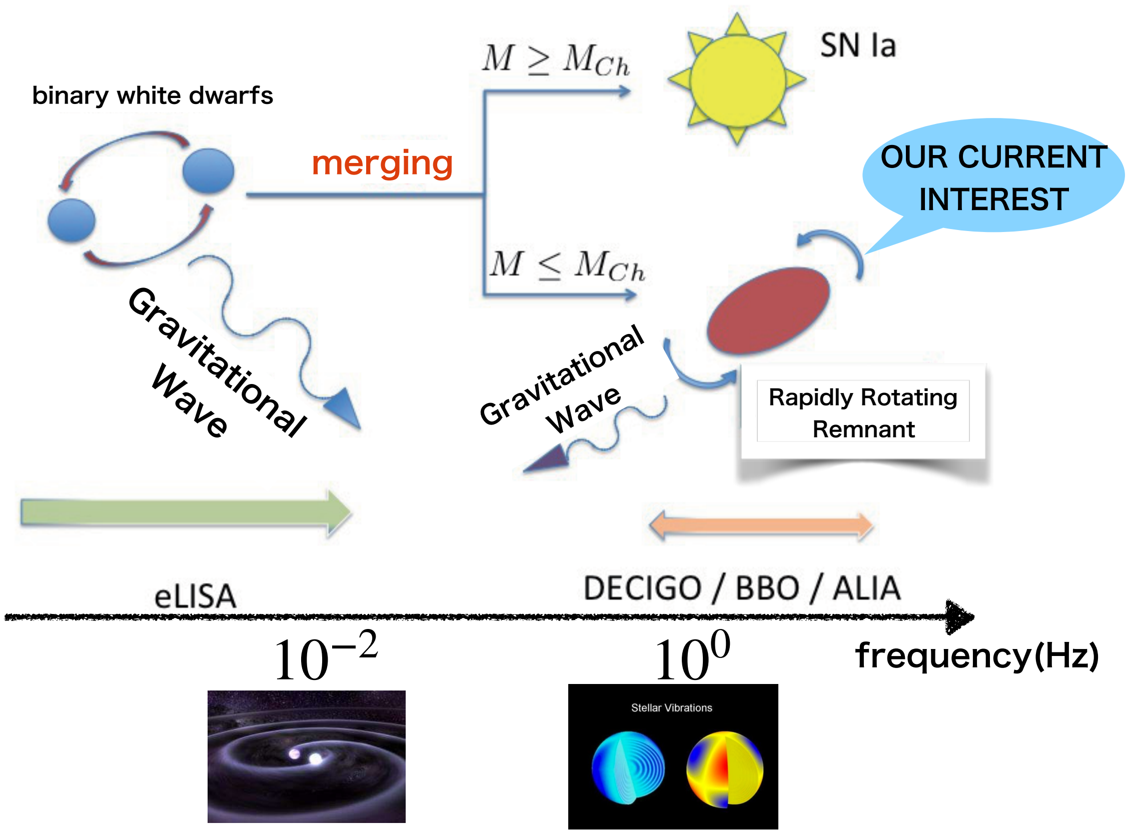

$f_{GW}^{max} = 5 \times 10^{-2}\text{Hz} \quad for\ M_2 = 0.6 M_{\odot},\ q = \frac{0.6}{0.9}$

$f_{\rm GW} \gtrsim 0.2 \left(\frac{M}{M_{\odot}}\right)^{\frac{1}{2}} \left(\frac{R}{0.01 R_{\odot}}\right)^{-\frac{3}{2}}$ Hz

Characteristic strain from binary WD merger remnants

$$h_c(f) = \sqrt{\frac{2f^2}{\dot{f}}}h_0 \quad ; \qquad h(t) = \sqrt{2}h_0 \exp(\phi(t)), \quad N_{cycl} = \frac{f}{2\pi}\frac{d\phi}{df} = \frac{f^2}{\dot{f}}$$

$$h_c(f) = 3\times 10^{-25} \cdot \sqrt{N_{cycl}} \left(\frac{D}{30\mathrm{Mpc}}\right)^{-1} \left(\frac{M}{M_\odot}\right) \left(\frac{R}{10^9\mathrm{cm}}\right)^2 \left(\frac{f}{1\mathrm{Hz}}\right)^2 \left(\frac{\epsilon}{0.1}\right)^2$$

Assuming N=3 polytrope

M: mass of the merger remnant
R: radius of the remnant
f: GW frequency
ε: dimensionless deformation (ellipticity)
Ncycl: # of cycles of quasi-periodic source

event rate (BWD merger)

Rueda et al. (2018)

merger rate per mass: $(1-80)\times 10^{-13}\ \mathrm{yr}^{-1}M_\odot^{-1}$ Maoz & Hallakoun (2017)

 # density of MW gals: $0.016\ \mathrm{Mpc}^{-3}$ Kalogera et al. (2001)

mass of MW gals.: $6.4\times 10^{10}\ M_\odot$

$$\rightarrow \quad \mathscr{R} = (0.74 - 5.9)\times 10^6\ \mathrm{Gpc}^{-3}\mathrm{yr}^{-1}$$

Assuming distance D to Virgo cluster = 30 Mpc'
# of merger per year

$$\mathscr{R}\times\frac{4\pi D^3}{3} = (83 \ - \ 671)\ \mathrm{yr}^{-1}$$

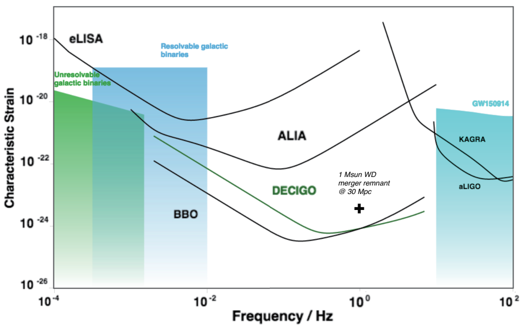

drawn with *http://gwplotter.com/*

Goal of the study

Assessment of GW from merger remnants by their oscillations

Early evolution of remnants including GW back-reaction

methodology

linear perturbation analysis of merger remnants

time domain
frequency domain

Before the study…

Remnant models to be perturbed needs to be constructed.

Debris of disrupted secondary accretes onto the primary
→ hot envelope + cold core

Merger of 2 orbiting stars
→ large angular momentum, differential rotation

[precedent studies] - outcomes of merger simulations
Guerrero et al. (2004), Yoon et al. (2007), Shen et al. (2012), Schwab et al. (2012)
Schwab et al. (2016)
Raskin et al. (2012), Zhu et al. (2013), Dan et al. (2014), Sato et al. (2015)
Kashyap et al. (2017)

Not useful for our current study
- no adiabatic index, sound speed provided
- "coarse grid"
- very early termination

of each simulation

Current study Obtaining remnant models that are to be used in linear perturbation analysis

— Equilibrium models with
differential rotation
thermal structure

II. FORMULATION

stationary & axisymmetric - after the dynamical accretion has ceased (< O[10^4] s)

thermal stratification

cold core (primary) - degenerate free electron EOS (cf. Chandrasekhar 1967)

hot envelope (secondary) - 'Helmholtz' EOS (Timmes & Swesty 2000)

partially degenerate e/e+
ions, photon

angular frequency profile

simplified profiles - analytic

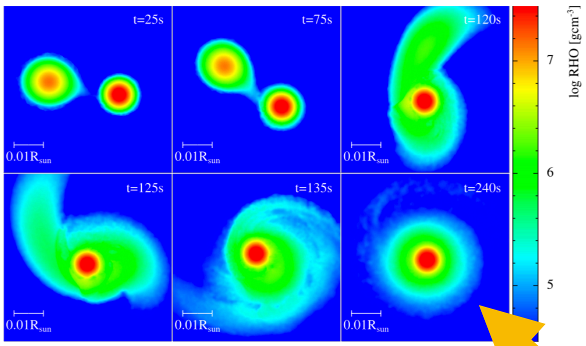

Figure 1. Density profiles in the equatorial plane for the dynamical evolution of our merger simulation. The mass combination is 1.1 ... and the resolution 500k $M_\odot^{-1}$. Colors indicate density on a logarithmic scale.

Sato et al. (2015)

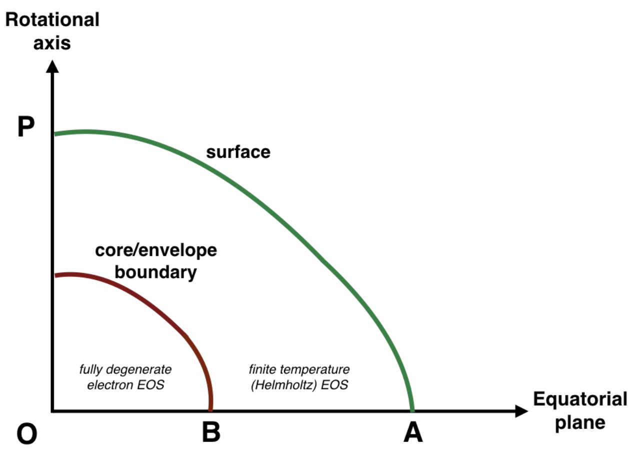

modified HSCF procedure (SY in preparation)

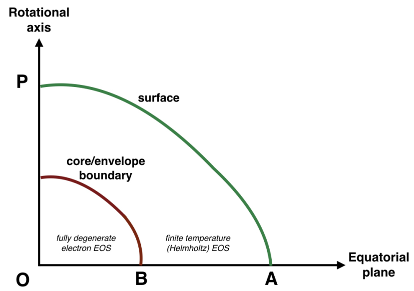

$$\int \frac{dp}{\rho} + \Phi - \int \Omega^2 R dR = C_{\mathrm{in/out}}$$

$$\Phi = -G \int \frac{\rho}{|\vec{r} - \vec{r'}|} d^3 \vec{r'}$$

fixed parameters: ρ_c

central density

temperature at the core-envelope boundary T_b

deformation OP/OA

chemical composition $X_{\mathrm{H}}, X_{\mathrm{He}}, X_{\mathrm{C}}, X_{\mathrm{O}}$

pressure ratio $f_p \equiv p(B)/p(O)$

1) give initial guess of enthalpy $h(\vec{r})$
2) invert EOS $h(\vec{r}) \rightarrow \rho(\vec{r})$
3) solve Poisson $\Phi(\vec{r})$
4) 1st integrals at O, B, A, P, and continuity of pressure (5 eqs) are solved for r(A), r(B), C's for core & envelope and $\Omega(O)$ (5 unknowns)
5) use 1st integrals to obtain $h_{\mathrm{updated}}(\vec{r})$
6) if not converged, GOTO 1)

Original HSCF (Hachisu 1986)

powerful method to compute configurations of rotating stars

stationary & axisymmetric

Equation of state (EOS) : barotropic

angular frequency : analytic profile

1st integral of hydrostationary balance

$$\int \frac{dp}{\rho} + \Phi - \int \Omega^2 R dR = C$$

Poisson

$$\Phi = -G \int \frac{\rho}{|\vec{r} - \vec{r'}|} d^3 \vec{r'}$$

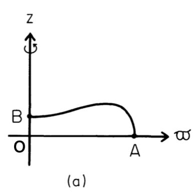

0) Fixing OB/OA, central density.
1) give initial guess of $\rho(\vec{r})$
2) integrate Poisson
3) solve for OA, C, $\Omega(O)$ by applying 1st integral at O,B,A
4) use 1st integral to obtain $\rho_{\mathrm{updated}}(\vec{r})$
5) if not converged, GOTO 2)

An assumption on the envelope : constant entropy

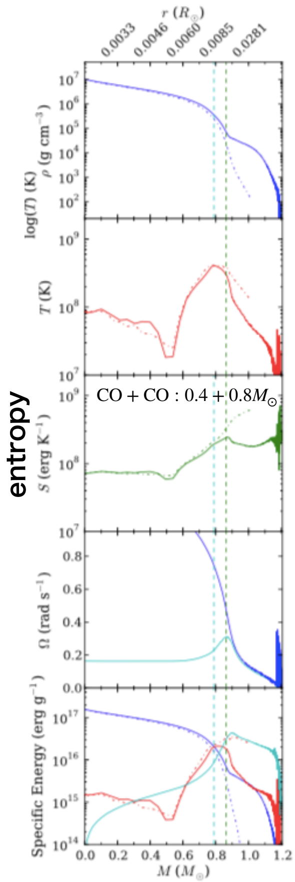

Zhu et al. 2013

- results from preceding simulations

- cooling envlps tend to be isentropic $\nabla s = 0$
  - hot envlp -> rad. cooling
    - -> convectively unstable (Loeb & Rasio 1994)
    - -> neutrally stable (cf. Kippenhahn & Weigert 1990)

Schwab et al. 2012

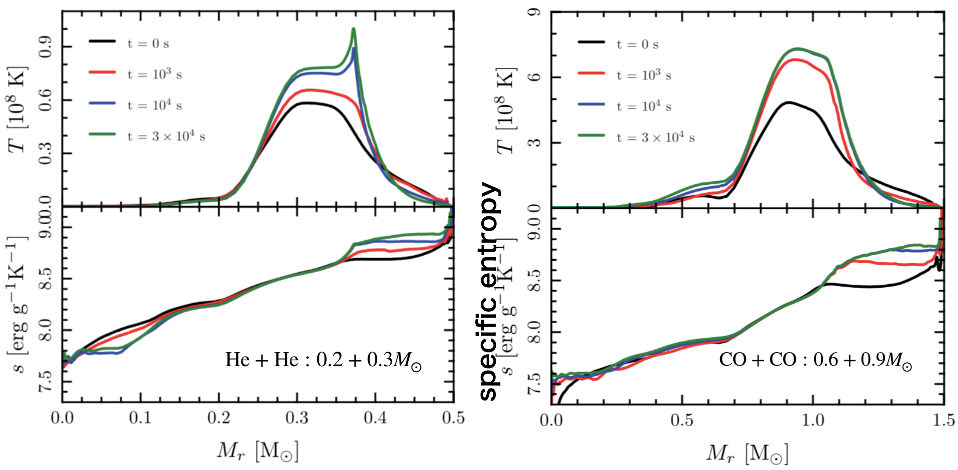

III. RESULTS

a. non-rotating models
b. uniformly rotating models
c. differentially rotating models
   c-1. Yoon07 rotational profile
   c-2. Kepler rotational profile
d. some sequences of interest

current results assume:

core - carbon or oxygen $X_Z = 1$

envelope - hydrogen+helium $X_H = 0.1,\ X_{He} = 0.9$

a. non-rotating models

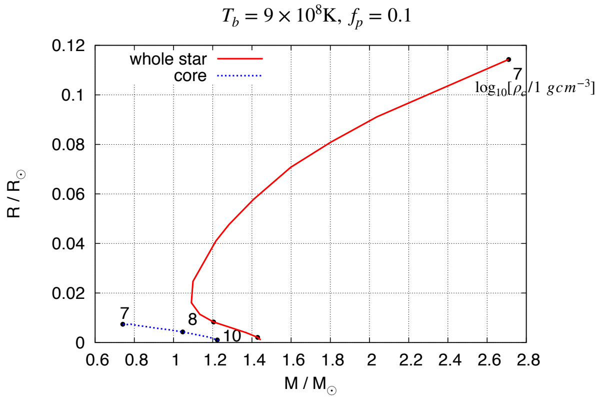

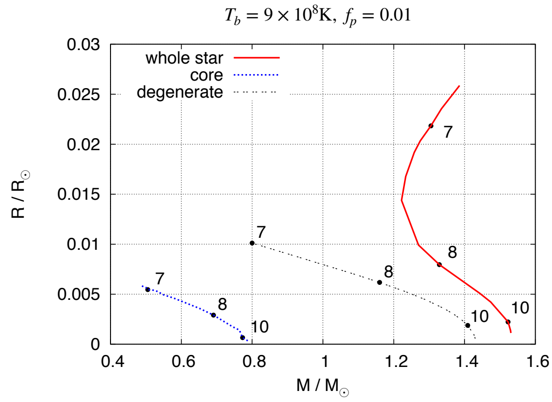

dependence of M on Tb

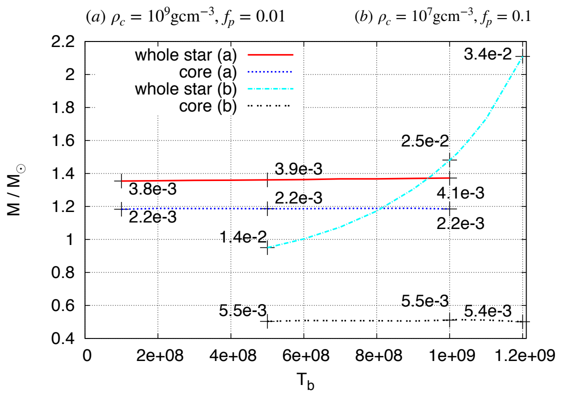

dependence of M-R on fp

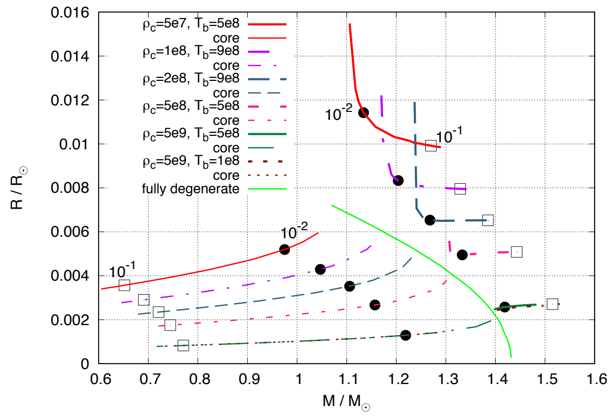

b. uniformly rotating models

$\rho_c = 10^8\mathrm{gcm}^{-3}, T_b = 5 \times 10^8\mathrm{K}, f_p = 0.1$

$M = 1.37M_\odot,\ M_{core} = 0.72M_\odot,\ T/W = 0.026\ (\Omega = 0.687\mathrm{Hz})$

T=kinetic energy
W=|gravitational energy|

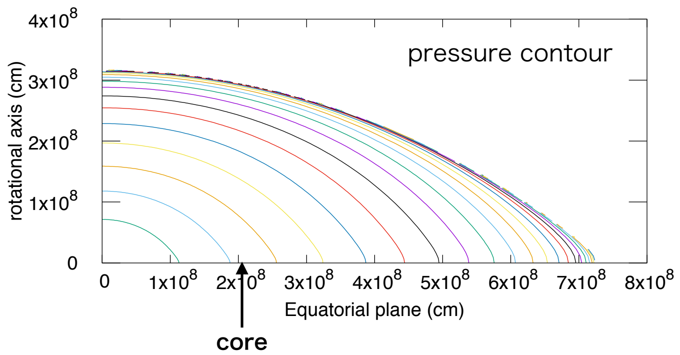

highly flattened by centrifugal force

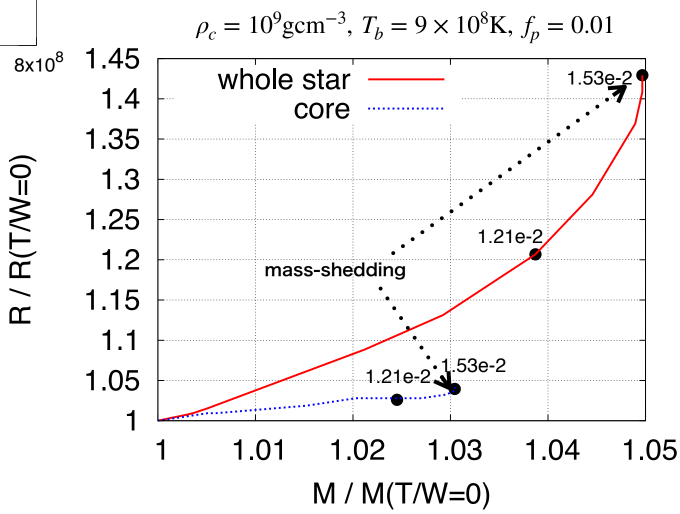

rotational effect

mass: Mtotal, Mcore at most a few %
radius: total radius a few tens %
core radius a few %

mass-radius parametrized by T/W

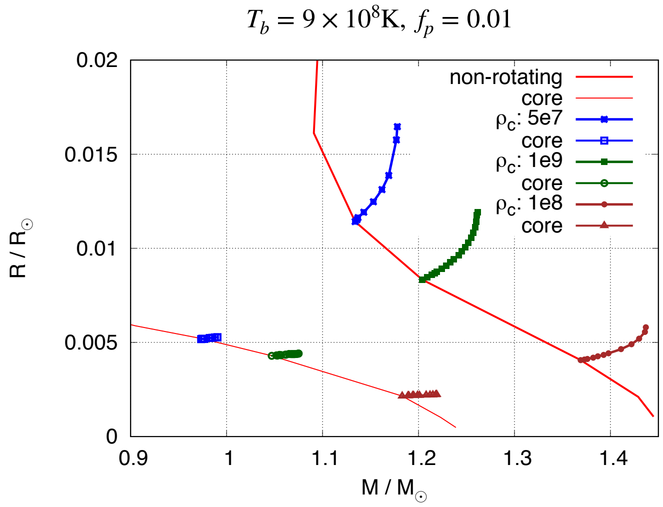

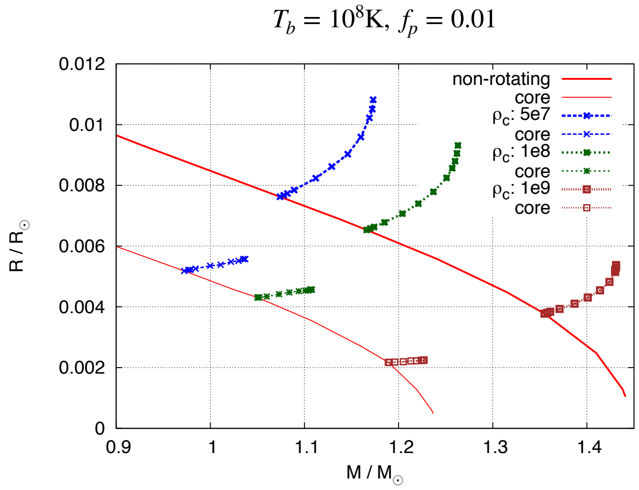

increment in max. mass never exceeds a few %

c. differentially rotating models

we compare 2 different profiles for Ω

1. ***Yoon07*** analytical fit of profile of a remnant in Yoon et al. (2007)

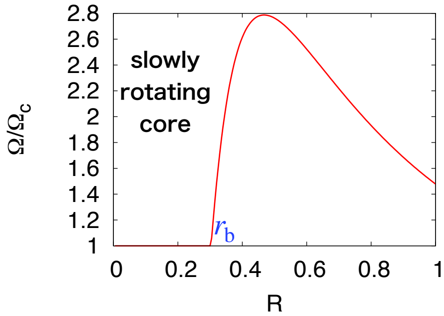

$$\Omega = \begin{cases} \sqrt{k_0} & (R \le r_b) \\ \sqrt{k_0}\,\frac{r_b^3}{\epsilon_b^{5/4}} R^{-3} (R-b)^{5/4} & (R \ge r_b) \end{cases}$$

$$b = r_b - \epsilon_b$$

r_b : equatorial core/envelope boundary

2. ***Kepler*** asymptotes to Keplerian profile for large R

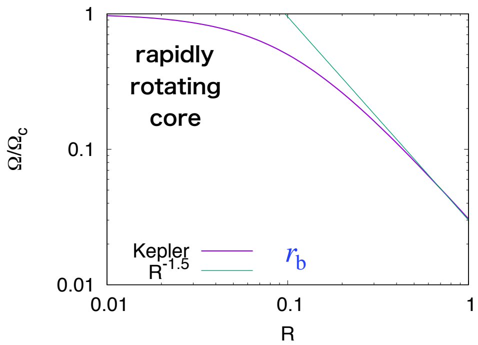

$$\Omega = \frac{\sqrt{k_0}}{R^{3/2} + r_b^{3/2}}$$

c-1. Yoon07 profile stars

$\rho_c = 10^8 \mathrm{gcm}^{-3}, T_b = 5 \times 10^8 \mathrm{K}, f_p = 0.1$

$M = 2.31 M_\odot,\ M_{core} = 0.785 M_\odot,\ T/W = 0.062\ (\Omega = 0.852\mathrm{Hz})$

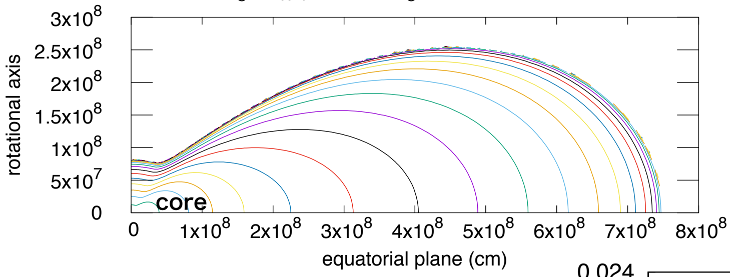

mass-radius relation of Yoon07 law models

$\rho_c = 10^8 \mathrm{gcm}^{-3},\ T_b = 5 \times 10^8 K$

as fp increases, envelope starts to dominate

uniform rotation : max M @ mass-shedding

Yoon07 :

core dominant star - max M reached

envelope dominant star - no max M

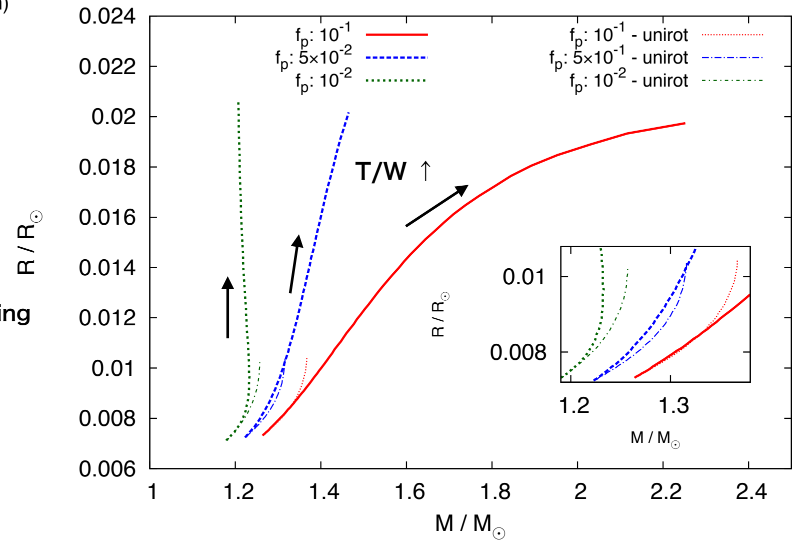

c-1. Yoon07 profile stars

mass and radius as functions of T/W Yoon07 law models

$\rho_c = 10^8 \mathrm{gcm}^{-3},\ T_b = 5 \times 10^8 \mathrm{K}$

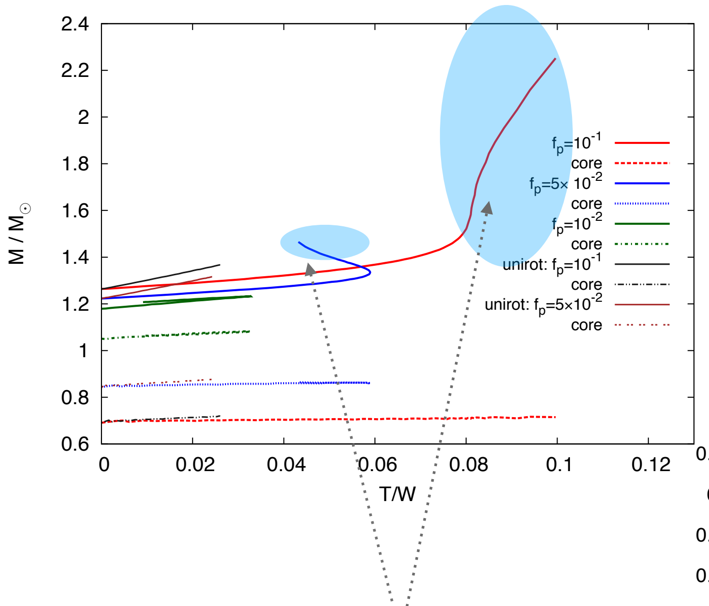

these models satisfies M(envelope)>M(core)

=> astrophysically implausible

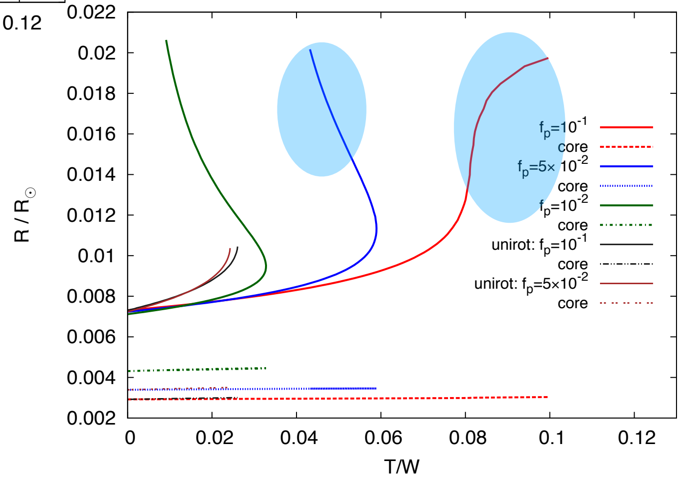

c-2. Kepler profile stars

$\rho_c = 10^8 \mathrm{gcm}^{-3}, T_b = 5\times10^8\mathrm{K}, f_p = 0.1$

$M = 3.15M_\odot,\ M_{core} = 1.56M_\odot,\ T/W = 0.211\ (\Omega = 0.488\mathrm{Hz})$

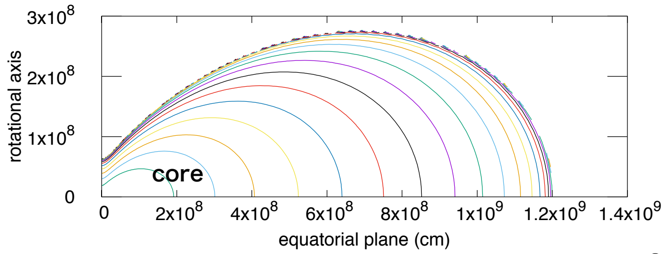

as fp increases, envelope starts to dominate

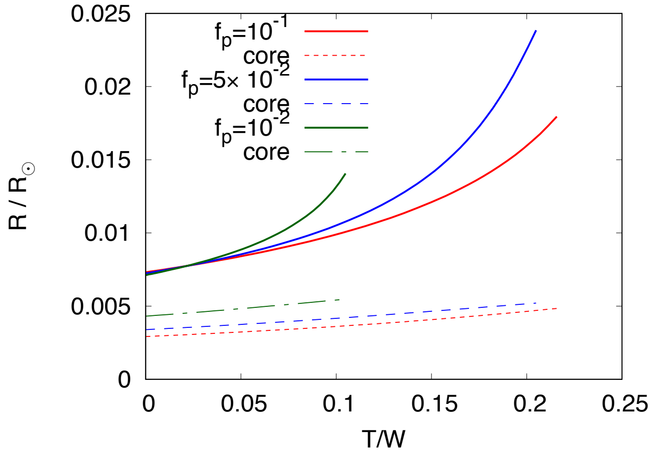

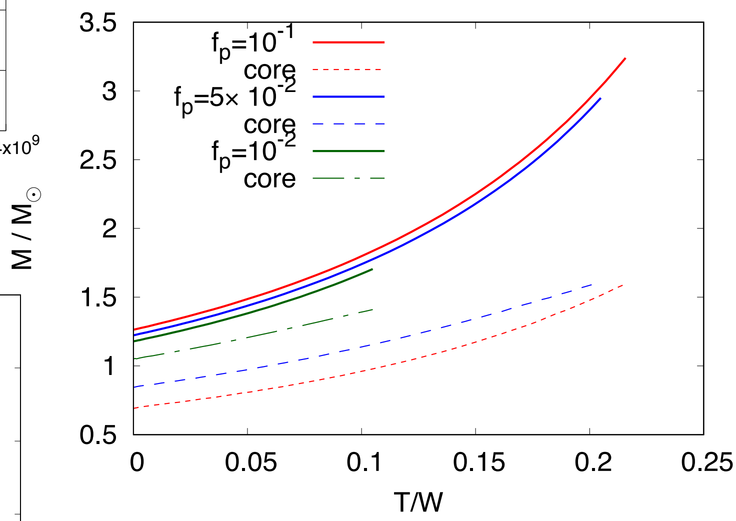

mass and radius of Kepler law models

$\rho_c = 10^8\mathrm{gcm}^{-3},\ T_\mathrm{b} = 5\times10^8\mathrm{K}$

d. some sequences of interest

quasi-evolutionary sequences
total mass = const.

We study two extreme cases without specifying details of the processes.

(1) rapid spin down — Tb=const.
(2) rapid cooling — J=const.

d-(2). M=const. & J=const.

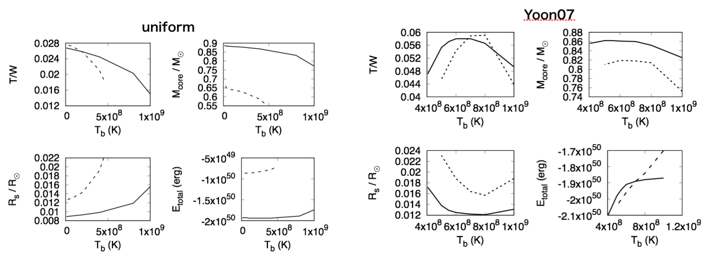

solid: M=1.29Msun, J=6.97e+49 erg s
dashed: M=0.86Msun, J=7.03e49 erg s

solid: M=1.37Msun, J=1.22e+50 erg s
dashed: M=1.35Msun, J=1.41e50 erg s

$\dfrac{dE_\mathrm{total}}{dT_\mathrm{b}} > 0$ E(total) decreases as Tb decreases
-> rapidly cooling down sequence

d-(1). M=const. & Tb=1e+8 K

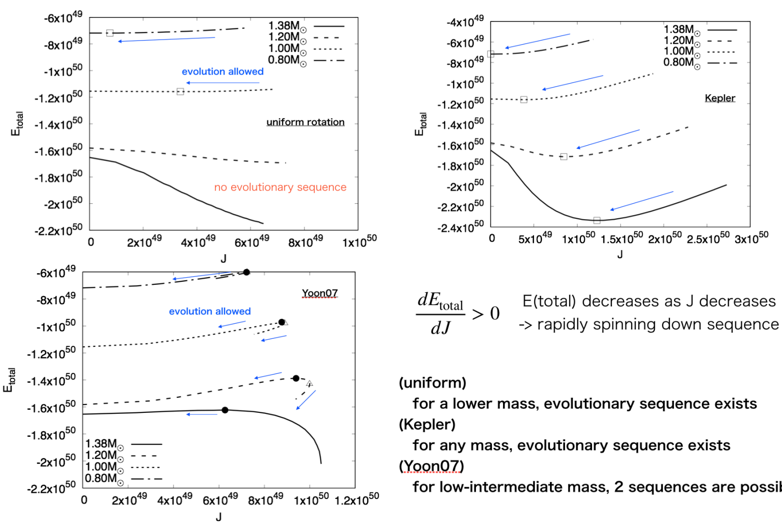

$\dfrac{dE_\mathrm{total}}{dJ} > 0$ E(total) decreases as J decreases
-> rapidly spinning down sequence

(uniform)
for a lower mass, evolutionary sequence exists
(Kepler)
for any mass, evolutionary sequence exists
(Yoon07)
for low-intermediate mass, 2 sequences are possible

IV. SUMMARY

* Numerical method & code to compute equilibrium merger remnants of BWD

  modified HSCF — cold degenerate core + hot envelope

* differential rotation + hot envelope

  => super-Chandrasekhar with relatively small core mass is possible

  ⚠ realistic merger process may prohibit M >2 Mch(cold)

* model evolutionary sequences : M=const.

  Tb=const. — rapid J removal

  physical sequences terminate at finite J

  J=const. — rapid cooling

  model sequences do not terminate at finite Tb

  and may cool down to entire degeneracy

secondary WD mass-radius
$$\frac{R_2}{0.01 R_\odot} = \left(\frac{M}{0.5 M_\odot}\right)^{-\frac{1}{3}}$$

Roche lobe radius of secondary
$$\frac{a_2}{D} = 0.462 \times \left(\frac{q}{1+q}\right)^{\frac{1}{3}} \qquad q \equiv M_2/M_1$$

if the Roche lobe is filled $(R_2 = a_2)$
$$\tilde{D} = \frac{0.01}{0.462}\left(\frac{M_2}{0.5 M_\odot}\right)^{-\frac{1}{3}}\left(\frac{1+q}{q}\right)^{\frac{1}{3}} R_\odot$$

$$\tilde{D} > R_1 + R_2 ? \quad \rightarrow \quad (1+q)^{\frac{1}{3}} > 0.462(1+q^{\frac{1}{3}}) \ ?$$

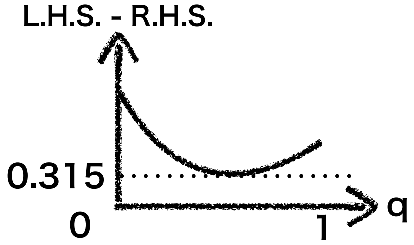

secondary fills its Roche lobe before the stars touch

expected temperature of envelope

specific heat $$C_V = \frac{3}{2} N k$$

energy avaiable in merger $$E \sim \frac{G M_1 M_2}{2 R_1}$$

mass-radius of primary* $$\frac{R_1}{0.01 R_\odot} = \left(\frac{M}{0.5 M_\odot} \right)^{-\frac{1}{3}}$$

* good for low mass WD
for high mass WD, R_1
may be much smaller
=> higher T

total particle # $$N = \frac{M_2}{A m_\mathrm{H}}$$

<ex.> $M_1 = 0.9 M_\odot,\ M_2 = 0.6 M_\odot$

$R_1 = 5.7 \times 10^8 \mathrm{cm} \quad \rightarrow \quad E \sim 1.2 \times 10^{50} \mathrm{erg}$

$N = 1.8 \times 10^{56}$

$$T_\mathrm{envlp} = \frac{E}{C_V} = 3 \times 10^9\ \mathrm{K}$$

Original HSCF (Hachisu 1986)

powerful method to compute configurations of rotating stars

stationary & axisymmetric
Equation of state (EOS) : barotropic
angular frequency : analytic profile

1st integral of hydrostationary balance
$$\int \frac{dp}{\rho} + \Phi - \int \Omega^2 R dR = C$$

Poisson
$$\Phi = -G \int \frac{\rho}{|\vec{r} - \vec{r'}|} d^3 \vec{r'}$$

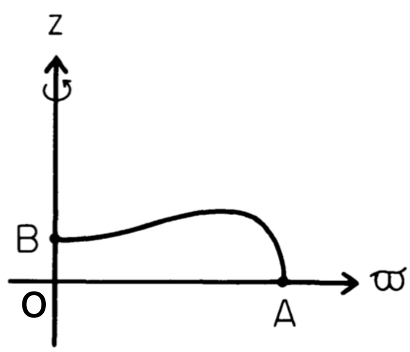

(a)

0) Fixing OB/OA, central density.
1) give initial guess of $\rho(\vec{r})$
2) integrate Poisson
3) solve for OA, C, $\Omega(O)$
by applying 1st integral at O,B,A
4) use 1st integral to obtain $\rho_\mathrm{updated}(\vec{r})$
5) if not converged, GOTO 2)

Norihiro Tanahashi
Institute of Mathematics for Industry, Kyushu University

“Separability of Maxwell equation in rotating black hole spacetime and its geometric aspects”

[JGRG28 (2018) PB26]

Separability of Maxwell equation in Rotating black hole spacetime and its Geometric aspects

Norihiro Tanahashi [Kyushu U]

with
Tsuyoshi Houri [NIT, Maizuru College]
Yukinori Yasui [Setsunan U]

Recently, a progress was made about Maxwell field perturbation on Kerr BH spacetime and its separability.
We try to find the geometric origin of this bland-new technique.

- Perturbations of Kerr black hole
- Recent breakthrough on separability
- Construction of commuting operators
- Summary

Perturbations of Kerr black hole

- Scalar field, Maxwell field, Metric perturbations on Kerr BH
- Important, but difficult

  Complicated PDE, many physical d.o.f. coupled with each other

- Teukolsky equation based on Newman-Penrose formalism

  [Teukolsky '72]

  EoM → decoupled PDEs that admit separation of variables

  → set of ODEs

Teukolsky eq. for Maxwell perturbations on 4D Kerr BH

$$ds^2 = \frac{1}{\Sigma}\Big\{-\Delta[dt - a\sin^2\theta d\phi]^2 + \sin^2\theta[(r^2+a^2)d\phi - adt]^2\Big\} + \Sigma\left[\frac{dr^2}{\Delta} + d\theta^2\right]$$

$$= -2\ell_{(\mu}n_{\nu)} + 2m_{(\mu}\bar{m}_{\nu)}$$

$$[\Delta = r^2 + a^2 - 2Mr,\ \Sigma = r^2 + a^2\cos^2\theta\,]$$

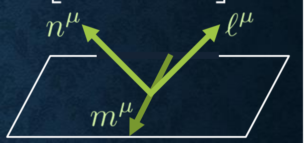

$$\begin{cases} F_{\mu\nu} = 2\left[\phi_1(n_{[\mu}l_{\nu]} + m_{[\mu}\bar{m}_{\nu]}) + \phi_2\, l_{[\mu}m_{\nu]} + \phi_0\, \bar{m}_{[\mu}n_{\nu]}\right] + c.c. \\ \psi_+ = \phi_0,\ \ \psi_- = \bar{\rho}^2\phi_2,\ \ \psi_s = e^{i\omega t + im\phi}R_s(r)S_s(\theta) \end{cases}$$

Maxwell equation $\nabla^\mu F_{\mu\nu} = 0$→ Teukolsky equation

$$\frac{1}{\Delta^s}\frac{d}{dr}\left[\Delta^{s+1}\frac{dR_s}{dr}\right] + \left[\frac{K(K-2isr)+2isMK}{\Delta} - 4is\omega r - \Lambda - (a\omega+m)^2 + m^2\right]R_s = 0$$

$$\frac{1}{\sin\theta}\frac{d}{d\theta}\left[\sin\theta\frac{dS_s}{d\theta}\right] + \left[(a\omega\cos\theta+s)^2 - \frac{(m+s\cos\theta)^2}{\sin^2\theta} + s(1-s) + \Lambda\right]S_s = 0$$

$$(s = \pm 1,\ \rho = r + ia\cos\theta,\ K = (r^2+a^2)\omega - am)$$

✓ ϕ_0 and ϕ_2 are solved by Teukolsky eq. (while PDE for ϕ_1 cannot be separated)

✓ Works only in 4D: separation of variables NOT achieved in higher dim.

Recent breakthrough on Separability

◆ Lunin's new ansatz [Lunin '17]

$$\begin{cases} \ell^\mu A_\mu = G_+(r)\ell^\mu\partial_\mu\Psi \\ n^\mu A_\mu = G_-(r)n^\mu\partial_\mu\Psi \\ m^\mu A_\mu = F_+(\theta)m^\mu\partial_\mu\Psi \\ \bar{m}^\mu A_\mu = F_-(\theta)\bar{m}^\mu\partial_\mu\Psi \end{cases}$$

Teukolsky's ansatz

$$\begin{aligned} \ell^\mu A_\mu &= \frac{2ia}{r} l^\mu\partial_\mu[e^{i\omega t+im\phi}g_+(r)f_+(\theta)] \\ n^\mu A_\mu &= \frac{2ia}{r} n^\mu\partial_\mu[e^{i\omega t+im\phi}g_-(r)f_-(\theta)] \\ m^\mu A_\mu &= -\frac{2ia}{ia\cos\theta} m^\mu\partial_\mu[e^{i\omega t+im\phi}f_+(\theta)g_+(r)] \\ \bar{m}^\mu A_\mu &= -\frac{2ia}{ia\cos\theta} \bar{m}^\mu\partial_\mu[e^{i\omega t+im\phi}f_-(\theta)g_-(r)] \end{aligned}$$

- ✓ $G_\pm(r)$, $F_\pm(\theta)$ chosen to achieve separation of variable
- ✓ Separable equations for all the variables $\left(\Psi = e^{i\omega t+im\phi}R(r)S(\theta)\right)$
- ✓ Works even in higher dimensions

◆ Covariant version of Lunin's ansatz [Krtouš, Frolov, Kubizňák '18]

$$A^\mu = B^{\mu\nu}\nabla_\nu Z \qquad \text{with} \qquad B^{\mu\nu} = (g_{\mu\nu} - \beta\, h_{\mu\nu})^{-1}$$

$h_{\mu\nu}$: Principal tensor = non-degenerate closed conformal Killing-Yano tensor

= "square root" of Killing tensor $K_{\mu\nu} = (*h)_\mu{}^\rho(*h)_{\rho\nu}$

Killing tensor $K_{\mu\nu}$ $(\nabla_{(\mu}K_{\nu\rho)} = 0)$ ≈ "Hidden symmetry" of spacetime: $K_{\mu\nu}p^\mu p^\nu$ = (constant of motion)

Killing vector ξ^μ $(\nabla_{(\mu}\xi_{\nu)} = 0)$ ≈ Symmetry of spacetime: $\xi^\mu p_\mu$ = (constant of motion)

Covariant ansatz [Krtouš, Frolov, Kubizňák '18]

◆ Most-general $2N$ dim. spacetime admitting $h_{\mu\nu}$ = Kerr-NUT-(A)dS

$$ds^2 = \sum_{\mu=1}^{N}\left[\frac{U_\mu}{X_\mu}dx_\mu^2 + \frac{X_\mu}{U_\mu}\left(\sum_{j=0}^{N-1}A_\mu^{(j)}d\psi_j\right)^2\right]$$

$x^\mu = \{r, y(\theta), \dots\}$ nontrivial directions

$\psi^i = \{\tau, \phi, \dots\}$ Killing directions

$$\begin{aligned} X_\mu &= X_\mu(x^\mu) \\ U_\mu &= \prod_{\nu\neq\mu}(x_\nu^2 - x_\mu^2) \\ A_\mu^{(j)} &= \sum_{\nu_1<\dots<\nu_j\neq\mu} x_{\nu_1}^2\dots x_{\nu_j}^2 \\ A_\mu &= \sum_{j=0}^{N-1}A_\mu^{(j)}\beta^{2j} \end{aligned}$$

Maxwell equation $\mathcal{C}_0 Z \equiv \left(\Box + 2\beta\xi_k B^{kn}\nabla_n\right)Z = 0$

Lorenz gauge $\mathcal{C}Z \equiv \nabla_m\left(B^{mn}\nabla_n Z\right) = 0$ $\quad\left(A^\mu = B^{\mu\nu}\nabla_\nu Z\right)$

$$\left[\mathcal{C} = \sum_\nu \frac{A_\nu}{U_\nu}\tilde{\mathcal{C}}_\nu,\ \mathcal{C}_k = \sum_\nu \frac{A_\nu^{(k)}}{U_\nu}\tilde{\mathcal{C}}_\nu,\ \mathcal{L}_k = -i\frac{\partial}{\partial\psi_k},\ \tilde{\mathcal{C}}_\nu = (1+\beta^2x_\nu^2)\frac{\partial}{\partial x_\nu}\left[\frac{X_\nu}{1+\beta^2x_\nu^2}\frac{\partial}{\partial x_\nu}\right] - \frac{1}{X_\nu}\tilde{\mathcal{L}}_\nu^2 + i\beta\frac{1-\beta^2x_\nu^2}{1+\beta^2x_\nu^2}\beta^{2(1-N)}\mathcal{L}\right]$$

✓ Both equations given by commuting operators $[\mathcal{C}_k, \mathcal{C}_l] = [\mathcal{C}_k, \mathcal{L}_l] = [\mathcal{L}_k, \mathcal{L}_l] = 0$

→ Z is given by simultaneous eigenfunctions of $\mathcal{C}_k$, $\mathcal{L}_k$

Eigenvalues C_k, L_k ≈ Separation constants

$$\left.\begin{aligned} \mathcal{C}_k Z &= C_k Z \\ \mathcal{L}_k Z &= L_k Z \end{aligned}\right\} \longrightarrow Z = Z(\beta; C_0, C_1, \dots, C_{N-1}, L_0, \dots, L_{N-1})$$

?: What is the geometric origin & covariant form of the commuting operators?

Construction of commuting operators

1. Express perturbation equations in terms of gauged Laplacian:
   $(\nabla^\mu - iq\mathcal{A}^\mu)(\nabla_\mu - iq\mathcal{A}_\mu) + \cdots = 0$

2. Express it as $\hat{\Box}\psi = 0$ by applying the Eisenhart-Duval lift: $g_{\mu\nu} \to \hat{g}_{AB}$
   [Eisenhart 1928, Duval+ 1985]

3. It turns out that the geodesic equation for the lifted metric $\hat{g}_{AB}$ admits separation of variables completely. [Benenti '91]
   Then, there exists the Killing tensors $\hat{K}_{AB}$ s.t. $\left\{\hat{g}_{AB}p^A p^B, \hat{K}_{AB}p^A p^B\right\} = 0.$

4. By quantization $p_\mu \to -i\nabla_\mu$ it follows $\left[\hat{g}^{AB}\hat{\nabla}_A\hat{\nabla}_B, \hat{\nabla}_A\hat{K}^{AB}\hat{\nabla}_B\right] = \frac{4}{3}\nabla_A\left(\hat{K}_C{}^{[A}\hat{R}^{B]C}\right)\hat{\nabla}_B.$

5. Then, if the anomaly-free condition $\nabla_A\left(\hat{K}_C{}^{[A}\hat{R}^{B]C}\right) = 0$ is satisfied,
   it follows $\left[\hat{g}^{AB}\hat{\nabla}_A\hat{\nabla}_B, \hat{\nabla}_A\hat{K}^{AB}\hat{\nabla}_B\right] = 0.$ [Carter 1977]

6. The commuting operators s.t. $\left[\hat{\Box}, \mathcal{C}_K\right] = 0$ is then given by $\mathcal{C}_k = \hat{\nabla}_A\hat{K}^{AB}\hat{\nabla}_B.$

Construction of commuting operators

- Lunin's equation $\left(\Box + 2\beta\xi_k B^{kn}\nabla_n\right) Z = 0$
- Teukolsky equation $\left(\Box + f_1^\mu\nabla_\mu + f_2\right)\psi = 0$

Both given by gauged wave equation $(\nabla^\mu - iq\mathcal{A}^\mu)(\nabla_\mu - iq\mathcal{A}_\mu) + \cdots = 0$

Can be expressed as wave operator in higher dimensions $\hat{\Box}\psi = 0$
by lifting the metric $g_{\mu\nu}$ to a higher-dimensional one $\hat{g}_{\mu\nu}$ [Eisenhart 1928, Duval+ 1985]

$ds^2 = \hat{g}_{AB}dx^A dx^B = g_{\mu\nu}dx^\mu dx^\nu + 2q\mathcal{A}_\mu dx^\mu du + 2dudv - 2V du^2$, $\hat{\psi}(x^A) = \psi(x^\mu)e^{iv}$

$\hat{\Box}\hat{\psi} = e^{iv}\left(\Box_\mathcal{A} - 2V\right)\psi$ $\left[\Box_\mathcal{A} = \Box - 2iq\mathcal{A}^\mu\nabla_\mu - q^2\mathcal{A}^\mu\mathcal{A}_\mu - iq\nabla_\mu\mathcal{A}^\mu\right]$

- It turns out that the geodesic eq. for the uplifted metric $\hat{g}_{AB}$ admits separation of variable completely. [Benenti '91]

- Separation of variable for geodesics
  → $\exists$ Constants of motion
  → $\exists$ Killing tensor satisfying $\left\{\hat{H}, \hat{K}_{AB}p^A p^B\right\} = 0$
  → Commuting operators $[\hat{\Box}, \hat{\nabla}_A(\hat{K}^{AB}\hat{\nabla}_B)] = 0$ by quantization $p_\mu \to -i\hat{\nabla}_\mu$
  if anomaly-free condition $\nabla_A\left(\hat{K}_C{}^{[A}\hat{R}^{B]C}\right) = 0$ is satisfied.

$$\left(\begin{array}{l}\hat{H} = \hat{g}_{AB}p^A p^B \\ \{f,g\} = \dfrac{\partial f}{\partial x_i}\dfrac{\partial g}{\partial p^i} - \dfrac{\partial f}{\partial p^i}\dfrac{\partial g}{\partial x_i}\end{array}\right)$$

Construction of commuting operators

ex.) Teukolsky eq. for 4D Kerr BH

$$\left[\frac{1}{\Delta^s}\frac{\partial}{\partial r}\left(\Delta^{s+1}\frac{\partial}{\partial r}\right)+\frac{1}{\sin\theta}\frac{\partial}{\partial\theta}\left(\sin\theta\frac{\partial}{\partial\theta}\right)+\frac{K(K-2isr)+2isMK}{\Delta}-4is\omega r\right.$$
$$\left.-(a\omega+m)^2+m^2+(a\omega\cos\theta+s)^2-\frac{(m+s\cos\theta)^2}{\sin^2\theta}+s(1-s)\right]\psi=0$$

$$\left(\Box-2iq\mathcal{A}^\mu\nabla_\mu-q^2\mathcal{A}^\mu\mathcal{A}_\mu-iq\nabla_\mu\mathcal{A}^\mu-2V\right)\psi=0$$

$$ds^2=\hat{g}_{AB}dx^Adx^B=g_{\mu\nu}dx^\mu dx^\nu+2q\mathcal{A}_\mu dx^\mu du+2dudv-2Vdu^2$$

Metric

$$\hat{g}^{\mu\nu}=g^{\mu\nu}\quad \hat{g}^{\mu u}=0\quad \hat{g}^{rv}=g^{rr}\frac{is(M-r)}{\Delta}$$
$$\hat{g}^{\theta v}=0\quad \hat{g}^{\phi v}=g^{rr}\frac{isa(M-r)}{\Delta^2}+g^{\theta\theta}\frac{s\cos\theta}{\sin^2\theta}$$
$$\hat{g}^{tv}=g^{rr}is\left(\frac{r}{\Delta}+\frac{M(a^2-r^2)}{\Delta^2}\right)+g^{\theta\theta}(-sa\cos\theta)$$
$$\hat{g}^{uv}=1\quad \hat{g}^{vv}=g^{\theta\theta}s^2\cot^2\theta$$

$\Rightarrow$

Killing tensor

$$\hat{K}^{\mu\nu}=K^{\mu\nu}_{\rm Kerr}\quad \hat{K}^{iu}=0\quad K^{rv}=K^{rr}\frac{is(M-r)}{\Delta}$$
$$K^{\theta v}=0\quad K^{\phi v}=K^{rr}\frac{isa(M-r)}{\Delta^2}+K^{\theta\theta}\frac{s\cos\theta}{\sin^2\theta}$$
$$K^{tv}=K^{rr}is\left(\frac{r}{\Delta}+\frac{M(r^2-a^2)}{\Delta^2}\right)+K^{\theta\theta}(-sa\cos\theta)$$
$$K^{uv}=0\quad K^{vv}=K^{\theta\theta}s^2\cot^2\theta$$

$\Rightarrow$ $\{\hat{g}^{AB}p_Ap_B,\hat{K}_{AB}p^Ap^B\}=0$ $\Rightarrow$ $[\hat{\Box},\hat{\nabla}_A(\hat{K}^{AB}\hat{\nabla}_B)]=0$ **if** $\nabla_A\left(\hat{K}_C{}^{[A}\hat{R}^{B]C}\right)=0$

✓$\nabla_A\left(\hat{K}_C{}^{[A}\hat{R}^{B]C}\right)=0$ is indeed satisfied, hence $\hat{\nabla}_A\hat{K}^{AB}\hat{\nabla}_B$ becomes a commuting op.

✓This procedure works also for 4D Kerr-NUT-AdS spacetime

Construction of commuting operators

ex.) D-dim. Kerr-NUT-AdS spacetime ($D = 2n + \varepsilon$)

$$g^{-1}=\sum_{\mu=1}^{n}(X_\mu\otimes X_\mu+X_{\hat{\mu}}\otimes X_{\hat{\mu}})+\epsilon X_0\otimes X_0=\sum_{\mu=1}^{n}g^{\mu\mu}\left(\frac{\partial}{\partial x_\mu}\right)^2+\sum_{k,\ell=0}^{n-1+\epsilon}g^{k\ell}\frac{\partial}{\partial\psi_k}\frac{\partial}{\partial\psi_\ell}$$

$$\left(g^{\mu\mu}=Q_\mu,\quad g^{kl}=\sum_{\mu=1}^{n-1+\epsilon}\zeta^{kl}_{(\mu)}(x_\mu)Q_\mu,\quad \zeta^{k\ell}_{(\mu)}=\frac{(-1)^{k+\ell}x_\mu^{2(2n-2-k-\ell)}}{X_\mu^2}+\frac{(-1)^{n+1}}{cx_\mu^2X_\mu}\delta_{nk}\delta_{n\ell}\right)$$

$$\left(\begin{aligned}&X_\mu=\sqrt{Q_\mu}\frac{\partial}{\partial x_\mu}\\&X_{\hat{\mu}}=\sum_{k=0}^{n-1+\epsilon}\frac{(-1)^kx_\mu^{2(n-1-k)}}{\sqrt{Q_\mu}U_\mu}\frac{\partial}{\partial\psi_k}\\&X_0=\frac{\sqrt{S}}{c}\frac{\partial}{\partial\psi_n}\\&Q_\mu=\frac{X_\mu}{U_\mu},\quad S=\frac{c}{A^{(n)}}\end{aligned}\right)$$

Perturbation eq. $\left(\Box+2\beta\xi_kB^{kn}\nabla_n\right)Z=0$ → gauge field $q\mathcal{A}^a=2i\beta\xi_bB^{ba}$

Lifted metric $\hat{g}^{\mu\mu}=g^{\mu\mu},\quad \hat{g}^{k\ell}=g^{k\ell},\quad \hat{g}^{\mu v}=-qg^{\mu\mu}\mathcal{A}_\mu,\quad \hat{g}^{kv}=-qg^{k\ell}\mathcal{A}_\ell,\quad \hat{g}^{vv}=-iq\,{\rm div}\mathcal{A},\quad \hat{g}^{uv}=1$

$$\Leftrightarrow\quad \hat{g}^{\mu\mu}=Q_\mu,\quad \hat{g}^{AB}=\sum_{\mu=1}^{n}\zeta_\mu^{AB}(x_\mu)\sigma_j(\hat{x}_\mu)Q_\mu\quad (A=B\neq\mu)$$

By Benenti's construction, the Killing tensor $\hat{K}_{(j)AB}$ of the lifted metric $\hat{g}_{AB}$ is given by

$$\hat{K}^{\mu\mu}_{(j)}=\sigma_j(\hat{x}_\mu)Q_\mu,\quad \hat{K}^{AB}_{(j)}=\sum_{\mu=1}^{n}\zeta_\mu^{AB}(x_\mu)\sigma_j(\hat{x}_\mu)Q_\mu\quad (A=B\neq\mu)$$

The anomaly-free condition $\nabla_A\left(\hat{K}_C{}^{[A}\hat{R}^{B]C}\right)=0$ turns out to be satisfied by $\hat{K}_{(j)AB}$,

hence the operator $\hat{\nabla}_A(\hat{K}^{AB}_{(j)}\hat{\nabla}_B)$ commutes with the Laplacian $\hat{\Box}$: $[\hat{\Box},\hat{\nabla}_A(\hat{K}^{AB}_{(j)}\hat{\nabla}_B)]=0$

✓ The operator $\hat{\nabla}_A(\hat{K}^{AB}_{(j)}\hat{\nabla}_B)$ coincides with the commuting operators $\mathcal{C}_k$ up to (Killing vector)$^\mu\nabla_\mu$

Summary

✓New ansatz for Maxwell perturbations on Kerr BH

✓EoMs given by commuting operators → Separability for all variables

◆Tried to give geometric interpretation to the commuting operators

- Master eq. = scalar field eq. with gauged wave operator

  = scalar eq. with (non-gauged) wave op. in higher dimensions
- Uplifted higher-dimensional metric possesses Killing tensors
- This Killing tensor generates commuting operators $[\hat{\Box}, \hat{\nabla}_A(\hat{K}^{AB}\hat{\nabla}_B)] = 0$
- Procedure above works for Teukolsky eq. and also Lunin's eq.

■Future tasks

- Uplifted spacetimes corresponding to Teukolsky eq. and Lunin's eq. are apparently different. What is the essential difference?
- Can we apply this procedure to gravitational perturbations in higher D?

Takuma Kajihara
Department of Physics, Rikkyo University

“Newton-V experiment: Test of gravitational inverse square law at a micrometer scale”

[JGRG28 (2018) PB30]

Newton-V experiment: Test of gravitational inverse square law at a micrometer scale

T. Kajihara, M. Hatori, S. Inaba, K. Ninomiya, S. Saiba, H. Shibaguchi,
N. Shinozaki, Y. Tanaka and J. Murata

Department of Physics, Rikkyo University, 3-34-1 Nishi-Ikebukuro, Tokyo 171-8501, JAPAN:

Contact Address: takumakajihara@rikkyo.ac.jp

Abstract

According to the large extra-dimension model[1], a deviation from the Newtonian inverse square law is expected at sub-millimeter scale. We have developed an experimental method using a wire cantilever with a digital image analysis system, aiming to test Newton's gravitational law in a laboratory experiment. We report the status of the experiment at the micrometer scale using the wire cantilever.

1. Physics motivation

Fundamental interaction	Relative force
Strong force	1
Weak force	10^{-5}
Electromagnetic force	10^{-2}
gravity	10^{-38}

Why gravity is extremely weak?

→Hierarchy problem

Only gravity propagates toward extra dimensions

Large Extra Dimension Model [1]
There is the possibility of compacted extra dimensions below mm scale.

Deviation from Newton's inverse square law is expected at below mm scale.

Modification of Newton's inverse square law

$$F_{r>>\lambda} = G\frac{Mm}{r^2}$$

$$F_{r<<\lambda} = G_{4+d}\frac{Mm}{r^{2+d}}$$

λ : interaction length
d : the number of extra dimension
(ADD model ⋯ d=2, λ=0.1mm)

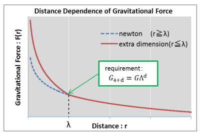

parameter in Yukawa potential

$$V(r) = -G\frac{Mm}{r}(1+\alpha e^{-\frac{r}{\lambda}})$$

λ : interaction length
α : coupling constant

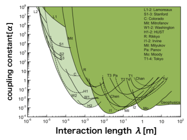

Limits on the Yukawa interaction [2]

2. Newton project

We have tested gravitational inverse square law at cm ~mm scale using torsion pendulum.
Because torsion pendulum is too large to measure gravity on μm scale, we introduce a wire cantilever to measure gravity.

Torsion pendulum | Wire cantilever

cm scale measurement | mm scale measurement | μm scale measurement

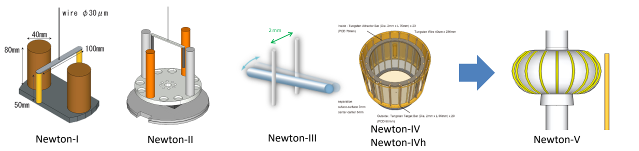

3. principle of Measurement

We have established how to measure the gravitational force using a wire cantilever and seventeen wires.

Wire cantilever (Target)

Wire cantilever is made of 50μm tungsten wire.

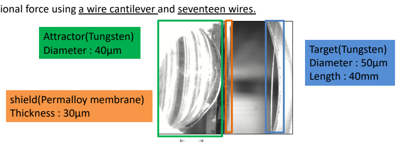

Gravity source

Gravity source is composed of a toroidal shaped acrylic resin and tungsten wires(attractor).
They are put on a rotating rod which is rotated by a stepping motor.
In addition, they are covered by a electromagnetic shield which is made by an aluminum box and a permalloy membrane.

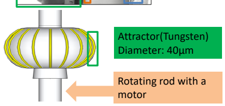

By rotating the wires(attractor) near the wire cantilever, periodical gravitational signal is expected as periodical motion of gravity of attractor.

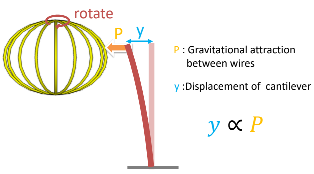

Whole apparatus

The entire system set in a vacuum chamber , which its vacuum level is 1Pa.

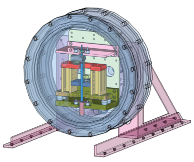

Section of whole apparatus

4. Analysis technics

The digital image analysis system is our original system.
We set up a digital microscope outside on side of chamber, which captures the motion of the wire cantilever as a movie data.
This movie data is converted as pixel intensity information. Finally, the displacements of the wire cantilever are determined using data.

Digital image analysis system [3]

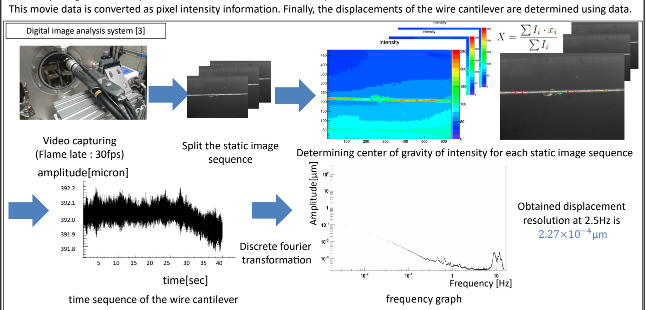

5. Frequency analysis

We tested the Newtonian inverse square law using a frequency analysis. This analysis performs Fourier transformation for the periodical gravitational signal, and calculate the gravitational force from the peak height.

The attractor continuously rotates near the wire cantilever.
The wire cantilever oscillates periodically because of gravity of the attractor.
In this case, the rotating frequency ω_d of the attractor is set to 924mrad/s (0.147Hz), so the corresponding gravitational signal frequency is 2.5Hz ($17\omega_d$).

Result of the frequency analysis

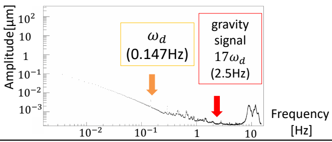

6. Result

Our device is placed on the basement of Rikkyo University Building 13. It is because vibration effects from the buildings and temperature changing are relatively small.

This measurement was tested with a duration of about 7.84days.Each data is measured for about 11 minutes.

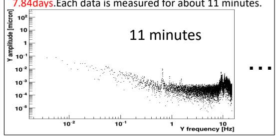

all data

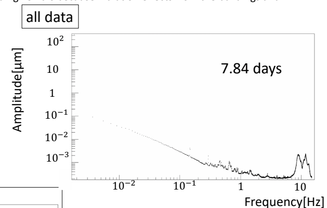

Result of the averaging data

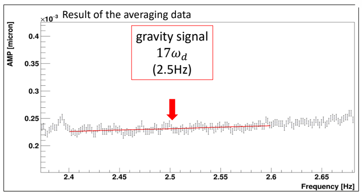

Test of displacement of cantilever
$-4.00\times10^{-13} \pm 1.42\times10^{-12}$ m

Red line : Gauss + Noise fitting

In this test, it is difficult to bring Target closer to Attractor.

By fitting the averaging data using Gauss and Noise fitting around 2.5Hz, displacement of cantilever is obtained as Gauss height -4.00×10^{-13} m.

7. Discussion

Parameterized in Yukawa potential

We can set upper limit on the alpha-lambda plot using the experiment data.
→143.3μm, 7.84days 2018result
X axis is the interaction length "λ" , Y axis is the coupling constant "α" .

$$V(r) = -G\frac{Mm}{r}(1+\alpha e^{-\frac{r}{\lambda}})$$

Center distance : 188.3μm
Closest distance : 143.3μm

We aim to set new upper limit on the alpha-lambda plot .
→75μm, 30days expected result (statistical error only)

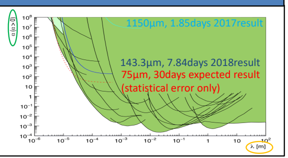

8. Future Plan

We are developing next generation device aiming to achieve the most precise test of the inverse square law at μm scale.
For the new gravity source, the an acrylic resin is going to be changed to tungsten. 18 trenches is patterned in stead of 17 tungsten wires. This enables us to bring the target closer to the attractor than now.

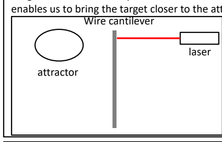

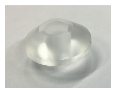

new attractor model

We will change the detector from the digital microscope to the Laser displacement sensor.
This laser can measure 5000 data per second (more than 100 times more data per second than the digital microscope).

9. Conclusion

✔ We are developing a new device aiming the highest precision experiment at μm scale..

Reference

[1] N. Arkani-Hamed, S. Dimopoulos, and G.Dvali, Physics Letter B, 429, 263 (1998)
[2] J. Murata and S. Tanaka CQG. 32(2015)033001
[3] K. Ninomiya, et al. In Journal of Physics: Conference Series Vol. 65, p. 012019. IOP Publishing,2009